

**COUPLING OF ECOLOGICAL AND WATER QUALITY MODELS FOR
IMPROVED WATER RESOURCE AND FISH MANAGEMENT**

A Dissertation

by

DOROTHY HAMLIN TILLMAN

Submitted to the Office of Graduate Studies of
Texas A&M University
in partial fulfillment of the requirements for the degree of

DOCTOR OF PHILOSOPHY

December 2008

Major Subject: Civil Engineering

**COUPLING OF ECOLOGICAL AND WATER QUALITY MODELS FOR
IMPROVED WATER RESOURCE AND FISH MANAGEMENT**

A Dissertation

by

DOROTHY HAMLIN TILLMAN

Submitted to the Office of Graduate Studies of
Texas A&M University
in partial fulfillment of the requirements for the degree of

DOCTOR OF PHILOSOPHY

Approved by:

Chair of Committee,
Committee Members,

Head of Department,

Ralph Wurbs
Anthony Cahill
Ann Kenimer
Frances Gelwick
David Rosowsky

December 2008

Major Subject: Civil Engineering

ABSTRACT

Coupling of Ecological and Water Quality Models for Improved Water Resource and Fish Management. (December 2008)

Dorothy Hamlin Tillman, B.S.; B.Eng.; M. Eng., Mississippi State University

Chair of Advisory Committee: Dr. Ralph Wurbs

In recent years new ideas for nutrient management to control eutrophication in estuarine environments have been under consideration. One popular approach being considered in the Chesapeake Bay Program is called the “top down” approach based on the premise that restoring algal predators, such as oysters and menhaden, will limit excess phytoplankton production and possibly eliminate costly nutrient control programs. The approach is being considered to replace or use in conjunction with the “bottom up” approach of reducing nutrient loads. The ability to model higher trophic levels such as fish, as well as the eutrophication processes driving production of primary producers in an aquatic ecosystem is needed. CE-QUAL-ICM (ICM) and Ecopath were two models selected for this research. ICM is a time- and spatial-varying eutrophication model that uses nutrient loads to predict primary producers, while Ecopath is a static mass balance model representing an average time period (e.g., season or year) and uses values of primary producers and other groups to predict fish biomass. Linking the two models will provide the means of going up the food chain by trophic levels. The Chesapeake Bay was chosen as the study site since both models are in use there.

Before coupling ICM and Ecopath, common links between the two models were found. Ten groups were identified with such variables as production rates, consumption rates, and unassimilated food/consumption. A post-processor/subroutine was developed for ICM to

aggregate output data from 3-D to 0-D to be used in Ecopath. Two Ecopath runs were developed with data from ICM and the Chesapeake Bay (CB) Ecopath model to see how network interactions differed with data representing the same system. Four additional runs were made, creating perturbations (i.e., increased phytoplankton production) using the CB Ecopath model and replacing the primary producers with data from ICM. Final runs of ICM were conducted looking at adjusting three parameters to try to restore the Bay back to 1950 conditions. It was demonstrated that ICM data can be coupled with Ecopath to study management strategies in eutrophication. Because of model formulations there was no data exchange from Ecopath back to ICM.

DEDICATION

First, I would like to dedicate this to God. With Him every thing is possible. Most importantly, I dedicate this to my family:

Russ, Blair, Barbara (Mom), Chris, Tom, Marte, Martine, Ulf, Soeren, and all the cats (Sandy, Carlee, Salem, Tom) and dogs (Sherbert, Houston and Chesley).

ACKNOWLEDGEMENTS

I would like to thank my committee chair, Dr. Wurbs, for allowing me to work with him as a distance student. It has not been easy, but he has been there whenever I needed him and always made it seem like nothing was impossible. I admire his professionalism and hope I can emulate him. He was one of the first professors to welcome me to Texas A&M for the short time I was there and every time I go back, he is there with a smile. I will always be indebted to him and remember his kindness. I would also like to thank the rest of my committee members, Dr. Cahill, Dr. Kenimer, and Dr. Gelwick for their support throughout the course of this research. They are all amazing for taking on a student they knew nothing about. I do not remember if any of them were teaching at Texas A&M when I was a student, but I thank them for accepting an unknown.

I would especially like to thank a colleague of mine, Dr. Carl Cerco. If it had not been for Carl, I would not have had a research project to work on. After six years of writing proposals to get funding and not being successful, he asked me to work with him on this project. He has provided unlimited guidance and a wealth of knowledge. With his knowledge of the Chesapeake Bay, he is “Mr. Chesapeake Bay.” I will always be grateful to him. Like Dr. Wurbs, he is a true professional.

I cannot forget all the great people I work with either. They have all given me support and encouragement along the way, and I thank them for it. I think of them as my second family.

Finally, thanks to my family. My husband, Russ, has taken up the slack when I have been too immersed in work to take care of things at home. I love him and appreciate all that he has done. I’d like to thank my daughter, Blair, for being with me at Texas A&M. She was a child

when she went off to school with me and now she is a young woman in college herself. She finally understands we were not just on vacation.

NOMENCLATURE

CBEM	Chesapeake Bay Eutrophication Model
CBEMP	Chesapeake Bay Environmental Model Package
CE	US Army Corps of Engineers
DIN	Dissolved Inorganic Nitrogen
DO	Dissolved Oxygen
DOC	Dissolved Organic Carbon
DOV	Dissolved Oxygen Volume Day
EBFM	Ecosystem-Based Fisheries Management
EE _i	Ecotrophic Efficiency
EPA	US Environmental Protection Agency
ERDC	US Army Engineer Research and Development Center
EWE	Chesapeake Bay Ecopath with Ecosim
ICM	CE-QUAL-ICM
MTI	Mixed Trophic Impact
NOAA	National Oceanic and Atmospheric Administration
NPP	Net Primary Production
POC	Particulate Organic Carbon
PP	Primary Production
RMBR	Restored Mid-Bay Run
SAV	Submerged Aquatic Vegetation
STAC	Chesapeake Bay Program Scientific and Technical Advisory Committee
SOD	Sediment-Oxygen Demand

TN	Total Nitrogen
TP	Total Phosphorus
TPP	Total Primary Production
TST	Total System Throughput
WES	US Army Engineer Waterways Experiment Station

TABLE OF CONTENTS

	Page
ABSTRACT	iii
DEDICATION	v
ACKNOWLEDGEMENTS	vi
NOMENCLATURE	viii
TABLE OF CONTENTS	x
LIST OF FIGURES	xii
LIST OF TABLES	xvi
CHAPTER	
I GENERAL INTRODUCTION	1
1.1 Background	3
1.2 Research Objectives	5
1.3 Dissertation Organization.....	6
II FUNDAMENTALS OF THE CE-QUAL-ICM AND ECOPATH WATER QUALITY AND NETWORK MODEL.....	8
2.1 Background	8
2.2 Chesapeake Bay Study Site.....	10
2.3 CE-QUAL-ICM Model Descriptions.....	12
2.4 Ecopath Model Description.....	15
III COMMON CONCEPTUAL PROCESSES BETWEEN CE-QUAL-ICM AND ECOPATH	18
3.1 Background	18
3.2 Finding the “Links”	19
3.3 Parallels between Ecopath and ICM	34
3.4 ICM and Ecopath Base Runs	43
3.5 3-D ICM Data Aggregated to 0-D Ecopath Data	49
3.6 Summary and Conclusions.....	70
IV ECOSYSTEM PROJECTIONS FROM CE-QUAL-ICM.....	73

CHAPTER	Page
4.1 Background	73
4.2 Analysis Procedure.....	76
4.3 Mass Balancing EWE	79
4.4 Results and Discussion.....	80
4.5 Conclusions	97
 V RECREATING HISTORICALLY DOCUMENTED CONDITIONS OF THE CHESAPEAKE BAY WITH CE-QUAL-ICM	 100
5.1 Background	100
5.2 Approach	103
5.3 Sensitivity Result Presentation.....	109
5.4 1950's Restored Bay Result Presentation	117
5.5 Results and Discussion.....	144
5.6 DO Volume-Day	155
5.7 Summary and Conclusions.....	159
 VI SUMMARY AND CONCLUSIONS	 162
 REFERENCES	 166
 APPENDIX A	 178
 APPENDIX B.....	 209
 VITA	 213

LIST OF FIGURES

FIGURE	Page
1.1 Coupling a Eutrophication Model with a Network Model (STAC 2005).....	5
2.1 Chesapeake Bay Study Site.....	9
2.2 Conceptual View of a Zero-Dimensional Water Body	15
3.1 Conceptual Illustration Showing Pathways of the Carbon Cycle in the Water Column and Sediments in CE-QUAL-ICM	21
3.2 Schematic of the Sediment Diagenesis Model (Cercio and Tillman, 2008)	27
3.3 Schematic of Benthic Algae Model (Cercio and Tillman, 2008).....	29
3.4 SAV Model State Variables (boxes) and Mass Flows (arrows) (Cercio and Tillman, 2008).....	30
3.5 Schematic of Benthos Model (Cercio and Tillman, 2008).....	32
3.6 “Basic Input” Screen for Ecopath	35
3.7 “Diet Composition” Screen from Ecopath	36
3.8 “Detritus Fate” Screen from Ecopath.....	37
3.9 Physical and Computational Grid of the 13000 Cell Chesapeake Bay Model (Cercio and Noel, 2004).....	45
3.10 Three Regions of Chesapeake Bay.....	47
3.11 Aggregate 3-D Temporally and Spatially Varying Data to O-D Snapshot of Well Mixed System.....	50
3.12 Ecopath Input Screens with ICM Common Variables (upper - “Basic Input,” middle - “Diet Composition,” and lower - “Detritus Fate,”)	59
3.13 Basic Estimates After Mass Balance for Ecopath with ICM Common Variables	60
3.14 Basic Estimates After Mass Balance for Ecopath-CB Ecopath Common Variables	61

FIGURE	Page
3.15 Lindeman Chain with Combined Primary Producer and Detrital Flow (gC m ⁻² d ⁻¹) for Transfer Efficiency Designated Between Boxes for Ecopath Run with ICM Variables	62
3.16 Lindeman Chain with Combined Primary Producer and Detrital Flow (gC m ⁻² d ⁻¹) for Transfer Efficiency Designated Between Boxes for Ecopath Run with CB Ecopath Variables	63
3.17 Mixed Trophic Impact (MTI) from Ecopath ICM Run.....	69
4.1 Primary Producer Biomass from EWE Base and EWE-M20% (Blue), EWE-ICM Base (Maroon), and EWE-ICM 20%P (Light Yellow) Runs	82
4.2 P/B Ratios for Primary Producers All EWE Runs	82
4.3 Network Interactions Through Detrital Flow (Black Arrows) and Predators (Orange Arrows) of Groups with EE > 1	84
4.4 Adjusted Predator Biomasses of Microphytobenthos, DOC, and Sediment POC from the EWE Base, EWE-ICM Base, and EWE-M20% Runs.....	85
4.5 Sum of System Production and TST Including Variables Making Up TST.....	89
4.6 Primary Producer Biomass from EWE Base (Blue) and EWE-ICM 90%R (Maroon) Runs.....	90
4.7 Predators of Net Phytoplankton in the EWE Base (Blue), EWE-ICM 90%R (maroon), and EWE 1950s Restored Bay (Light Yellow) Runs	92
5.1 Chesapeake Bay Program Segments.....	108
5.2 Phytoplankton Limitation Results for Base, SR1, and SR2 in the Mid Chesapeake Bay.....	111
5.3 Benthic Algae Limitation Results for Base, SR1, and SR2, in the Mid Chesapeake Bay.....	112
5.4 SAV Limitation Results for Base, SR1, and SR2 in the Mid Chesapeake Bay	113
5.5 Comparison of Biomasses for Each Group Common to ICM and Ecopath.....	114
5.6 Comparison of P/B Ratios from ICM Values Used in Ecopath.....	115

FIGURE	Page
5.7 Comparison of Q/B Ratios from ICM to Values Used in Ecopath	116
5.8 Comparison of UA/B Ratios from ICM to Values Used in Ecopath	117
5.9 Comparison of Surface Chlorophyll <i>a</i> for Base and 1950's RMB2 Results in the Upper, Mid, and Lower Regions of the Chesapeake Bay.....	119
5.10 Comparison of Surface DO for Base and 1950's RMB2 Results in the Upper, Mid, and Lower Regions of the Chesapeake Bay	120
5.11 Comparison of Surface TN for Base and 1950's RMB2 Results in the Upper, Mid, and Lower Regions of the Chesapeake Bay	121
5.12 Comparison of Surface TP for Base and 1950's RMB2 Results in the Upper, Mid, and Lower Regions of the Chesapeake Bay	122
5.13 Comparison of Surface Light Extinction for Base and 1950's RMB2 Results in the Upper, Mid, and Lower Regions of the Chesapeake Bay.....	123
5.14 Comparison of the Pycnocline Chlorophyll <i>a</i> for Base and 1950's RMB2 Results in the Upper, Mid, and Lower Regions of the Chesapeake Bay	124
5.15 Comparison of Pycnocline DO for Base and 1950's RMB2 Results in the Upper, Mid, and Lower Regions of the Chesapeake Bay	125
5.16 Comparison of the Pycnocline TN for Base and 1950's RMB2 Results in the Upper, Mid, and Lower Regions of the Chesapeake Bay	126
5.17 Comparison of the Pycnocline TP for Base and 1950's RMB2 Results in the Upper, Mid, and Lower Regions of the Chesapeake Bay	127
5.18 Comparison of the Deep Chlorophyll <i>a</i> for Base and 1950's RMB2 Results in the Upper, Mid, and Lower Regions of the Chesapeake Bay.....	128
5.19 Comparison of the Deep DO for Base and 1950's RMB2 Results in the Upper, Mid, and Lower Regions of the Chesapeake Bay	129
5.20 Comparison of the Deep TN for Base and 1950's RMB2 Results in the Upper, Mid, and Lower Regions of the Chesapeake Bay	130
5.21 Comparison of the Deep TP for Base and 1950s RMB2 Results in the Upper, Mid, and Lower Regions of the Chesapeake Bay	131
5.22 Areal Concentrations of Chlorophyll <i>a</i> for the Upper Chesapeake Bay for Base and 1950's RMB2.....	132

FIGURE	Page
5.23 Areal Concentrations of Chlorophyll <i>a</i> for the Mid Chesapeake Bay for Base and 1950's RMB2.....	133
5.24 Areal Concentrations of Chlorophyll <i>a</i> for the Lower Chesapeake Bay for Base and 1950's RMB2.....	134
5.25 Comparison of Summer Averaged (1985-1987) Chlorophyll <i>a</i> Results Longitudinally from the Susquehanna River (≈ 325 km) to the Open Ocean (≈ 70 km).....	135
5.26 Comparison of Summer Averaged (1985-1987) DO Results Longitudinally from the Susquehanna River (≈ 325 km) to the Open Ocean (≈ 70 km).....	136
5.27 Comparison of Summer Averaged (1985-1987) TN Results Longitudinally from the Susquehanna River (≈ 325 km) to the Open Ocean (≈ 70 km).....	137
5.28 Comparison of Summer Averaged (1985-1987) TP Results Longitudinally from the Susquehanna River (≈ 325 km) to the Open Ocean (≈ 70 km).....	138
5.29 Comparison of Summer Averaged (1985-1987) Light Extinction Results Longitudinally from the Susquehanna River (≈ 325 km) to the Open Ocean (≈ 70 km).....	139
5.30 DO Volume-Day for Upper Chesapeake Bay Region for DO ≤ 0.1 , 1.0, 2.0, and 5.0.....	141
5.31 DO Volume-Day for Mid Chesapeake Bay Region for DO ≤ 0.1 , 1.0, 2.0, and 5.0.....	142
5.32 DO Volume-Day for Lower Chesapeake Bay Region for DO ≤ 0.1 , 1.0, 2.0, and 5.0.....	143
5.33 ICM Normalized DO Volume Water at Three Intervals: Upper – DO ≤ 0.1 , Middle – DO ≤ 1.0 , and Lower – DO ≤ 2.0	157
5.34 Hagy et al. (2004) Normalized DO Volume Water at Three Intervals: Upper – DO ≤ 0.1 , Middle – DO ≤ 1.0 , and Lower – DO ≤ 2.0	158

LIST OF TABLES

TABLE	Page
2.1 Water Quality Model State Variables	14
2.2 Parameters From Main Equations in Ecopath.....	16
3.1 Groups Modeled in ICM and Ecopath Application to Chesapeake Bay (from Cerco and Tillman 2008)	38
3.2 Basic Input Parameters for Ecopath Derived from ICM Formulations (Cerco and Tillman 2008)	39
3.3 Prey Utilization Formulas Derived from ICM (Cerco and Tillman 2008).....	40
3.4 Derived Detrital Fate for ICM Variables	41
3.5 Groups of the Chesapeake Bay Ecopath Model (Cerco and Tillman 2008)	48
3.6 Biomass, Production, and Production/Biomass in the Three Regions as Denoted by Ecopath and ICM.....	51
3.7 Biomass Distribution from the Ecopath-ICM and Ecopath CB Ecopath Runs	64
3.8 System Statistics for Ecopath CB Ecopath (Left Value) and Ecopath ICM (Right Value).....	66
4.1 Total Biomass by Trophic Levels for All EWE Runs.....	86
4.2 Transfer Efficiency (%) from Producers (First #) and Detritus (Second #) Between Trophic Levels	88

CHAPTER I

GENERAL INTRODUCTION

Water is continually being renewed and recycled through hydrological processes. This would lead one to believe that we have a continuous supply of water. However, with the industrialization of our country, increased population growth, and increased agriculture, water is not always replaced at the same rate it is used, inevitably becoming a finite resource (Kiely 1997). Consequently, water resource managers cannot always meet the demands of the consumers. It is ironic that highly populated regions and industrialized areas are usually found where low rainfall occurs and water demand is the greatest in the summer (Mason 1991). Agricultural regions also tend to be in drier parts of the country that require irrigation. Engineering-based interventions have been used to help in the shortfall of water supplies in some areas, such as redistribution of water, channelization and damming of streams, and diversion from one catchment to another.

Each water use (e.g., irrigation, water supply, industrial use, transportation, power generation, recreation, flood control, waste transportation) can have specific impacts on water resources and the aquatic environment. This relates to the quality of the aquatic environment in terms of the physicochemical conditions and the state of the flora and fauna (Kiely 1997).

Water resource managers and planners constantly put forth an effort to minimize the impact of human activities on water quality and damage to the aquatic environment. They have been instrumental in developing potential engineering controls to help alleviate impacts to the

This dissertation follows the style of *Journal of Water Resources Planning and Management*.

environment and assure high quality water supplies and suitable habitats for the aquatic environment. An understanding of the physical, chemical, and biological characteristics of water and the requirements for the various water uses, methods to improve water quality, and methods to predict impacts resulting from environmental changes to water quality are necessary to lessen environmental impacts (Tchobanoglous and Schroeder 1987). This requires a blending of disciplines (i.e., engineers and biologists) to address all levels of ecosystem management (Nestler 2005).

Water resource managers and planners frequently have to deal with eutrophication caused by the overabundance of nutrients (nitrogen and phosphorus) delivered to surface waters via point and non point sources. A eutrophic environment favors plant life over animal. Surface water in agricultural areas is especially susceptible to eutrophication via runoff. According to Chambers et al. (2006), some of the problems caused by eutrophication include increased rates of plant growth and decay, reduction or loss of plant species, anoxia, and changes to diversity and abundance of organisms (i.e., invertebrates, fish, birds and mammals). Engineers and scientists frequently rely on water quality and ecological models to assess potential impacts to a water body. There are many models available to address eutrophication in the aquatic environment. Some of the well known eutrophication models are CE-QUAL-ICM, EDFC Water Quality, and WASP7. Using a eutrophication model, the water resource manager can explore the effects of the “bottom up” controls for reducing the nutrient loads to manage the eutrophication. Questions relating to changes in primary production and phytoplankton biomass can be answered. However, most eutrophication models only address the lower trophic levels and do not go beyond phytoplankton. This limits finding answers to eutrophication effects to higher trophic levels such as fish.

By coupling a eutrophication model and a fishery management model, higher trophic levels could be modeled, and eutrophication concerns could conceivably be explored using a “top down” control. This type of approach would consider the restoration of algal predators that could control or reduce eutrophication. Unfortunately, a modeling framework hoping to address all interactions and processes representing a complete ecosystem cannot be restricted to either a “bottom up” or a “top down” approach. Korpjen et al. (2007) found that both approaches interact. Loeuille and Loreau (2004) add to these findings with the observation that the dominant control depends on biotic or abiotic conditions, and for this reason it is critical in understanding factors influencing the dominance of that control. Thus, a coupling of both modeling approaches could provide managers a tool to support decisions as to the best approach for reducing eutrophication and also for supporting fisheries management in a complex ecosystem.

1.1 Background

In recent years new ideas for nutrient management to control eutrophication in estuarine environments have been under consideration. One popular approach being considered in the Chesapeake Bay Program is called the “top down” approach based on the premise that restoring algal predators, such as oysters and menhaden, will limit excess phytoplankton production and possibly eliminate costly nutrient control programs. The approach is being considered to replace or to use in conjunction with the “bottom up” approach of reducing nutrient loads. Guidance for nutrient control programs is frequently obtained from eutrophication models such as CE-QUAL-ICM (Cercio and Cole 1994). Eutrophication models provide temporal representations of carbon, nutrient, and oxygen cycling on a discrete spatial grid. These models usually represent the rate of primary production and/or phytoplankton biomass but extend no further to higher trophic levels. More complex eutrophication models that incorporate higher trophic levels (i.e., zooplankton and oysters) have limits and can run into numerical difficulties from multiple interacting partial

differential equations needed to describe the food web. Presently there are no models available to provide guidance for “top down” management.

One approach to modeling the complex materials and/or energy transfers that describe interactions between higher trophic levels such as zooplankton, benthos, and fish is the network model. Network models provide complexity in representing the food web at the cost of simplicity in temporal and spatial resolution. At their basic level, network models consider steady-state mass flows with little or no spatial resolution. They are equivalent to ledger sheets in which mass and/or energy flows must balance.

A combination of eutrophication and network models (Figure 1.1) is needed to address questions such as:

1. How does management in a watershed affect fisheries harvest in adjacent water bodies?
2. How does fisheries management affect water quality problems such as low dissolved oxygen?
3. How do changes in net primary production (NPP) of primary producers affect fish populations?
4. How does a cleaner water body affect primary producer biomass as well as fish populations?

No straightforward means of coupling the two modeling approaches is available or apparent although Kenny Rose of LSU has conducted studies where fish models were linked to or embedded in ecosystem computations (Scientific and Technical Advisory Committee (STAC) 2005). These fish models were individual-based stage-specific models and not mass balanced.

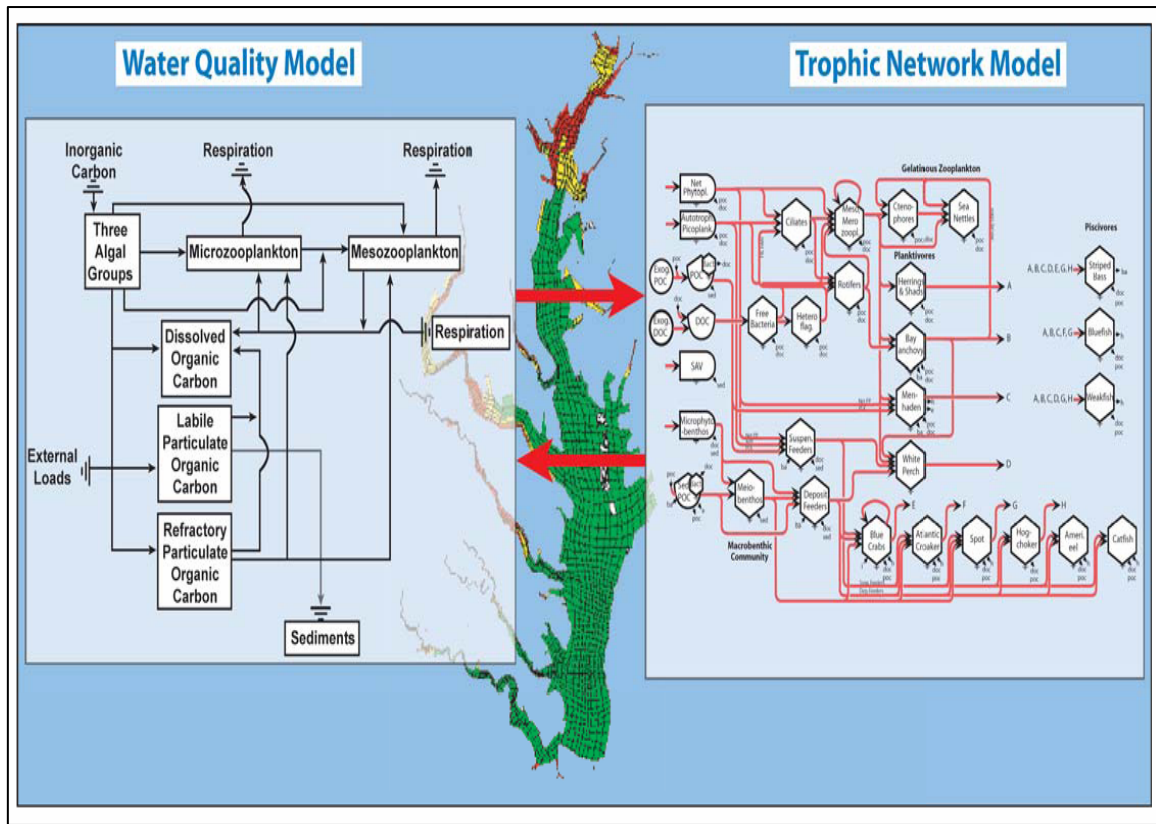


Figure 1.1. Coupling a eutrophication model with a network model (STAC 2005).

1.2 Research Objectives

The objectives of this research are: (1) investigate the coupling of the eutrophication model, CE-QUAL-ICM (ICM), with the network model, Ecopath, (2) apply the results to a specific problem, and (3) recommend a general procedure for future endeavors in this area.

Steps in the order of importance to meet research objectives are:

- Identify links where interactions may occur between ICM and Ecopath models. These include: 1) phytoplankton and benthic algal biomass and production, 2) zooplankton biomass

and production, 3) benthos biomass and production, 4) grazing rates on primary producers, and 5) predation rates on invertebrates.

- Spatially and temporally aggregate output from an ICM run to the scales of the network model. With this aggregated output of variables representing common links between the two models, examine variables for consistency (e.g., magnitudes of fundamental rates and processes).
- Manually couple the two models by using a manual interface for information exchange between the models. Perform a major alteration in a fundamental process, e.g. reduce phytoplankton primary production, and examine the behavior of the two models.
- Automate coupling by making Ecopath a subroutine of ICM and having information exchanged between the two models. Information will flow two ways and possibly require many iterative model runs. Once models are coupled, perform the same major alteration in a fundamental process as was conducted in the manual coupling.

1.3 Dissertation Organization

This dissertation is comprised of six chapters. Chapter II gives a description of the study site, criteria for models selected, and a description of each model and their basic fundamentals as they apply to this research. Chapter III continues with comparing and finding similarities (“links”) between model parameters and once found, checking the constituency between those parameters. This chapter concludes with a discussion of setting up two Ecopath models using common variables from a Chesapeake Bay application of CE-QUAL-ICM and the same common variables from an existing Ecopath model of the Chesapeake Bay. Chapter IV explores modeling perturbations to parameters affecting biomasses and production rates of primary producers of the lower trophic levels of a system. By taking the output from this model application and using it in the application of the second model, effects to higher trophic levels

are revealed. Chapter V examines specific historical water quality conditions in the Chesapeake Bay and through adjustments to model parameters, considers whether it is feasible to restore the Bay back to previous conditions as was attempted using the Ecopath model of the Chesapeake Bay. Finally, Chapter VI discusses general conclusions and future directions for this research.

CHAPTER II

FUNDAMENTALS OF THE CE-QUAL-ICM AND ECOPATH WATER QUALITY AND NETWORK MODEL

2.1 Background

Although the idea of studying ecosystems through network analysis sounds like a simple approach, in reality it requires many hours of gathering the appropriate data which are quite extensive. Certain parameters are hard to come by because they are not always collected. Equally important is the fact that data needed to develop the cause-and-effect relationship between variables (i.e., change in nutrient loads) and conditions (i.e., increased turbidity and increased flow) may not have been collected at the most opportune time. When data are available, sampling strategies and analysis procedures may not be the same from one sampling time to the next especially if collected by a different group introducing some uncertainty into the mix (Wolfe et al. 1987). Data monitoring programs are very expensive to maintain and unless critical are usually the first item cut in funding shortages (Wolfe et al. 1987); consequently, projects with short-term monitoring durations that are readily applicable to management decision-making are emphasized. Because of funding constraints, this research project required a study site with long-term data collected frequently and readily available. With this in mind, databases from prior projects were considered and the Chesapeake Bay site (Figure 2.1) chosen. This site is data rich because of efforts to pin point the decline in water quality from man induced stresses (i.e., increased nutrient loads) which prompted the Environmental Protection Agency (EPA) to take action in protecting it by establishing the Chesapeake Bay Program in 1976. This led to beginning a Bay-wide monitoring program with sampling schedules of every 2 to 4 weeks



Figure 2.1. Chesapeake Bay study site.

collecting water and biota samples at 50 plus stations starting in 1984 and continuing today (Harding et al. 2002).

More importantly, this site was also chosen because a fisheries network model (Ecopath with Ecosim, EWE) and a eutrophication model (CE-QUAL-ICM) already exist in current use that have strong organizational backing within and outside the Army Corps of Engineers (CE). The Chesapeake Bay Environmental Model Package (CBEMP) is a combination of a highly modified HSPF watershed model (Bicknell et al. 1996, Linker et al. 2000), the CH3D-WES hydrodynamic model (Johnson et al. 1991) and the CE-QUAL-ICM (ICM) eutrophication model (Cercio and Cole 1994; Cercio and Noel 2004). The hydrodynamic and eutrophication components of the CBEMP are CE codes. The Chesapeake Bay model effort has been supported for 17 years by the EPA Chesapeake Bay Program and the Baltimore District, USACE.

Ecopath is a network model employed in fisheries management (Christensen et al. 2000). It is a freely distributed model supported by the Fisheries Centre, University of British Columbia. Recently, NOAA has funded an effort to apply ECOPATH to fisheries management

in the Bay. Jim Hagy (2002) conducted one of the early ECOPATH modeling efforts on Chesapeake Bay. The model is in use at the NOAA Chesapeake Bay Office, the Virginia Institute of Marine Science, and the University.

This chapter will begin with a brief description of the Chesapeake Bay study site. It will follow with descriptions of the fundamentals of each model chosen to conduct this research.

2.2 Chesapeake Bay Study Site

The Chesapeake Bay has been described as the largest and most productive estuary of the mainland United States. Drainage into the Bay is from a watershed covering 64,000 square miles that includes six states and the District of Columbia. The origin of its name is believed to be an Algonquian word from the Powhatan Indian tribe that means the “Great Shellfish Bay” (<http://www.baydreaming.com/history.htm>). It has a length of approximately 300 km beginning at the most downstream end of the Susquehanna River flowing south and east to the Atlantic Ocean. The narrowest point of the Bay (6.4 km wide) can be found near Annapolis, Maryland and the widest (50 km wide) near the mouth of the Potomac River. The average depth of the Bay is about 9 meters (m) with the shallowest areas being less than 2m.

The climate of the Chesapeake Bay has been described as being humid subtropical, with hot and humid summers to mild and freezing winters. It is rare for the surface of the Bay to freeze in the winter but the mouth of the Susquehanna River and the wetlands nearby are prone to freezing. Historical average rainfall in the Chesapeake Bay is approximately 39.25 inches (in).

The highest freshwater inflow into the Chesapeake Bay occurs typically during the spring from the spring freshet which is a pulse of water mostly coming from spring snow melt (Harding and Perry 1997). This comes from the Susquehanna River that supplies about 60% of the freshwater flow and can have impacts to the salinity, nutrient loads, dissolved oxygen concentrations, and turbidity (USGS 2000). Other major freshwater tributary inflows as

identified by Cerco and Cole (1994) are from the Potomac River (19%) and the James River (12%).

Dissolved oxygen (DO) depletion has been observed in the Bay as early as the 1930's (Newcombe and Horner 1938). Anoxic waters in estuaries are formed from two processes acting together: stratification and aerobic respiration (Crump et al. 2007). Limited DO exchange to the bottom waters resulting from stratification in the water column diminishes the rate oxygen can be put back to the estuary bottom layers (Kemp et al. 1992). Density differences from freshwater inflows to water entering at the Atlantic Ocean have led to vertical stratification which reduces the mixing zone often leading to the formation of hypoxia and anoxia in the bottom waters (Hagy et al. 2004). Gradually, since the 1950's anoxic conditions have infringed on more of the bottom waters of the Bay and remained for longer extended periods of time (Hagy et al. 2004). With the increase in algal production in the spring from eutrophication, aerobic respiration has increased as well removing oxygen from the waters as a consequence (Crump et al. 2007). Communities of plants and animals have been affected by the poor water quality conditions of the Bay. The effects to these communities were viewed as indicators of the health in the system (Breitburg et al. 1997; Davis 1985; Boesch 2000) and resulted in the establishment of the Chesapeake Bay Program by the Environmental Protection Agency.

Although not as diverse, the present Chesapeake Bay is still home to aquatic communities of animals. In the food web, animal life ranges from the lower trophic levels of zooplankton to the higher trophic levels of fish such as striped bass. The plant communities house phytoplankton and submerged aquatic vegetation (SAV) which contribute the majority of the primary production and are considered the backbone of the food web. Compared to historical evidence, SAV beds of the Bay have declined to the extent of providing only a small fraction of the production needed to maintain the community (Davis 1985). Because of eutrophication, the

phytoplankton communities make up this loss of production to a certain extent but contribute to the decline in SAV (Orth and Moore 1983; Davis 1985). Once known for its abundance of seafood, the Bay of today is less productive as the result of anthropogenic influences (Harding and Perry 1997).

2.3 CE-QUAL-ICM Model Descriptions

CE-QUAL-ICM (ICM) was designed to be a flexible, widely applicable, state-of-the-art eutrophication model. Initial application was to Chesapeake Bay (Cерco and Cole 1994). Since the initial Chesapeake Bay study, the ICM model code has been generalized with minor corrections and model improvements. Subsequent additional applications of ICM included the Delaware Inland Bays (Cерco et al. 1994), Newark Bay (Cерco and Bunch 1997), the San Juan Estuary (Bunch et al. 2000), Florida Bay (Cерco et al. 2000), St. Johns River (Tillman et al. 2004) and Mississippi Sound (Bunch et al. 2003). Each model application employed a different combination of model features and required addition of system-specific capabilities.

General features of the model include:

- a. Operational in one-, two-, or three-dimensional configurations
- b. Twenty-four state variables including physical properties.
- c. Sediment-water oxygen and nutrient fluxes may be computed in a predictive sub-model or specified with observed sediment-oxygen demand rates (SOD)
- d. State variable may be individually activated or deactivated.
- e. Internal averaging of model output over arbitrary intervals.
- f. Computation and reporting of concentrations, mass transport, kinetics transformations, and mass balances.

- g. Debugging aids include ability to activate and deactivate model features, diagnostic output, volumetric and mass balances.
- h. Operates on a variety of computer platforms. Coded in ANSI Standard FORTRAN F77.

ICM is limited by not computing the hydrodynamics of the modeled system.

Hydrodynamic variables (i.e., flows, diffusion coefficients, and volumes) must be specified externally and read into the model. Hydrodynamics may be specified in binary or ASCII format and are usually obtained from a hydrodynamic model such as the CH3D_WES model (Johnson et al. 1991).

2.3.1 Conservation of Mass Equation

The foundation of CE-QUAL-ICM is the solution to the three-dimensional mass-conservation equation for a control volume. Control volumes correspond to cells on the model grid. CE-QUAL-ICM solves, for each volume and for each state variable, the equation:

$$\frac{\delta V_j C_j}{\delta t} = \sum_{k=1}^n Q_k C_k + \sum_{k=1}^n A_k D_k \frac{\delta C}{\delta x_k} + \sum S_j \quad \text{Eq. 2.1}$$

in which V_j is the volume of j^{th} control volume (m^3), C_j is the concentration in j^{th} control volume (g m^{-3}), t and x are temporal and spatial coordinates, n is the number of flow faces attached to j^{th} control volume, Q_k is the volumetric flow across flow face k of j^{th} control volume ($\text{m}^3 \text{ s}^{-1}$), C_k is the concentration in flow across face k (g m^{-3}), A_k is the area of flow face k (m^2), D_k is the diffusion coefficient at flow face k ($\text{m}^2 \text{ s}^{-1}$), and S_j is the external loads and kinetic sources and sinks in j^{th} control volume (g s^{-1}).

The solution of equation 2.1 on a personal or mainframe computer requires discretization of the continuous derivatives and specification of parameter values. The equation

is solved explicitly using upwind differencing or the QUICKEST algorithm (Leonard 1979) to represent C_k . The time step, determined by stability requirements, is automatically adjusted. For notational simplicity, the transport terms are dropped in the reporting of kinetics formulations.

2.3.2. State Variables

CEQUAL-ICM incorporates 24 state variables in the water column including physical variables, multiple algal groups, and multiple forms of carbon, nitrogen, phosphorus, and silica (Table 2.1). Two zooplankton groups, microzooplankton and mesozooplankton, are available and can be activated when desired.

Table 2.1. Water quality model state variables

Temperature	Salinity
Fixed Solids	Cyanobacteria
Diatoms	Other Phytoplankton
Dissolved Organic Carbon (DOC)	Refractory Particulate Organic Carbon
Labile Particulate Organic Carbon	Nitrate + Nitrite Nitrogen (NO ₃)
Ammonium (NH ₄)	Dissolved Organic Nitrogen (DON)
Refractory Particulate Organic Nitrogen	Labile Particulate Organic Nitrogen
Total Phosphate (TP)	Dissolved Organic Phosphorus (DOP)
Refractory Particulate Organic Phosphorus	Labile Particulate Organic Phosphorus
Chemical Oxygen Demand (COD)	Dissolved Oxygen (DO)
Dissolved Silica	Particulate Biogenic Silica
Zooplankton 1	Zooplankton 2

2.4 Ecopath Model Description

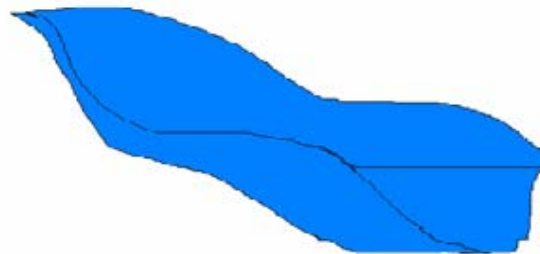
The governing equations of Ecopath originate from Polovina (1984) but are no longer assumed to be steady state. Variable estimations are based on mass balance over an arbitrary period, usually a year but can also be over growing seasons. The system is assumed to be a zero-dimensional, well-mixed system (Figure 2. 2). Two main equations are implemented in Ecopath: 1) one to describe the production term and 2) one to balance the energy input and output of the system.

The production term in Ecopath is written as:

$$P_i = Y_i + B_i - M 2_i + E_i + BA_i + P_i \quad (1 - EE_i) \quad Eq. 2.2$$

This equation can be rearranged as

$$EE_i = \frac{Y_i + E_i + BA_i + M 2_i - B_i}{P_i} \quad Eq. 2.3$$



Zero-Dimensional

Figure 2.2. Conceptual view of a zero-dimensional water body.

A set of linear equations representing the different groups in a system is set up and solved for one of the following four parameters of the groups: 1) biomass, 2) production/biomass ratio, 3) consumption/biomass ratio; or 4) ecotrophic efficiency (EE_i). The unknown parameter is usually EE_i since there is no procedure available for field estimation (Christensen et al. 2004). Energy balance of the system is then calculated once the missing parameters have been estimated and mass balance is maintained with the following equation:

$$C_i = P_i + R_i + U_i \quad \text{Eq. 2.4}$$

Terms for both equations are listed in Table 2.2.

Table 2.2. Parameters from main equations in Ecopath

Parameter	Definition	Units
B_i	Average Biomass	mgC m ⁻²
C_i	Consumption	mgC m ⁻² d ⁻¹
P_i	Production	mgC m ⁻² d ⁻¹
R_i	Respiration	mgC m ⁻² d ⁻¹
U_i	Unassimilation = Egestion plus Excretion	mgC m ⁻² d ⁻¹
E_i	Net Emigration minus Immigration or net export of	mgC m ⁻² d ⁻¹
Y_i	Fisheries removals of biomass from i th	mgC m ⁻² d ⁻¹
BA_i	Accumulation or depletion of biomass	mgC m ⁻² d ⁻¹
$M2_i$	Biomass specific mortality rate due to predation	d ⁻¹
EE_i	Ecotrophic efficiency	Unit-less

The system of linear equations representing Eq. 2.1 for n groups is written as:

$$\begin{array}{r}
 B_1 \times (P/B)_1 \times EE_1 - B_1 \times (Q/B)_1 \times DC_{11} - B_2 \times (Q/B)_2 \times DC_{22} \dots B_n \times (Q/B)_n \times DC_{nn} \\
 \dots - Y_n - E_n - BA_n = 0 \\
 B_2 \times (P/B)_2 \times EE_2 - B_1 \times (Q/B)_1 \times DC_{12} - B_2 \times (Q/B)_2 \times DC_{22} \dots B_n \times (Q/B)_n \times DC_{nn} \\
 \dots - Y_2 - E_2 - BA_2 = 0 \\
 \vdots \quad \vdots \quad \vdots \quad \vdots \quad \vdots \quad \vdots \quad \vdots \quad \vdots \quad \vdots \quad \vdots \quad \vdots \quad \vdots \\
 B_n \times (P/B)_n \times EE_n - B_1 \times (Q/B)_1 \times DC_{1n} - B_2 \times (Q/B)_2 \times DC_{2n} \dots B_n \times (Q/B)_n \times DC_{nn} \\
 \dots - Y_n - E_n - BA_n = 0 \quad Eq. 2.5
 \end{array}$$

They can be rewritten as:

$$a_{11} \times X_1 + a_{12} \times X_{12} + a_{1m} \times X_m = Q_1$$

$$a_{21} \times X_1 + a_{22} \times X_2 + a_{2m} \times X_m = Q_2$$

$$\vdots \quad \vdots \quad \vdots \quad \vdots \quad \vdots$$

$$a_{n1} \times X_1 + a_{n2} \times X_2 + a_{nm} \times X_m = Q_n$$

Eq. 2.6

or in Matrix notation

$$[A]_{nm} \times [X]_m = [Q]_m$$

CHAPTER III
COMMON CONCEPTUAL PROCESSES BETWEEN
CE-QUAL-ICM AND ECOPATH

3.1 Background

Studying food webs and energy flow to different compartments in an ecosystem through network analysis gives insight into the dynamics of that system (Heymans and McLachlan 1996). For instance in the Baltic Sea, Worm et al. (2000) found that increased nitrogen (N) and phosphorus (P) loads created shifts in algal species composition. This was offset by grazers selectively consuming dominant annual algal species that overshadowed the perennial species as a result of nutrient abundance. Many scientists believe it is better to study the system as a whole than to separate into components because once reassembled, the reconstructed system may not behave the same as the whole (Patricio and Marques 2006). With this in mind, fishery management has taken a new direction to be more effective by taking a more holistic approach and looking at the ecosystem first rather than just at the target fish species. This has been termed as ecosystem-based fishery management, EBFM (Pikitch et al. 2004).

To continue this thought, in 1998 the Chesapeake Bay Program's Scientific and Technical Advisory Committee (STAC) also considered a more ecosystem encompassing view of management and recommended a multispecies approach to assist regional managers in developing the best options to meet future fishery goals. One of the tools developed after this initiative was the fisheries network model for the Chesapeake Bay using Ecopath with Ecosim (Christensen et al. 2000). Through network analysis, the Ecopath model looks at the Bay on many trophic levels to describe interactions of the whole system. Since the Chesapeake Bay Program already has a well established watershed, water quality and hydrodynamic modeling

package in use (Cercio and Noel 2004), the idea of coupling the Chesapeake Bay water quality model and the Ecopath model was formed. By coupling the models manually or through automation, predictions from scenarios testing management options could be used for guidance in deciding future actions for fishery management in the Bay.

This chapter presents the steps taken to couple the ICM and Ecopath models. Formulations and data requirements of both models will be presented as they were examined to find similar variables and processes that may be substituted from output of one model to drive the predictions of the other. The ICM can provide information for the lower trophic levels of Ecopath such as biomass and production rates (among other parameters) of certain groups as affected by strategies initiated through resource management (i.e., as nutrient reduction or changes in DO concentrations). This is the premise behind the development of an Ecopath and ICM coupled model package.

In the final sections of this chapter, comparison of common link variables found between the original ICM and Ecopath runs (identified as “base” simulations of both models) will be compared. Then using these variables, two Ecopath runs were conducted: 1) an Ecopath model developed using values of common links from Hagy’s Ecopath base run and 2) an Ecopath model developed using common links from Cercio and Noel’s ICM base run. Results from two Ecopath model runs will be compared for the upper Chesapeake Bay region. The focus of this discussion will center on the similarities and differences of the ecosystem interactions produced by the models as interpreted by the network analysis. Any substantial quantitative differences (i.e., order-of-magnitude) between common variables will also be noted.

3.2 Finding the “Links”

Coupling ICM and Ecopath began by finding common “hooks” or “links” between the two models. Knowing that both models are or can be carbon based, the carbon cycle in ICM was

the starting point to look for common links. Although Ecopath (as well as ICM) could have been investigated for other trophic exchanges, the developer of the Ecopath Chesapeake Bay model (Hagy 2002) chose carbon as the currency because more information was available for the Chesapeake Bay describing carbon interactions than for other elements. Most researchers from literature use carbon as the currency as well (Meyer and Poepperl 2004; Neira and Arancibia 2004; Ortiz and Wolff 2002). For this reason, keeping carbon as the currency for the Ecopath/ICM coupling was unchanged.

Figure 3.1 presents the different pathways of carbon interactions in ICM where common links were investigated for variables or formulations similar to what is found in Ecopath. Blue boxes represent constituents in the water column, and yellow boxes represent constituents living in or on the sediments. It is within these pathways that common links with Ecopath variables were assessed. Some examples of common links that were readily identified are: 1) phytoplankton and benthic algal biomass and production, 2) zooplankton biomass and production, 3) benthos biomass and production, 4) grazing rates on primary producers, and 5) predation rates on invertebrates. A brief discussion of each group associated with the carbon cycle and its formulation as described by CE-QUAL-ICM in the water column and sediments is presented in the next section and came from Cerco and Cole (1994) and Cerco and Noel (2004). From these formulations, common links between Ecopath and ICM were found (Tillman et al. 2006; Cerco and Tillman 2008). Common links found between the models will be presented in tabular format which contain the model formulations and computer code names with the associated Ecopath variable. These computer names are recognizable in the equations presented for each group below.

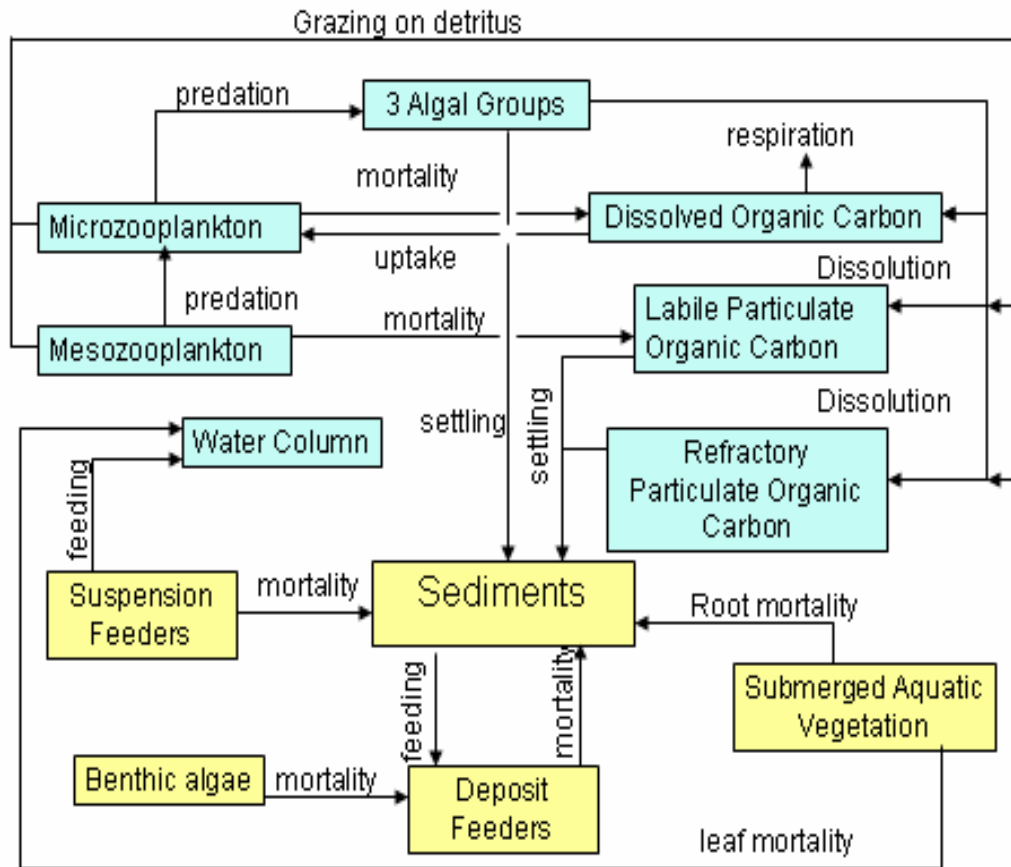


Figure 3.1. Conceptual illustration showing pathways of the carbon cycle in the water column and sediments in CE-QUAL-ICM.

3.2.1. Algae

Sources and sinks of algae in the conservation equation include production, metabolism, predation, and settling. The equation including these terms is written:

$$\frac{\delta}{\delta t} B = \left(G - BM - Wa \times \frac{\delta}{\delta z} \right) B - PR \quad \text{Eq. 3.1}$$

in which B is the algal biomass expressed as carbon (g C m^{-3}), G is the growth (d^{-1}), BM is the basal metabolism (d^{-1}), Wa is the algal settling velocity (m d^{-1}), PR is the predation ($\text{g C m}^{-3} \text{d}^{-1}$), and z is the vertical coordinate.

The growth and metabolism functions are described in Cerco and Noel (2004). The predation term is made up of four groups or populations: microzooplankton, mesozooplankton, filter-feeding benthos, and other planktivores.

Zooplankton grazing terms are discussed below. Predation by benthos only affects the cells interacting with the bottom and is represented as a loss term. It is assumed that other planktivore predators clear a specific volume of water per unit biomass:

$$PR = F \times B \times M \quad \text{Eq. 3.2}$$

in which F is the filtration rate ($\text{m}^3 \text{g}^{-1} \text{predator C d}^{-1}$) and M is the planktivore biomass (g C m^{-3}).

It is difficult to find or collect detailed spatially and temporally varying distributions of the predator population. So for this reason, Cerco and Noel (2004) assumed that predator biomass is proportional to algal biomass, $M = \gamma B$, in which case Equation 3.2 was rewritten:

$$PR = \gamma \times F \times B^2. \quad \text{Eq. 3.3}$$

Since γ and F are not known, a term (Phl) representing their product is combined and adjusted during the model calibration procedure.

3.2.2. Zooplankton

The same production equation is used for both zooplankton groups:

$$\frac{\delta}{\delta t} Z = (Gz - BMz - Mz) \times Z - PRz \quad \text{Eq. 3.4}$$

in which Z is the zooplankton biomass (g C m^{-3}), Gz is the growth rate of zooplankton group Z (d^{-1}), BMz basal metabolic rate of zooplankton group z (d^{-1}), and Mz is mortality (d^{-1}), and PRz is the predation on zooplankton group z ($\text{g C m}^{-3} \text{d}^{-1}$).

What makes the equation unique for each group is that it has parameter values and prey compositions specific to a particular group. In Cerco and Noel (2004) details describing individual terms in the production equation are found. In relation to variables common to Ecopath, prey composition and selection are discussed below.

3.2.2.1. Prey Composition and Selection

Zooplankton grazing is found using Monod type formulation similar to what is used in representing algal nutrient uptake and is:

$$G_z = \frac{PA_z}{KHC_z + PA_z} \times RMAX_z \quad Eq. 3.5$$

where G_z is the carbon grazed by zooplankton group z ($g \text{ prey C g}^{-1} \text{ zooplankton C d}^{-1}$), PA_z is the prey available to zooplankton group z ($g \text{ C m}^{-3}$), KHC_z prey density at which grazing is halved ($g \text{ C m}^{-3}$), and $RMAX_z$ is the maximum ration of zooplankton group z ($g \text{ prey C g}^{-1} \text{ zooplankton C d}^{-1}$).

Estimation of prey for zooplankton uses the equation:

$$BA_{xz} = \text{Max}(B_x - CT_z, 0) \quad Eq. 3.6$$

in which BA_{xz} is the portion of algal group x available to zooplankton group z ($g \text{ C m}^{-3}$), and CT_z threshold concentration below which prey will not be utilized by zooplankton group z ($g \text{ C m}^{-3}$).

Food sources for the microzooplankton are dissolved organic carbon (DOC) and three phytoplankton groups (i.e., diatoms, cyanobacteria, and green algae). In reality, microzooplankton also utilizes heterotrophic bacteria as a major food source, but bacteria are not a state variable in ICM. For this reason, DOC replaces bacteria as a food source. Since DOC is one of the primary food sources for the bacteria, it becomes a good replacement for a food source of microzooplankton. Mesozooplankton have similar sources of food as

microzooplankton. They graze on three algal groups, microzooplankton, and organic detritus. The total prey available to each group is determined by “utilization” parameters, which are weighting terms and range between zero and unity. For example, the prey available to microzooplankton is estimated as:

$$\begin{aligned}
 PAsz &= UDsZ \times DOCAsz \\
 &+ \sum UBxsz \times BAxsz + ULsZ \times LPOCAsz + URsZ \times RPOCAsz
 \end{aligned}
 \tag{Eq. 3.7}$$

in which $PAsz$ is the prey available to microzooplankton (g C m^{-3}), $UDsZ$ is utilization of dissolved organic carbon by microzooplankton, $UBxsz$ is utilization of algal group x by microzooplankton, $ULsZ$ is utilization of labile particulate organic carbon by microzooplankton, $URsZ$ is utilization of refractory particulate organic carbon by microzooplankton, $DOCAsz$ is the dissolved organic carbon available to microzooplankton (g C m^{-3}), $BAxsz$ is the algal group x available to microzooplankton (g C m^{-3}), $LPOCAsz$ is the labile particulate organic carbon available to microzooplankton (g C m^{-3}), and $RPOCAsz$ refractory particulate organic carbon available to microzooplankton (g C m^{-3}).

The fraction of the total ration removed from each prey group is estimated based on the fraction of each utilizable prey group relative to the total utilizable prey.

3.2.2.2. Predation on Zooplankton

Since micro- and mesozooplankton are the highest trophic levels represented in the water column, a quadratic term similar to Equation 3.4 is used to represent predation on both zooplankton groups by organisms not included in the model.

3.2.3. Organic Carbon

Organic carbon dissolution and respiration are treated as first-order processes in which the reaction rate is proportional to the concentration of the reactant. Dissolution and respiration

are related to temperature using an exponential. The equation used to model dissolved organic carbon sources and sinks is:

$$\begin{aligned} \frac{\delta}{\delta t} DOC = & FCDa \times BMa \times B + FCDPa \times PRa \\ & + FCDz \times (BMz + Mz) \times Z + FCDPz \times Z \\ & + Kl_{poc} \times LPOC + Kr_{poc} \times RPOC - Kdoc \times DOC + S \end{aligned} \quad Eq. 3.8$$

in which DOC is dissolved organic carbon (g m^{-3}), $LPOC$ is labile particulate organic carbon (g m^{-3}), $RPOC$ is refractory particulate organic carbon (g m^{-3}), $FCDa$ is the fraction of algal respiration released as DOC ($0 < FCDa < 1$), $FCDPa$ is the fraction of predation on algae released as DOC ($0 < FCDPa < 1$), $FCDz$ is the fraction of zooplankton respiration released as DOC ($0 < FCDz < 1$), $FCDPz$ is the fraction of predation on zooplankton released as DOC ($0 < FCDPz < 1$), Kl_{poc} is the dissolution rate of $LPOC$ (d^{-1}), Kr_{poc} is the dissolution rate of $RPOC$ (d^{-1}), $Kdoc$ is the respiration rate of DOC (d^{-1}), S loading from external sources ($\text{g m}^{-3}\text{d}^{-1}$).

Labile particulate organic carbon sources and sinks in ICM are modeled as:

$$\begin{aligned} \frac{\delta}{\delta t} LPOC = & FCLa \times BMa \times B + FCLPa \times PRa + FCLz \times (BMz + Mz) \times Z \\ & + FCLPz \times PRz - Kl_{poc} \times LPOC - Wl \times \frac{\delta}{\delta z} LPOC + S \end{aligned} \quad Eq. 3.9$$

in which $FCLa$ is the fraction of algal respiration released as $LPOC$ ($0 < FCLa < 1$), $FCLPa$ is the fraction of predation on algae released as $LPOC$ ($0 < FCLPa < 1$), $FCLz$ fraction of zooplankton respiration released as $LPOC$ ($0 < FCLz < 1$), $FCLPz$ is the fraction of predation on zooplankton released as $LPOC$ ($0 < FCLPz < 1$), and Wl is the settling velocity of labile particles (m d^{-1}).

A similar equation describes refractory particulate organic carbon.

3.2.4. The Sediment Diagenesis Model

In the sediment flux model developed by Di Toro and Fitzpatrick (1993) the benthic sediments were represented by two layers having a total depth of 10 centimeters. The upper layer is in contact with the water column and can be aerobic or anaerobic depending on the dissolved oxygen concentration in the overlying water. The lower sediment layer is always considered anaerobic. The depth of the upper layer depends on the diffusion of dissolved oxygen into the sediments. Even at its maximum thickness, the upper layer is only a small fraction of the total benthic layer (Cercio and Cole 1994).

As described by Cercio and Cole (1994), the sediment model actually consists of three basic processes. Figure 3.2 illustrates the processes of the sediment flux model. Deposition of particulate organic matter from the water column to the sediments is the first process considered. Since the upper layer is very thin, deposition of organic matters goes directly to the anaerobic layer where the second process of diagenesis (decay) occurs. Flux of the substances produced by diagenesis is the third process which is the most complicated. Flux has to be considered for reactions in both sediment layers, partitioning between fractions of particulate and dissolved materials, sedimentation from upper to lower layers and from the lower layer to the inactive sediments, particle mixing between sediment layers, diffusion between sediment layers, and mass transfer between the upper layer and water column.

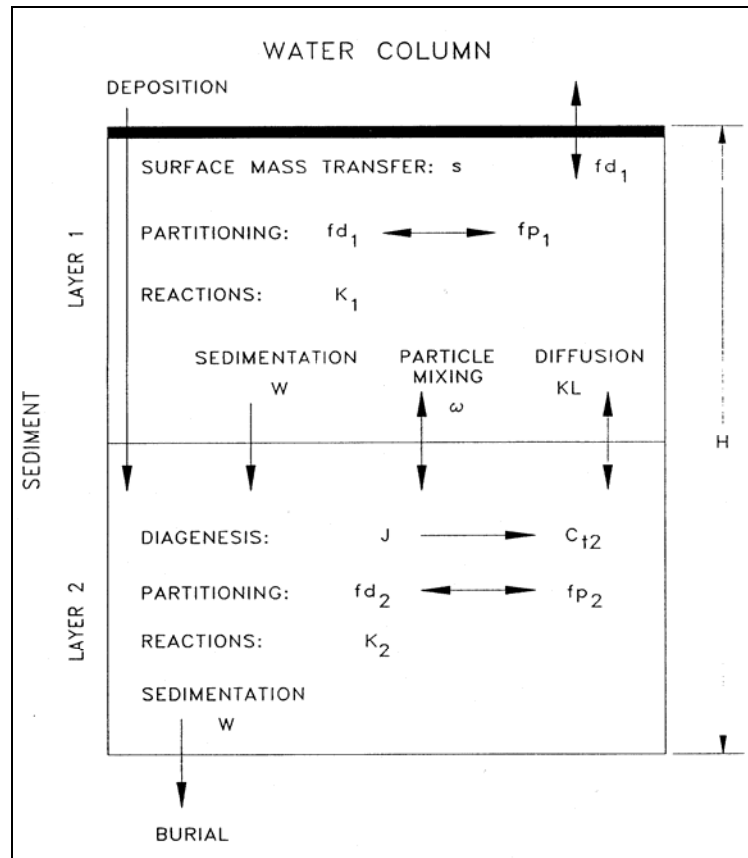


Figure 3.2. Schematic of the sediment diagenesis model (Cercio and Tillman, 2008).

From principles established by Westrich and Berner (1984), organic matter in the sediments was divided into three G classes. The differential decay rates of organic matter fractions determined which G class the matter was placed. The G1, labile, fraction has a half-life of 20 days. The G2, refractory, fraction has a half-life of one year. The G3, inert, fraction undergoes no significant decay before burial into deep, inactive sediments. Each G class has its own mass-conservation equation:

$$H \times \frac{\delta Gi}{\delta t} = W_{net} \times f_i \times C + S \times f_i - W \times Gi - H \times K_i \times Gi \times \theta_i^{(T-20)} \quad Eq. 3.10$$

in which H is the total thickness of sediment layer (m), Gi is the concentration organic matter in G class i (g m^{-3}), W_{net} is the net settling to sediments (m d^{-1}), C is the organic matter concentration in water column (g m^{-3}), f_i is the fraction of deposited organic matter assigned to G class i , S is the local source from *SAV*, benthic algae, and benthos ($\text{g m}^{-2} \text{d}^{-1}$), W is the burial rate (m d^{-1}), K_i is the decay rate of G class i (d^{-1}), and θ constant that expresses effect of temperature on decay of G class i .

The sediment model simulates diagenesis of carbon, nitrogen, phosphorus, and silica. Only carbon diagenesis is relevant to the linkage with Ecopath. Details of remaining substances and processes are found in DiToro and Fitzpatrick (1993).

3.2.5. The Benthic Algae Model

Benthic algae live in a thin layer between the water column and benthic sediments (Figure 3.3). Biomass within the layer is calculated by balancing the term of production, respiration, and losses to predation:

$$\frac{\delta BA}{\delta t} = (G - BM) \times BA - PR \quad Eq. 3.11$$

in which BA is algal biomass, as carbon (g C m^{-2}), G is the growth (d^{-1}), BM is the basal metabolism (d^{-1}), and PR is the predation ($\text{g C m}^{-2} \text{d}^{-1}$).

To find production, respiration, and predation the equations follow the formulations for phytoplankton (Cercio and Noel 2004). The ICM sediment module receives any carbonaceous byproducts from algal metabolism and predation.

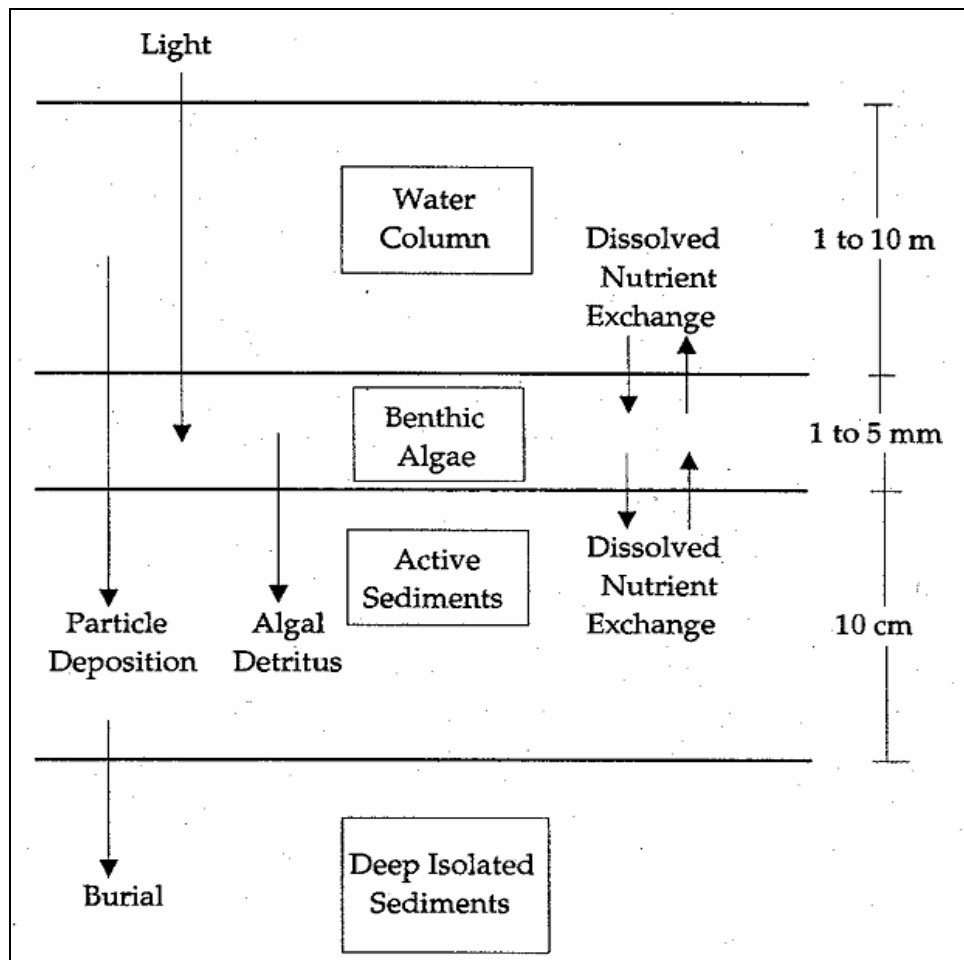


Figure 3.3. Schematic of benthic algae model (Cercu and Tillman, 2008).

3.2.6. Submerged Aquatic Vegetation

The SAV model is made up of three components: 1) a unit-level model of a plant, 2) an environmental model that provides light, temperature, nutrient concentrations, and other forcing functions and 3) a coupling algorithm that links the system-wide environmental model to the local-scale plant model. The SAV unit model (Figure 3.4) includes three state variables: shoots (above-ground biomass), roots (below-ground biomass), and epiphytes (attached growth).

Epiphytes and shoots transfer material with the water-column component of the eutrophication model, while roots exchange material with the diagenetic sediment flux model. Light available to the shoots and epiphytes is computed with a series of sequential attenuations by color, fixed and organic solids in the water column, and self-shading of shoots and epiphytes. Details of the model may be found in Cerco and Noel (2004).

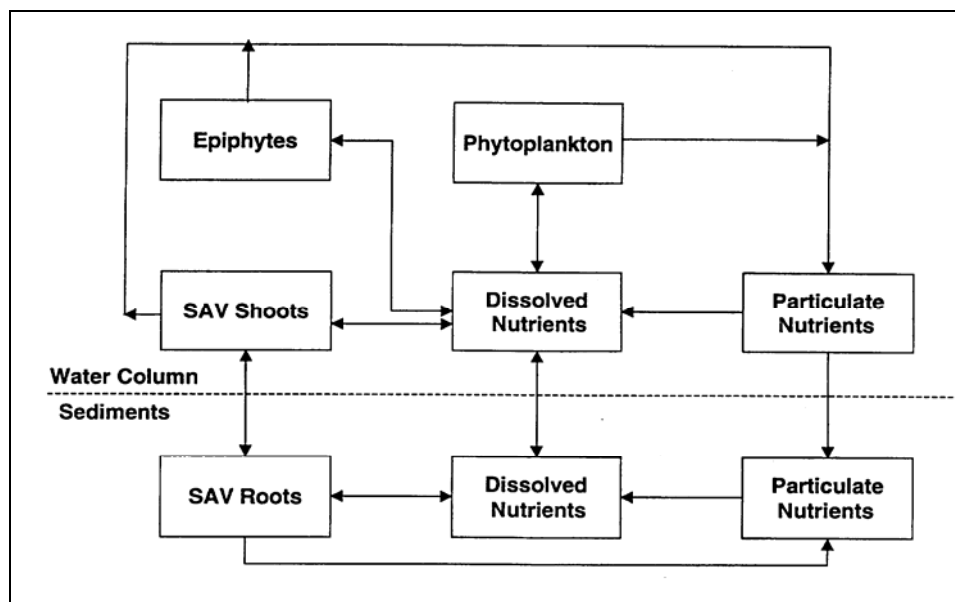


Figure 3.4. SAV model state variables (boxes) and mass flows (arrows)[Cerco and Tillman 2008].

3.2.6.1. Shoots

The governing equation for shoots solves for a balance between sources and sinks of the biomass above ground and is:

$$\frac{dSH}{dt} = [P \times (1 - Fpsr) - Rsh - SL] \times SH + Trs \times RT \quad Eq. 3.12$$

in which SH is the shoot biomass (g C m^{-2}), P is the production (d^{-1}), $Fpsr$ is the fraction of production routed from shoot to root, Rsh is shoot respiration (d^{-1}), SL is the sloughing (d^{-1}), Trs

is the rate at which carbon is transported from root to shoot (d^{-1}), and RT is the root biomass ($g\ C\ m^{-2}$).

Carbonaceous material lost through shedding is routed to water column state variables using empirical distribution coefficients similar to those employed to distribute planktonic material.

3.2.6.2. Roots

The governing equation for roots establishes a balance between sources and sinks of below-ground biomass:

$$\frac{dRT}{dt} = Fpsr \times P \times Sh - Rrt \times RT - Trs \times RT \quad Eq. 3.13$$

in which Rrt is the root respiration (d^{-1}).

Empirical distribution coefficients are used to route any carbonaceous material lost through root respiration to the sediments. Epiphytes have a negligible role in the carbon cycle and are not considered further.

3.2.6.3. From the Unit to the System

In the CE-QUAL-ICM formulation of SAV, SAV beds form a ribbon of littoral cells along the land-water margin of the system. Because the goal of SAV restoration has been set to the two-meter contour line, width of littoral cells in the model is represented as the distance to the two-meter contour (Cercio and Tillman 2008). To allow SAV to grow within a cell, a variable called patchiness was adjusted. It represents the fraction of bottom area covered by plants. This variable is found in the equation for estimating abundance within a cell and is:

$$M = SH \times A \times TE \times C \times P \quad Eq. 3.14$$

of which M is the above ground abundance (g C), A is the cell surface area (m^2), TE is the truncation error, C is the coverage, and P is the patchiness.

3.2.7 Benthos

Benthos serves as an important food source for crabs, finfish, and other economically and ecologically significant biota. Additionally, they have a great influence on water quality through filtration of overlying waters. Benthos is modeled as two groups: deposit feeders and filter feeders (3.6). The deposit-feeders live within bottom sediments and feed on deposited material while the filter-feeders live at the sediment surface and feed by filtering overlying water.

The benthos model (Figure 3.5) was developed by HydroQual (2000). The formulations below describe model state variables and fundamental processes within the modeled carbon cycle.

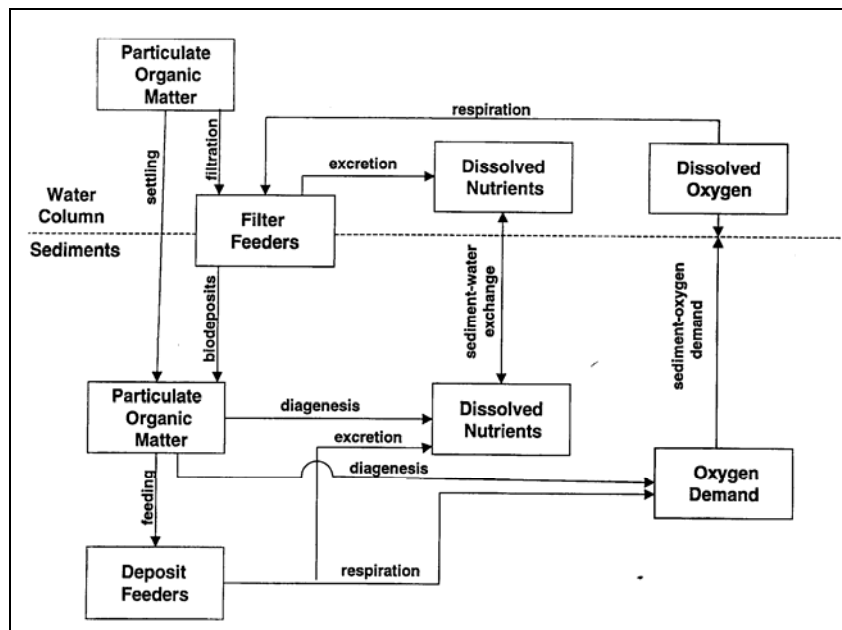


Figure 3.5. Schematic of benthos model (Cercio and Tillman, 2008).

3.2.7.1. Deposit Feeders

The mass-balance equation for deposit feeders is:

$$\frac{dDF}{dt} = \alpha \times \frac{I}{m} \times \frac{POC \times Khdf}{POC + Khdf} \times DF - r \times DF - \beta \times DF^2 - hmr \times DF \quad Eq. 3.15$$

in which DF is the deposit feeder biomass (mg C m^{-2}), α is the assimilation efficiency ($0 < \alpha < 1$), m is the sediment solids concentration (mg m^{-3}), I is the ingestion rate ($\text{mg sediment mg}^{-1}$ deposit feeder C d^{-1}), POC is the sediment particulate organic carbon (mg m^{-3}), $Khdf$ is the half-saturation concentration for carbon uptake (mg m^{-3}), r is the specific respiration rate (d^{-1}), β is the predation rate ($\text{m}^2 \text{mg}^{-1}$ deposit feeder C d^{-1}), hmr is the mortality rate due to hypoxia (d^{-1}), and t is the time (d).

The assimilation efficiency and half-saturation concentration are specified depending on whether it is G1 (labile) or G2 (refractory) carbon. G3 (inert) carbon is not utilized. An inverse “Michaelis-Menton” function determines ingestion. At low carbon concentrations ($POC \ll Khdf$), ingestion is proportional to available carbon ($\approx I \times POC$). At high concentrations ($POC \gg Khdf$), ingestion approaches a constant value ($\approx I \times Khdf$). All material eaten comes from bottom sediments, and from the processes of mortality and predation, byproducts of carbon are returned to the sediments.

3.2.7.2. Filter Feeders

The model allows for multiple filter-feeding groups. Each is governed by the same mass-balance equation:

$$\frac{dFF}{dt} = \alpha \times Fr \times POC \times FF - r \times FF - \beta \times FF^2 - hmr \times FF \quad Eq. 3.16$$

in which FF is the filter feeder biomass (mg C m^{-2}), α is the assimilation efficiency ($0 < \alpha < 1$), Fr is the filtration rate ($\text{m}^3 \text{mg}^{-1}$ filter feeder C d^{-1}), POC is the particulate organic carbon in

overlying water (mg m^{-3}), r is the specific respiration rate (d^{-1}), β is the predation rate ($\text{m}^2 \text{mg}^{-1}$ filter feeder C d^{-1}), hmr is the mortality rate due to hypoxia (d^{-1}), and t is the time (d).

The assimilation efficiency is specified individually for each form of particulate organic matter in the water column, including phytoplankton. Like deposit feeders, byproducts of carbon coming from mortality and respiration are routed to the model sediment component.

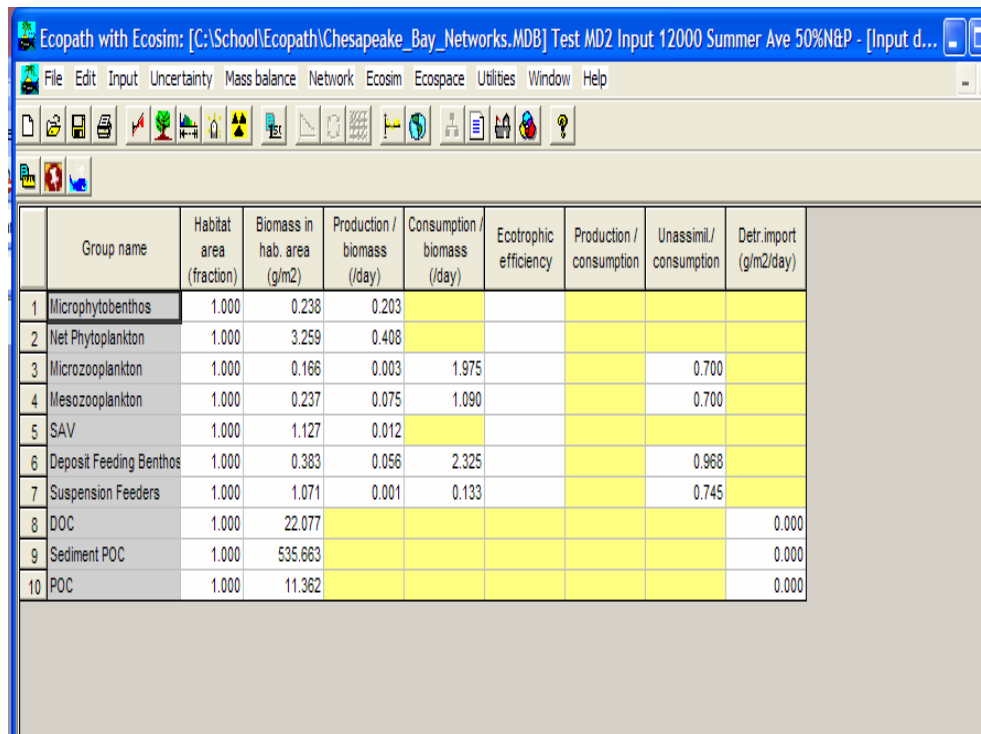
3.3. Parallels between Ecopath and ICM

Beginning with Ecopath data requirements, there are three input data screens of parameters required for an Ecopath application. These screens are identified as: “Basic Input”, “Diet Composition”, and “Detritus Fate”. They are displayed as sheets of column data similar to an Excel worksheet. Examples of input screens are shown in Figures 3.6 through 3.8, respectively. The “Basic Input” screen is the first screen data are required (Figure 3.6). “Group Name” is the first entry required before any other because the groups modeled determine the remaining data needed for a simulation. The groups in Ecopath can be living or non-living. Living groups are primary producers or consumers, and the non-living group is detritus.

To determine what groups can be used from an ICM simulation, we go back to Figure 3.1. From Figure 3.1, all the groups contributing to the carbon cycle were chosen to represent a group for an Ecopath run. Tables 3.1 and 3.2 list the ICM constituents/groups and their formulas (respectively) to be used as a group in Ecopath. All the ICM groups listed in Table 3.1 are considered generic. To clarify this, the groups coming out of ICM can stand alone or be substituted into another Ecopath model developed previously. If they are used as stand alone to create an Ecopath model, they can be used as they come out of ICM. If the information is coupled with an existing Ecopath model, you may have to establish the correspondence between the ICM groups and groups being modeled in the Ecopath model. In the next chapter this will be demonstrated using the Ecopath model developed for the Chesapeake Bay and ICM output. The

only circumstance requiring the addition of a new group to the list would be the addition of a new state variable to the carbon cycle in ICM.

In Table 3.1, a listing of the actual computer code name for the common groups are listed and can be found in the equations discussed previously. The remaining parameters on the “Basic Input” screen include production-to-biomass ratio (primary producers and consumers), consumption-to-biomass ratio (consumers only), and unassimilated consumption (consumers only). Equivalent variables from ICM representing these Ecopath variables were not always a single variable (i.e., phytoplankton or zooplankton production) but a formula computing that variable.



The screenshot shows the 'Basic Input' screen of the Ecopath software. The window title is 'Ecopath with Ecosim: [C:\School\Ecopath\Chesapeake_Bay_Networks.MDB] Test MD2 Input 12000 Summer Ave 50%N&P - [Input d...'. The menu bar includes File, Edit, Input, Uncertainty, Mass balance, Network, Ecosim, Ecospace, Utilities, Window, and Help. The toolbar contains various icons for file operations and modeling. The main area displays a table with the following data:

	Group name	Habitat area (fraction)	Biomass in hab. area (g/m2)	Production / biomass (/day)	Consumption / biomass (/day)	Ecotrophic efficiency	Production / consumption	Unassimil./ consumption	Detrit import (g/m2/day)
1	Microphytobenthos	1.000	0.238	0.203					
2	Net Phytoplankton	1.000	3.259	0.408					
3	Microzooplankton	1.000	0.166	0.003	1.975			0.700	
4	Mesozooplankton	1.000	0.237	0.075	1.090			0.700	
5	SAV	1.000	1.127	0.012					
6	Deposit Feeding Benthos	1.000	0.383	0.056	2.325			0.968	
7	Suspension Feeders	1.000	1.071	0.001	0.133			0.745	
8	DOC	1.000	22.077						0.000
9	Sediment POC	1.000	535.663						0.000
10	POC	1.000	11.362						0.000

Figure 3.6. “Basic Input” screen for Ecopath.

	Prey \ Predator	3	4	6	7
1	Microphytobenthos				
2	Net Phytoplankton	0.474	0.791		0.376
3	Microzooplankton		0.001		
4	Mesozooplankton				
5	SAV				
6	Deposit Feeding Bent				
7	Suspension Feeders				
8	DOC	0.385			
9	Sediment POC			1.000	
10	POC	0.141	0.208		0.624
11	Import				
12	Sum	1.000	1.000	1.000	1.000

Figure 3.7. “Diet Composition” screen from Ecopath.

The “Diet Composition” screen (Figure 3.7) contains the Diet Composition (DC) of each consumer which is the fraction of a consumer’s diet that comes from each prey of that consumer. Table 3.3 lists the prey of each consumer group (predator) and the equivalent ICM formula used to calculate the fraction of diet coming from that prey. Calculating the DC fraction that goes into the “Diet Composition” screen table used the following equation:

$$DC_{\text{fraction } i} = \frac{\text{prey}_i \text{ biomass utilized}}{\sum_1^n \text{all prey}_i \text{ biomass of predator utilized}} \quad \text{Eq. 3.17}$$

in which $DC_{\text{fraction } i}$ is the Diet Composition fraction coming from a prey (i) up to n prey, and prey_i biomass utilized is the amount of prey (i) biomass available. For a particular predator/consumer the $DC_{\text{fraction } i}$ for all prey must sum to one.

The third Ecopath screen requiring ICM equivalent values was the “Detritus Fate” screen (Figure 3.8). For production that is not consumed or respired, it is directed into the detritus pool. In particular, detritus in Ecopath can be exported out of the system or go to at least one detrital compartment. For this study detritus was transported to three compartments: DOC, POC, and sediment POC. Table 3.4 contains the derived ICM variables of detrital fate with formulas for each (from Cerco and Tillman 2008). The fraction going to each compartment was estimated with the same form of *Eq. 3.1*.

	Source \ Fate	DOC	Sediment POC	POC	Export	Sum (must = 1)
1	Microphytobenthos	0.000	1.000	0.000	0.000	1.000
2	Net Phytoplankton	0.175	0.052	0.773	0.000	1.000
3	Microzooplankton	0.250	0.000	0.750	0.000	1.000
4	Mesozooplankton	0.250	0.000	0.750	0.000	1.000
5	SAV	0.504	0.121	0.375	0.000	1.000
6	Deposit Feeding Be	0.000	1.000	0.000	0.000	1.000
7	Suspension Feeder	0.000	1.000	0.000	0.000	1.000
8	DOC	0.000	0.000	0.000	1.000	1.000
9	Sediment POC	0.000	0.000	0.000	1.000	1.000
10	POC	0.140	0.860	0.000	0.000	1.000

Figure 3.8. “Detritus Fate” screen from Ecopath.

**Table 3.1. Groups modeled in ICM and Ecopath application to Chesapeake Bay
(from Cerco and Tillman 2008)**

ICM Variable	Ecopath Variable	ICM Formula
Phytoplankton (spring diatoms, green algae)	Picoplankton, Net Phytoplankton	$B2 + B3$
Submerged Aquatic Vegetation	Submerged Aquatic Vegetation	$PATCH \times SH$
Benthic Algae	Microphytobenthos	BBM
Microzooplankton	Heteroflagellates, Ciliates, Rotifers, Meroplankton	SZ
Mesozooplankton	Mesozooplankton	LZ
Deposit Feeders	Deposit-Feeding Benthos	DF
Filter Feeders	Filter-Feeding Benthos	$SF(1) + SF(2) + SF(3)$
Particulate Organic Carbon	Particulate Organic Carbon	$LPOC + RPOC$
Dissolved Organic Carbon	Dissolved Organic Carbon	DOC
Sediment Organic Carbon	Sediment Carbon	$G1 + G2 + G3$

Table 3.2. Basic Input parameters for Ecopath derived from ICM formulations (Cercu and Tillman 2008)

Production-to-biomass ratio derived from ICM variables.		
Group	Formula	Units
Phytoplankton	$Pa_{lg} \times (1 - PRSPa_{lg}) - BMa_{lg}$	d^{-1}
SAV	$Psav - BMsav - SL$	d^{-1}
Benthic Algae	$Pba - BMba$	d^{-1}
Microzooplankton	$Esz \times (1 - RFSz) \times Rsz - BMSz$	d^{-1}
Mesozooplankton	$Elz \times (1 - RFlz) \times Rlz - BMLz$	d^{-1}
Deposit Feeders	$Gdf - Rdf$	d^{-1}
Filter Feeders	$(TCONff - UCONff - RESPff) / SF$	d^{-1}
Consumption-to-biomass ratio derived from ICM variables		
Group	Formula	Units
Microzooplankton	Rsz	d^{-1}
Mesozooplankton	Rlz	d^{-1}
Deposit Feeders	$xki0 \times (POC1 + POC2 + POC3) / M2$	d^{-1}
Filter Feeders	$FILTCT \times (B2 + B3 + LPOC + RPOC)$	d^{-1}
Unassimilated consumption derived from ICM variables		
Group	Formula	Units
Microzooplankton	$1 - Esz$	< 1
Mesozooplankton	$1 - Elz$	< 1
Deposit Feeders	$\frac{(1 - \alpha1 \times xpoc1 \text{ lim}) \times POC1 + (1 - \alpha2 \times xpoc2 \text{ lim}) \times POC2 + POC3}{POC1 + POC2 + POC3}$	< 1
Filter Feeders	$\frac{CFECES + RCFECES + CPSFEC + RCPSFEC}{SF \times FILTCT \times (B2 + B3 + LPOC + RPOC)}$	< 1

Table 3.3. Prey utilization formulas derived from ICM (Cercio and Tillman 2008)

Predator	Prey	Fraction	Units
Microzooplankton	Dissolved Organic Carbon	$\frac{UDOCsz \times DOC}{PRAsz}$	< 1
	Phytoplankton	$\frac{UB2sz \times B2 + UB3sz \times B3}{PRAsz}$	< 1
	Particulate Organic Carbon	$\frac{ULsz \times LPOC + URsz \times RPOC}{PRAsz}$	< 1
Mesozooplankton	Microzooplankton	$\frac{USZlz \times SZ}{PRAlz}$	< 1
	Phytoplankton	$\frac{UB2lz \times B2 + UB3lz \times B3}{PRAlz}$	< 1
	Particulate Organic Carbon	$\frac{ULlz \times LPOC + URlz \times RPOC}{PRAlz}$	< 1
Deposit Feeders	Bed Sediments	100%	
Filter Feeders	Phytoplankton	$\frac{B2 + B3}{B2 + B3 + LPOC + RPOC}$	< 1
	Particulate Organic Carbon	$\frac{LPOC + RPOC}{B2 + B3 + LPOC + RPOC}$	< 1

Table 3.4 Derived detrital fate for ICM variables

Source	Fate	Formula	Units
Phytoplankton	Detritus Production, CP	$(P_2 + PRSP \times BMR_2) \times B_2 + (P_3 + PRSP \times BMR_3) \times B_3$	$\text{g C m}^{-3} \text{d}^{-1}$
	DOC Production, DOCalg	$FCD \times CP + FCDP \times (PR_2 + PR_3)$	$\text{g C m}^{-3} \text{d}^{-1}$
	POC Production, POCalg	$(1 - FCD) \times CP + (1 - FCDP) \times (PR_2 + PR_3)$	$\text{g C m}^{-3} \text{d}^{-1}$
	Sedimentation, SEDalg	$WS_2 NET \times B_2 + WS_3 NET \times B_3$	$\text{g C m}^{-2} \text{d}^{-1}$
	Fraction to DOC	$\frac{H \times DOCalg}{H \times DOCalg + H \times POCalg + SEDalg}$	< 1
	Fraction to POC	$\frac{H \times POCalg}{H \times DOCalg + H \times POCalg + SEDalg}$	< 1
	Fraction to Sediments	$\frac{SEDalg}{H \times DOCalg + H \times POCalg + SEDalg}$	< 1
SAV	Fraction to DOC	$\frac{(BMSH \cdot FCDSH + SL \cdot FCDSL) \cdot SH}{(BMSH \cdot FCDSH + SL) \cdot SH + BMRT \cdot RT}$	< 1
	Fraction to POC	$\frac{(1 - FCDSL) \times SL \times SH}{(BMSH \times FCDSH + SL) \times SH + BMRT \times RT}$	< 1
	Fraction to Sediments	$\frac{BMRT \cdot RT}{(BMSH \cdot FCDSH + SL) \cdot SH + BMRT \cdot RT}$	< 1
Benthic Algae	Fraction to Sediments	100%	
Microzooplankton	Fraction to DOC	$FDOCsz$	< 1
	Fraction to POC	$1 - FDOCsz$	< 1
Mesozooplankton	Fraction to DOC	$FDOClz$	< 1
	Fraction to POC	$1 - FDOClz$	< 1
Deposit Feeders	Fraction to Sediments	100%	
Filter Feeders	Fraction to Sediments	100%	
Dissolved Organic Carbon	Export	100% (This is an Ecopath default value, ICM creates no DOC detritus)	
Particulate Organic Carbon	Amount to Sediments, POC2SED	$WSLNET \times LPOC + WSRNET \times RPOC$	$\text{g C m}^{-2} \text{d}^{-1}$
	Amount to DOC, POC2DOC	$H \times (KLPOC \times LPOC + KRPOC \times RPOC)$	$\text{g C m}^{-2} \text{d}^{-1}$
	Fraction to Sediments	$\frac{POC2SED}{POC2DOC + POC2SED}$	< 1
	Fraction to DOC	$\frac{POC2DOC}{POC2DOC + POC2SED}$	< 1
Sediment Organic Carbon	Export	100% (This is an Ecopath default value, ICM creates no detritus from sediment organic carbon)	

Coding modifications were made to the ICM program to write the equivalent ICM variables or formula derived variables from Tables 3.1 through Table 3.4 to an Ecopath designated output file containing only variables required to complete the three screens listed above in Ecopath. A post-processor was written to read the new Ecopath output file and perform data manipulations to get the common variable output in the final format necessary for use by Ecopath. Procedures for ICM data manipulations will be discussed in a section below. The program listing for the post-processor is in Appendix A. A listing and explanation of all terms in formulas from ICM in Tables 3.1 to 3.4 can be found in Appendix B and came from Cerco and Tillman (2008).

The post-processor that was written specifically to output ICM information for Ecopath was developed into a subroutine of ICM containing the basic equations of Ecopath solving for the ecotrophic efficiency defined as the fraction of production that is utilized in the system. This number should range between zero and one; one being highly utilized and zero meaning very little or no utilization. The intent of developing the subroutine was to help automate the process of determining the status of the Chesapeake Bay system without having to set up an Ecopath model, in particular is the model mass balanced as is. This subroutine could be modified for use by other eutrophication models being applied to any system. Correspondence to Ecopath for the groups coming out of the eutrophication model would have to be established similar to how the variables and formulas for ICM were done. The application of ICM to the Chesapeake Bay was used as a test case for this subroutine.

During this research it was determined that a true coupling of ICM with Ecopath (i.e., exchanging of information from one model to the other and back) could not be accomplished because the model frameworks are too different. In spite of this, the exchange of information from ICM to Ecopath is very worthwhile. Although not a part of my research, I am providing

input into the development of a gui to automate the exchange of data from ICM to Ecopath. Using the gui, users will have the choice of developing an Ecopath model using ICM output data alone or they can combine the ICM data with an existing Ecopath model. To combine ICM information with an existing Ecopath model, a data file from Ecopath is exported that has an *.eii extension and contains all the information that has to be entered on the “Basic Input” screen, the “Diet Composition” screen, and the “Detritus Fate” screen. The *.eii file is a comma delimited file so it is easily read as long as one knows the variable formats. This file is read into the gui along with the Ecopath specific output file from the ICM post-processor. Once in the gui, any of the ten groups from ICM and their associated parameters can replace the variables in the Ecopath model. The user can exchange all or be more specific and exchange particular groups (i.e., only primary producers). Coupling the models in this way will allow modeling of upper trophic levels such as fish without adding to the computational burden of developing new state variables for ICM.

3.4 ICM and Ecopath Base Runs

In the previous sections, the common links of ICM to Ecopath were identified. This was considered the correspondence between the two model formulations and variables. Knowing this, common links of ICM output can now be used to develop a new or modify an existing Ecopath model. If a new Ecopath model is developed for the Chesapeake Bay using only ICM output, it would signify only the lower trophic levels of the system since the highest trophic level modeled in ICM is zooplankton. This model would contain two trophic levels and 10 groups. If a previously developed Ecopath model of the Chesapeake Bay (i.e. from Hagy 2002) were modified using the common variables from ICM as input to Ecopath, this would signify a system of many trophic levels with 34 groups.

The final sections of this chapter will present the development of two Ecopath models using only the common variables of both models discussed in sections below. Before this can be done, the steps leading up to the actual model runs will be presented. These are: 1) descriptions of the ICM and Ecopath runs (identified as base for each) previously conducted by Cerco and Noel (2004) and Hagy (2002), respectively, 2) aggregation of ICM output data to the form needed for Ecopath, 3) comparison of the values of the base ICM common variables after aggregation to the variables used in the original Chesapeake Bay Ecopath run, and 4) comparison of results from two new Ecopath models developed using the common data from the ICM base run designated Ecopath-ICM in the text and the Ecopath base run designated Ecopath-CB Ecopath in the text.

3.4.1. ICM Chesapeake Bay Base Application

There have been several versions of the ICM model developed but the version used for the model runs in this research was Cerco and Noel (2004) 2002 Chesapeake Bay Eutrophication Model (CBEM). This version contains 24 state variables in the water column (Table 2.1) and is linked to a sediment diagenesis model developed by Di Toro and Fitzpatrick (1993). The sediment diagenesis model calculates predictions for up to 10 state variables and 6 fluxes.

The grid used in the model application contained close to 13000 cells (see Figure 3.9 from Cerco and Noel 2004). There are approximately 2900 surface cells having non-orthogonal curvilinear coordinates in a horizontal plan. The z coordinates are in the vertical direction with the deepest part of the Bay being up to 19 layers deep. Layer thickness is fixed at 1.5 m for the subsurface layers while the surface layer can vary as a result of forcing functions such as winds and tides.

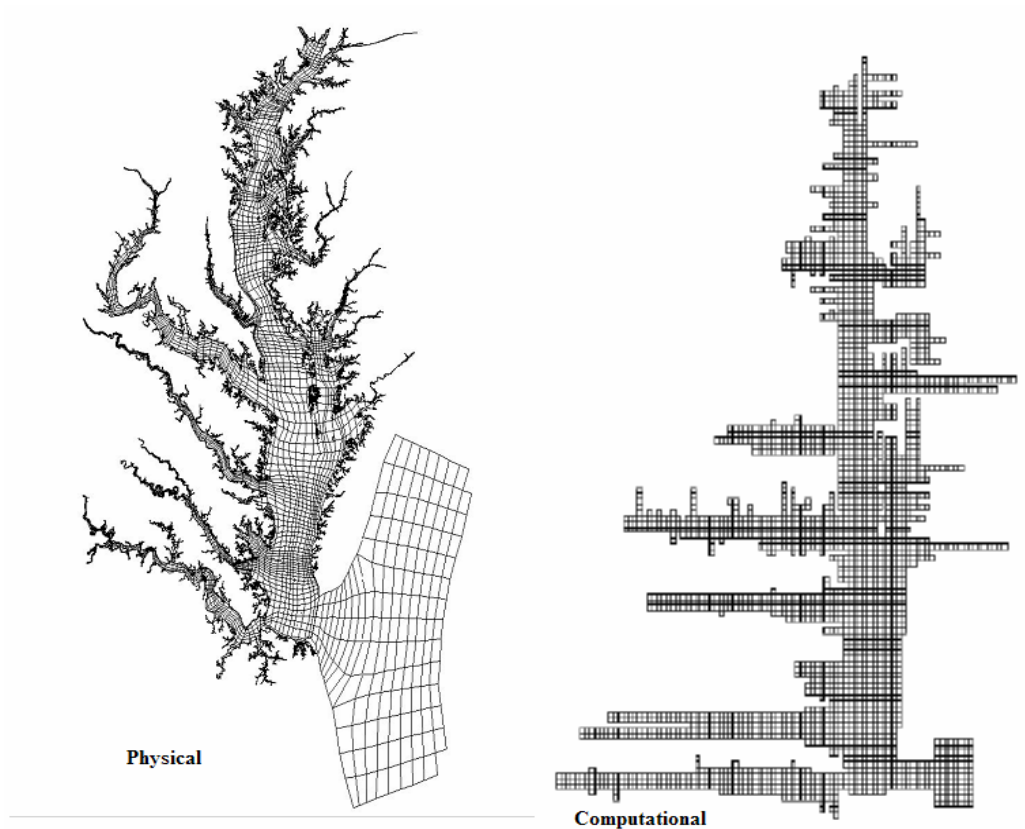


Figure 3.9. Physical and computational grid of the 13000 cell Chesapeake Bay model (Cercio and Noel, 2004).

The hydrodynamics model used to link with ICM was CH3D-WES (Johnson et al. 1993). CH3D-WES produced three-dimensional predictions of velocity, diffusion, surface elevation, salinity, and temperature for each grid cell. Numerically, CH3D is a finite-difference formulation having a grid of discrete cells. Inputs to drive the hydrodynamics model included wind speed, air temperature, tributary freshwater inflows, surface heat exchange, tides, and the time-varying vertical distributions of temperature and salinity at the open boundary

(Johnson et al. 1993). Ten years, 1985-1994, are simulated continuously using a five minute time step, and from these, two-hour hydrodynamics were determined as arithmetic means to be used in the water quality model. The use of intra-tidal hydrodynamics for this application differed from the earliest model application (Cerco and Cole 1994) where Lagrangian-average hydrodynamics were stored at 12.4-hour intervals (Dortch et al. 1992).

The grid characteristics of the hydrodynamics model were the same as described above for the water quality model. The range of the grid is from the heads of tide on the tributaries to the continental shelf in the Atlantic Ocean.

3.4.2. Ecopath Chesapeake Bay Base Application

One of the first applications of the Ecopath model to Chesapeake Bay resulting from the STAC initiatives is documented in Hagy (2002); although as early as 1986, Ulanowicz and Baird (1986) compiled existing data of ecological transfers to use in the network analysis of the system. Hagy (2002) modeled the summer (June–August) conditions for three regions of the Bay (Figure 3.10) using carbon as currency. The application was typical of conditions in the bay for the years 1985–1999. Similarly, an application was created that represented the Bay of the 1950s to early 1960s. Ecopath input files, as well as documentation, were provided by the originator of these applications (J. D. Hagy).

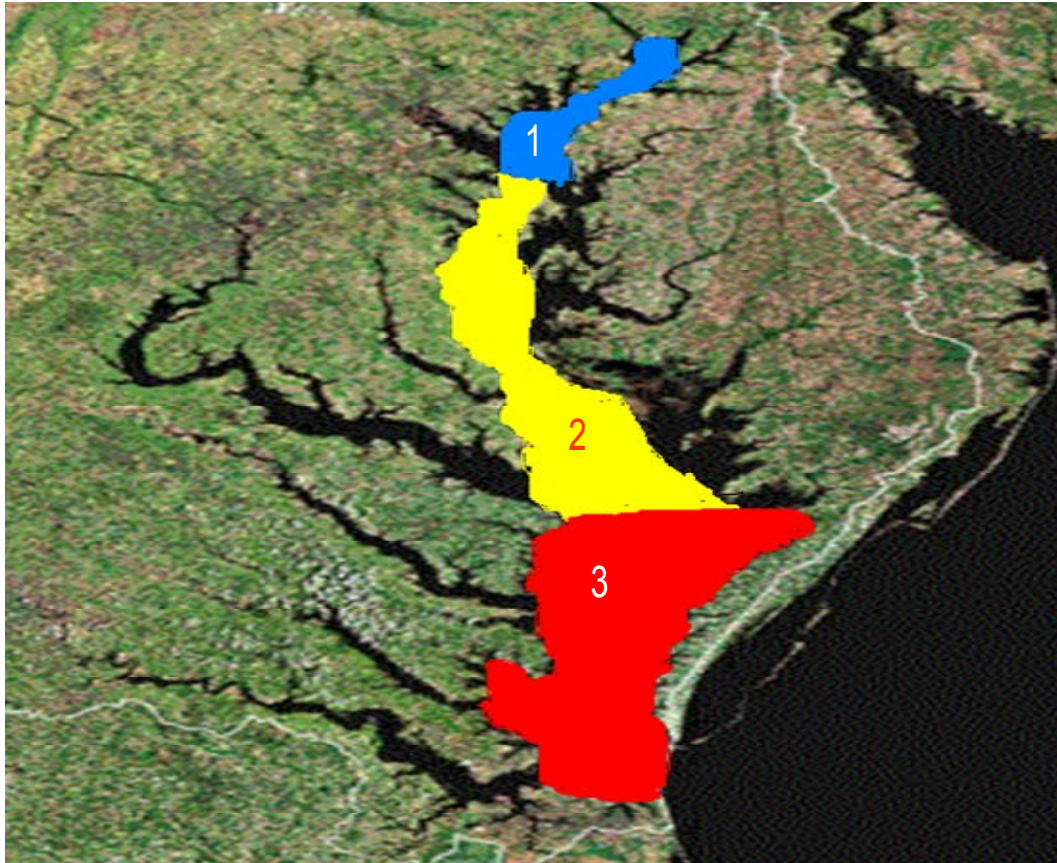


Figure 3.10. Three regions of Chesapeake Bay.

All Ecopath applications from Hagy (2002) included 34 groups (Table 3.5), separated into 3 detrital pools, 4 primary producers, 9 planktonic consumers, 5 benthic consumers, and 13 nektonic consumers. An Ecopath application requires extensive searches of databases and documentation of information sources. For the Chesapeake Bay application, Hagy (2002) compiled more than 150 sources including data from the Chesapeake Bay Monitoring Program to peer-reviewed literature.

**Table 3.5 Groups of the Chesapeake Bay Ecopath model
(Cercu and Tillman, 2008)**

Group Number	Description	Trophic Class
1	Net Phytoplankton	Primary Producer
2	Picoplankton	Primary Producer
3	Free Bacteria	Planktonic Consumer
4	Attached Bacteria	Planktonic Consumer
5	Heteroflagellates	Planktonic Consumer
6	Ciliates	Planktonic Consumer
7	Rotifers	Planktonic Consumer
8	Meroplankton	Planktonic Consumer
9	Mesozooplankton	Planktonic Consumer
10	Ctenophores	Planktonic Consumer
11	Chrysora	Planktonic Consumer
12	Microphytobenthos	Primary Producer
13	Submerged Aquatic Vegetation	Primary Producer
14	Benthic Bacteria	Benthic Consumer
15	Meiobenthos	Benthic Consumer
16	Deposit-Feeding Benthos	Benthic Consumer
17	Suspension-Feeding Benthos	Benthic Consumer
18	Oysters	Benthic Consumer
19	Blue Crab	Nektonic Consumer
20	Menhaden	Nektonic Consumer
21	Bay Anchovy	Nektonic Consumer
22	Herring/Shad	Nektonic Consumer
23	White Perch	Nektonic Consumer
24	Spot	Nektonic Consumer
25	Croaker	Nektonic Consumer
26	Hogchoker	Nektonic Consumer
27	American Eel	Nektonic Consumer
28	Catfish	Nektonic Consumer
29	Striped Bass	Nektonic Consumer
30	Bluefish	Nektonic Consumer
31	Weakfish	Nektonic Consumer
32	Dissolved Organic Carbon	Detritus
33	Sediment Carbon	Detritus
34	Particulate Organic Carbon	Detritus

3.5. 3-D ICM Data Aggregated to 0-D Ecopath Data

Before comparisons of common links between the ICM and Ecopath models could begin, model differences had to be considered and modifications to output data implemented. For instance, ICM results and process rates had to be spatially and temporally aggregated to the scales of the network model (see Figure 3.11). Specifically, concentrations from ICM have units of volume (i.e., gm m⁻³) while Ecopath quantifies biomass and other similar parameters on an areal basis (i.e. mgC m⁻²). Temporal results from the ICM were output as a summer average, and then averaged over a 3-year study period. Spatially, the Ecopath Chesapeake Bay model represented the main stem Chesapeake Bay as three regions identified as the upper, mid, and lower Chesapeake Bay (Figure 3.6). Tributaries were not included in the Ecopath modeling effort, only the main channel of the Chesapeake Bay. Thus, output from ICM was temporally and spatially integrated through the water column that represented the cells encompassing the three regions modeled with Ecopath (Cercio and Tillman 2008). All modifications made to ICM results were through a post-processor or subroutine developed in ICM for this study and not through embedded code modifications. Program listing for the post processor/subroutine can be found in Appendix A.

The equation used to find the temporal average was:

$$C_{ave} = \frac{1}{T} \times \sum_{i=1}^n C_i \times \Delta t \quad Eq . 3 . 18$$

where C_i is concentration of group at time interval i , C_{ave} is temporal average of C_i , Δt is the model time step, T is the duration of the averaging interval, and n is the number of time steps over the averaging interval. Once the temporal average was found, an areal average was found using:

$$C_{areal} = \sum_I^n C_{ave} \times \Delta z \quad Eq. 3.19$$

where C_{areal} is the areal average of the quantity, Δz is the cell layer thickness, and n is the number of cells in the water column. The final step in data aggregation, averaging data over the region representing upper, mid, or lower Chesapeake Bay is represented by:

$$C_{reg} = \frac{I}{A_{reg}} \times \sum_I^n C_{areal} \times A_i \quad Eq. 3.20$$

where C_{reg} is the regional and temporally averaged quantity used in comparison to equivalent Ecopath value, A_{reg} is the regional area, A_i is the surface area of the water column for cell i , and n is the number of surface cells in a region.

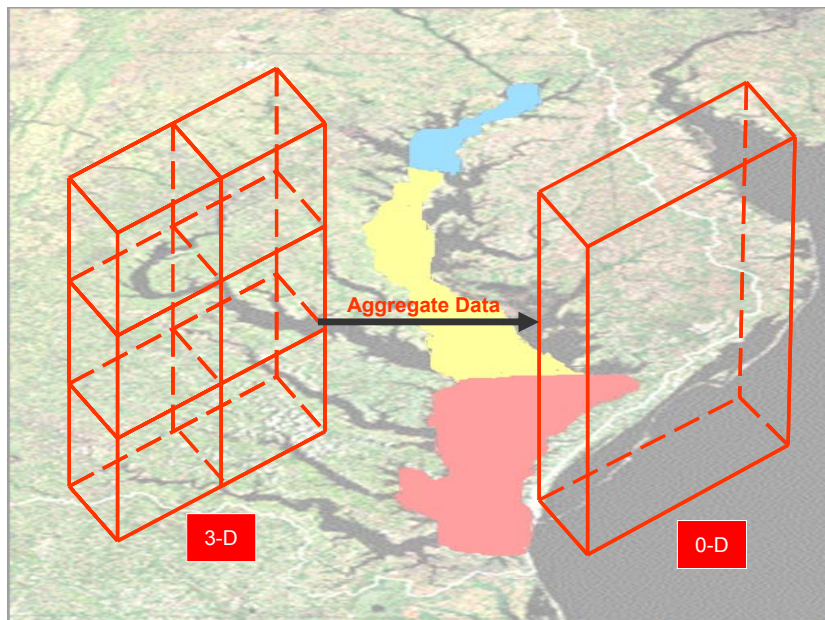


Figure 3.11. Aggregate 3-D temporally and spatially varying data to 0-D snapshot of well mixed system.

3.5.1 Comparison of ICM Base Aggregated Data to Ecopath Base Data

Table 3.6 lists the common groups between the ICM and Ecopath base runs for Chesapeake Bay and their associated “Basic Input” parameters for the three regions modeled (per Hagy 2002). A comparison is presented below of the correspondence between the biomass and production parameters for all common groups. The goal of this exercise is to question whether the representation of the same system by two different models at the lower trophic levels is comparable enough to be useful to the overall goal of this research. With one model using cited literature data to get a “steady-state” approximation of system behavior and the other using temporally-varying monitored data to predict system behavior, is there too substantial a difference in common variables that it renders the assumptions moot? Comparative system behavior (i.e., production rates) and quantitative differences were the focus of this exercise and will be discussed for each common variable. Differences within a factor of two appear to be reasonable.

Table 3.6. Biomass, production, and production/biomass in the three regions as denoted by Ecopath and ICM

Upper Chesapeake Bay									
Group	Biomass			Production			P/B		
	Ecopath gC m ⁻²	ICM gC m ⁻²	Ratio	Ecopath gC m ⁻² d ⁻¹	ICM gC m ⁻² d ⁻¹	Ratio	Ecopath (d ⁻¹)	ICM (d ⁻¹)	Ratio
Phytoplankton	1.60	1.60	1.000	0.904	0.898	0.993	0.567	0.561	0.989
Benthic Algae	0.29	0.05	0.172	0.176	0.003	0.017	0.600	0.075	0.125
SAV	2.09	0.47	0.225	0.017	0.015	0.882	0.008	0.032	4.000
Microzooplankton	0.08	0.05	0.625	0.171	0.0001	0.001	2.060	0.01	0.005
Mesozooplankton	0.28	0.06	0.214	0.107	0.003	0.028	0.380	0.057	0.150
Deposit Feeders	3.07	0.4	0.13	0.083	0.025	0.301	0.027	0.064	2.370

Table 3.6. Continued

Filter Feeders	27.23	0.36	0.013	0.218	0.001	0.005	0.008	0.003	0.375
DOC	12.50	13.30	1.064						
POC	5.25	5.90	1.124						

Mid Chesapeake Bay

Group	Biomass			Production			P/B		
	Ecopath gC m ⁻²	ICM gC m ⁻²	Ratio	Ecopath gC m ⁻² d ⁻¹	ICM gC m ⁻² d ⁻¹	Ratio	Ecopath (d ⁻¹)	ICM (d ⁻¹)	Ratio
Phytoplankton	3.91	3.26	0.834	2.463	1.330	0.540	0.630	0.408	0.648
Benthic Algae	0.27	0.283	1.048	0.159	0.057	0.358	0.600	0.203	0.338
SAV	0.53	1.127	2.126	0.005	0.014	2.800	0.009	0.012	1.333
Microzooplankton	0.19	0.166	0.874	0.382	0.0001	0.000	2.030	0.0001	0.000
Mesozooplankton	0.53	0.237	0.447	0.263	0.018	0.068	0.500	0.075	0.150
Deposit Feeders	1.52	0.384	0.253	0.049	0.022	0.449	0.032	0.056	1.750
Filter Feeders	0.42	1.071	2.550	0.006	0.001	0.167	0.014	0.001	0.071
DOC	28.20	22.08	0.783						
POC	10.30	11.36	1.103						

Lower Chesapeake Bay

Group	Biomass			Production			P/B	Production	P/B
	Ecopath gC m ⁻²	ICM gC m ⁻²	Ratio	Ecopath gC m ⁻² d ⁻¹	ICM gC m ⁻² d ⁻¹	Ratio	Ecopath (d ⁻¹)	ICM (d ⁻¹)	Ratio
Phytoplankton	2.49	3.17	1.273	2.131	1.13	0.530	0.856	0.356	0.416
Benthic Algae	0.29	0.192	0.662	0.234	0.041	0.175	0.799	0.213	0.267
SAV	1.99	1.377	0.692	0.018	0.009	0.500	0.009	0.007	0.778
Microzooplankton	0.13	0.219	1.685	0.236	0.0001	0.000	1.890	0.0005	0.000
Mesozooplankton	1.07	0.256	0.239	0.268	0.016	0.060	0.250	0.063	0.252
Deposit Feeders	4.79	0.523	0.109	0.105	0.026	0.248	0.022	0.05	2.273

Table 3.6. Continued

Group	Biomass			Production			P/B	Production	P/B
	Ecopath gC m ⁻²	ICM gC m ⁻²	Ratio	Ecopath gC m ⁻² d ⁻¹	ICM gC m ⁻² d ⁻¹	Ratio	Ecopath (d ⁻¹)	ICM (d ⁻¹)	Ratio
Filter Feeders	6.96	0.323	0.046	0.097	0.0001	0.001	0.014	0.0003	0.021
DOC	26.92	19.864	0.738						
POC	8.31	10.023	1.206						

3.5.1.1. Phytoplankton

Values for algal biomass (identified as net phytoplankton in Table 3.6) from ICM compare favorably in all regions, but are higher (1.27:1) in the lower region than values used in Ecopath. There are two possible reasons for the discrepancies between the models. Both are related to averaging procedures used in post processing ICM output to get comparable values to Ecopath. First, comparisons were made between values representing different time periods. For instance, ICM values represented a summer average (June 1 to August 31) for the years 1985 through 1987 while Ecopath's values represented a summer period (June 1 to August 31) for the years 1984 through 1986. Second, ICM's areal average of grid cells to get regional values may not exactly match the areas representing Hagy's regions. Hagy's surface areas of the three regions were 472, 2338, and 2661 km² for the upper, mid and lower Bay, respectively. ICM calculated surface areas of 936.8, 3513.5, and 3424.9 km², respectively. ICM's region with the largest surface area was the mid Bay while Hagy's region with the largest surface area was the lower Bay. This may explain why the largest difference was in the phytoplankton biomass of the lower Bay.

There are noted differences in primary production between models (Table 3.6). ICM values are approximately half the value in the mid and lower Bay and about the same in the

upper Bay. Hagy (2002) estimated values for Ecopath from literature while values in ICM are calculated based on intensity of light, nutrient availability, and ambient temperature. These model parameters are influenced by the temporal and spatial averaging as well.

3.5.1.2. Benthic Phytoplankton

Benthic algal biomass values from ICM are less than values from Ecopath in all regions except the mid Bay. For benthic algae, again we must look at how comparing values from different time periods affect comparison results, and also consider whether taking an areal average of the ICM values over the entire region instead of just where benthic algae occur (i.e., in shallow water where light penetrates to the bottom) was the right averaging approach.

Another benthic algal common link showing differences was net benthic primary production (Table 3.6). For all regions, ICM values are orders of magnitude less than Ecopath values. It is strongly suspected that differences come from taking an areal average over the entire region more so than comparing different time periods. If discrepancies are not the result of averaging procedures, then model formulation for components of primary productivity need to be examined.

3.5.1.3. Zooplankton Group 1

Zooplankton group 1 (microzooplankton) biomass from ICM in Table 3.6, are between 60% to 90% of the values of Ecopath in the upper and mid regions of Chesapeake Bay and are 60 % greater than Ecopath's value in the lower region. The reasons for the discrepancies are noted above under phytoplankton. Moreover, with more phytoplankton in the lower region providing more food the discrepancy may in part be due to that. Although there are differences, it is unrealistic to assume the values from each model will be exactly the same given the difference in their frame work.

Zooplankton group 1 production and production rate were almost nonexistent in the mid and lower Bay and not much better in the upper Bay (Table 3.6). As has been pointed out by Cerco and Noel (2004) the disparity can be traced back to the temperature function associated with grazing forcing a decline of grazing in the summer months. As temperatures become higher than 25 °C, respiration increases resulting in a decline in filtration. Thus, the overall effect is reduced biomass. Although different, the values fall within the factor of two range established as the guide post. Given the different model framework, it is not expected for values to be exactly the same.

Like phytoplankton, different rates for microzooplankton in ICM are calculated internally and consider factors such as prey availability, temperature, predation by organisms not modeled, low dissolved oxygen, etc. (Cerco and Noel 2004) while values for Ecopath came from literature. Due to the almost nonexistence in production, this may indicate a need to revisit the components of production for zooplankton.

3.5.1.4. Zooplankton Group 2

Zooplankton group 2 (mesozooplankton) values from ICM in Table 3.6, are about 20% to 40% the values used in Ecopath in all regions of the Bay. Again, this was believed to be an acceptable comparison given the discrepancies caused by the grazing formulation. Similar to zooplankton group 1, zooplankton group 2 production and production rates were low compared to values use in Ecopath. These low values in ICM warrant a revisit to the equations estimating production to improve values coming from ICM.

3.5.1.5. Dissolved and Particulate Organic Carbon (DOC/POC)

DOC and POC biomass values from ICM (identified as DOC and POC in Table 3.6) compare favorably with Ecopath values. By regions, ICM values are 75% or better the value used in Ecopath. The most differences are noted for DOC in the mid and lower regions. In the upper Bay, the comparison is the most favorable. Reasons for the discrepancies in the mid and lower Bay are probably attributed to the difference in region sizes between Hagy's and the area ICM calculated. This can be adjusted easily in ICM because the region size is controlled by the cell numbers designated by the modeler for each region then read into the post-processor for aggregating purposes.

3.5.1.6. Submerged Aquatic Vegetation (SAV)

SAV biomass values from ICM show the most disparity in the upper and lower Bay as far as having less biomass whereas the mid Bay has almost twice as much. These differences are still within the factor of two range for comparison. In the upper Bay, the reason the value may be so low is that ICM is estimating a higher light extinction compared to the other areas of the Bay. This could be from more particulate matter resulting from algal die-off in the shallower upper Bay and has stunted SAV growth. Increased light extinction has been documented as the most likely cause of SAV demise in the Bay (Kemp et al. 2005; Davis 1985). In addition to this, as discussed above taking an areal average over the whole Bay should be reconsidered. In hind sight, an average should be calculated just for the areas SAV grows (i.e., along shallow shorelines). It is not clear why the mid Bay has values almost double the Ecopath value other than most of the nutrients probably end up in the mid Bay.

Production and P/B ratios are both lower in the mid and lower Bay and highest in the upper Bay. This may indicate high predation in this area.

3.5.1.7. Deposit and Filter Feeders

In ICM, deposit and filter feeders are sediment dwelling organisms. Deposit feeders are benthos organisms that live within the bottom sediments and feed on deposited materials while filter feeders live at the sediment water interface and filter over water. Their biomass values from ICM are two to four times less than values used in Ecopath for all regions. As with all other constituents discussed above, discrepancies between the two models are most likely produced by post processing averaging procedures of ICM output. However, if this proves not to be the case, then model formulations need to be examined for improvements. Cerco and Noel (2005) have documented the shortfalls of the benthos component developed by HydroQual (2000).

3.5.2. New Ecopath Models Developed from Chesapeake Bay ICM and Ecopath Base Model Data

Two new Ecopath model applications were developed from data contained in Table 3.6 along with other parameters common to ICM and Ecopath for the upper Bay region. These were considered test runs to see how each network model run characterizes the system with one model input being developed from data cited in literature and the other model input based on predictions from equations of first principles. The upper Bay region was chosen because it shows the most disparity between the common variables.

The three input screens for each run were populated with data from the ICM and Ecopath base runs. In Figure 3.12, examples of the “Basic Input”, “Diet Composition”, and “Detritus Fate” screens are shown containing the aggregated data from ICM output. A couple of differences between the groups modeled in ICM and Ecopath had to be rectified before simulations could be completed. Namely in ICM only one group of microzooplankton are modeled but in the CB Ecopath three microzooplankton groups were modeled. Similarly for

phytoplankton, in ICM net phytoplankton includes picoplankton, but in Ecopath picoplankton was treated as a separate group from net phytoplankton. To develop the Ecopath model using base Ecopath variables, it was decided to combine the three microzooplankton groups into one group. Knowing the values for P/B , Q/B , UA/Q and B (see Table 2.1 for definition of terms) of each group, the production, consumption, and unassimilated food could be found for each (i.e., $B * P/B = \text{Production}$; $B * Q/B = \text{Consumption}$; $Q * UA/Q = \text{Unassimilated Food}$). A sum was calculated for each parameter and B , then total production, consumption, or unassimilated food was found dividing by the total B to get the values of the parameters for one group of microzooplankton. Combining picoplankton and net phytoplankton was handled in the same manner.

Once both models were set-up, mass balance exercises were initiated similar to the procedure described by Ortiz and Wolff (2002) and Kavanagh et al. (2004). The steps followed included adjusting the diet composition of predators and/or reducing predator biomasses of groups having $EE > 1$. This was an iterative procedure, since making these adjustments did not always produce $EE < 1$ for a group. Sometimes if a predator biomass was reduced too much, $EE > 1$ resulted for other groups utilizing that predator. When this happened, adjustments had to be made again until the EE s of all groups involved were less than one.

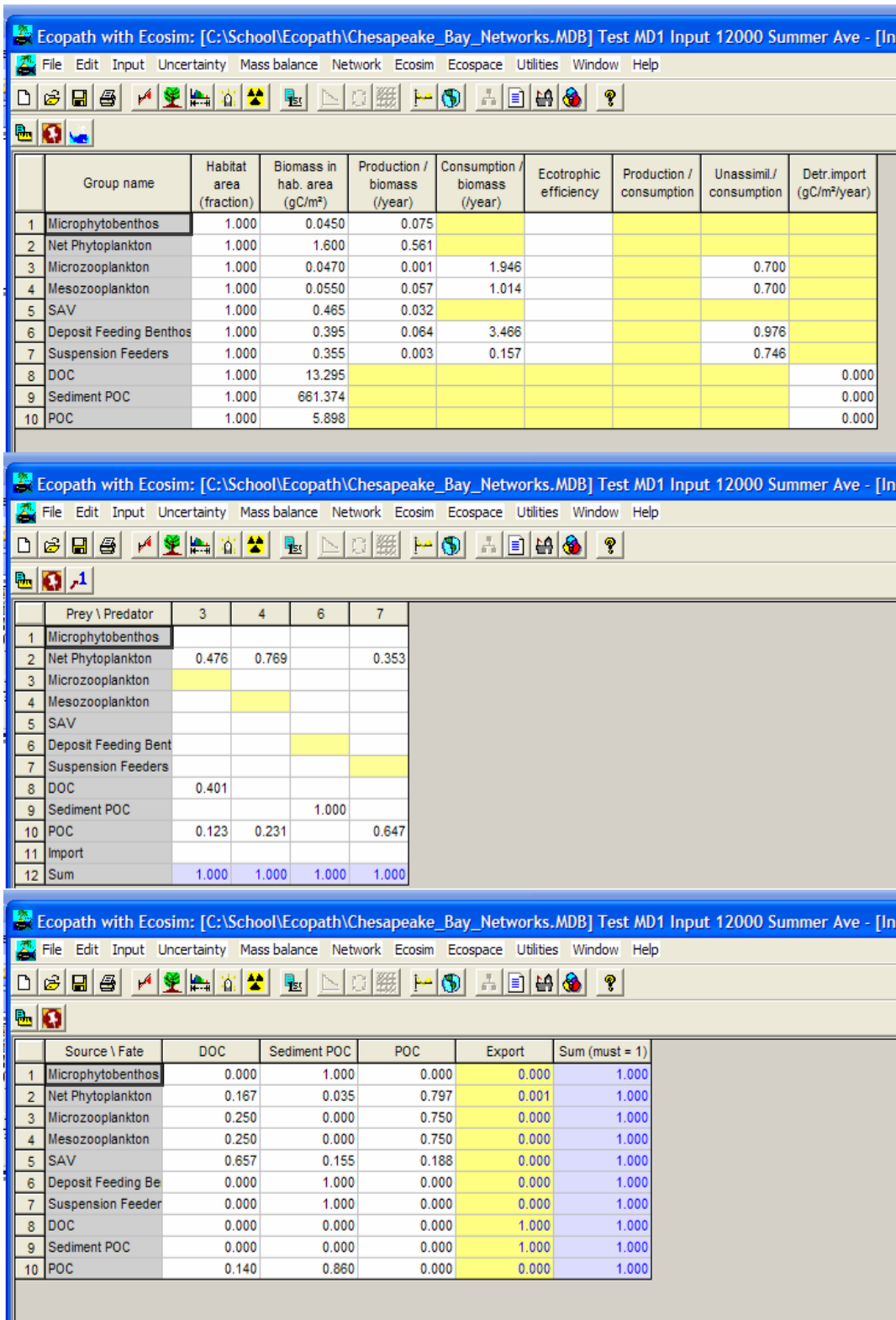


Figure 3.12. Ecopath input screens with ICM common variables (upper – “Basic Input”, middle – “Diet Composition”, and lower – “Detritus Fate”).

3.5.2.1. Results and Discussion

Analysis of the similarities and differences of the output from the two Ecopath runs using the common variables of the Chesapeake Bay base ICM and Ecopath runs employed several Ecopath routines for output analysis. The routines that will be discussed below are the system statistics, the network analysis aggregated trophic flows (Ulanowicz 1986), mixed trophic impacts, and EE. Figures 3.13 and 3.14 contain the basic estimates after mass balance of the two runs, Ecopath ICM common variables and Ecopath CB Ecopath common variables, respectively.

The screenshot shows the Ecopath software interface with a menu bar (File, Edit, Input, Uncertainty, Mass balance, Network, Ecosim, Ecospace, Utilities, Window, Help) and a toolbar. The main window displays a table titled "Results form: displays mass-balance solution". The table has 10 rows and 10 columns. The columns are: Group name, Trophic level, Habitat area, Biomass in habitat area (gC/m²), Biomass (gC/m²), Prod./ biom. (/day), Cons./ biom. (/day), Ecotrophic efficiency, and Production / consumption. The rows represent different trophic groups: 1 Microphytobenthos, 2 Net Phytoplankton, 3 Microzooplankton, 4 Mesozooplankton, 5 SAV, 6 Deposit Feeding Benthos, 7 Suspension Feeders, 8 DOC, 9 Sediment POC, and 10 POC.

	Group name	Trophic level	Habitat area	Biomass in habitat area (gC/m ²)	Biomass (gC/m ²)	Prod./ biom. (/day)	Cons./ biom. (/day)	Ecotrophic efficiency	Production / consumption
1	Microphytobenthos	1.00	1.000	0.0450	0.0450	0.075	-	0.000	-
2	Net Phytoplankton	1.00	1.000	1.600	1.600	0.561	-	0.118	-
3	Microzooplankton	2.00	1.000	0.0470	0.0470	0.001	1.946	0.000	0.001
4	Mesozooplankton	2.00	1.000	0.0550	0.0550	0.057	1.014	0.000	0.056
5	SAV	1.00	1.000	0.465	0.465	0.032	-	0.000	-
6	Deposit Feeding Benthos	2.00	1.000	0.395	0.395	0.064	3.466	0.000	0.018
7	Suspension Feeders	2.00	1.000	0.355	0.355	0.003	0.157	0.000	0.019
8	DOC	1.00	1.000	13.295	13.295	-	-	0.141	-
9	Sediment POC	1.00	1.000	661.374	661.374	-	-	0.685	-
10	POC	1.00	1.000	5.898	5.898	-	-	0.084	-

Figure 3.13. Basic estimates after mass balance for Ecopath with ICM common variables.

The screenshot shows the 'Results form: displays mass-balance solution' window in Ecopath with Ecosim. The table below represents the data displayed in this window.

	Group name	Trophic level	Habitat area	Biomass in habitat area (gC/m ²)	Biomass (gC/m ²)	Prod. / biom. (/day)	Cons. / biom. (/day)	Ecotrophic efficiency	Production / consumption
1	Microphytobenthos	1.00	1.000	0.293	0.293	0.600	-	0.519	-
2	Net Phytoplankton	1.00	1.000	1.595	1.595	0.570	-	0.957	-
3	Microzooplankton	2.44	1.000	0.110	0.110	2.400	5.580	0.996	0.430
4	Mesozooplankton	2.49	1.000	0.282	0.282	0.380	0.910	0.192	0.418
5	SAV	1.00	1.000	2.086	2.086	0.008	-	0.000	-
6	Deposit Feeding Benthos	2.00	1.000	2.368	2.368	0.014	0.070	0.000	0.200
7	Suspension Feeders	2.00	1.000	27.232	27.232	0.008	0.041	0.000	0.195
8	DOC	1.00	1.000	12.504	12.504	-	-	0.520	-
9	Sediment POC	1.00	1.000	201.670	201.670	-	-	0.000	-
10	POC	1.00	1.000	5.249	5.249	-	-	0.772	-

Figure 3.14. Basic estimates after mass balance for Ecopath CB Ecopath common variables.

These two runs represent very simple networks compared to many cited in literature (Crales-Hernandez et al. 2005; Villanueva et al. 2005; Bundy 2005; Meyer and Poepperl 2004; and Neira and Arancibia 2004). A system most similar as far as network structure to this one was an application conducted by Ortiz and Wolff (2002) looking at management strategies of increasing standing stocks of *A. purpuratus* and *Ch. chamissoi* in seagrass and sand-gravel habitats, and removal of the seastar *M. gelatinosus* from seagrass beds seems justified. These systems were similar in that they look at the lower trophic level interactions. Figures 3.15 and 3.16 illustrates the Lindeman (1942) chain for combined primary producer and detrital flow (gC m⁻² d⁻¹) with transfer efficiency flow charts of biomass showing trophic interactions of the groups included in the two Ecopath models.

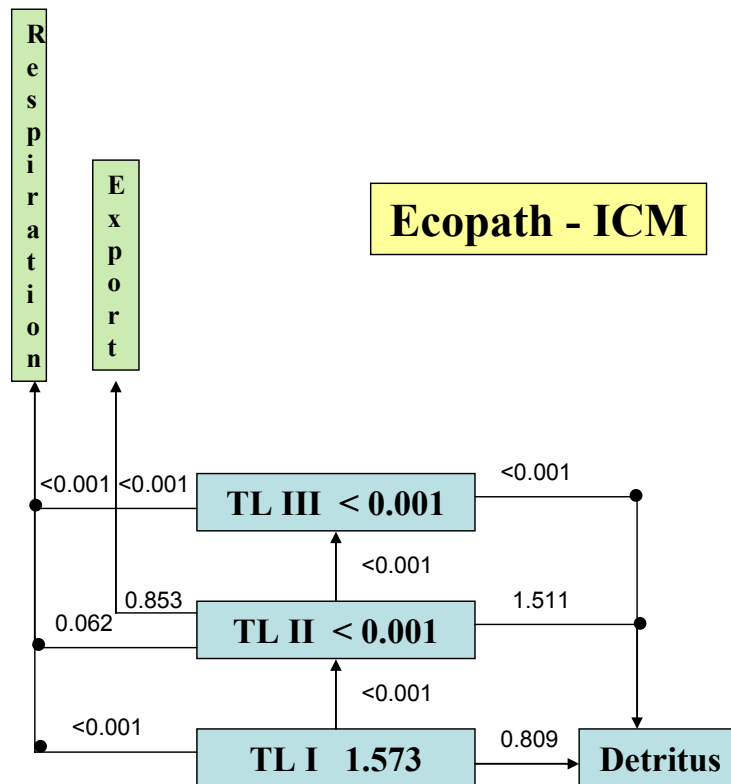


Figure 3.15. Lindeman chain with combined primary producer and detrital flow ($\text{gC m}^{-2} \text{d}^{-1}$) for transfer efficiency designated between boxes for Ecopath run with ICM variables.

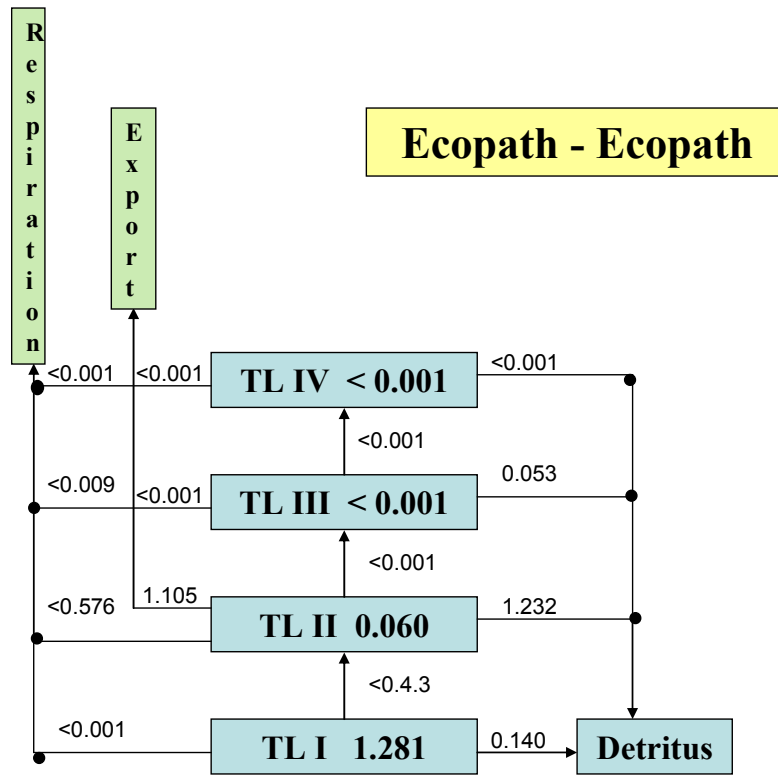


Figure 3.16. Lindeman chain with combined primary producer and detrital flow (gC m⁻² d⁻¹) for transfer efficiency designated between boxes for Ecopath run with CB Ecopath variables.

The biomass distribution in the Ecopath ICM network system was heavily weighted in trophic level 1 (TL I) while the biomass distribution of the Ecopath CB Ecopath network showed most of the biomass in TL II (Table 3.7). Villanueva et al. (2006) reported similar findings of high biomass in TL I at the Ebrie lagoon and Lake Nokoue which they believe indicates a bottom-up control in the ecosystems. Since there was such a large difference in suspension feeder biomass between the two model runs (27.2 as opposed to 0.36 gC m⁻²), this was most likely the reason for the difference in the biomass distribution. Of all the common groups between the two base models of the Chesapeake Bay, this group showed the most disparity.

Although the P/B ratios were very similar, the production was actually two orders-of-magnitude less for the Ecopath-ICM run. As discussed before, this may require a revisit to the production formulation for suspension feeders and has been previously noticed by Cerco and Noel (2004).

Table 3.7. Biomass distribution from the Ecopath ICM and Ecopath CB Ecopath runs

Trophic Level	Total Biomass (gC m⁻²) for Ecopath ICM run	Total Biomass (gC m⁻²) for Ecopath CB Ecopath
IV	-	<0.001
III	<0.001	0.074
II	0.852	29.918
I	2.110	3.974

Consumption by predators in the trophic flow diagram from the Ecopath-ICM application has most of their food source originate from the detritus compartment (93%) with only a small fraction (7%) coming from primary producers. Meyer and Poepperl (2004) saw similar behavior on the Steina, a mountain stream in southern Germany. Sediment POC contributed about 69% as recycled material back to the living groups of the system. Of the living groups, deposit feeders contributed the most (65%) of the material recycled back to the detritus pool. Consumption by predators in the Ecopath CB Ecopath application mostly relies on primary producers as their food source (75%) while detritus only provided about 25% to their diet. In this application suspension feeders have such a high population compared to the other groups that their diet preference (almost 60% net phytoplankton) heavily weights the food source to primary producers. Thus, suspension feeders are by far the most important consumers.

Most of the transfer efficiencies (calculated as the ratio of the sum of exports plus flow that is transferred from one trophic level to the next to the throughput on the concerned trophic level) were less than the 10-20% commonly described in literature (Odum 1971; Baird and Ulanowicz, 1989; and Heymans and Baird, 2000). This was the case for both Ecopath runs (Figures 3.15 and 3.16). The Ecopath ICM application had such low transfer efficiency that it did not register on the table created in Ecopath. This happens if the values are less than 0.001. This is a sign of low transfer of food from one trophic level to the next, but since only the lower trophic levels are being considered in the network, this seems reasonable. If more predators (higher trophic levels) were added to the group list, transfer efficiencies would probably increase. Poepperl (2003) observed low ecotrophic efficiencies from not including fish in a network on a lowland stream in northern Germany.

System statistics are presented in Table 3.8 for the two Ecopath applications. The total system throughput (TST) is defined as the sum of all flows in a system and includes consumption, exports, respiratory flows, and detritus flows. It represents the “size of the entire system in terms of flow” (Ulanowicz 1986). For both applications the TST and the sum of all production carry the same value of 5 and 1 $\text{gm m}^{-2} \text{d}^{-1}$, respectively. This does not seem possible, but when looking at the components of TST the largest differences between the two are in the respiratory flows and the flows to detritus. The Ecopath ICM application has very low respiratory flows ($0.062 \text{ gm m}^{-2} \text{ d}^{-1}$ compared to $0.585 \text{ gm m}^{-2} \text{ d}^{-1}$) probably due to the low biomass total when compared to the Ecopath CB Ecopath application. Detritus flow is double for this application compared to the Ecopath CB Ecopath as noted above. There is a large transfer of matter at the lower levels, and this implies the system is driven by flows passing through the detrital pools. Using TST with total system biomass (B), a ratio (B/TST) can be found that is directly proportional to the maturity of the system (Christensen 1995). The B/TST ratio was

compared for the two applications and indicated that the Ecopath ICM application is an ecosystem in development while the Ecopath CB Ecopath application is a mature system. Since both systems have the same TST, this indicator is heavily influenced by the biomass. Another indicator of system maturity is the ratio of total primary production (TPP) to total respiration (TR). Odum (1971) points out that when a system is in early development production exceeds respiration, and in a mature system it approaches one. Systems suffering anoxia have ratios less than one. Similar to the B/TST, the TPP/TR ratio shows the Ecopath ICM application to be in development while the Ecopath-CB Ecopath application is approaching maturity. The values for TPP/TR are 14.853 and 1.884, respectively. The Ecopath ICM value is higher than others that have been reported but the Ecopath CB Ecopath value is in line with the Northern Gulf of California documented by Morales-Zarate et al. (2003) and with the Somme Bay documented by Rybarczyk et al. (2003).

Table 3.8. System statistics for Ecopath CB Ecopath (left value) and Ecopath ICM (right value)

Parameter	Value		Units
Sum of all consumption	2.153	1.573	gC/m ² /day
Sum of all exports	1.105	0.853	gC/m ² /day
Sum of all respiratory flow	0.585	0.062	gC/m ² /day
Sum of all flows into detritus	1.449	2.973	gC/m ² /day
Total system throughput	5.00	5.000	gC/m ² /day
Sum of all production	1.00	1.000	gC/m ² /day
Calculated total net primary production	1.102	0.916	gC/m ² /day
Total primary proproduction/total respiration	1.884	14.853	
Net total system production	0.517	0.854	gC/m ² /day

Table 3.8. Continued.

Parameter	Value		Units
Total primary production/total biomass	0.032	0.309	
Total biomass/total system throughput	6.793	0.592	
Total biomass	33.966	2.962	gC/m ²
Total catches	–		gC/m ² /day
Connectance Index	0.265	0.163	
System Omnivory	0.267	–	

Assuming the trophic structure stays the same, direct and indirect interactions between groups in a food web can be assessed by changing the biomass of one group and noting the effect to others. This is called mixed trophic impact (MTI) and is scaled from -1 to 1 with negative numbers indicating negative impacts and positive numbers indicating a positive impact (Christensen et al. 2000). Bradford-Grieve et al. (2003) observe that all living groups have a negative impact on themselves from competition for resources. This is illustrated in Figure 3.16 which shows that when there is a noticeable impact of one group on itself it is negative. The MTI from both Ecopath runs show similar impact behavior on groups even though biomasses differ more in this region compared to the other regions. The group with the most positive impacts to other compartments is net phytoplankton. In both runs, net phytoplankton impacts the groups, microzooplankton, mesozooplankton, and suspension feeders although more equally for the Ecopath ICM run. This is because on the “Diet Composition” screen these groups have been designated as predators of phytoplankton. When phytoplankton biomass increases these groups’

biomasses will more than likely increase as well. This is in agreement with Fetahi and Mengistou (2007) who found that phytoplankton and detritus have positive impacts on most other groups but especially their major predators. Groups from the Ecopath ICM run using detritus as a food source (as indicated on the “Diet Composition” screen in Figure 3.12) do show positive impacts from a change in biomass of the detrital groups. For the Ecopath ICM run, there are greater positive impacts to the other groups than in the Ecopath CB Ecopath run. As stated before this may suggest that the Ecopath ICM trophic system could indicate a bottom-up control is present since a number of groups feed on detritus. The microphytobenthos group is shown to have no impacts to the other groups for the Ecopath ICM application and a positive impact to the deposit feeders for the Ecopath CB Ecopath run. Again this can be traced back to the diet composition specified. In the Ecopath ICM run there are no predators on the microphytobenthos, but in the Ecopath CB Ecopath run, deposit feeders prey on microphytobenthos. Microphytobenthos having no predators in the Ecopath ICM run stems back to the formulation for microphytobenthos in ICM, thus only through indirect organic matter decay (through death) do they serve as a food source to other groups.

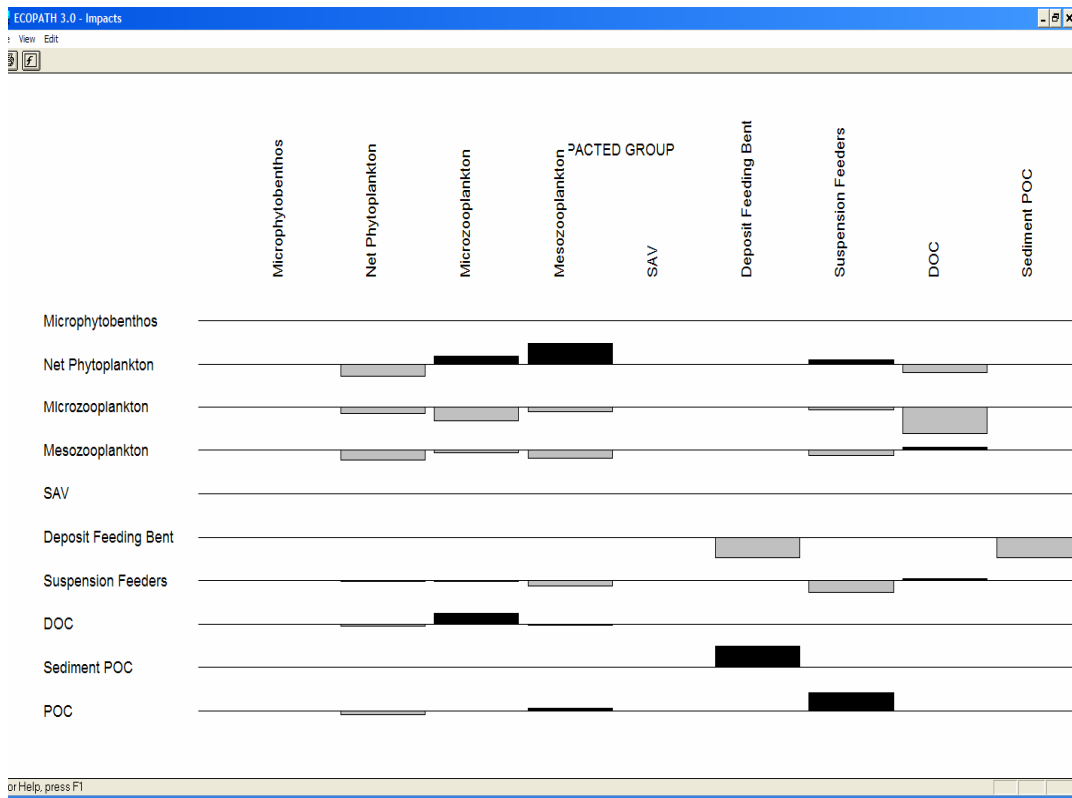


Figure 3.17. Mixed trophic impact (MTI) from Ecopath ICM run.

Ecotrophic efficiency (EE) is an indication of the utilization of one group by the others, namely the portion of production consumed by predators or exported from the system. The value ranges from zero (no utilization) to one (highly utilized). Results from the Ecopath CB Ecopath run (Figure 3.10) show that three groups are highly utilized (i.e., net phytoplankton, microzooplankton, and POC) with values of 0.957, 0.996, and 0.772, respectively. These values are typical and are similar to values from Angelini and Agostinho (2004) and Neira and Arancibia (2004). Results from the Ecopath ICM run are quite different from these although EE for sediment POC (0.695) is very similar to POC (0.772) of the Ecopath CB Ecopath run. The

EE for phytoplankton in the Ecopath ICM run was calculated as 0.114 indicating very low utilization. This is not a typical value for a major primary producer. This value was similar to one seen by Fetahi and Mengistou (2007) for Lake Awassa (Ethiopia) for phytoplankton. They explained this low value as a result of low predation from zooplankton, thus a major portion of phytoplankton dies off and goes to detritus. That appears to be similar to what is seen here. They also point out bacteria was excluded from their study and may also have some effect indirectly since zooplankton feed on bacteria. This study excludes bacteria too but, ICM formulation allows zooplankton to feed directly on dissolved organic carbon (DOC) [from Cerco and Noel (2004)].

3.6. Summary and Conclusions

The possibility of coupling a eutrophication model to a fisheries network model was explored. Coupling of these two models will provide managers a new perspective on how to improve management strategies and help answer questions such as: 1) how will management of watershed impact fisheries, or 2) can management of fisheries replace/supplement nutrient control? The models being considered were CE-QUAL-ICM and Ecopath with Ecosim, (Ecopath), respectively. CE-QUAL-ICM is a time and spatially varying multi-dimensional water quality model, and Ecopath is a fisheries network model with no temporal or spatial resolution. Both models have previously been applied to the Chesapeake Bay.

Common links between the two models were identified. Because ICM's and Ecopath's model frameworks were so vastly different, results from ICM were aggregated temporally and spatially so that its values could be compared to values used in Ecopath. Results from comparisons indicate that generally ICM and Ecopath values were similar to each other (e.g., within an order of magnitude or less). It is unreasonable to expect values from both models to be exactly the same especially since model formulations are different. Many of the constituents and

rates in ICM are calculated based on environmental conditions while Ecopath values are estimated from literature. Although most values compared reasonably well, some of the rates for benthic associated groups were orders of magnitude different. The temporal and spatial averaging of ICM output during post processing possibly produced some of the differences. To verify this, post processing averaging procedures were revisited to:

- Check consistency in the temporal averaging interval.
- Check consistency in spatial averaging of ICM cells to represent Hagy's three regions.
- Check consistency of spatial averaging of SAV and benthic algae over only part of regions where they occur instead of the entire region.

Differences were rectified, but the production rates and biomasses of zooplankton (in the upper and lower regions) and benthic groups (in all regions) were still being under-predicted. Limitations such as ICM model formulation for zooplankton grazing were recognized as a process needing reconsideration and possibly a new formulation for model improvement. The problems with the zooplankton grazing formulation had to do with limitations placed on grazing when temperatures are too warm during hot periods causing no production. The inability to predict higher values of benthos organism biomasses and production rates had been previously noted by Cerco and Noel (2004). Under-predicting of biomass in the lower Bay stems from ICM's model formulation solving for bivalve filter feeders which are negligible in the lower Bay. Conversely, bivalves are included in the biomass estimate for deposit feeders (Hagy, 2002) in the Ecopath CB Ecopath run.

From this work, future modifications to ICM formulations will be implemented to improve ICM's predictive capabilities to provide the information needed to address ecosystem questions. If anything, this research has provided guidance in critical areas for code re-formulation so that ICM will be beneficial in meeting future management support.

Two Ecopath models were created using common links from an ICM base run and the Ecopath CB Ecopath input data for the upper Chesapeake Bay region. This exercise was performed to see Ecopath's interpretation of the same system using two different data sources. Because ICM predicted lower concentrations and production rates for the benthic organism than was used in the Ecopath CB Ecopath run, Ecopath viewed the ecosystem as a developing environment. Conversely, the Ecopath CB Ecopath model results were viewed as a system approaching maturity. The statistic variable used in describing the Ecopath view of the system was the B/TST ratio. This statistic (B/TST) is biomass dependent so it is understandable that this different view point of the same system occurs. Also from network analysis, the Ecopath ICM model suggest that there is a bottom-up control present in this ecosystem since most of the food source originates and flows back to the detrital compartment. In contrast, the Ecopath CB Ecopath run's food source mostly originates from the primary producers. Again, this difference is believed to arise from the disparity in benthos and zooplankton biomasses causing a lack of predators of phytoplankton. Biomasses and production rates for phytoplankton were reasonable (within an order of magnitude); therefore, they were growing but had no demands on them. That being the case, they die adding to the detrital compartment. Improvements to ICM formulations for some of the groups identified (i.e., benthos) will help to enhance the ICM predictive capabilities and bring ICM's view of the ecosystem more in line with Ecopath's so that through coupling their information, answers can be found for nutrient and fishery management questions.

CHAPTER IV

ECOSYSTEM PROJECTIONS FROM CE-QUAL-ICM

4.1. Background

Nutrient enrichment and the problems associated with it have been receiving world wide attention (Boesch et al. 2001). The environmental effects are numerous and include initiation of hypoxia and anoxia (Boesch et al. 2001), change in biodiversity as well as species dominance, and harmful algal blooms (Loeuille and Loreau 2004). A quandary arose as to which the most important factors are controlling species in an ecosystem food web, the resources or the predators (Loeuille and Loreau 2004). This initiated the dispute of which control, “top-down” versus “bottom-up,” is more critical to the ecosystem. Since the late eighties and early nineties, the Chesapeake Bay Program has been practicing “bottom-up” nutrient controls with some success. One popular approach being considered in the Chesapeake Bay Program is called the “top down” approach based on the premise that restoring algal predators, such as oysters and menhaden, will limit excess phytoplankton production and possibly eliminate costly nutrient control programs. Managing nutrients based on a “top down” approach by increasing algal predators requires the ability to model higher trophic levels such as fish, as well as the eutrophication processes driving production of primary producers in an aquatic ecosystem. ICM and Ecopath were two models selected for linkage to investigate the “top down” approach of nutrient control. ICM is a time- and spatial-varying eutrophication model that uses nutrient loads to predict primary producers, while Ecopath is a static mass balance model representing an average time period (e.g., season or year) and uses values of primary producers and other groups to predict fish biomass. Linking the two models will provide the means of going up the food chain by trophic levels from supplying nutrients to primary producers, then primary producers to

fish. As a first attempt in understanding this process, ICM production can be inserted into Ecopath to see if fish biomass can be supported in the mid Chesapeake Bay.

Primary producers are seen as the backbone of a viable ecosystem. In an aquatic system, all groups of phytoplankton are the major primary producers. They provide the necessary energy in the form of carbon production for increased biomass. They are the bottom tier of the food chain and pass energy and nutrients up through a chain of consumers to help sustain life at upper trophic levels (Kiely 1997).

Net primary production is the rate at which new organic matter or energy of a system accumulates minus energy needed for respiration (Campbell 1987). This variable, along with primary producer biomass, is common to ICM and Ecopath. Since both models have been applied to the Chesapeake Bay mainstem (Hagy 2002; Cerco and Cole 1994; Cerco and Noel 2004), replacing these Ecopath parameters with ICM's made it possible to examine questions of higher trophic level sustainability. Although the modeling frameworks of the models are vastly different, a mass balanced system results once both models have been calibrated. As demonstrated by Tillman et al. (2006), ICM can reasonably predict the rate of primary production and phytoplankton biomass similar to values used in the Ecopath calibration run given the appropriate boundary conditions.

With net primary production of carbon by phytoplankton being an essential process to sustain upper trophic levels, an analysis was devised to see the implications of substituting values of net primary production predicted by ICM into the Ecopath calibration input data set developed by Hagy from literature values for the mid bay (Hagy 2002). Interchanging ICM's values with Ecopath's will also help further the possibility of linking the two models or if not linking, then perhaps using both models simultaneously to answer management questions for

fishery improvement or nutrient control. A number of questions addressed during this analysis were:

1. Are the biomasses of fish and other trophic levels (higher than phytoplankton) computed in Ecopath consistent with primary production computed in ICM? This run was conducted to see if simply replacing ICM primary producers and production/biomass (P/B) ratios could maintain mass balance and give similar results to Hagy's Ecopath base run. If not, what has to be done to re-establish mass balance?
2. Are the biomasses of fish and other trophic levels (higher than phytoplankton) computed in the Ecopath base run consistent with primary production computed in ICM from the 90% nutrient reduction run? Reducing ICM nutrients loads by 50% was an attempt to produce primary producer biomasses similar to what Hagy used for his 1950s restored Bay run. ICM nutrients loads were initially reduced by 50%. Reducing nutrients by themselves did not produce the results needed so ICM loads were further reduced by 90%.
3. What happens when the menhaden biomass is increased 20% in the Ecopath base input data file? Is this consistent with increasing predation by 20% in the ICM base run and substituting the resulting primary producer biomasses in Ecopath? Do these Ecopath runs produce similar results? In one run the predators are increased, while in the other the preys are decreased.
4. How does the Ecopath 1950s restored bay run compare to the Ecopath base run where values for primary producer biomass and P/B ratios were replaced with ICM values from the 90% nutrient reduction run? According to Hagy (2002), conditions in the Chesapeake Bay were very different than they are now. For one thing, the bay water was much clearer than what exists today. Will simply changing primary producer biomass produce the same biomass elsewhere?

4.2. Analysis Procedure

4.2.1. Model Applications to the Chesapeake Bay

The Ecopath application to Chesapeake Bay is documented in Hagy (2002). Summer (June–August) conditions were modeled for three regions of the Bay (Figure 3.6) using carbon as currency. The application represented conditions in the bay typical of the years 1985–1999. An application was also created that pictured the bay following nutrient load reductions sufficient to restore phytoplankton production to levels typical of the 1950s to early 1960s. Ecopath input files, as well as documentation, were provided to us by the originator.

The Ecopath application considered 34 groups (Table 3.5), including 3 detrital pools, 4 primary producers, 9 planktonic consumers, 5 benthic consumers, and 13 nektonic consumers. Application and validation of Ecopath require extensive searches of databases and documentation of information sources. More than 150 sources, ranging from raw data to peer-reviewed literature, provided input to the Ecopath simulation.

For this analysis, two calibrated models that had been applied to the same study area (e.g., mid bay) were used: ICM and Ecopath. The Cerco and Noel (2004) kinetics were adapted to the Cerco and Cole (1994) grid to produce the ICM calibration run representing 26 water quality constituents. Data used in this calibration effort were collected under the Chesapeake Bay Monitoring Program for 1984–1994, and results from the calibration run for 1984 were used for this study. Hagy (2002) had previously calibrated Ecopath for a total of 34 groups. He also used data in the Ecopath calibration from the Chesapeake Bay Monitoring Program for the same years as ICM calibration as well as data from literature. These calibration runs were considered base runs and will be referred to as such for this analysis.

Several steps were performed in completing the analysis, including:

1. Making three ICM model runs to get values for common variables of primary producer biomasses and P/B ratios to substitute into the Ecopath runs.
2. Substituting ICM common variables of primary producer biomasses and P/B ratios from the three ICM runs into the Ecopath base run.
3. Re-establishing mass balance in the modified Ecopath model runs containing the ICM primary producer biomasses and P/B ratios when necessary.
4. Making a run of the Ecopath base model with the original menhaden biomass increased and re-establishing mass balance if necessary.

The modeling effort began by conducting ICM runs to get values for common variables/“hooks” used in substitution into the Ecopath base input data files originally developed by Hagy. There were three runs conducted: (1) the ICM calibration run, considered the base run, (2) the ICM 90% reduced nutrient loading run, and (3) the ICM 20% increase in predation run. ICM output from these runs was then processed for the common “hooks” between the two models into units and regional/seasonal averages compatible to Ecopath units. All “hooks” had previously been identified by Tillman et al. (2006), but as mentioned above, only the “hooks” of primary producer biomasses and net primary production rates were needed for this analysis.

The Ecopath runs made were those starting with the Ecopath base input data file and substituting the ICM common “hooks” of primary producer biomasses and P/B ratios for all three ICM runs. Also an Ecopath base run was conducted with the menhaden biomass increased by 20%. No new Ecopath models were created from scratch. In all, four modified Ecopath base runs were made.

Model and data preparations to make runs to address the questions posed above were similar for all runs. Beginning with the first question, values for primary producer biomasses and P/B ratios from the ICM base run were substituted into the Ecopath base run input data file.

Groups considered primary producers were net phytoplankton, picoplankton, microphytobenthos, and submerged aquatic vegetation (SAV). Because the ICM net phytoplankton value includes picoplankton, the picoplankton biomass used for substitution had to be estimated. The percentage of picoplankton compared to net phytoplankton in the Ecopath data set was found by summing the values of net phytoplankton and picoplankton, dividing this number into picoplankton biomass, and multiplying by 100. ICM net phytoplankton biomass was then multiplied by this percentage to get the picoplankton biomass needed for substitution. The ICM original net phytoplankton value was then adjusted to account for the picoplankton value used in the modified Ecopath input data file. The ICM value for P/B ratio for all groups except picoplankton was calculated by dividing the net primary production of a group by the biomass of that group. Like biomass, the picoplankton P/B value used for substitution was estimated based on the percentage of picoplankton production to the total production (calculated as the sum of net phytoplankton and picoplankton production) in the Ecopath base input data. Adjustment to the ICM net phytoplankton P/B ratio was made to account for this. The new values of primary producer biomasses and P/B ratios were substituted into the Ecopath base input data set, with all other groups remaining unchanged. This was saved as a modified Ecopath base model identified as EWE-ICM base.

Addressing the second question above, again involved substituting ICM “hooks” of primary producer biomasses and P/B ratios into the Ecopath base run, but this time from the ICM run with nutrient loads reduced by 90%. This run was conducted to see if replacing the Ecopath base values with values from the ICM reduced nutrient run could produce results similar to the Ecopath 1950s restored bay run conducted by Hagy. The same groups discussed above were considered primary producers. ICM net phytoplankton and picoplankton biomasses were estimated as before, as well as their P/B ratios. Again, only the primary producer biomasses and

P/B ratios were substituted for the Ecopath values, while all other groups remained unchanged. This was saved as a modified Ecopath base model identified as EWE-ICM 90%R.

Making two runs using a modified version of the Ecopath base run addressed the third question. First, modifications were made to the Ecopath base input data file by simply increasing menhaden biomass by 20% without using any ICM output. Ortiz and Wolff (2002) performed a similar assessment on increased scallops (*A. purpuratus*) in the subtidal area in Tongoy Bay (Chile). They increased or decreased biomass of commercial or undesirable species to test management strategies. All other group variables remained the same for this run. This run was saved as a modified Ecopath base model identified as EWE-M20%. The second run to address question 3 was made by replacing primary producer biomasses in the Ecopath base input data file with values from an ICM run with predators increased by 20%. This ICM run was performed to emulate the Ecopath run with menhaden increased by 20%. This run was saved as another modified Ecopath base model identified as EWE-ICM 20%P. These model runs were called the menhaden runs.

The final question was addressed without making any new runs with ICM or Ecopath. By using results from the Ecopath 1950s restored mid bay run developed by Hagy and the modified EWE-ICM 90%R run, comparisons were made.

4.3. Mass Balancing EWE

With all the ICM runs completed and substitutions of common “hooks” made into the Ecopath base model, mass balance had to be re-established for the modified Ecopath models. This was done through reparameterization of the model [similar to the procedure described by Ortiz and Wolff (2002) and Kavanagh et al. (2004)].

In Ecopath, a set of linear equations representing all the groups modeled is set up and solved for one of four parameters [for a discussion of the equations and parameters, see

Christensen et al. (2004)]. These parameters are biomass, P/B ratio, consumption/biomass ratio (C/B), and ecotrophic efficiency (EE). In this study, the unknown parameter was EE which is defined as the portion of production utilized by the system. The value of EE must be between zero and one. Having $EE > 1$ for a group indicates that the system is over utilizing that group, so other steps have to be taken to reach mass balance. These steps included adjusting the diet composition of predators when necessary and/or reducing predator biomasses of groups having $EE > 1$. This was an iterative procedure, since making these adjustments did not always produce $EE < 1$ for a group. Sometimes if a predator biomass was reduced too much, $EE > 1$ resulted for other groups utilizing this predator. When this happened, adjustments had to be made again until the EEs of all groups involved were less than one.

4.4. Results and Discussion

ICM was used to predict carbon production for the mid CB for three separate runs to replace common variables of primary producer biomasses and P/B ratios in the original Ecopath base model developed by Hagy. This was an exercise to see if ICM predictions could maintain the higher trophic level organisms in Ecopath for the mid CB. In addition to the three Ecopath models developed from using ICM variables, another Ecopath model was developed by increasing the original menhaden biomass by 20%. Results from these model runs are presented in Figures 4.1–4.10. In the figure legends and axis titles, the Ecopath runs are identified with the following abbreviations:

- EWE Base is Hagy's original mid CB run.
- EWE-ICM Base is Hagy's original mid CB EWE run with ICM base values of primary producer biomasses and P/B ratios substituted.
- EWE-ICM 90%R is Hagy's original mid CB EWE run with ICM 90% nutrient reduction values of primary producer biomasses and P/B ratios substituted.

- EWE-ICM 20%P is Hagy's original mid CB EWE run with values of primary producer biomasses and P/B ratios from the ICM run with a predation increase of 20% substituted.
- EWE-M20% is Hagy's original mid CB run with menhaden increased by 20%.
- EWE 1950s restored bay is Hagy's original mid CB Ecopath 1950s restored bay run.

4.4.1. ICM Base Primary Production Replaced in EWE Base Run

Differences in biomass between the Ecopath (blue) and ICM (red) values of primary producers for the base runs are shown in Figure 4.1. In terms of biomass, net phytoplankton was the most important of the primary producers. Values for net phytoplankton and estimated picoplankton from the ICM base run were similar to the ECOPATH base values Hagy obtained from literature and monitored data. The greatest differences between the ICM and Ecopath primary producers occurred for microphytobenthos and SAVs. ICM's microphytobenthos biomass was slightly less than half of the Ecopath value, and ICM's SAV biomass was more than double the Ecopath value. Comparison of P/B ratios in Figure 4.2 shows that values from the ICM base run (red) are less than the Ecopath values (blue) except for picoplankton. This suggests that net primary production rates from ICM are lower. The picoplankton P/B ratio is about the same as Ecopath's value.

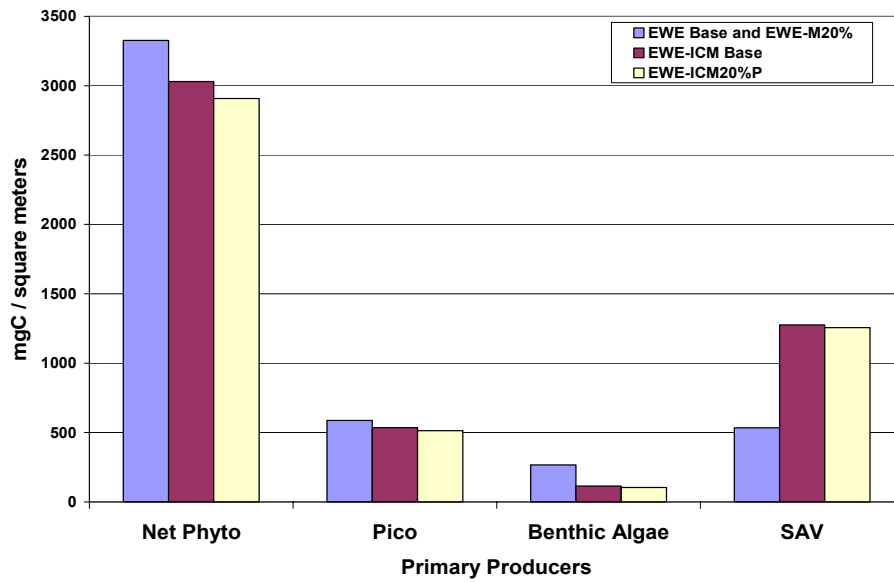


Figure 4.1. Primary producer biomass from EWE base and EWE-M20% (blue), EWE-ICM base (maroon), and EWE-ICM 20%P (light yellow) runs.

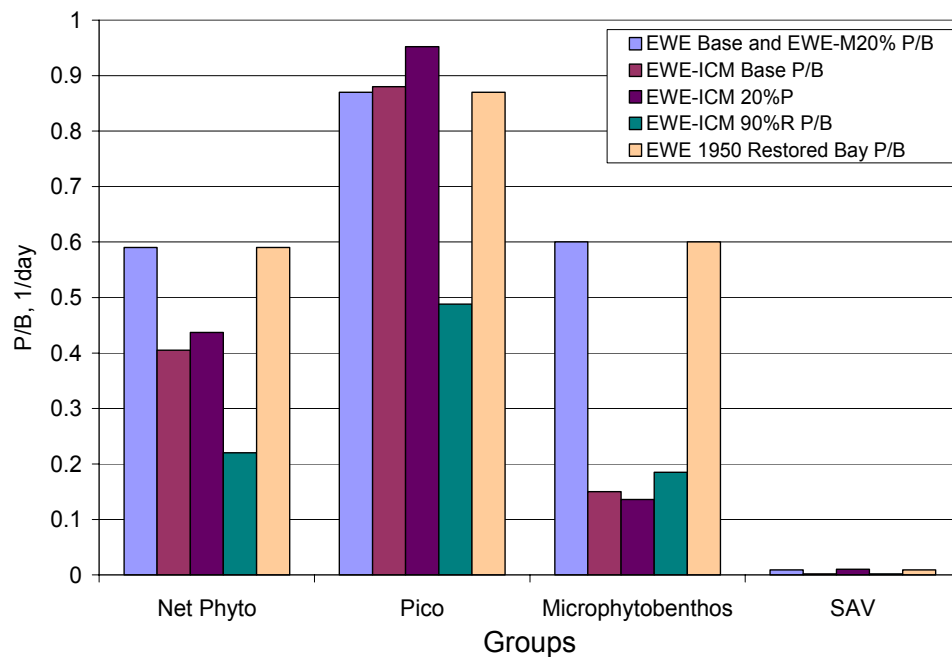


Figure 4.2. P/B ratios for primary producers all EWE runs.

Substituting ICM's primary producer biomasses and P/B ratios for Ecopath values and reparameterizing Ecopath produced some initial EEs > 1 for the following groups: microphytobenthos, dissolved organic carbon (DOC), and sediment particulate organic carbon (POC). Their EE values were 4.5, 1.35, and 1.16, respectively. These values indicate that all of these groups are being over utilized and that the model is not mass balanced. Figure 4.2 illustrates the interactions between groups with EEs > 1 and is only a small portion of the overall network of the groups modeled. In Figure 4.3, yellow boxes represent groups providing only detrital flow between groups; blue boxes represent groups providing detrital flow and/or predator/prey interaction with other groups. Additionally, black arrows indicate detrital flow pathways, while orange arrows indicate predator/prey interactions. Efforts to reduce the EEs began by reducing the biomass of their predators. Ecopath original predator biomass values were compared to the reduced values and are shown in Figure 4.4. Predator biomasses were reduced approximately 20–40%, depending on the effect to EE values. Reducing predator biomass helped reduce EEs for all groups except microphytobenthos. Although the EE for this group had not been reduced to less than one, its initial EE value had been reduced from 4.5 to 2.7. The difference between the original Ecopath base microphytobenthos biomass and the ICM biomass was so great that simply reducing the predator biomass was not enough to reach mass balance. To further reduce the EE of microphytobenthos, the diet compositions of its predators (again meiofauna and DFB) were modified. By comparison, the diet composition of the meiofauna changed the most of the two predators. Originally 50% of meiofauna's diet came from microphytobenthos but was modified to 17.5%, with more of its diet coming from benthic bacteria and sediment POC. This seemed like a reasonable change to diet composition since the preferred prey was no longer available or limited.

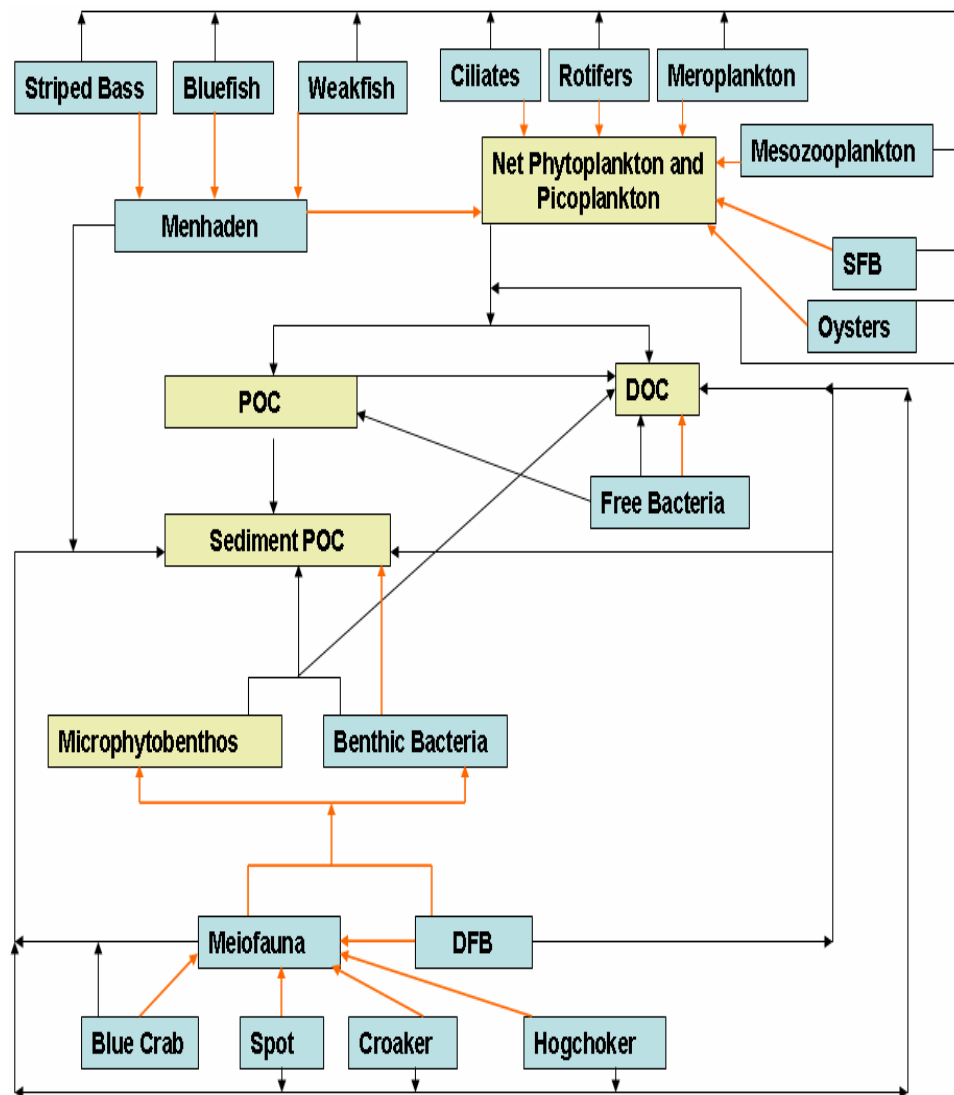


Figure 4.3. Network interactions through detrital flow (black arrows) and predators (orange arrows) of groups with $EE > 1$.

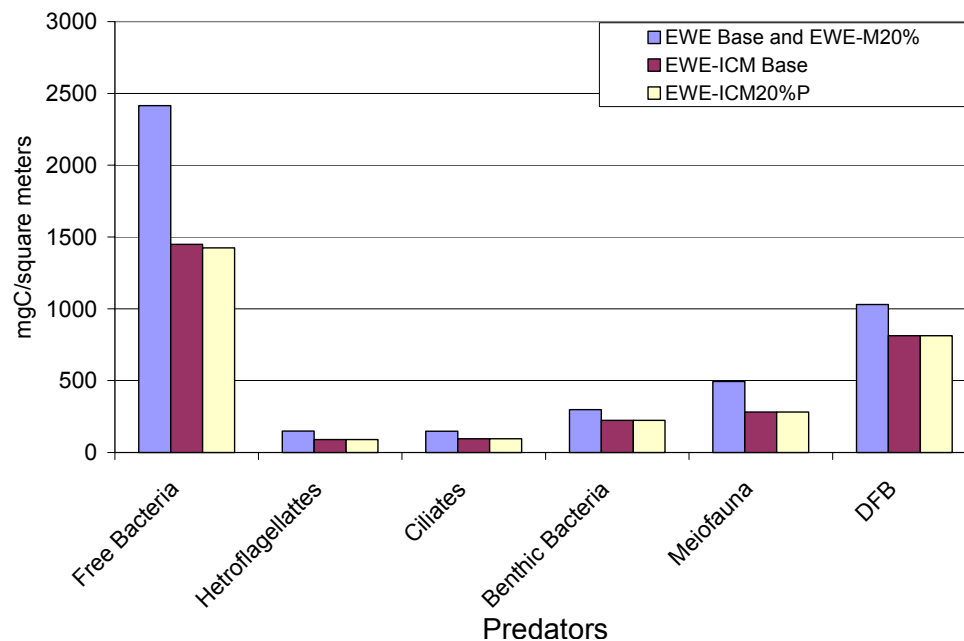


Figure 4.4. Adjusted predator biomasses of microphytobenthos, DOC, and sediment POC from the EWE base, EWE-ICM base, and EWE-M20% runs.

There were many options available to perform mass balance on the modified EWE-ICM base model, but in this study changes in lower trophic level groups were preferred over changes in upper trophic level groups unless it was necessary. This ensured that the original fish biomasses were maintained. Table 4.1 shows the total biomass of the system broken down by trophic level for the Ecopath base run and all modified Ecopath base runs. From the table, the majority of the total biomass is found in the lower trophic levels (i.e., trophic levels I, II, and III). This is normal for most network analysis as cited by the originator of the Ecopath model (Christensen et al. 2005) and is illustrated in Meyer and Poepperl (2002). In Table 4.1, the top three groups found in each trophic level are listed. Data in Table 4.1 also show changes in biomass distribution from run to run. Most of the biomass in EWE runs by Hagy have the larger

amounts of biomass in the trophic level II (TL II). This indicates a larger community of herbivores than EWE-ICM runs.

Table 4.1. Total biomass by trophic level for all EWE runs

Trophic Level / Major 3 Groups within Level	EWE Base total biomass (mgC m⁻²)	EWE 1950s restored bay total biomass (mgC m⁻²)	EWE-M20% total biomass (mgC m⁻²)	EWE-ICM base total biomass (mgC m⁻²)	EWE-ICM 20%P total biomass (mgC m⁻²)	EWE-ICM 90%R total biomass (mgC m⁻²)
IX / Chrysaora, Bay Anchovy	0.019	0.001	–	–	–	0.000
VIII / Mesozooplankton, Ctenophores, and Chrysaora	0.393	0.174	0.043	0.043	0.043	0.049
VII / Ctenophores, Chrysaora, Bay Anchovy	7.200	9.249	5.416	5.412	5.412	4.173
VI / Mesozooplankton, Ctenophores, and Bay Anchovy	45.117	57.82	42.181	43.651	43.396	37.504
V / Meroplankton, Mesozooplankton, and Bay Anchovy	150.997	100.158	138.226	163.595	170.459	100.559
IV / Ciliates, Mesozooplankton, and Bay Anchovy	593.799	420.228	563.86	587.701	596.945	438.322
III / Hetroflagellates, Mesozooplankton, and Ciliates	1928.96	2584.011	1974.55	1772.672	1769.841	1553.734
II / Free Bacteria, Benthic Bacteria, and Mesozooplankton	6794.818	12958.45	7088.576	5367.958	5329.808	5225.112
I / Net Phytoplankton, DOC, and Sediment POC	4711.00	9057.00	4711.000	4952.00	4778.00	3650.00

After mass balance was reached for the modified EWE-ICM base run, comparisons were made between system statistical parameters for this run and the EWE base run. These parameters included such variables as total system throughput (TST), all variables making up TST, and the sum of all production. As discussed in Chapter III, TST is defined as the size of the whole system in terms of flow (Christensen et al. 2004) and is found by summing total consumption, total export, total respiration, and total flows to detritus. Values of TST for the EWE-ICM base run were reduced by approximately 30% from 16,822 mg C m⁻² day⁻¹ (EWE base run) to 11,759 mg C m⁻² day⁻¹. This reduction is also seen for the parameters making up TST except total export (Figure 4.5). Total export [defined by Christensen et al. (2005) is the part of production that is exported from or consumed by predators of the system] increased from 9.25 to 59.14 mg C m⁻² day⁻¹. ICM net primary production rates for all primary producers were less than the values in the EWE base; this means that less carbon is produced. This is reflected in the sum of all production being 33% less for the EWE-ICM base run (Figure 4.5) than for the EWE base run. With less carbon production, there is less material to sustain the system as originally modeled. Adjustments made to the system were restricted to the lower trophic levels; thus, the fish populations were able to be maintained at the original level using ICM production.

The final statistic examined as far as system response was the transfer efficiency (how well was the food transferred through the trophic levels). Table 4.2 contains the transfer efficiency for all the runs simulated during this part of the research. Comparing EWE base with the EWE-ICM base, we see similar results in that detritus for both runs is transferred at a higher percentage and to higher trophic levels than flow from producers. Overall, a large amount of matter is transferred from the lower trophic levels illustrating how important these groups are to the production of a system.

Table 4.2. Transfer efficiency (%) from producers (first #) and detritus (second #) between trophic levels

Trophic Level / Major 3 Groups within Level	EWE-base TE %	EWE 1950s restored bay TE %	EWE-M20% TE %	EWE-ICM base TE %	EWE-ICM 20%P TE %	EWE-ICM 90%R TE %
VIII / Mesozooplankton, Ctenophores, and Bay Anchovy	– 0.9	– 1.7	- 0.9	– 0.9	– 0.9	– 1.4
VII / Ctenophores, Chrysaora, Bay Anchovy	– 2.1	– 2.6	– 2.1	– 2.1	– 2.1	– 2.6
VI / Mesozooplankton, Ctenophores, and Bay Anchovy	0.9 5.9	1.7 6.6	0.9 5.8	0.9 5.9	0.9 5.9	1.3 6.5
V / Meroplankton, Mesozooplankton, and Bay Anchovy	2.3 20.2	2.5 25.5	2.3 20.4	2.1 20.1	2.1 20.1	3.1 26.0
IV / Ciliates, Mesozooplankton, and Bay Anchovy	6.5 23.6	5.4 39.5	6.4 23.7	5.7 32.0	5.5 32.1	7.1 30.1
III / Hetroflagellates, Mesozooplankton, and Ciliates	15.6 13.9	13.3 24.2	15.6 13.9	15.6 16.8	15.3 16.5	18.9 24.6
II / Free Bacteria, Benthic Bacteria, and Mesozooplankton	20.8 33	17.5 23.5	20.2 34.6	24.6 31.1	24.5 31.2	26.8 31.8

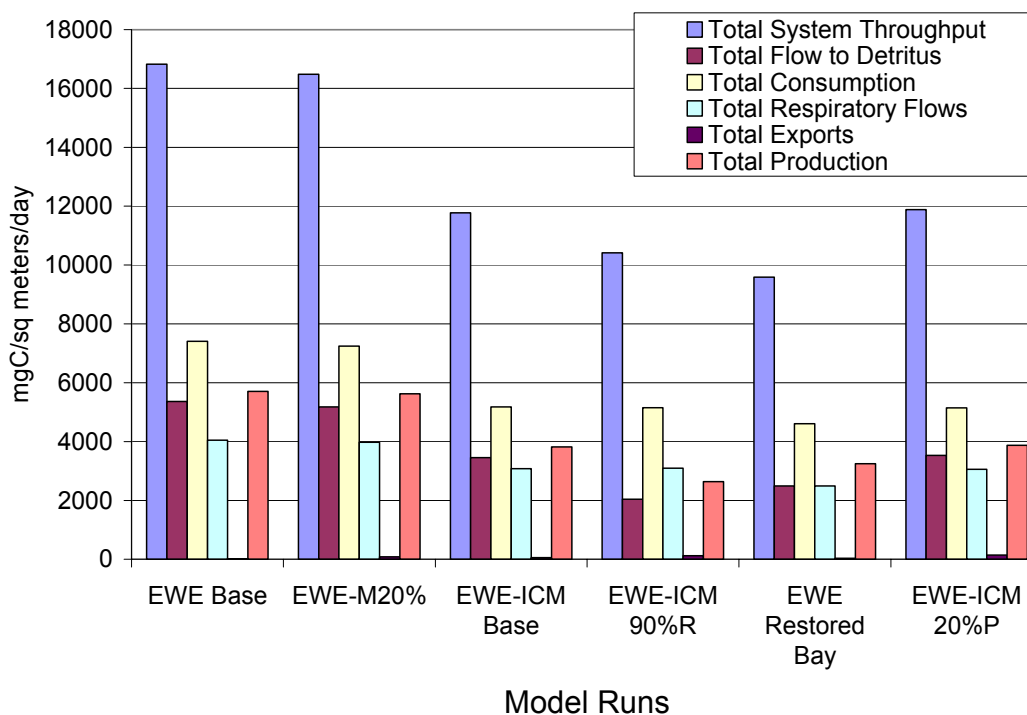


Figure 4.5. Sum of system production and TST including variables making up TST.

4.4.2. ICM 90% Nutrient Reduction Primary Production Replaced in EWE Base Run

Replacing values of primary producers and P/B ratios in the EWE base run with ICM values from the 90% nutrient reduction run was an attempt to emulate the EWE 1950s restored bay run developed by Hagy (2002). Differences between the EWE base values of primary producers and the EWE-ICM 90%R values are shown in Figure 4.6. Biomass values for net phytoplankton and estimated picoplankton were less than about half the values set in the EWE base run. ICM's microphytobenthos biomass was slightly greater than the EWE base values, and again ICM's SAV biomass was more than double the EWE base values. Although net phytoplankton biomass was less than half the value set in the EWE base run, this group and SAVs were the most important of the primary producers based on biomass (Table 4.1).

Differences in P/B ratios (Figure 4.2) were also evident between the two runs. Values of net primary production rate from ICM were again less for all primary producers than values used by Hagy for EWE Base.

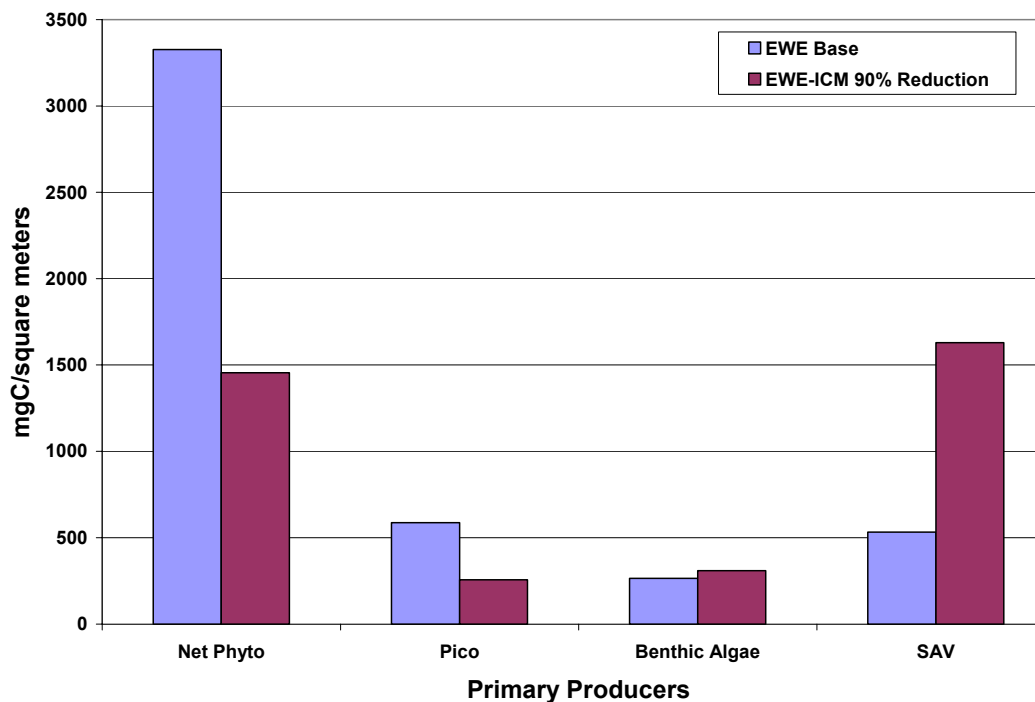


Figure 4.6. Primary producer biomass from EWE base (blue) and EWE-ICM 90%R (maroon) runs.

Substituting ICM values of primary producer biomass and P/B ratios from the 90% nutrient reduction run in for the EWE base values and reparameterizing EWE produced EEs > 1 for a number of groups. These groups included net phytoplankton, picoplankton, microphytobenthos, DOC, and sediment POC. Their initial EE values were 2.86, 1.46, 1.34, 2.84, and 1.3, respectively. These were the same groups, with the inclusion of net phytoplankton

and picoplankton, having EEs > 1 from the EWE-ICM base run. With biomass of net phytoplankton and picoplankton being half of the original values and all other groups remaining the same, producing EE values for these groups of greater than one is no surprise. Efforts to reduce the EE of these groups to re-establish mass balance began as before by reducing the biomass of their predators. Figure 4.7 shows the EWE base predator biomass values (blue) and the reduced values (maroon) from the EWE-ICM 90%R run. As before, changing lower trophic level groups was preferred over changing the upper trophic level groups so that the original fish biomasses could be maintained. Unfortunately, for this EWE run, upper trophic level groups had to be modified to re-establish mass balance. Net phytoplankton biomass from ICM was reduced so much from the original EWE value that reducing fish biomass could not be avoided. Its major predator biomass, menhaden, could be reduced only so much until its EE was affected. Consequently, there were not enough menhaden to sustain their predators (Figure 4.3). As discussed previously, all predator biomasses were reduced until EEs < 1 were re-established or the EE of other groups became adversely affected. After much iteration, all groups' EEs except net phytoplankton and DOC had been reduced to less than one. The EEs for these groups were still 2.115 and 2.579, respectively.

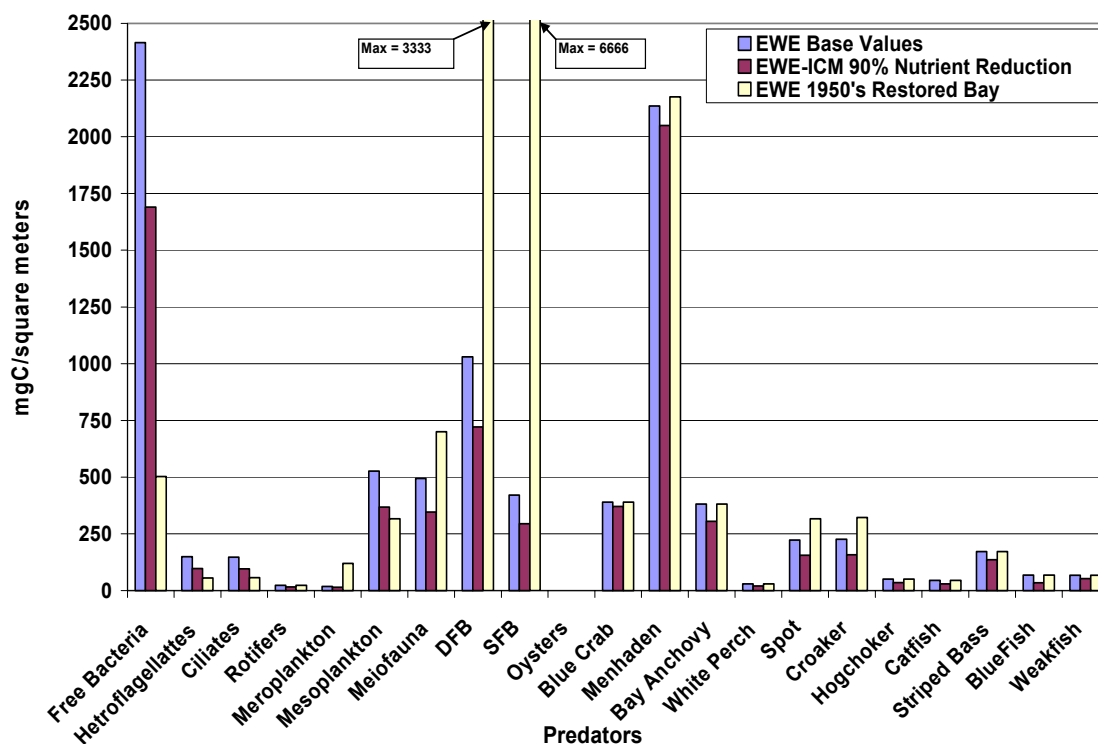


Figure 4.7. Predators of net phytoplankton in the EWE base (blue), EWE-ICM 90%R (maroon), and EWE 1950s restored bay (light yellow) runs.

To further reduce the EE of net phytoplankton and DOC, diet compositions for a number of predators were adjusted. Free bacteria were the only predator of DOC. There was only enough DOC biomass to provide 35% of its diet. For this reason, a DOC import of 65% was included to reduce the EE of DOC to less than one. In EWE, an import was considered consumption of a prey not part of the system (Christensen et al. 2004); for the EWE-ICM 90%R run, free bacteria are consuming DOC outside the system. In the same vein, Hagy had to import organic matter in the form of sediment POC and/or DOC for his EWE base run and 1950s restored bay run to get a balanced model. He identified his carbon source as resuspension of the spring algal bloom (Hagy 2002).

Getting a net phytoplankton $EE < 1$ proved to be more complicated than what had been done previously for the EWE-ICM base run. It was complicated in that many more iterations had to be made because of the complex interactions from changing the diets of so many predator groups (Figure 4.3). All of the predators came from the lower trophic levels of I, II, or III. The diet composition of each predator of net phytoplankton was shifted from net phytoplankton to other groups that were preyed on. Changes to diet compositions of all net phytoplankton predators saw the largest change to menhaden diet. They went from consuming 90% of net phytoplankton to 40% with most of their remaining diet being consumed from POC.

The value of TST for the EWE-ICM 90%R run is $10,417 \text{ mg C m}^{-2} \text{ day}^{-1}$. This value is about 38% less than the EWE base run and about 10% more than the EWE 1950s restored bay run. The difference between TST values for the EWE base run and the EWE-ICM 90%R run was expected because the primary producer biomasses were reduced by about half in the EWE-ICM 90%R run and the net primary production rate was also lower. As a result, the sum of all production is also less than 50% (Figure 4.5). It was surprising to see that the TST was quite similar between the EWE 1950's restored bay run and the EWE-ICM 90%R run, since the total biomass (excluding detritus) for the EWE restored bay run was almost double that of the EWE-ICM 90%R run (Table 4.1). The difference in total biomass was attributed to EWE 1950's values for bottom dwellers [i.e., see in Figure 4.7 DFB and suspension feeding benthos (SFB)] and SAVs (see Figure 4.6) being set to very high concentrations compared to the EWE-ICM 90%R run and even the EWE base run. In Hagy's EWE 1950s restored bay run, most other group values were set lower (some more so than others) than the EWE-ICM 90%R run or remained the same (Figure 4.7) with the exception of a few higher trophic level groups. They included menhaden, spot, and croaker. After Hagy made changes to the lower trophic level groups, he made changes to these groups by allowing EWE to solve for biomass rather than EEs.

Hagy set the SAVs biomass to the high value because the bay in the 1950s was clearer with more light penetration (Kemp et al. 2005; Davis, 1985; Cooper and Brush 1993), thus stimulating more SAV growth. In addition, he points out that during this period there is more activity in the benthic community (Smith et al. 2003), and based on biomass measurements from similar regional areas, he set these groups' biomasses accordingly.

The transfer efficiency for this run compared to the EWE base, EWE-ICM., and 1950s restored bay run shows similar TE even though biomass of net phytoplankton have been reduced by half. Benthic algae and SAV make up some of the loss by their increase in biomass (Figure 4.6). Transfer efficiencies from detritus are highest for TL II and TL IV while for producers it is TL II and TL III. As before, a large amount of matter is transfer from the lower trophic levels illustrating how important these groups are to the production of a system.

4.4.4. EWE Base Run with Menhaden Increased 20%

This EWE run was different from the others. There was no substitution of ICM values in EWE, only an increase in the original menhaden biomass in the EWE base run by 20%. All other group values remained the same. The same procedure was followed to balance the model; the new menhaden biomass was substituted into the input data, and EWE was reparameterized. By increasing menhaden biomass a slight imbalance of the system occurred. This was demonstrated by values of EEs being slightly > 1 for DOC and sediment POC. Their values were 1.01 and 1.002, respectively. With more menhaden preying on net phytoplankton, there is less of this group going to DOC and POC as detritus. Ultimately, there is less POC that goes to sediment POC and DOC. These detrital groups seem to be sensitive to system changes since their EEs were greater than one in all modified EWE runs. This is probably because their original EEs were very close to 1 in the EWE base run; any small change to groups that interact with these groups produces $EE > 1$. Predator biomasses of DOC and sediment POC were reduced—free

bacteria by 10% and benthic bacteria by 5%. Both predators are in the lower trophic level II as calculated by EWE. DOC and sediment POC EE values were so close to one that only one iteration was necessary to attain mass balance.

Increasing the menhaden biomass causes slight changes to the TST compared to the value from the EWE base run (Figure 4.5). The TST value for this run is $16,482 \text{ mgC m}^{-2} \text{ day}^{-1}$, compared to $16,822 \text{ mg C m}^{-2} \text{ day}^{-1}$. All values of parameters that make up TST have been reduced 3–5% except total exports. The value of total export changed from approximately 9 to $80 \text{ mg C m}^{-2} \text{ day}^{-1}$. Increased menhaden biomass seemed to have produced this change since menhaden are predators of net phytoplankton.

The transfer efficiency for this run is very similar to the EWE base. This suggests that the increase in menhaden did not have as big an influence as thought. The most noticeable change is a slight increase in detrital flow from TL II to TL III.

4.4.5. ICM 20% Increase in Predation Primary Production Replaced in EWE Base Run

For this run, ICM-generated values of primary producers and P/B ratios replaced values for these groups in the EWE base run. Increasing the predators by 20% in this ICM run was a way to imitate the EWE-M20% discussed previously, since higher trophic levels such as menhaden are not actually modeled in ICM. Increasing predation would be equivalent to increasing predator biomasses in EWE. Biomasses from this ICM run for the primary producers were slightly less for all groups when compared to the primary producer biomasses in the EWE base, EWE-M20%, and EWE-ICM base runs (Figure 4.1). As discussed above, the primary producer biomasses and P/B ratios of the EWE base and EWE-M20% were the same; thus the blue bar in Figure 33 represents both. In terms of biomass, net phytoplankton was again the most important primary producer. Differences in P/B ratios for primary producers of this run (Figure 4.2) were also noticeable when compared to values set in the EWE base/EWE-M20% and EWE-

ICM base runs. Values of net primary production rate except for microphytobenthos used to calculate P/B ratios were higher for this ICM run (even though biomasses were lower) than the other ICM runs conducted. The reason for this could be because although there is more production the increased predation negates the growth spurred by more nutrients thus there is less net phytoplankton, picoplankton, and SAV biomasses. Cerco and Tillman (2008) point out that increased grazing releases nutrients with the effect of relaxing nutrient limitation on algal growth.

Substituting ICM's primary producer biomasses and P/B ratios in for the EWE values and reparameterizing EWE produced some initial EEs > 1 for microphytobenthos, DOC, and sediment POC. Their EE values were 5.45, 1.32, and 1.15, respectively, and were very similar to the initial EE values from the EWE-ICM base run. This being the case, predator values were initially reduced by the same amount (Figure 4.4) as the EWE-ICM base run. This was enough to produce $EE < 1$ for the sediment POC but not the DOC. Thus, free bacteria biomass (i.e., predator of DOC; see network interactions in Figure 4.3) was reduced slightly from this initial value to produce an EE value for DOC of less than one.

As discussed for the EWE-ICM base run, microphytobenthos predator biomasses of meiofauna and DFB could only be reduced so much before they started affecting the EEs of other groups. Following the procedure to reduce EE, the diet composition of microphytobenthos predators was modified. For each predator it was set to values used in the EWE-ICM base run. Only the diet composition of meiofauna had to be modified slightly from these values; the diet composition of DFB was the same. By comparison, the diet composition of the meiofauna changed the most of the two predators. Originally 50% of meiofauna's diet came from microphytobenthos, but it was modified to 12.5%, with more of its diet coming from benthic bacteria and sediment POC.

Substitution of primary producers and P/B ratios from the ICM run with predation increased 20% into EWE results in a TST value that is quite different than the TST value resulting from the EWE-M20% run (Figure 4.5). The TST value for this run was 11,883 mg C m⁻² day⁻¹, compared to 16,482 mg C m⁻² day⁻¹ for the EWE-M20% run. All values of variables making up TST are different as well. Most variables are less than those produced by the EWE-M20% run except for the total exports (142 versus mg C m⁻² day⁻¹, respectively). The results from this run mostly resemble the results from the EWE-ICM base run. With primary producer biomasses being slightly less for the EWE-ICM 20%P run compared to the EWE-ICM base run, it seems logical that they would produce similar results. The sum of all production (identified as Total Production in Figure 4.5) is also less for this run compared to the EWE-M20% run, but it is slightly more than the EWE-ICM base run. This occurs because of the relaxed nutrient limitation thus increasing the net production of the primary producers.

The transfer efficiency for this run is very similar to the EWE-ICM base. Like the EWE-base /EWE-M20% comparison, this suggests that the increase in menhaden did not have as big an influence as one might expect. The most noticeable change is a slight increase in detrital flow from TL II to TL III.

4.5. Conclusions

In general, the results from the three modified EWE-ICM runs indicate that some higher trophic level groups (i.e., blue crab, white perch, spot, croaker, hogchoker, and catfish) cannot be supported without adjustments to their prey biomasses and diet compositions. Although these higher trophic level groups have reasonable EEs, groups that provide some of their diet do not. Of the groups with EE greater than one, net phytoplankton, picoplankton, and sediment POC affected higher trophic level groups while microphytobenthos and DOC affected lower trophic level groups. The imbalance of the system for the three modified EWE runs was attributed to

lower ICM primary producer biomass values (especially for net phytoplankton and microphytobenthos) and lower values of ICM net primary production rates for all primary producers except for the EWE-ICM 20%P run. These runs demonstrate the usefulness of coupling information from ICM to an existing Ecopath model to test management strategies that would take years of data collection to verify.

One consideration in coupling the models is for the user to be aware of the limitations. Ecopath looks at a snapshot in time, while ICM is time and spatial varying requiring data manipulation to get data into the form Ecopath needs. However if one thinks about it, data from literature may have to be averaged over a time period (i.e. a year) so it is similar in that respect although data from ICM has the added concern of being 3-dimensional. Also, ICM has had trouble in the past with formulation shortcomings. One persistent problem is being able to predict reasonable values for zooplankton production in the summer due to temperature effects on grazing (Cercu and Tillman 2008). Because of the formulation, higher temperatures cause zooplankton production to be practically nonexistent. This was evident in this study as the simulation period for the runs were averaged over the summer months and predicted zooplankton production rates were low. This can be a problem with the transfer of food to the higher trophic levels. Another group under-represented in this study by ICM is the deposit feeder group. Cercu and Tillman (2008) point out the problem with this group is that the ICM formulation presents one species while Ecopath represents another. It is not understood what the ramifications of this are other than in the transfer of material in Ecopath.

Results from the EWE-M20% run do not indicate direct problems with higher trophic levels, but to maintain mass balance, changes to predator biomasses of lower trophic level groups were made. Adjustments to the diet composition of the predators were not necessary for this run. However, instead of changing predator biomasses, perhaps mass balance could have been

achieved simply through diet modification of the predators. This seems reasonable given the fact that more predation causes competition food a food source: thus a shift to maintain production would be feasible.

When biomasses of the upper and lower trophic groups of the EWE 1950s restored bay run were compared to values from the EWE-ICM 90%R run, similar biomass reductions in the lower trophic level groups had been made (e.g., the values for free bacteria were 587 mg C m^{-2} from the EWE base run compared to 294 mg C m^{-2} for the EWE restored bay run and 256 mg C m^{-2} for the EWE-ICM 90%R run). However, changes in some lower trophic level group biomasses (i.e., SAVs, DFB, and SFB) for the EWE 1950's restored bay run were much greater than for the EWE-ICM 90%R run. This was attributed to Hagy assuming that the 1950's bay was cleaner with a much more active benthic community. This was based on data and observations in the literature from similar regional areas. From this, Hagy set values of SAVs and bottom dweller biomasses to reflect this difference from what exist today. Although the biomasses for these groups from the EWE-ICM 90%R run were different, this run could be representative of what could happen if nutrients were reduced for present-day conditions in the mid CB. This ICM run only presents changes as a result of nutrient load reduction and does not consider changes to light extinction or total inorganic solids. This will be further examined in the next chapter.

CHAPTER V

RECREATING HISTORICALLY DOCUMENTED CONDITIONS OF THE CHESAPEAKE BAY WITH CE-QUAL-ICM

5.1 Background

Of all the estuaries in the continental United States of America, the Chesapeake Bay is by far the largest with over 4,479 square (sq) miles of surface area encompassing the bay and its major tributaries. Since the 1950's, regular water quality monitoring has been conducted on the Bay to help identify causes of anthropogenic induced eutrophication and anoxia (Bratton et al., 2003). Before the 1950's, most data describing the conditions in the Chesapeake Bay were from historical descriptive observations (Hagy 2002).

Leading up to the 1950's, historical data and observations have presented the Chesapeake Bay as a thriving and very productive estuary (Cooper and Brush 1993). Since the time of European settlement in the Chesapeake Bay area, a key contributor in the degradation of water quality has been identified as increased human activity and settlement (i.e., agriculture, deforestation, population growth, sewage treatment and industrialization) (Burnett 1997; Kemp et al. 2005). Before this, impacts to water quality in this area were influenced mostly through climate changes (e.g., hurricanes and heavy snow and rain storm events) and Native American activities (Cooper and Brush 1993). As late as the 1800's, waters at Albany, New York were still being described as "crystal clear" (Paul 2001). Much of the blame for increased erosion from agriculture has been credited to the invention of the moldboard plow by Thomas Jefferson around the 1830's. Add this to the attitude of ambivalence toward concern for land conservation and major silting occurred in the upper Chesapeake Bay and major tributaries (Paul 2001). Physical erosion in the Bay has been reduced since the 1940's (Brush 1995).

Over the past 100 years, signs of over enrichment of nutrients (eutrophication) and decreased water clarity were noted in the Chesapeake Bay from sediment core samples (Kemp et al. 2005; Cooper and Brush 1993; and Nielsen et al. 2002). An over abundance of nutrients resulting in eutrophication is complemented by higher primary productivity (Paerl 2006; and Scavia and Bricker 2006; and Jaworski et al. 1992) which has been linked to anoxic and hypoxic conditions in the Bay (Taft et al. 1980; Officer et al. 1984). In the 1950's there were short periods of seasonal low dissolved oxygen waters, but these periods were short compared to what occurs now (Officer et al., 1984). Episodic anoxia and hypoxia have increased in duration and extent in the bottom waters of the Bay (Cooper and Brush 1993; Kemp et al. 1992). Hypoxia can adversely affect biota and severely hinder ecological interactions leading to detrimental effects on biological communities (Breitburg 2002; Hagy et al. 2004).

The more recent time period of the 1950's was still considered to have good water quality compared to the modern Bay water quality. Since the 1960's and 1970's, water quality in the Chesapeake Bay has become poorer through over abundance of nutrients and reduced clarity (Kemp et al., 2005). Not only has the water quality become poorer, but biodiversity of the communities of plants and animals been severely affected to the point that trophic levels are being controlled by different groups. For example, Marshall (1994) demonstrated through microscope analyses that the phytoplankton communities in the Chesapeake Bay switched from being dominated by large cell groups to small cell groups. Zimmerman and Canuel (2002) also verified the shift in phytoplankton communities by looking at biomarker ratios of dinoflagellates and non-diatom algae relative to diatoms which showed a significant increase in the last century. Because observed historical data are scarce, paleobotanical studies have been conducted to study the ratio of various groups of diatoms to one another to see the change in the past two centuries (Cooper and Brush 1991; Brush 1995).

Plant and benthic communities of the Bay have also declined and shifted to different groups controlling the communities in the past 50 years (Bayley et al. 1978; Kemp et al. 1983; Orth and Moore 1983; Holland et al. 1987; Twilley and Barko 1990; Kemp et al. 2005). From over enrichment, benthic communities suffer from reduced diversity and function (Dauer et al. 2000). Back in the 1950's and 1960's, the dominant SAV groups were *Vallisneria Americana*, *Najas* spp. and *Elodea Canadensis*. Over time they have changed to *Myriophyllum spicatum* (Davis 1985). Decline in communities of SAV's and macrobenthic communities has been correlated to the increased nutrients and sediment inputs from watershed development and urbanization (Kemp et al. 1983; Kemp et al. 2005; Malone et al. 1988; and Paul 2001). Primarily this has affected the light attenuation in the water column and reduced the production of both communities (Paul 2001; Kemp et al. 2005).

One of the questions this research explored is that knowing what we know about the driving forces of over abundance of nutrients and decreased water clarity, can we go back to conditions that were found in the 1950's mid Bay? Making adjustments to loads and coefficients controlling eutrophication through a numerical water quality model is one way to study this problem. In the previous chapter, a run was made with only loads reduced (90%) to try to produce the primary production set in Chesapeake Bay Ecopath by Hagy (2002) for his 1950's restored Bay run. By doing this, net phytoplankton was reduced to the appropriate level but SAV and microphytobenthos biomass did not increase to the level Hagy set. This is because other factors are affecting their growth besides loads. In this chapter, an attempt will be made to try to improve the previous ICM predictions by adjusting other coefficients associated with SAV and microphytobenthos growth and adjusting the loads to what was found in the 1950's. The approach taken is to answer the question of whether we can go back in time to more pristine conditions found in the Chesapeake Bay with thriving communities of SAVs and fish.

5.2 Approach

5.2.1. Model Version

CE-QUAL-ICM was chosen as the water quality model to use for the exercise to recreate 1950's conditions in the Chesapeake Bay because it has a long history of being calibrated and applied to the system for over 17 years (Cercio and Cole 1994; and Cercio and Noel 2004). As mentioned in Chapter II, CE-QUAL-ICM (ICM) was designed to be a flexible, widely applicable, state-of-the-art eutrophication model. There have been several versions of the model developed but the version used for the model runs in this part of the research was the Cercio and Noel (2004) 2002 Chesapeake Bay Eutrophication Model (CBEM). This version contains 24 state variables in the water column (see Table 2.1 in Chapter II) and is linked to a sediment diagenesis model developed by Di Toro and Fitzpatrick (1993). The sediment diagenesis model calculates predictions for up to 10 state variables and 6 fluxes.

The grid used in the model application contained close to 13000 cells (see Figure 3.9 from Cercio and Noel, 2004). There are approximately 2900 surface cells having non-orthogonal curvilinear coordinates in a horizontal plan. The z coordinates are in the vertical direction with the deepest part of the Bay being up to 19 layers deep. Layer thickness is fixed at 1.5 m for the subsurface layers while the surface layer can vary with forcing functions such as winds and tides.

The hydrodynamics model used to link with ICM was CH3D-WES (Johnson et al. 1993). CH3D-WES produced three-dimensional predictions of velocity, diffusion, surface elevation, salinity, and temperature for each grid cell. Numerically, CH3D is a finite-difference formulation having a grid of discrete cells. Inputs to drive the hydrodynamics model included wind speed, air temperature, tributary freshwater inflows, surface heat exchange, tides, and the time-varying vertical distributions of temperature and salinity at the open boundary

(Johnson et al. 1993). Ten years, 1985-1994, are simulated continuously using a five minute time step, and from these, two-hour hydrodynamics were determined as arithmetic means to be used in the water quality model. The use of intra-tidal hydrodynamics for this application differed from the earliest model application (Cercio and Cole 1994) in which Lagrangian-average hydrodynamics was stored at 12.4-hour intervals (Dortch et al. 1992).

The grid characteristics of the hydrodynamics model were the same as described above for the water quality model. The range of the grid is from the heads of tide on the tributaries to the continental shelf in the Atlantic Ocean.

Cercio and Noel (2004) used data to set boundary conditions from the Chesapeake Monitoring Program collected from 1985 to 1994, the EPA Chesapeake Bay Watershed Model (WSM), and reports from regulatory agencies provided to the EPA Chesapeake Bay Program Office. The hydrology was represented by river inflows, lateral inflows and ocean boundary interfaces. Loads included in modeling the Chesapeake Bay system were from many sources and encompassed types such as non-point loads, point-source loads, atmospheric loads, bank loads, and wetlands loads. For a complete discussion of setting boundary conditions and loads see Cercio and Noel (2004).

Before each simulation was conducted, a spin-up period (20 years) was run to allow for changes in nutrients loadings, light extinction, and patchiness to reach their full effect and approach equilibrium to the new conditions. Cercio (1995) reported that it took approximately 10-years for the eutrophication model to show a near-complete response to nutrient load reductions, mostly due to the relatively slow rate of processes in the sediments. Before each scenario run was conducted, the eutrophication model was run for 20 years (i.e., looping twice over the 10 years of hydrodynamic data consecutively) and writing out the conditions at the end of the run to use as initial conditions to start the actual scenario runs (i.e. 50% reduction of

nitrogen (N) and phosphorus (P) or 50% light attenuation reduction). The output from each run was then compared to base results (calibration) and each other.

5.2.2. Model Runs

Five simulations using the 2002 CBEM were conducted with analyses only discussed for the mid Bay except when noted. All model runs were simulated for the same time period, 1985 through 1994, but only analyzed for the 1985 through 1987 period. This time period covered two of the same years Hagy (2002) had developed the Chesapeake Bay Ecopath with Ecosim (EWE) models. The first model run was termed the base run and was a re-simulation of the calibration run from the 2002 CBEM recalibration application. This run was used as a reference for comparison to other model runs. Discussion and plots of calibration results and statistics can be found in Cerco and Cole (1994) and Cerco and Noel (2004).

Leading up to the 1950's restored mid Bay run, two sensitivity runs were conducted to help understand which parameters had the greatest impacts to limiting conditions of the system. Parameters and perturbations for these simulations were:

- 50% reduction in nitrogen and phosphorus loads (i.e., point source, non-point source, and tributary)
- 50% reduction in nitrogen and phosphorus loads and light attenuation (i.e., the variable, KEISS, in CE-QUAL-ICM)

Setting parameters for the fourth and fifth CE-QUAL-ICM model runs identified as the 1950's restored mid Bay runs were based on observed and monitored historical values in hopes of producing water quality conditions representative of the 1950's. Changes were made to the same parameters (nutrient loads and light attenuation) modified in the sensitivity runs with the inclusion of an additional parameter, patchiness. Patchiness represents the fraction of the bottom

cell covered by plants within an SAV bed. Values chosen for these parameters for the 1950's restored mid Bay run are discussed below.

To help with run identification within the text, the following are identifiers for each run:

- 2002 calibration run: base
- Sensitivity run 1: SR-1
- Sensitivity run 2: SR-2
- 1950's restored mid Bay run 1: 1950's RMB1
- 1950's restored mid Bay run 2: 1950's RMB2

5.2.3. Nutrient Loading Modifications for Sensitivity and 1950's Runs

Nutrient concentrations of nitrogen and phosphorus in the 1950's were less than concentrations found in the mid modern Bay. To estimate how much to reduce values of nitrogen loads used in the 2002 CE-QUAL-ICM CBEM Model for the 1950 restored mid Bay run, a review of NO₃ loading data for the Susquehanna River presented in Hagy et al. (2004) was made. The Susquehanna River provides approximately 60% of the freshwater flow and 80% of the dissolved inorganic nitrogen (DIN) to the Chesapeake Bay so loading conditions should be representative of total loads coming into the Bay. Values of annual averaged NO₃ loads with river flow for the Susquehanna River at Harrisburg were graphically presented and showed that annual NO₃ loading during the 1945-1969 period was fairly constant averaging 20 Gg yr⁻¹ (Gg = 10⁹ g). To compare to total nitrogen (TN) load data from Cerco and Cole (1994), this value was converted to annual TN using the relationship Hagy et al. (2004) developed correlating the TN loading at Conowingo to NO₃⁻ loading at Harrisburg and is written: $L_{TN,C} = -0.16 + 1.99 * L_{NO3,H}$ ($r^2 = 0.90$). A ratio of historic Bay loads to Hagy et al. (2004) loads was calculated and used as the multiplication factor for reducing the 2002 Chesapeake Bay Model TN loads to values for the 1950's run. The calculated ratio was 0.58.

The multiplication factor for reducing total phosphorus (TP) loads to 1950 conditions was estimated based on atomic ratios. Using load data from the 1994 calibration, the ratio of TN to TP was found (by Carl Cerco) using the equation:

$$1950 N = 1985 N \times 0.58 \quad \text{Eq. 5.1}$$

and

$$1950 P = 1983 P \times \frac{0.58 \text{ kg } 1950 N}{1 \text{ kg } 1983 N} \times \frac{22.8 \text{ kg } 1983 N}{\text{kg } 1983 P} \times \frac{\text{kg } 1950 P}{18.9 \text{ kg } 1950 N} \quad \text{Eq. 5.2}$$

$$1950 P = 1983 P \times 0.703.$$

5.2.4. Light Attenuation for Sensitivity and 1950's Runs

From historical pictures of SAV beds and written observation, inference can be made that water clarity in the Chesapeake Bay was much clearer than present day (Orth and Moore, 1987). Based on this, Hagy (2002) assumed light attenuation was half of what the present day value of 0.8 m^{-1} is. Light attenuation (K_e) in CE-QUAL-ICM is modeled as spatially varying and is solved as:

$$K_e = a_1 + a_2 \times ISS + a_3 \times V_{ss} \quad \text{Eq. 5.3}$$

where a_1 is the background attenuation (m^{-1}), a_2 is the attenuation by inorganic suspended solids (m^{-1}), and a_3 is the attenuation by organic suspended solids (m^{-1}).

For each segment of the Chesapeake Bay (Figure 5.1) in the model domain, coefficients of the equation were determined. To be consistent with Hagy, calculated values of K_e are halved during the CE-QUAL-ICM 1950's restored mid Bay and sensitivity runs.

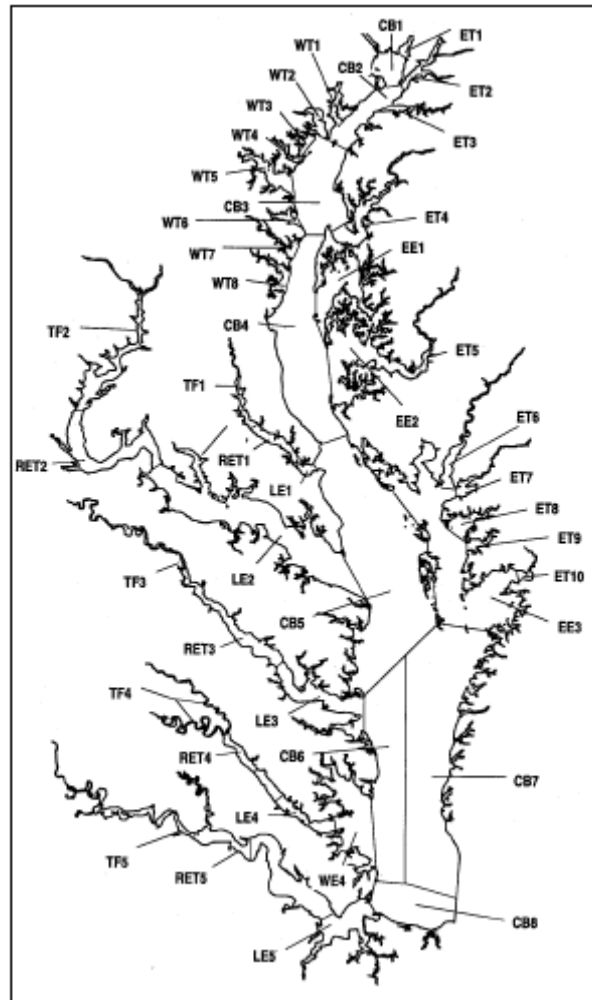


Figure 5.1. Chesapeake Bay program segments.

5.2.5. SAV Coverage for Sensitivity and 1950's Runs

Coverage of SAV beds in present day is believed to grow to about the 1 m depth while during the 1950's aerial photographs showed SAV coverage possibly grew in waters up to 2 m depth (Orth and Moore 1987). In the CE-QUAL-ICM formulation of SAV, SAV beds form a ribbon of littoral cells along the land-water margin of the system. Because the goal of SAV

restoration has been set to the two-meter contour line, width of littoral cells in the model is represented as the distance to the two-meter contour (Cercio and Noel 2004). To allow SAV to grow within a cell, a variable called patchiness was adjusted. It represents the fraction of bottom area covered by plants. This variable is found in the equation for estimating abundance within a cell and is:

$$M = SH \times A \times TE \times C \times P \quad \text{Eq. 5.4}$$

in which M is the above ground abundance (g C), A is the cell surface area (m²), TE is the truncation error, C is the coverage, and P is the patchiness.

For sensitivity runs patchiness remained at 0.1 however, for the 1950's restored mid Bay run, it was adjusted from 0.1 to 0.5.

5.3 Sensitivity Result Presentation

Two forms of graphical plots were used to compare base results with sensitivity results. The plots were time series of nutrient limitations and histograms of groups common to both CE-QUAL-ICM and Ecopath.

5.3.1. Time Series

Results for the CE-QUAL-ICM base model run were compared to results for both sensitivity model runs through daily time series plots of nutrient limitations for the primary producer groups: phytoplankton, benthic algae, and SAV. Daily time series plots were developed for the simulation period of 1985 through 1987. Since three groups of phytoplankton were modeled in the CE-QUAL-ICM applications (i.e., cyanobacteria, green, and diatoms), nutrient limitation values for the phytoplankton group were calculated as an averaged biomass weighted, areal average using the following equations:

$$Algae\ limit = \frac{\sum SA \times (B_1 \times FN + B_2 \times FN + B_3 \times FN) / (B_1 + B_2 + B_3)}{\sum RSA} \quad Eq. 5.5$$

where B_1 , B_2 , & B_3 are algal concentrations for algal groups 1, 2, & 3 (mgm m^{-3}), FN is the nutrient limitation (dimensionless), SA is the surface area of cell (m^2), Δz = layer thickness (m) RSA is the regional surface area.

Values of nutrient limitations for the other two primary producers (benthic algae and SAV) were calculated as an areal average using the equation below:

$$Benthic\ Algae\ Limit = \frac{\sum SA \times FN}{\sum RSA} \quad Eq. 5.6$$

where FN is the nutrient limitation (dimensionless), SA is the surface area of cell (m^2), RSA is the regional surface area.

These plots demonstrate the range of nutrient limitation where a value of zero is equivalent to total growth inhibition and a value of one is equivalent to no inhibition.

Limitations of the primary producers are shown in Figures 5.2 to 5.4.

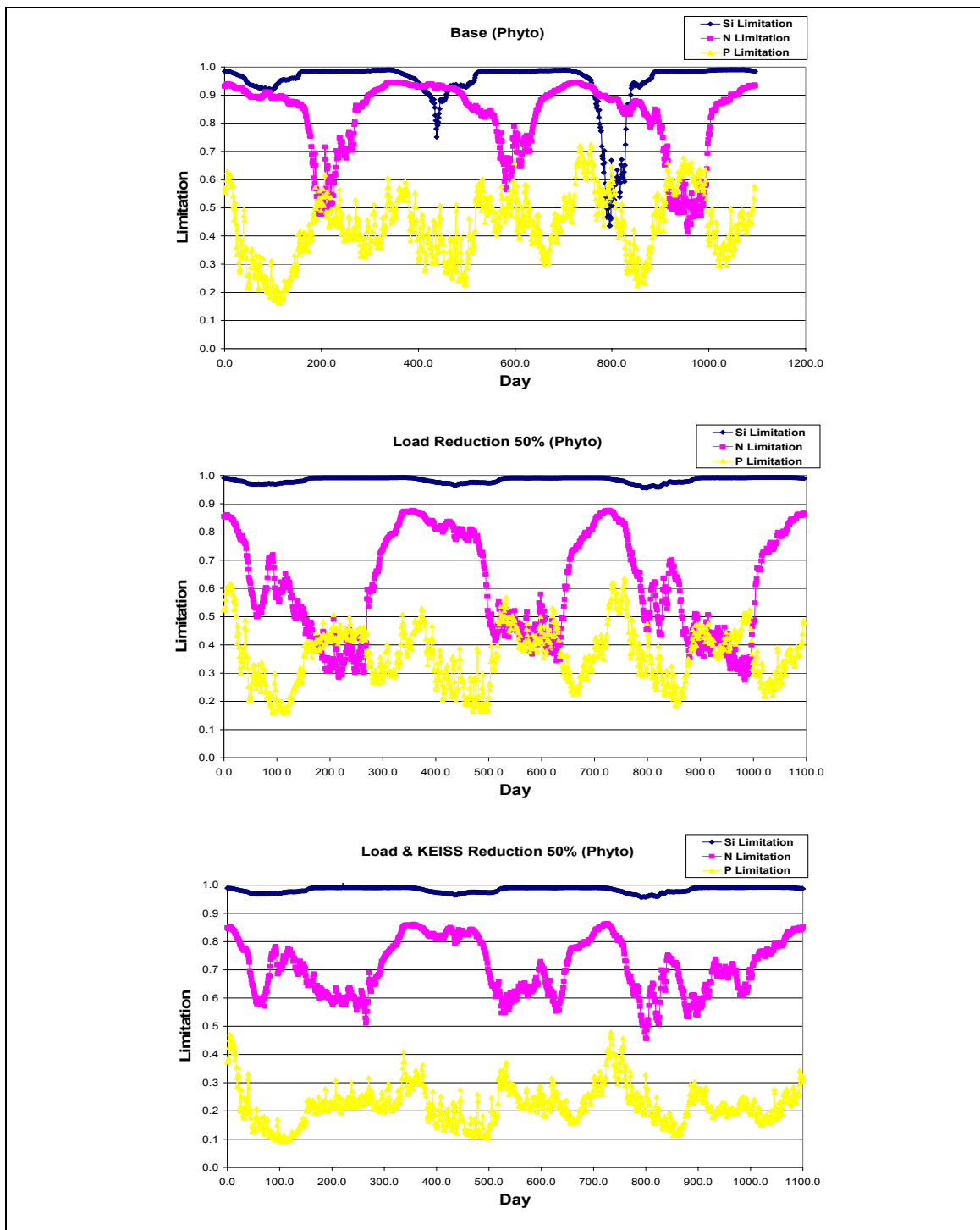


Figure 5.2. Phytoplankton limitation results for base, SR1, and SR2 in the mid Chesapeake Bay.

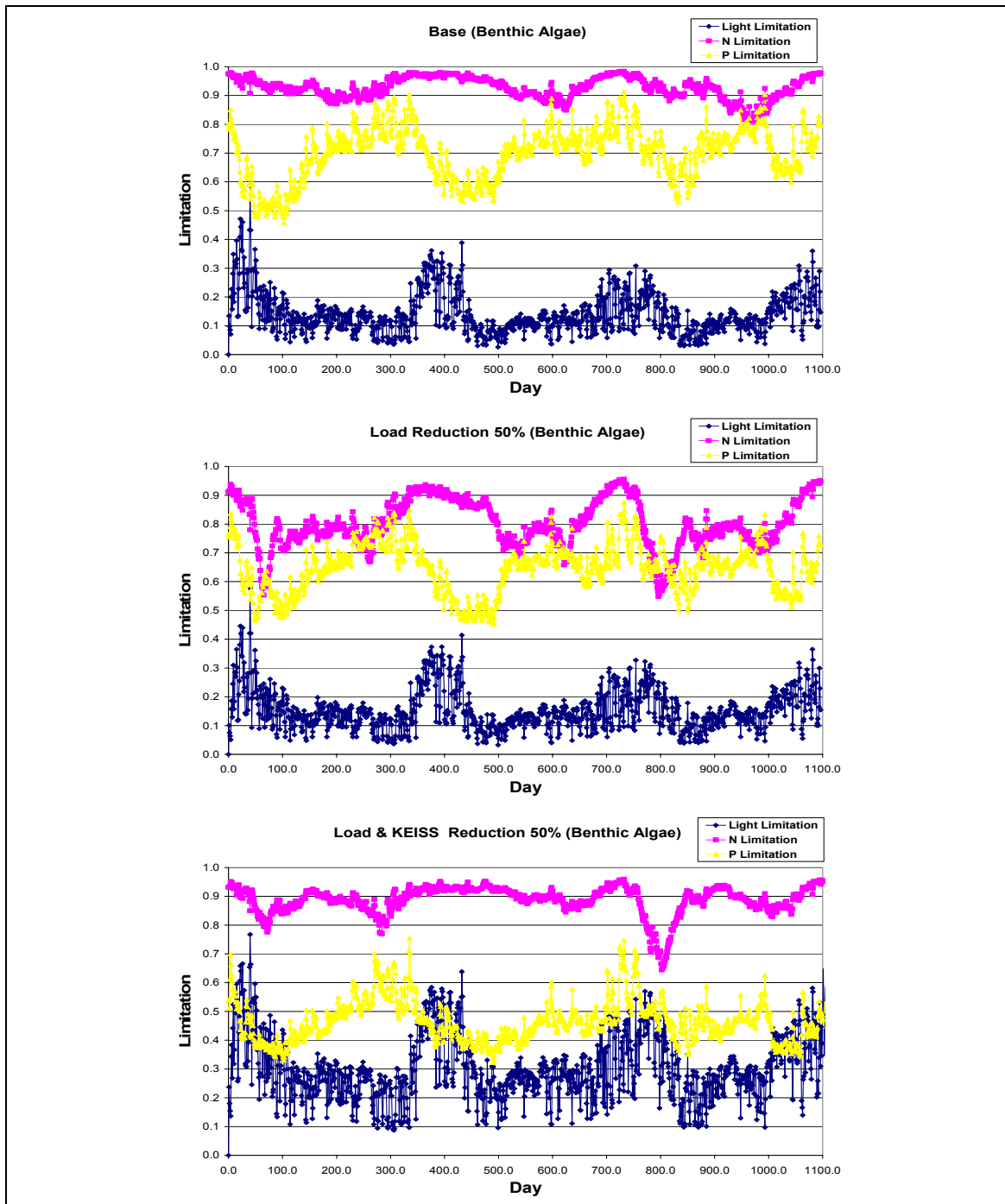


Figure 5.3. Benthic algae limitation results for base, SR1, and SR2 in the mid Chesapeake Bay.

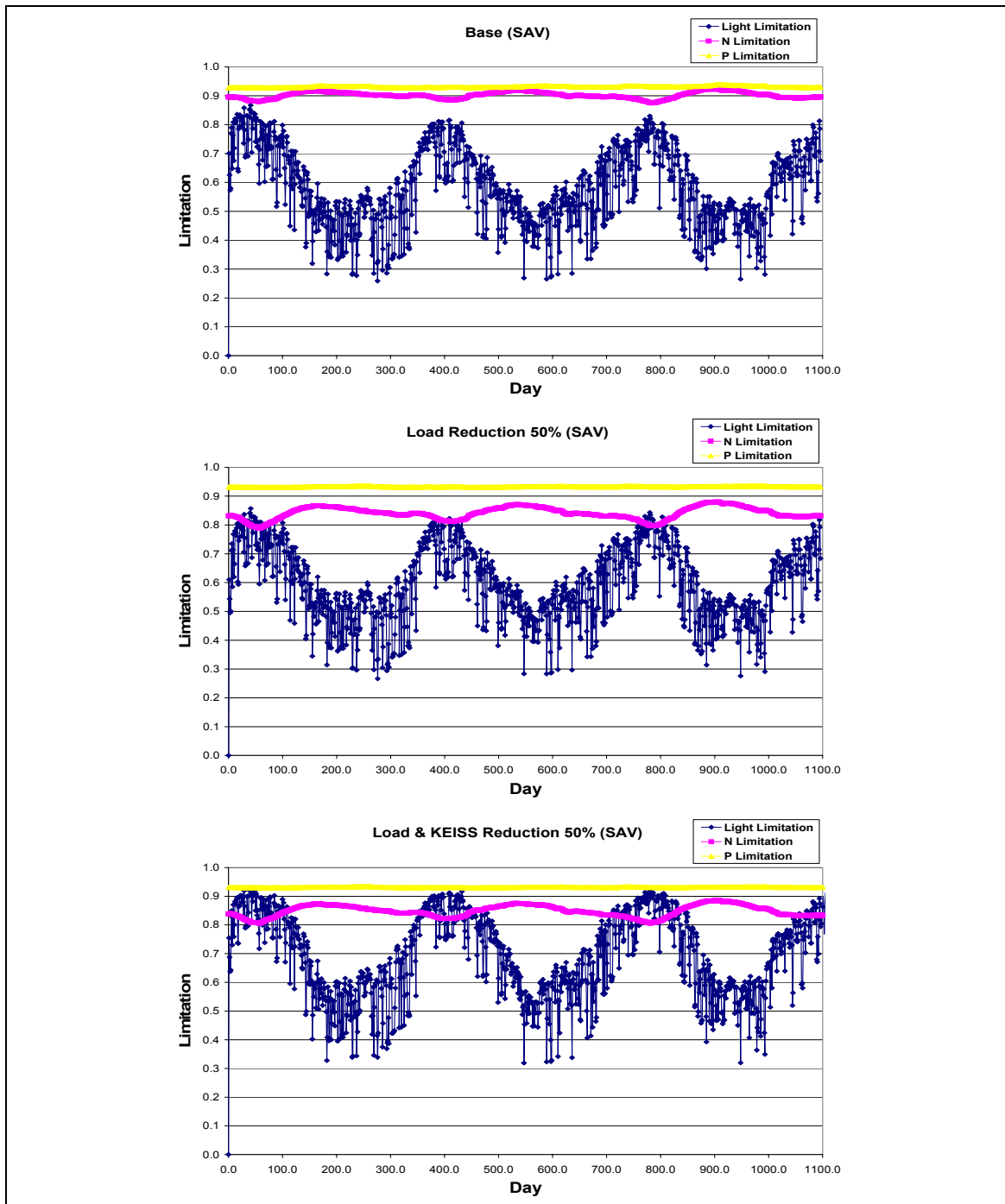


Figure 5.4. SAV limitation results for base, SR1, and SR2 in the mid Chesapeake Bay.

Histograms of biomass, P/B (production over biomass) ratios, Q/B (consumption over biomass) ratios and, UA/B (unassimilated food over biomass) ratios are presented for each group of interest in Figures 5.5 through 5.8. Each histogram represents the summer average of 1986 (June 1 through August 31) of each variable plotted from the groups of interest.

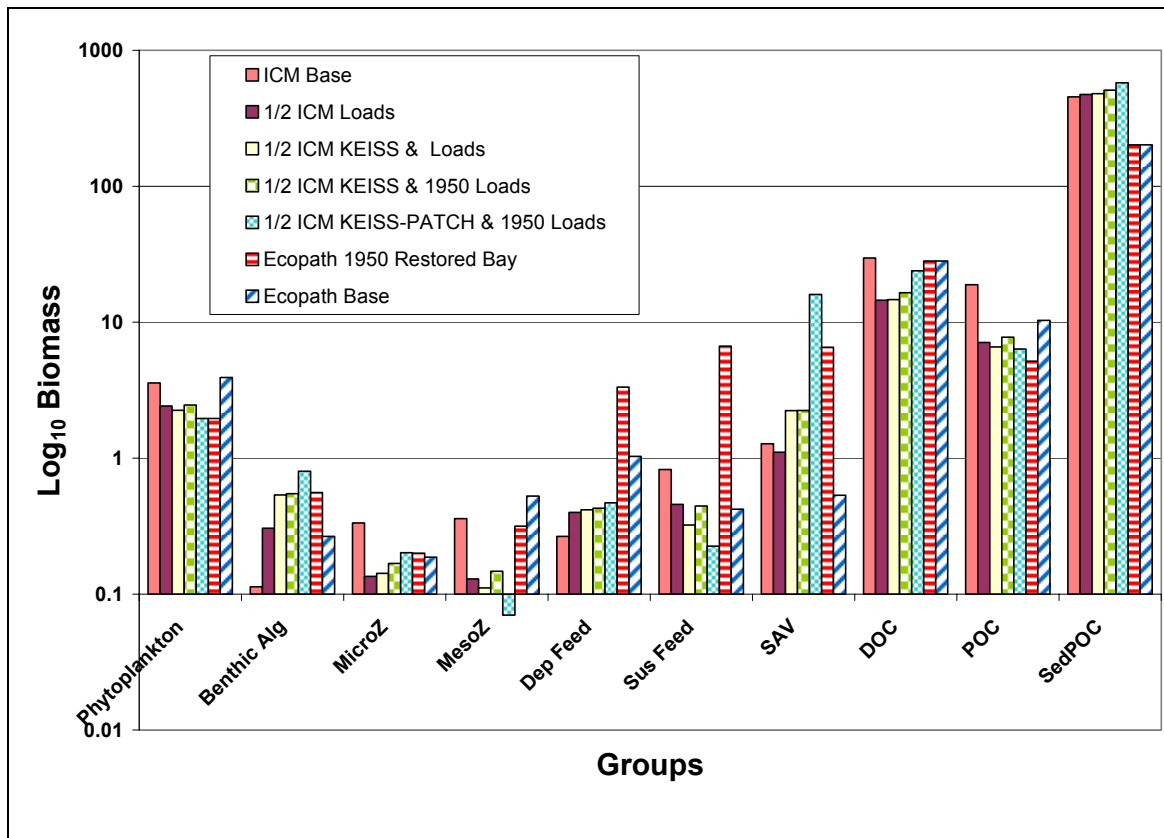


Figure 5.5. Comparison of biomasses for each group common to ICM and Ecopath.

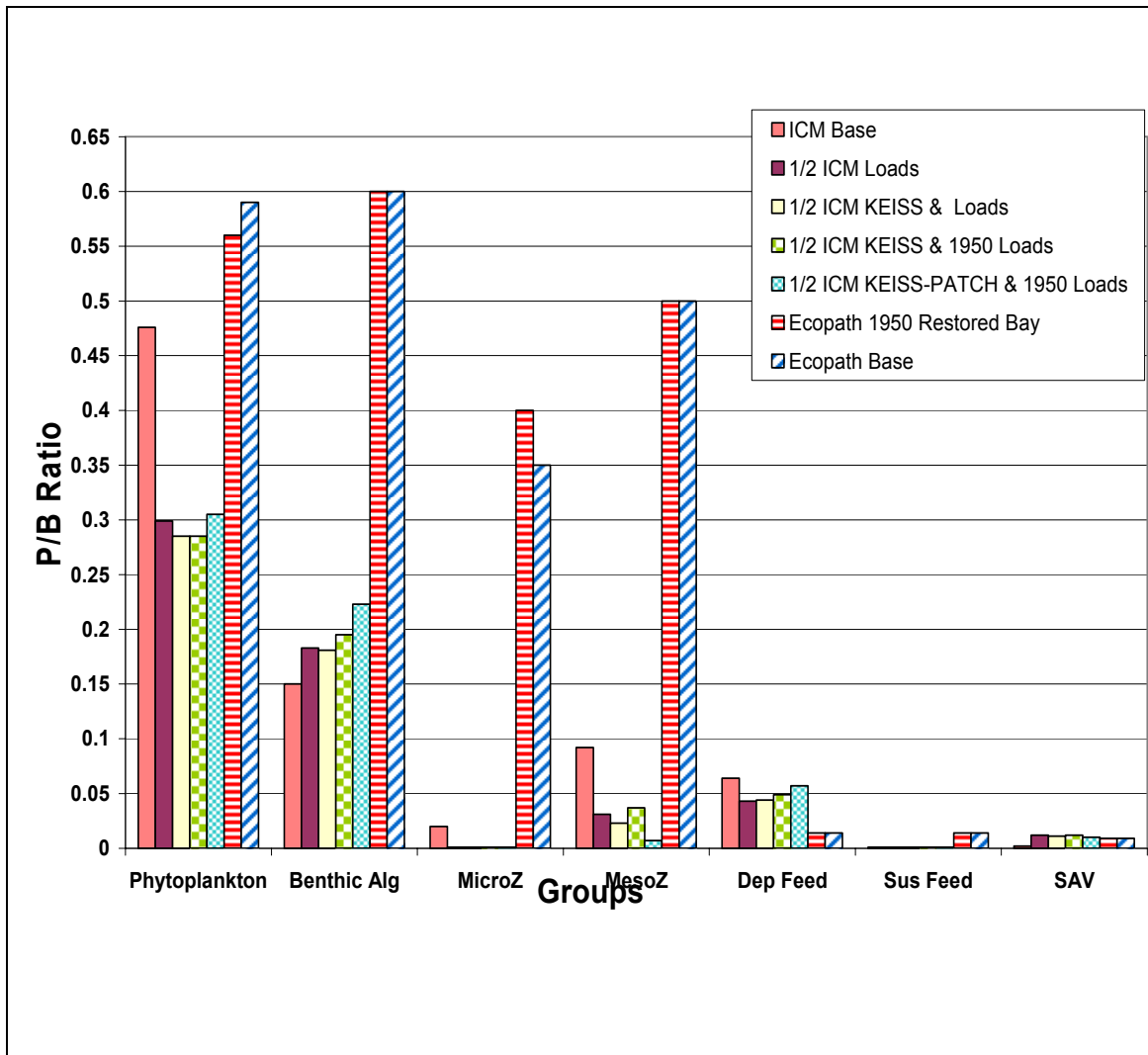


Figure 5.6. Comparison of P/B ratios from ICM to values used in Ecopath.

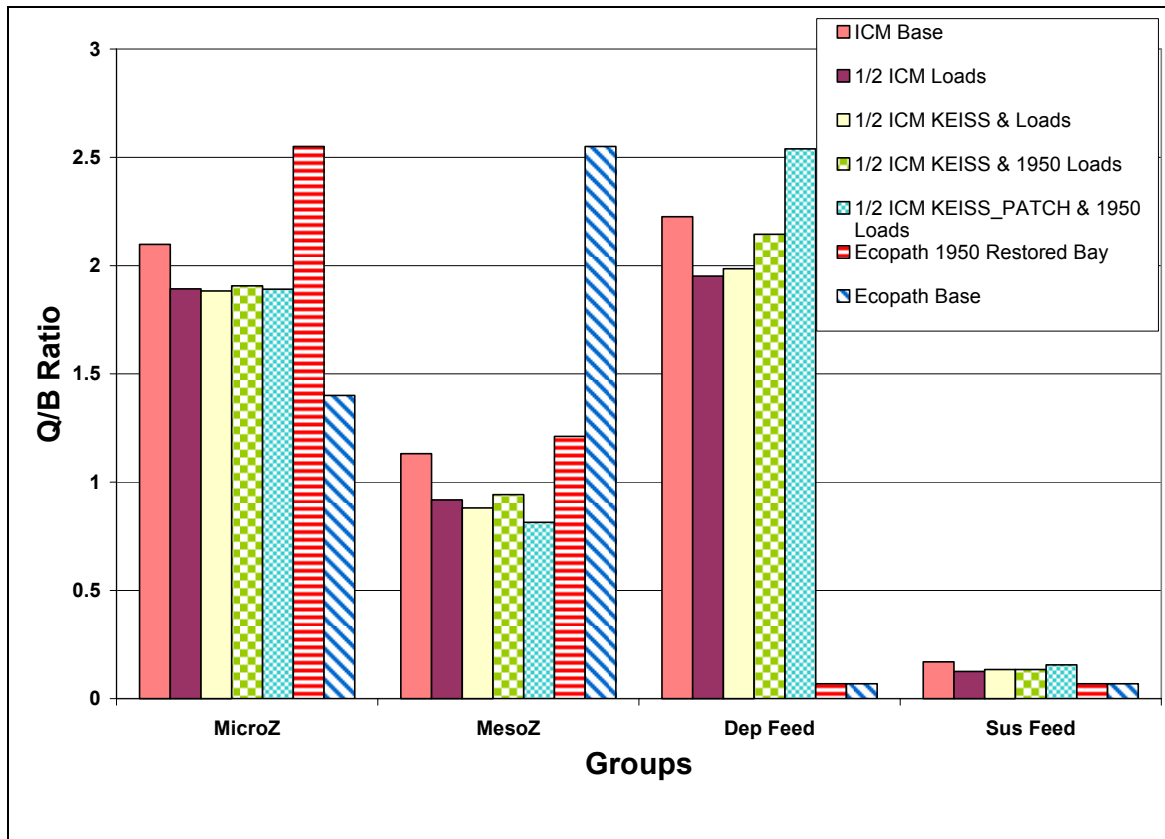


Figure 5.7. Comparison of Q/B ratios from ICM to values used in Ecopath.

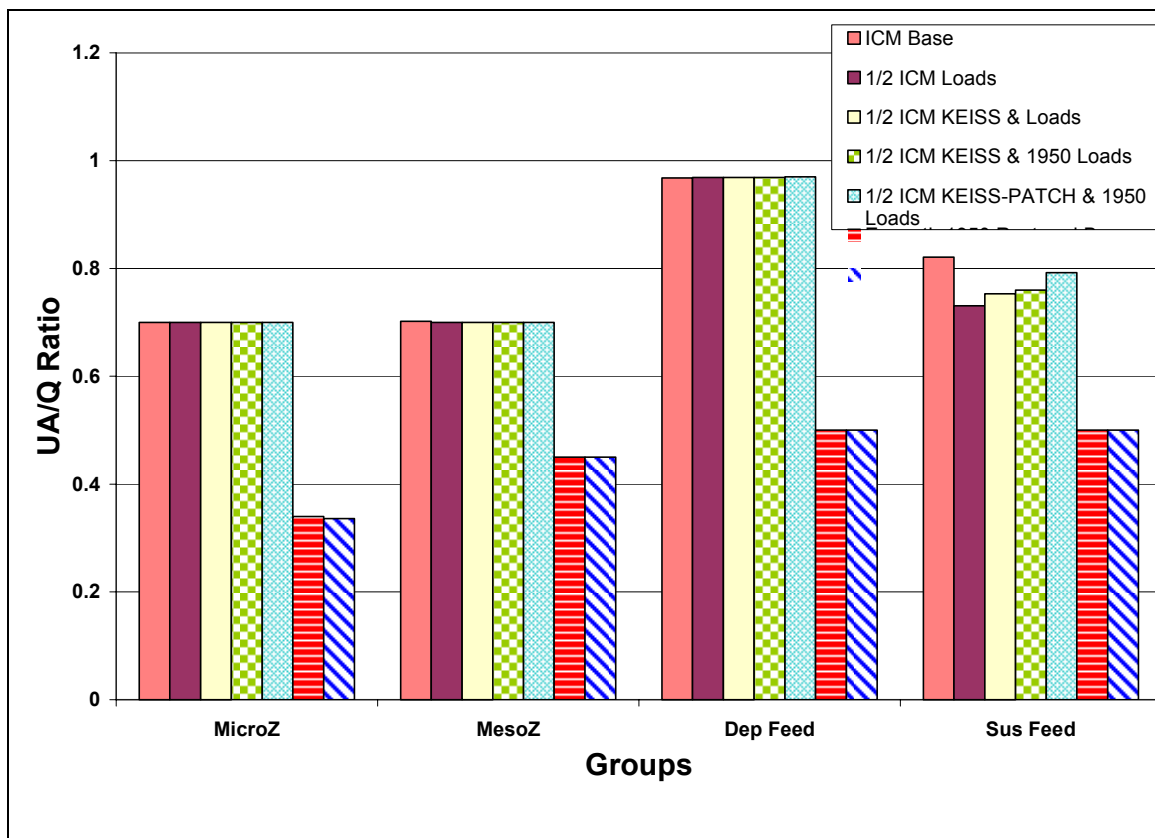


Figure 5.8. Comparison of UA/B ratios from ICM to values used in Ecopath.

Four forms of graphical plots were used to compare base results with the 1950's restored mid Bay results. They include time series, histograms, longitudinal, and DO Volume-day plots. Variables plotted as histograms were included on Figures 5.5- 5.8 discussed previously for the sensitivity run results. Other graphical forms used in comparison of the 1950's restored mid Bay results to base results are discussed below.

5.4. 1950's Restored Bay Result Presentation

5.4.1. Time Series

The CE-QUAL-ICM base model results were compared to 1950's mid modern Bay model results through time series plots. They were developed for the complete simulation period

(1985 through 1987) for all variables most affected by adjustments to nutrient loads and coefficients in an attempt to generate water quality conditions of the 1950's. These included the variables: chlorophyll *a*, dissolved oxygen (DO), total nitrogen (TN), total phosphorus (TP), nutrient and light limitations, and light extinction. These plots demonstrate model performance over time and provide indications of interactions between modeled parameters.

Results are shown for the three regions of the Chesapeake Bay (upper, mid, and lower as denoted in Figure 3.6) as defined by Hagy (2002). For each region, time series plots were developed for three levels in the water column which were:

- Surface level - upper four layers of grid (Figures 5.9 - 5.13).
- Pycnocline level - next four layers of grid (Figures 5.14 - 5.17).
- Deep water level - all cells below layer eight of grid (Figures 5.18 – 5.21).

A volumetric average of concentration is displayed on each plot for the variables listed previously. In addition to volumetric concentration time series for each region, time series were also developed to present algae as biomass per unit area (mg CHL m⁻²) using the formula:

$$Alg\ Biomass = \frac{\sum((B_1/cchl1 + B_2/cchl2 + B_3/cchl3) \times SA) \times \Delta z}{\sum RSA} \quad Eq. 5.7$$

where B₁, B₂, & B₃ = Algal concentrations for algal groups 1, 2, & 3 (mgm m⁻³), cchl1, cchl2, & cchl3 are the carbon to chlorophyll ratio, SA is the surface of cell, Δz is the layer thickness (m), and RSA (m²) is the regional surface area.

These time series are shown in Figures 5.22 through Figure 5.24.

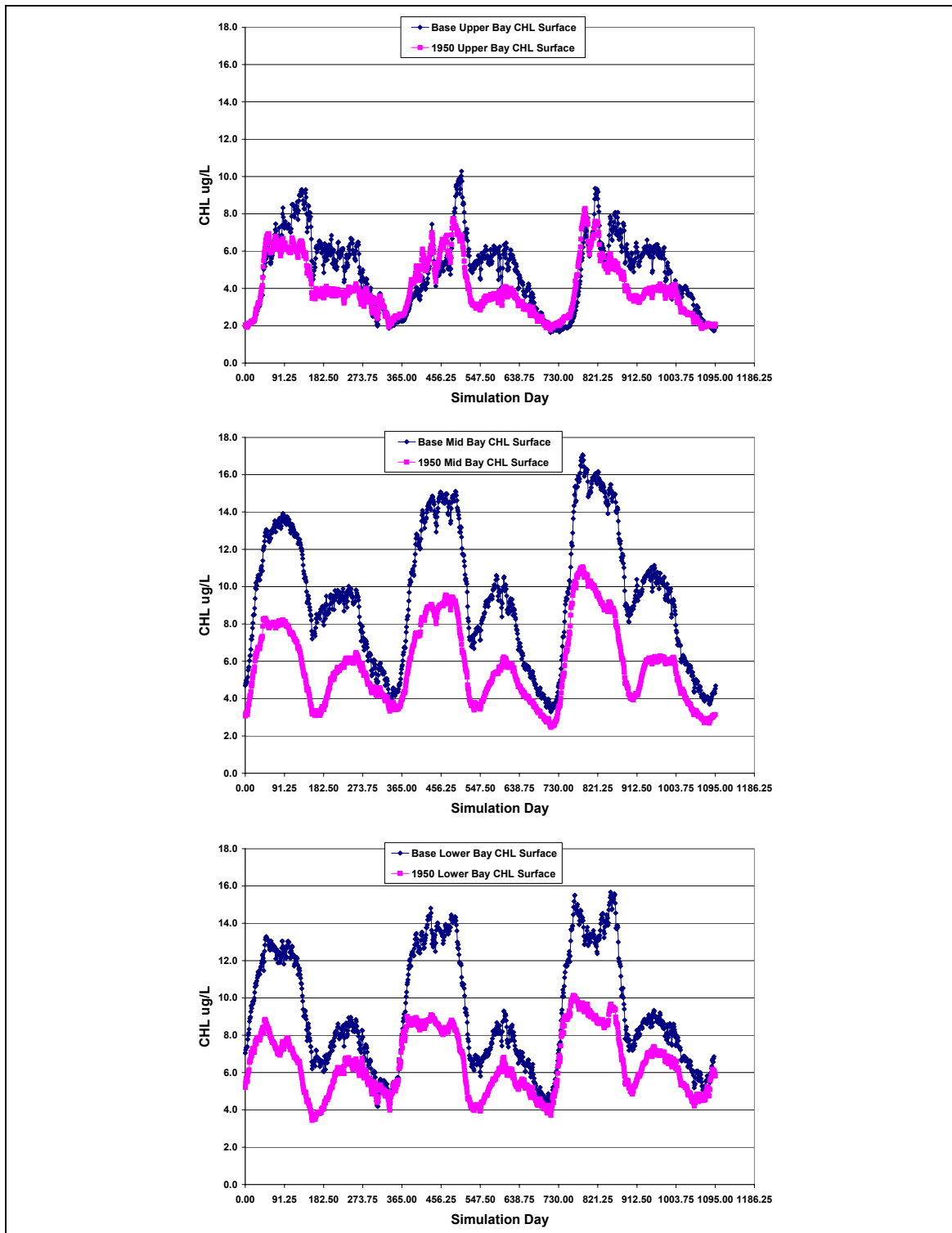


Figure 5.9. Comparison of surface chlorophyll *a* for base and 1950's RMB2 results in the upper, mid, and lower regions of the Chesapeake Bay.

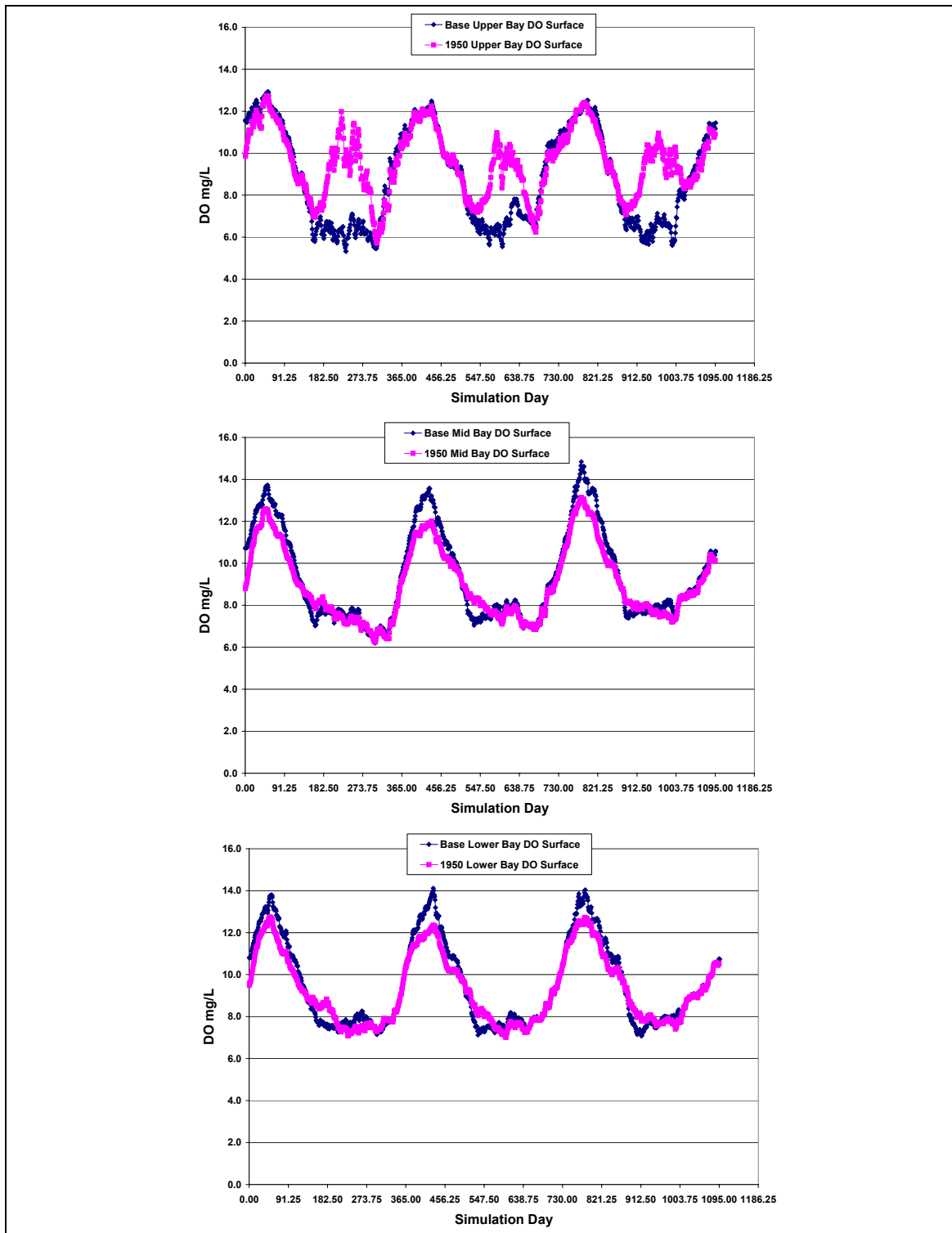


Figure 5.10. Comparison of surface DO for base and 1950's RMB2 results in the upper, mid, and lower regions of the Chesapeake Bay.

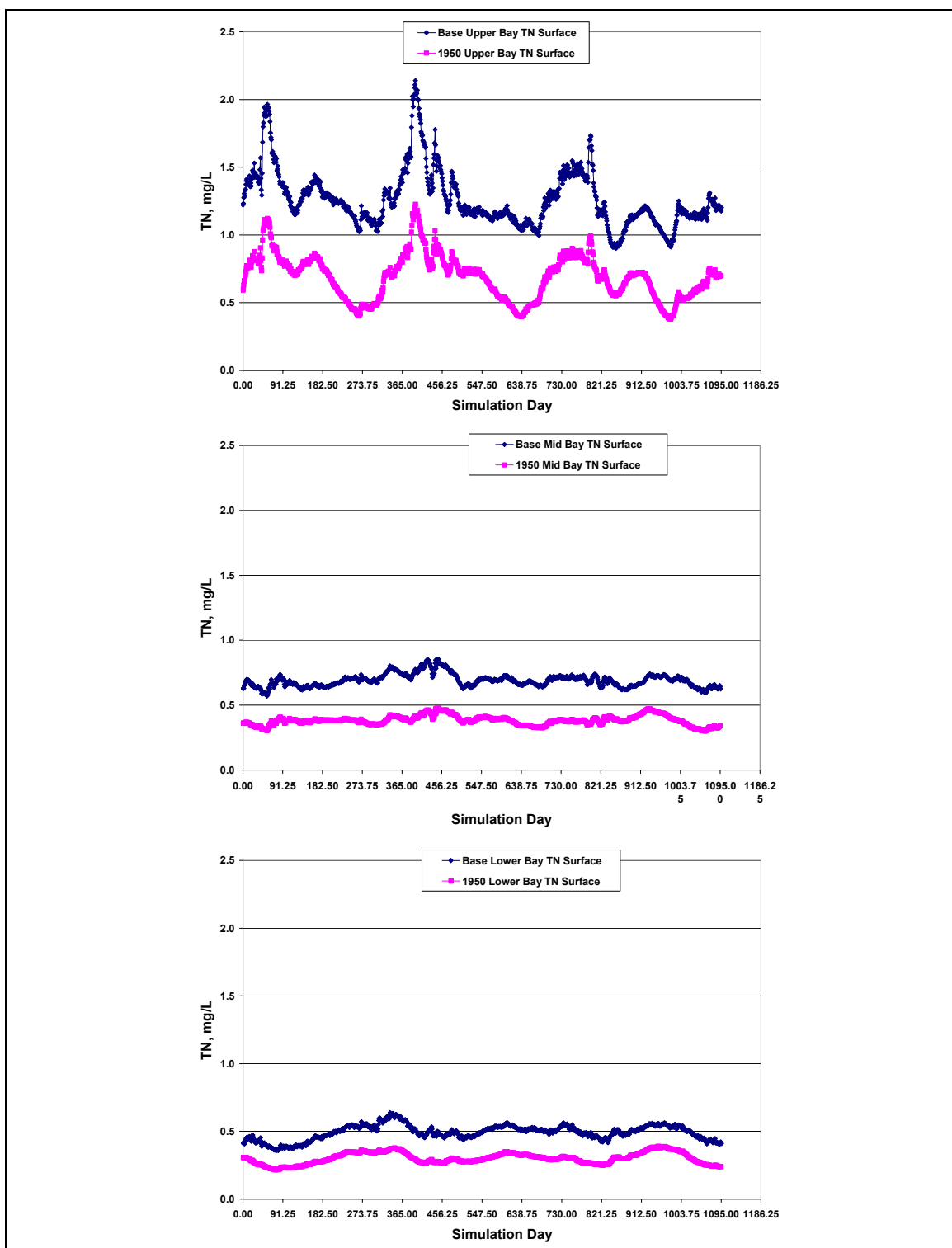


Figure 5.11. Comparison of surface TN for base and 1950's RMB2 results in the upper, mid, and lower regions of the Chesapeake Bay.

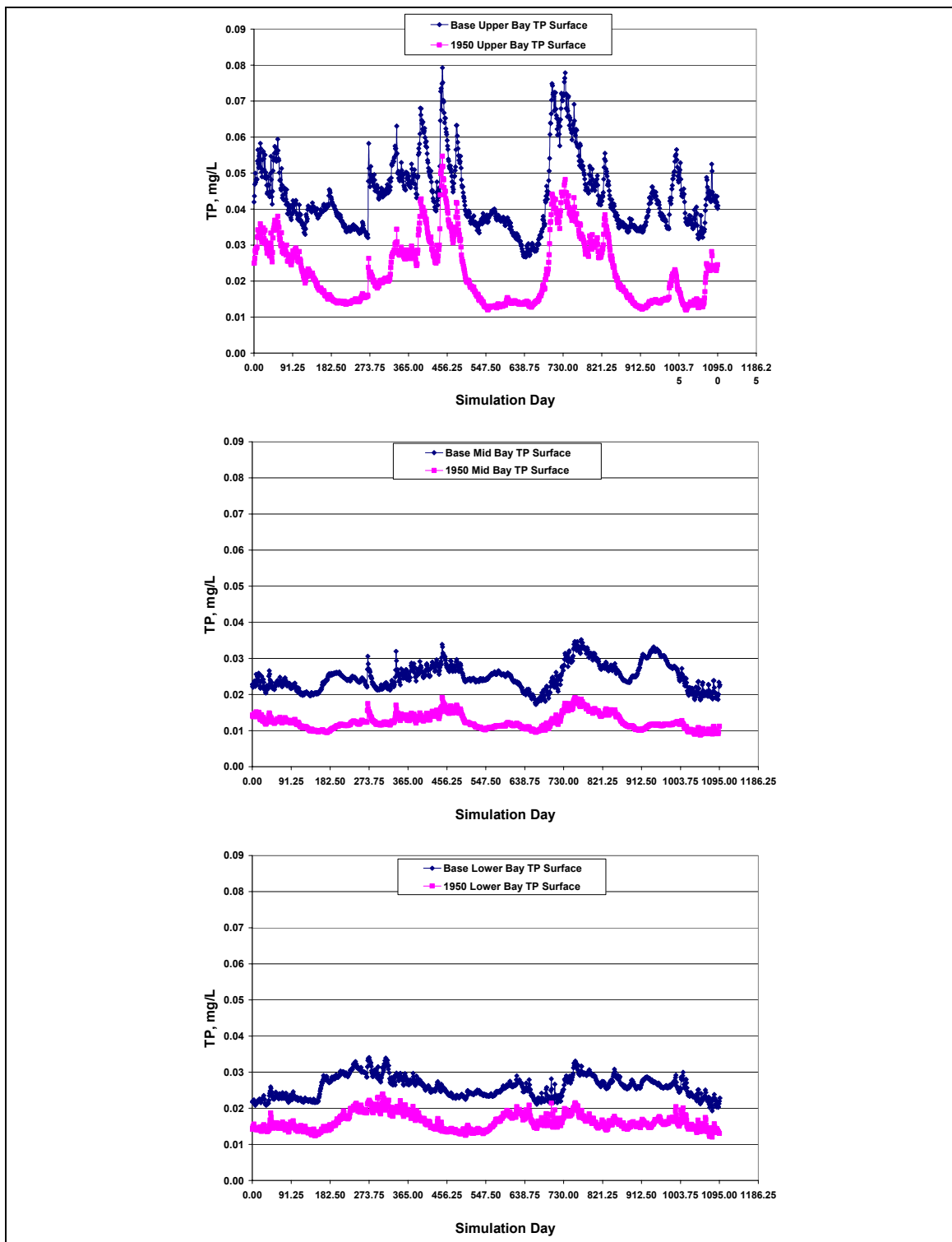


Figure 5.12. Comparison of surface TP for base and 1950's RMB2 results in the upper, mid, and lower regions of the Chesapeake Bay.

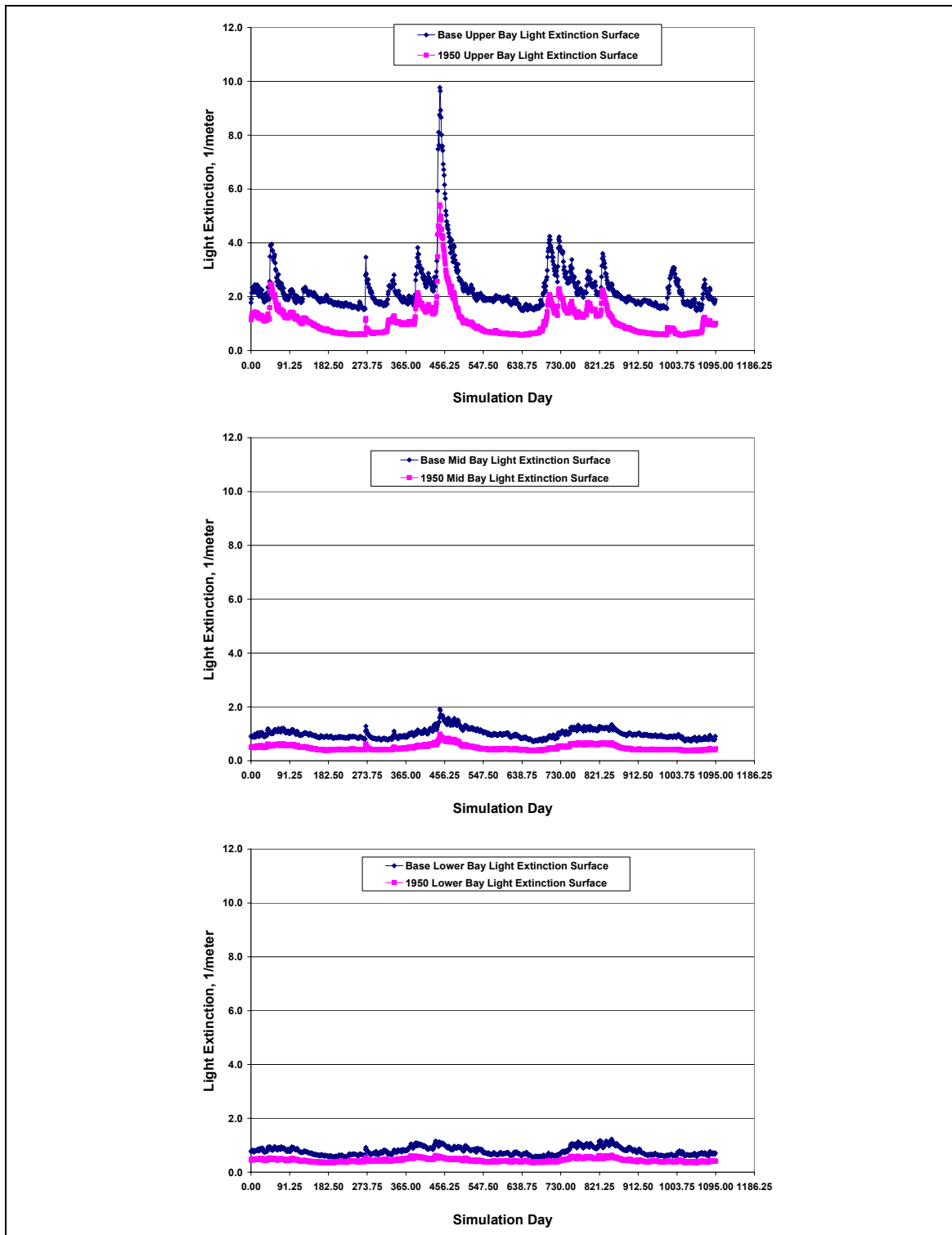


Figure 5.13. Comparison of surface light extinction for base and 1950's RMB2 results in the upper, mid, and lower regions of the Chesapeake Bay.

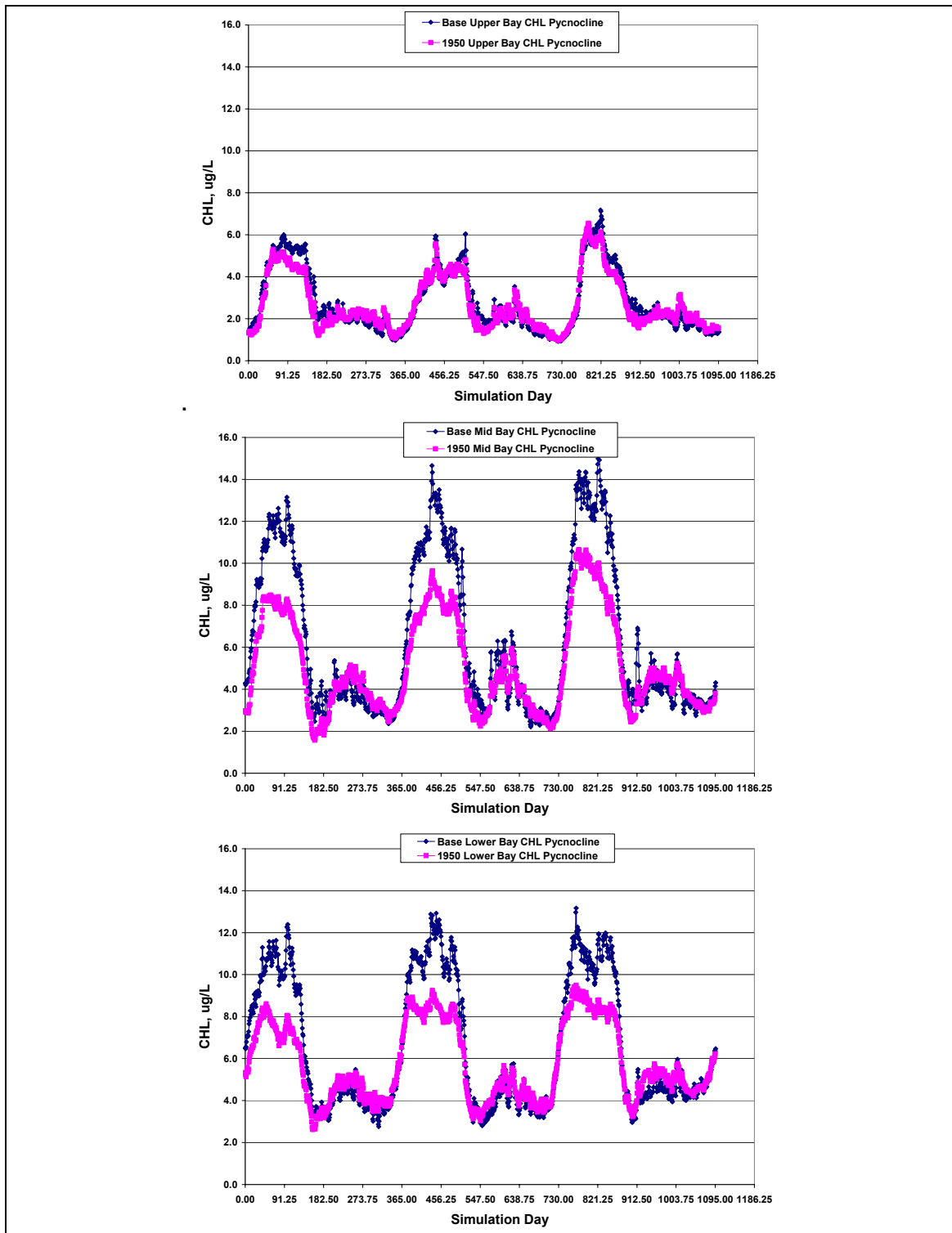


Figure 5.14. Comparison of the pycnocline chlorophyll *a* for base and 1950's RMB2 results in the upper, mid, and lower regions of the Chesapeake Bay.

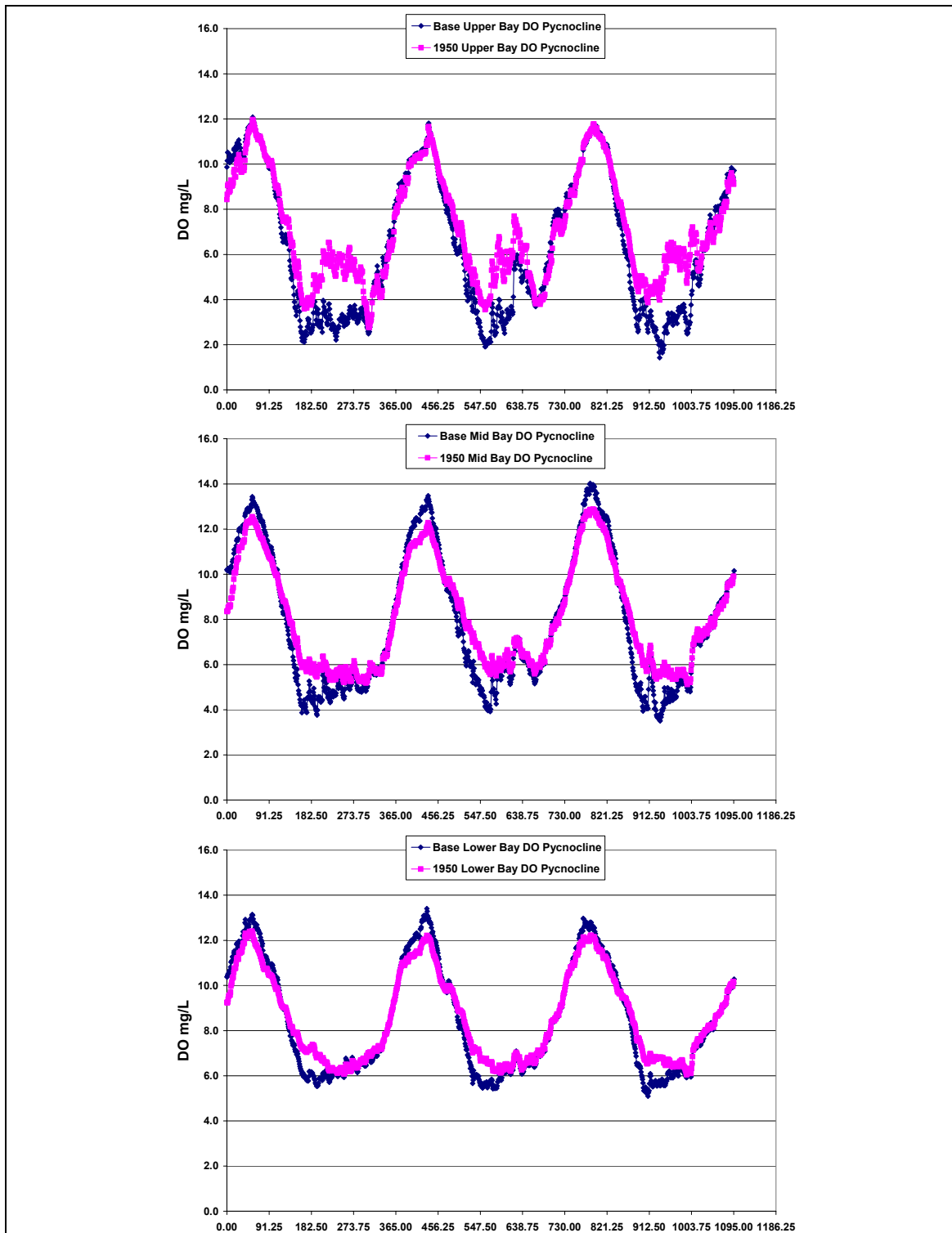


Figure 5.15. Comparison of the pycnocline DO for base and 1950's RMB2 results in the upper, mid, and lower regions of the Chesapeake Bay.

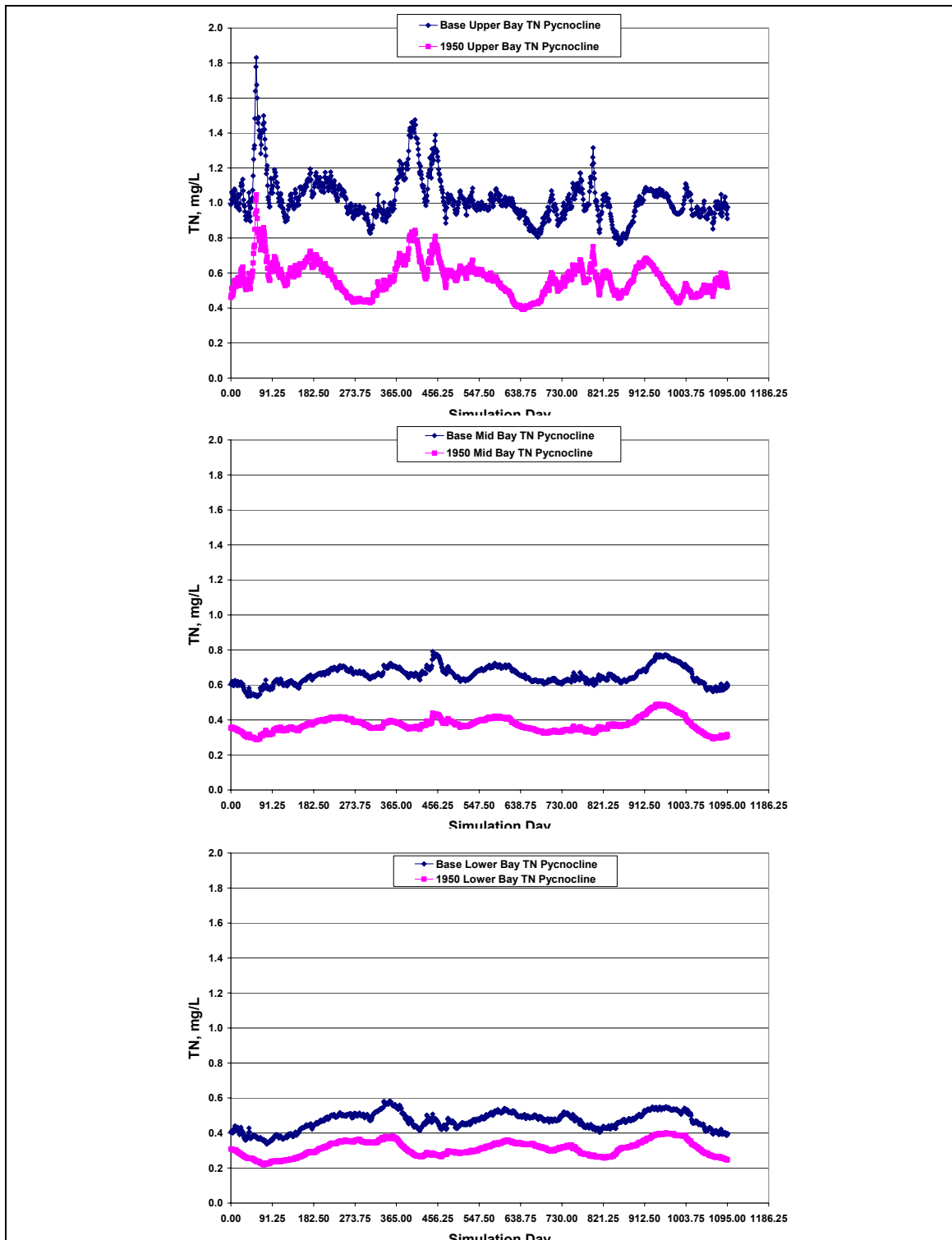


Figure 5.16. Comparison of the pycnocline TN for base and 1950's RMB2 results in the upper, mid, and lower regions of the Chesapeake Bay.

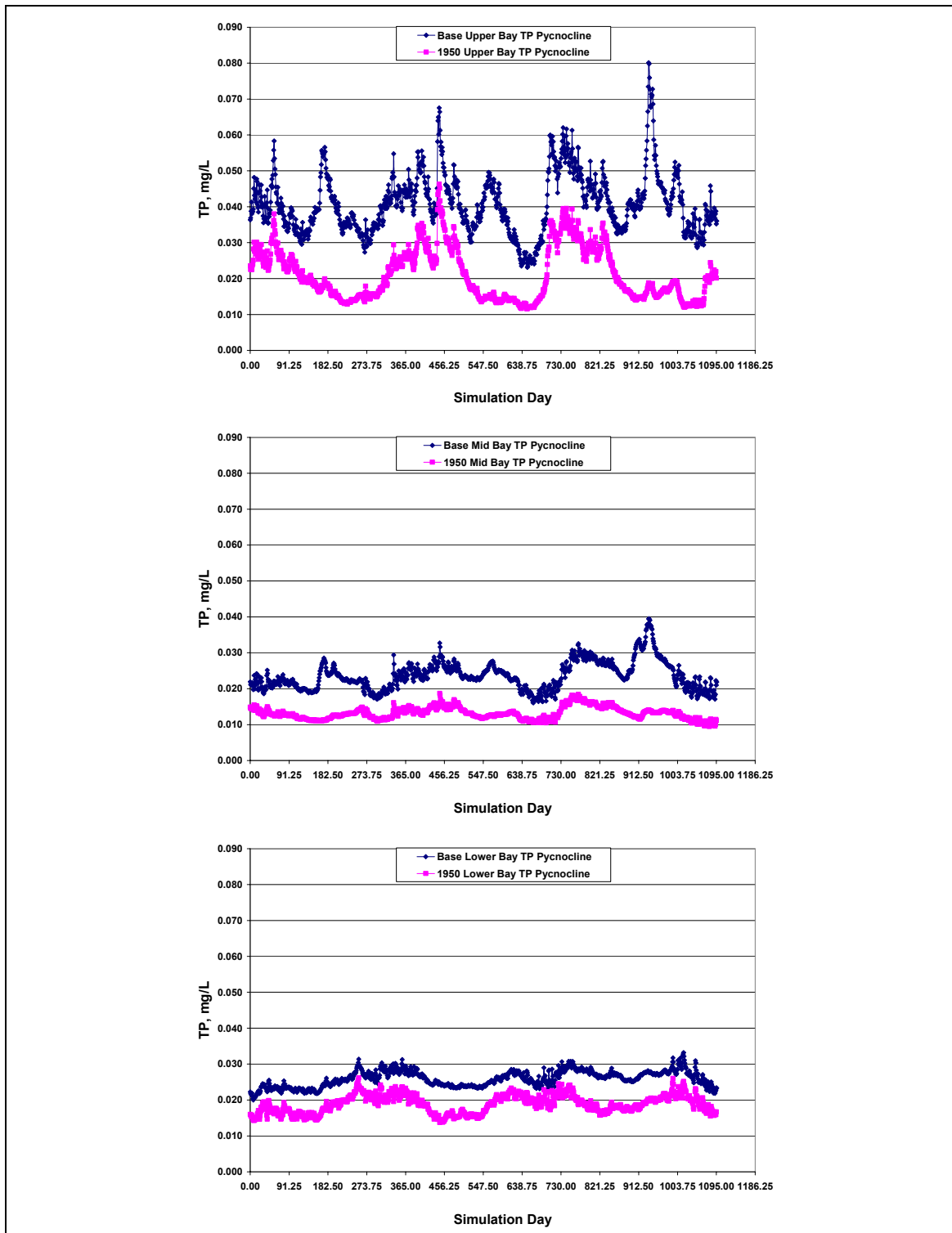


Figure 5.17. Comparison of the pycnocline TP for base and 1950's RMB2 results in the upper, mid, and lower regions of the Chesapeake Bay.

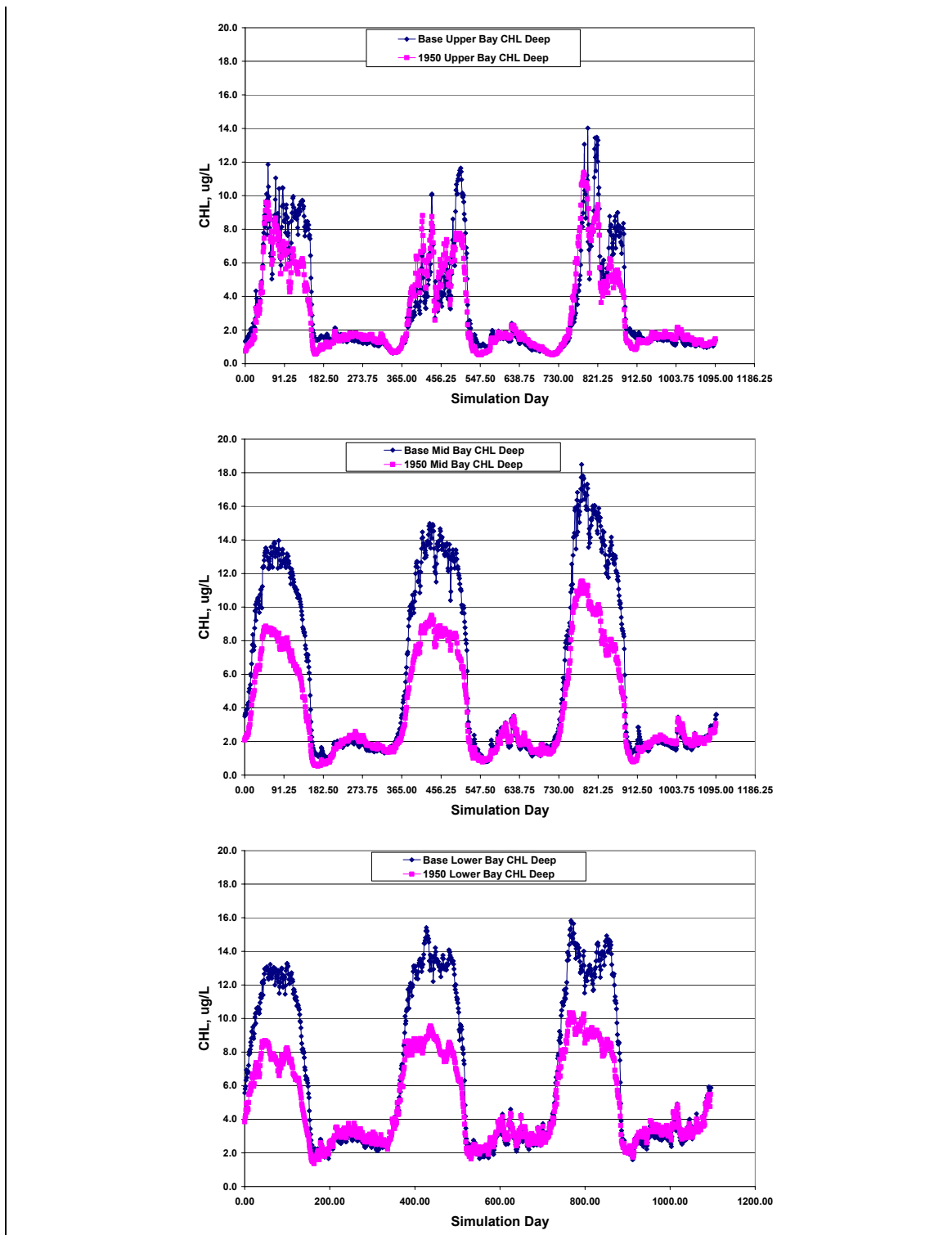


Figure 5.18. Comparison of the deep chlorophyll *a* for base and 1950's RMB2 results in the upper, mid, and lower regions of the Chesapeake Bay.

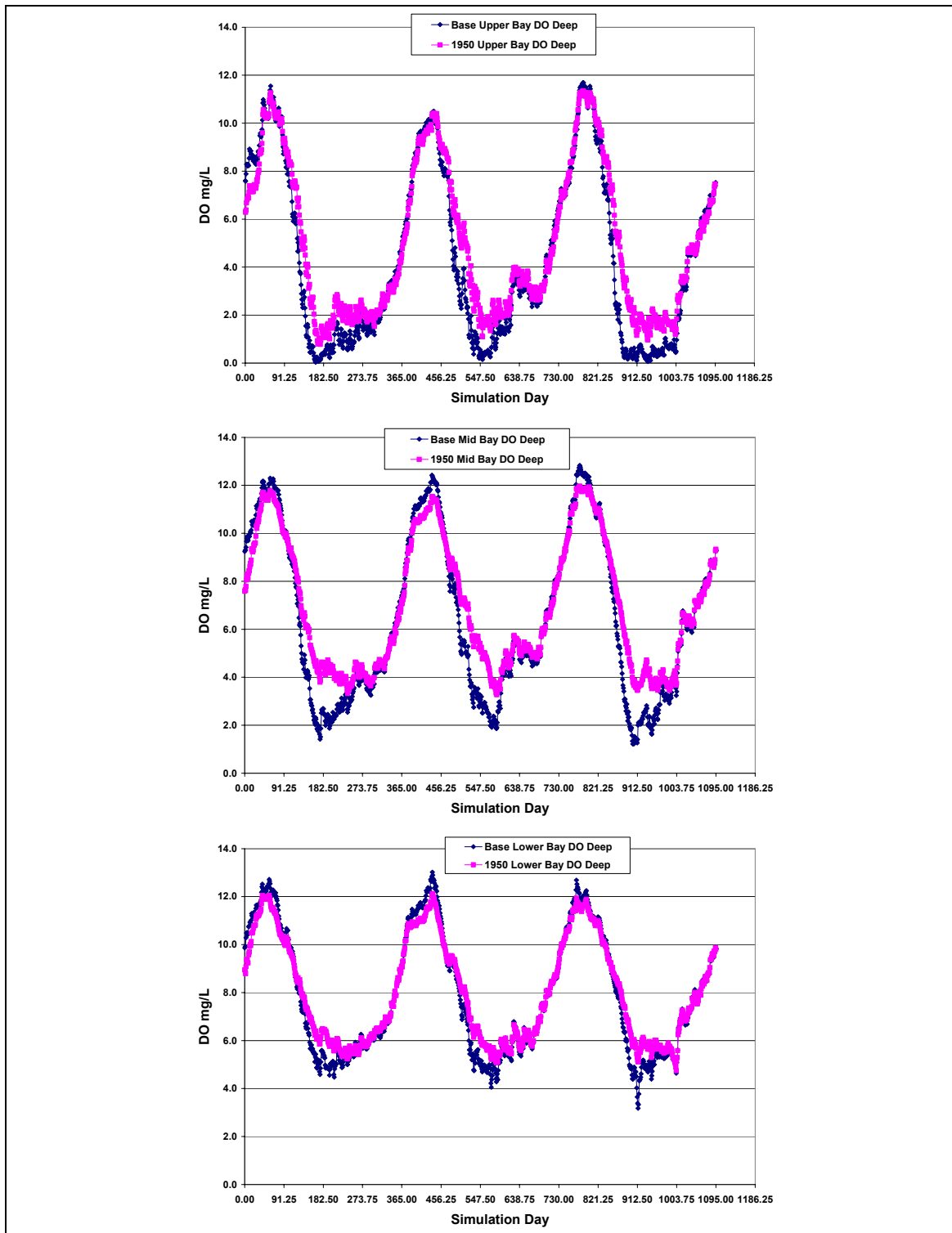


Figure 5.19. Comparison of the deep DO for base and 1950's RMB2 results in the upper, mid, and lower regions of the Chesapeake Bay.

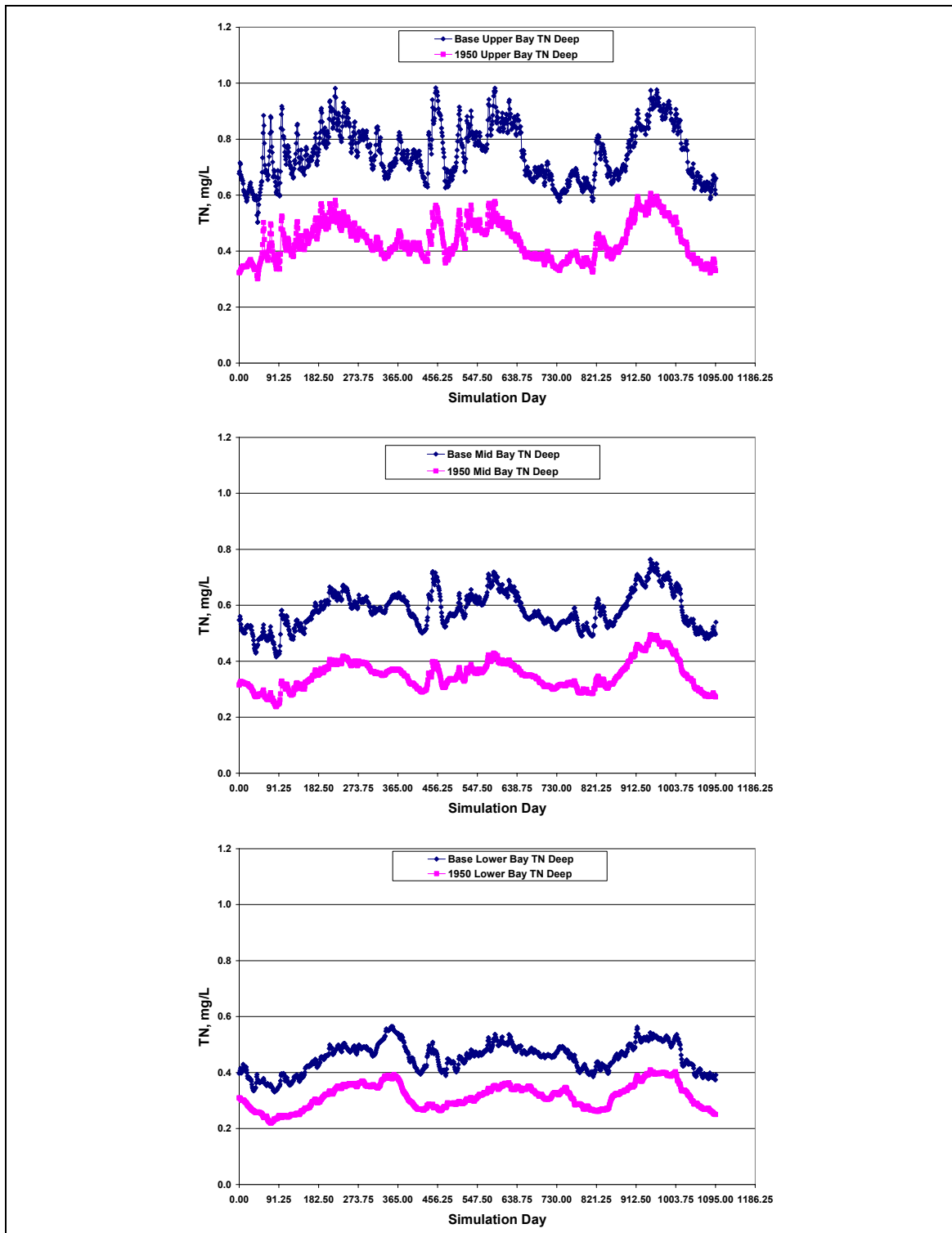


Figure 5.20. Comparison of the deep TN for base and 1950's RMB2 results in the upper, mid, and lower regions of the Chesapeake Bay.

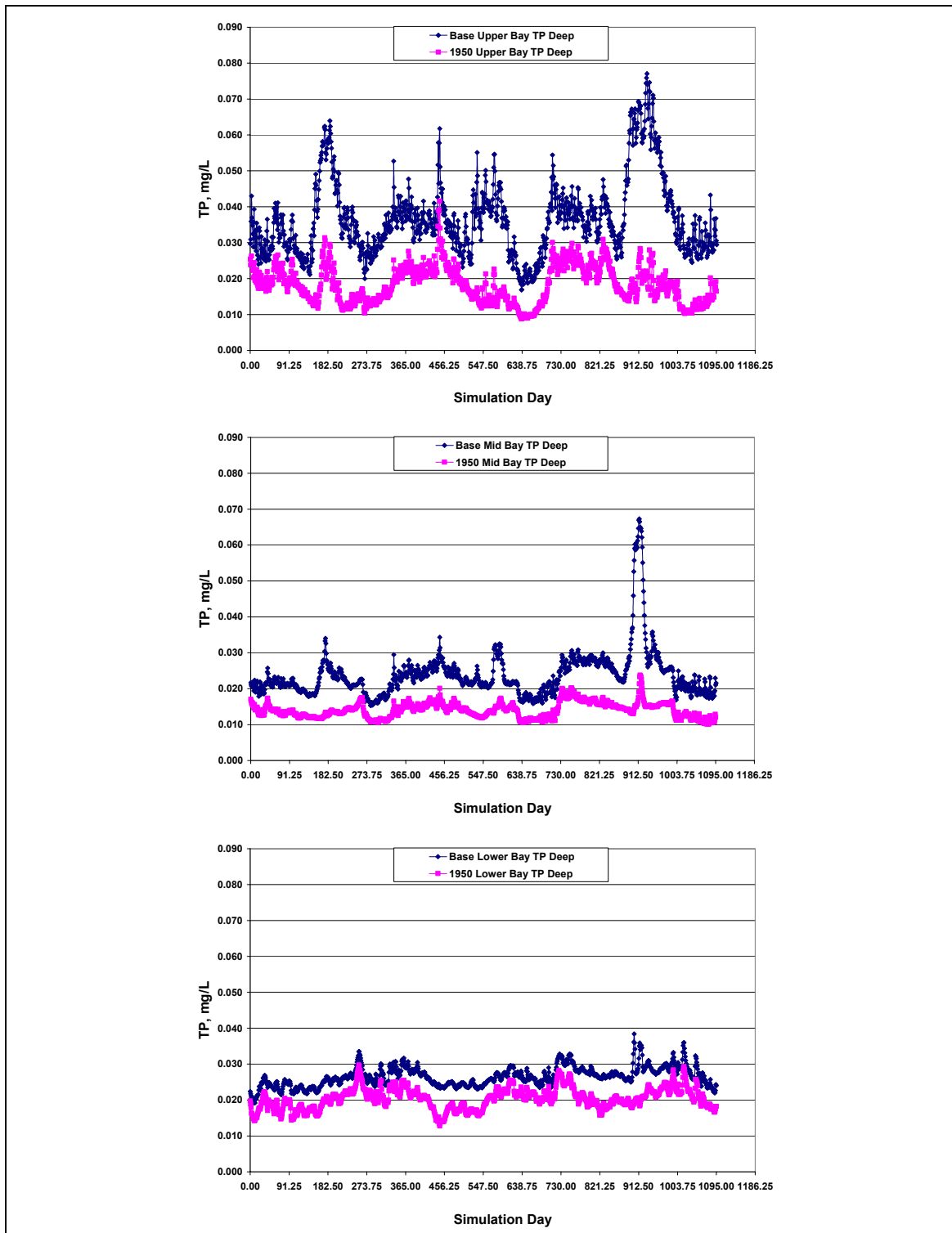


Figure 5.21. Comparison of the deep TP for base and 1950's RMB2 results in the upper, mid, and lower regions of the Chesapeake Bay.

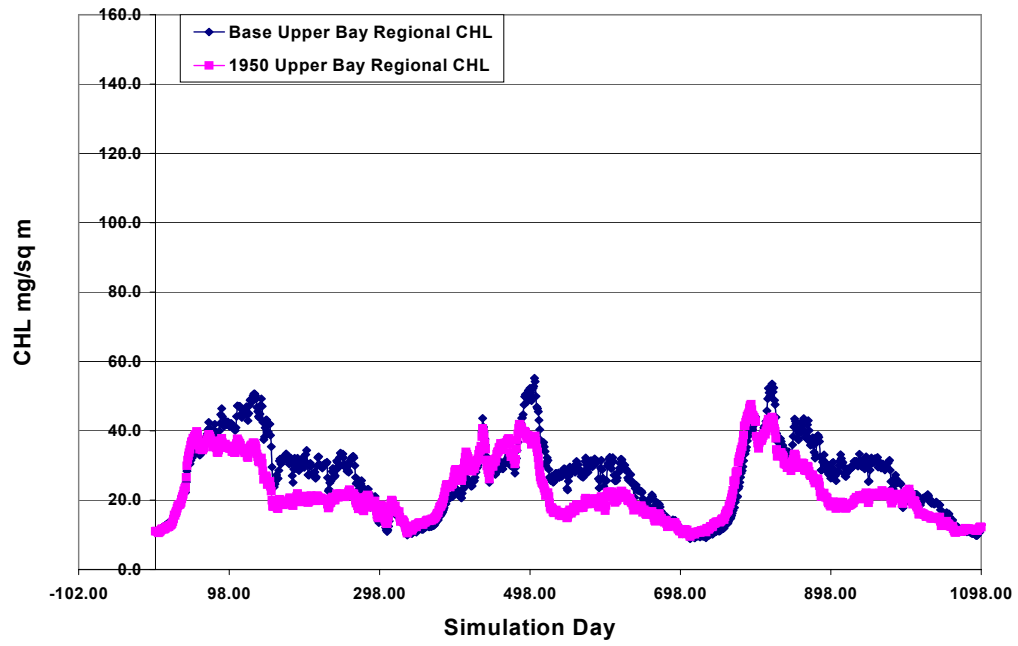


Figure 5.22. Areal concentrations of chlorophyll *a* for the upper Chesapeake Bay for base and 1950's RMB2.

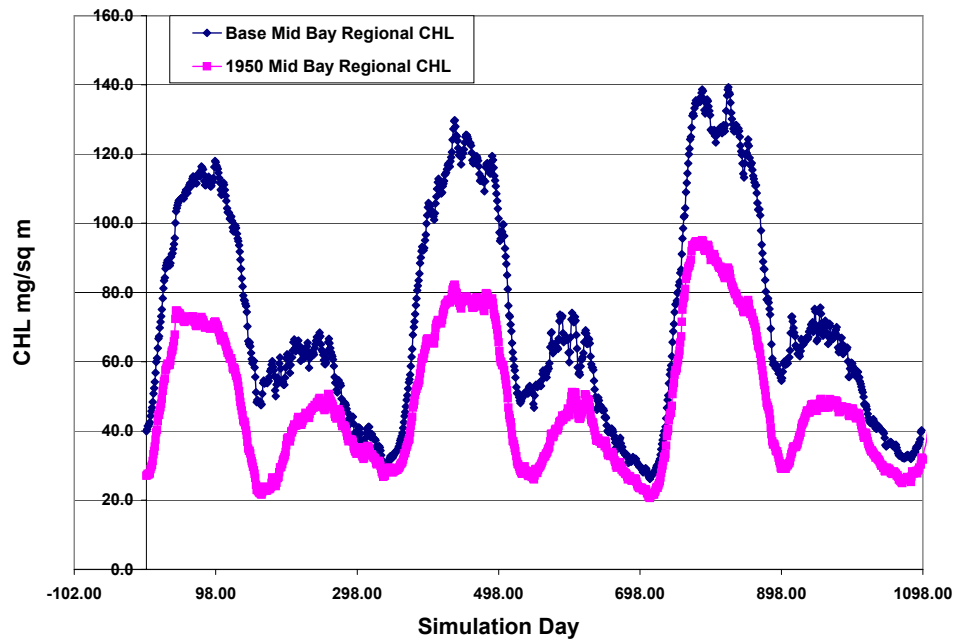


Figure 5.23. Areal concentrations of chlorophyll *a* for the mid Chesapeake Bay for base and 1950's RMB2.

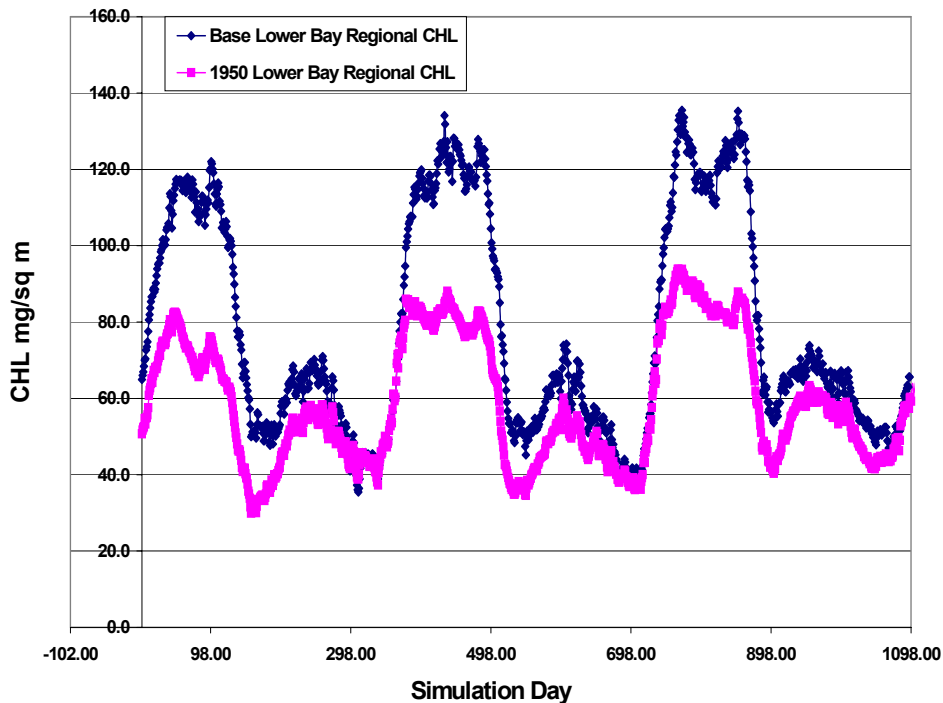


Figure 5.24. Areal concentrations of chlorophyll *a* for the lower Chesapeake Bay for base and 1950's RMB2.

5.4.2. Longitudinal Plots

Summer averages for all years modeled were calculated for chlorophyll *a*, DO, TN, TP, and light attenuation for the base run and the 1950's restored mid Bay run. Surface and bottom concentration of CHL *a*, DO, TN, and TP were plotted along the longitudinal distance from the confluence of the Susquehanna River with the mainstem of the Chesapeake Bay to the ocean boundary. Light attenuation was plotted for only the surface layer. These averages presented in longitudinal plots provide a synopsis of the changes occurring along the longitudinal profile of the main channel of the Chesapeake Bay resulting from modifications to nutrient loads, light attenuation, and SAV patchiness. Results for longitudinal profiles are presented in Figures 5.25 through Figure 5.28.

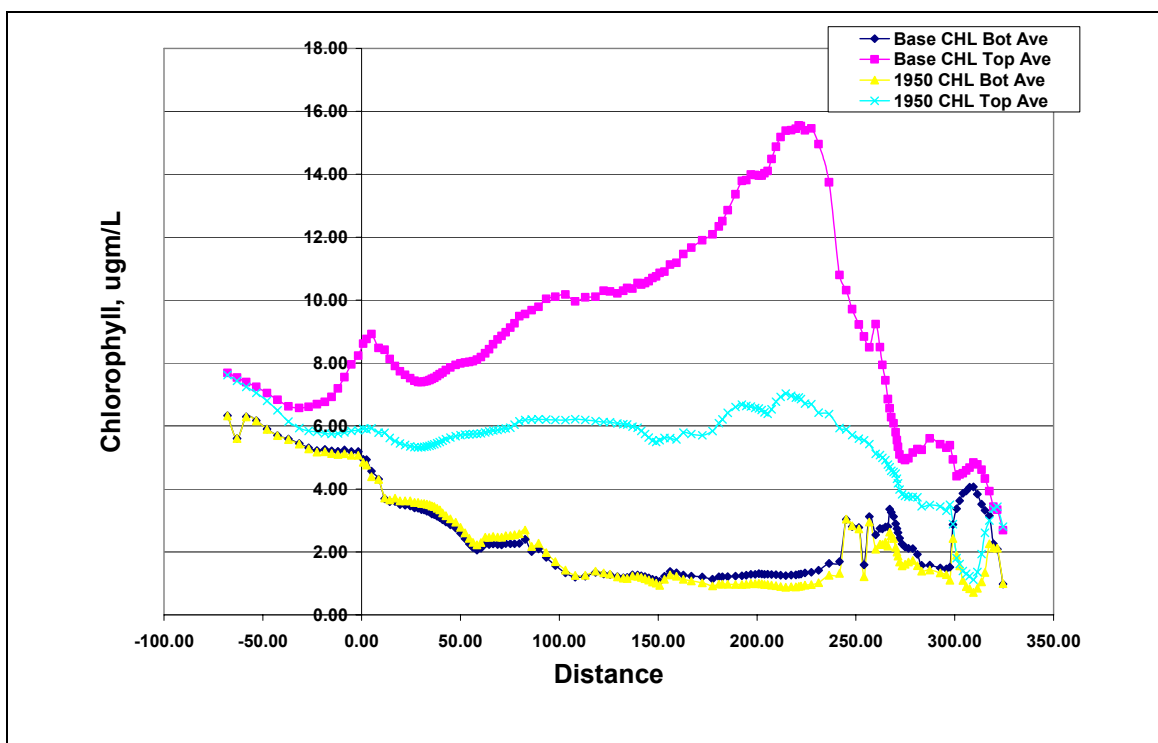


Figure 5.25. Comparison of summer averaged (1985-1987) chlorophyll *a* results longitudinally from the Susquehanna River (≈ 325 km) to the open ocean (≈ -70 km).

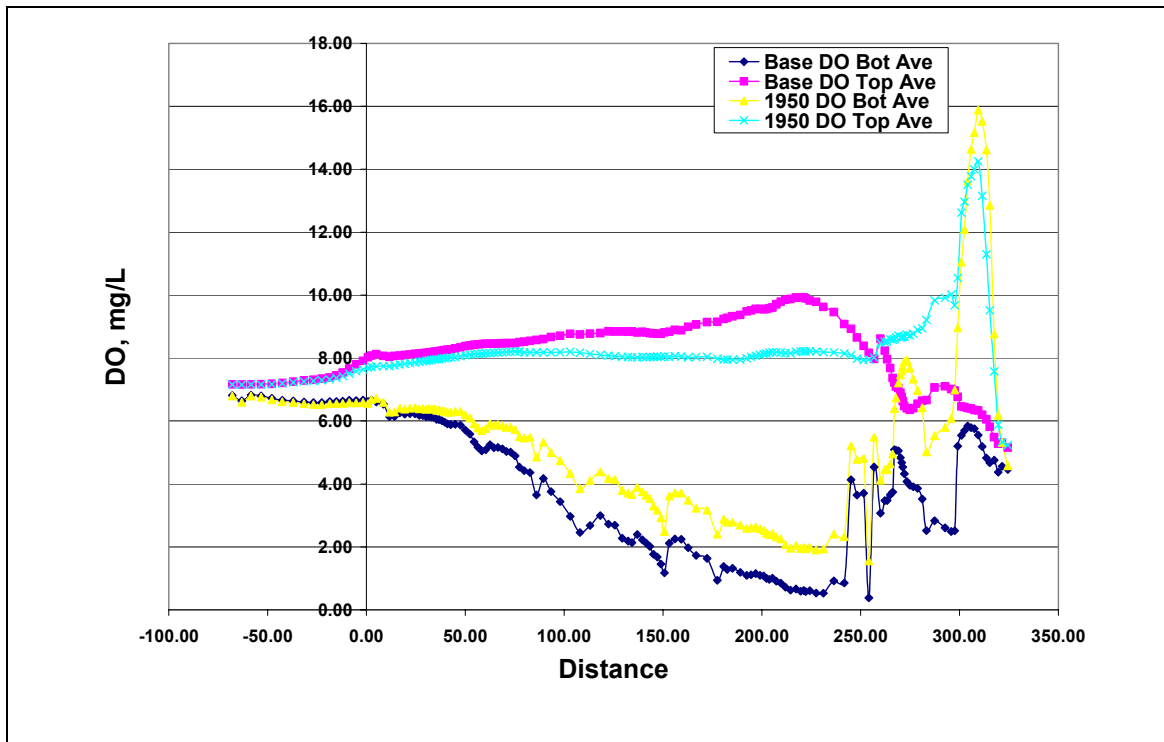


Figure 5.26. Comparison of summer averaged (1985-1987) DO results longitudinally from the Susquehanna River (≈ 325 km) to the open ocean (≈ -70 km).

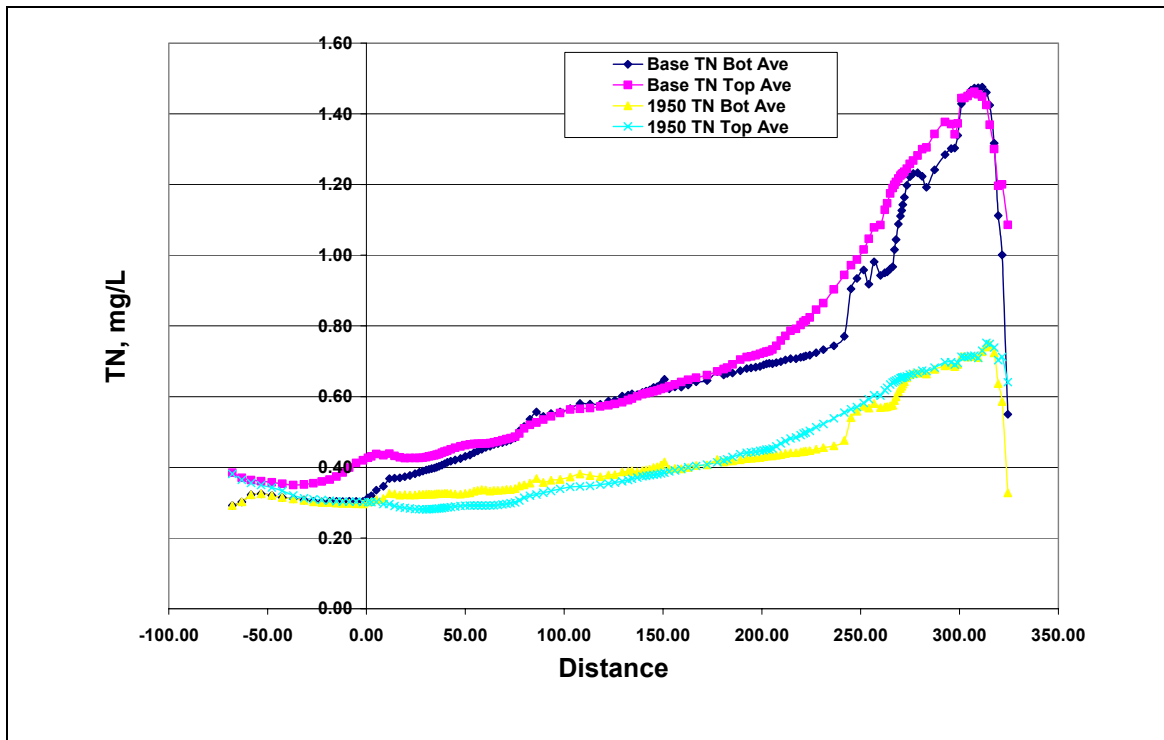


Figure 5.27. Comparison of summer averaged (1985-1987) TN results longitudinally from the Susquehanna River (≈ 325 km) to the open ocean (≈ -70 km).

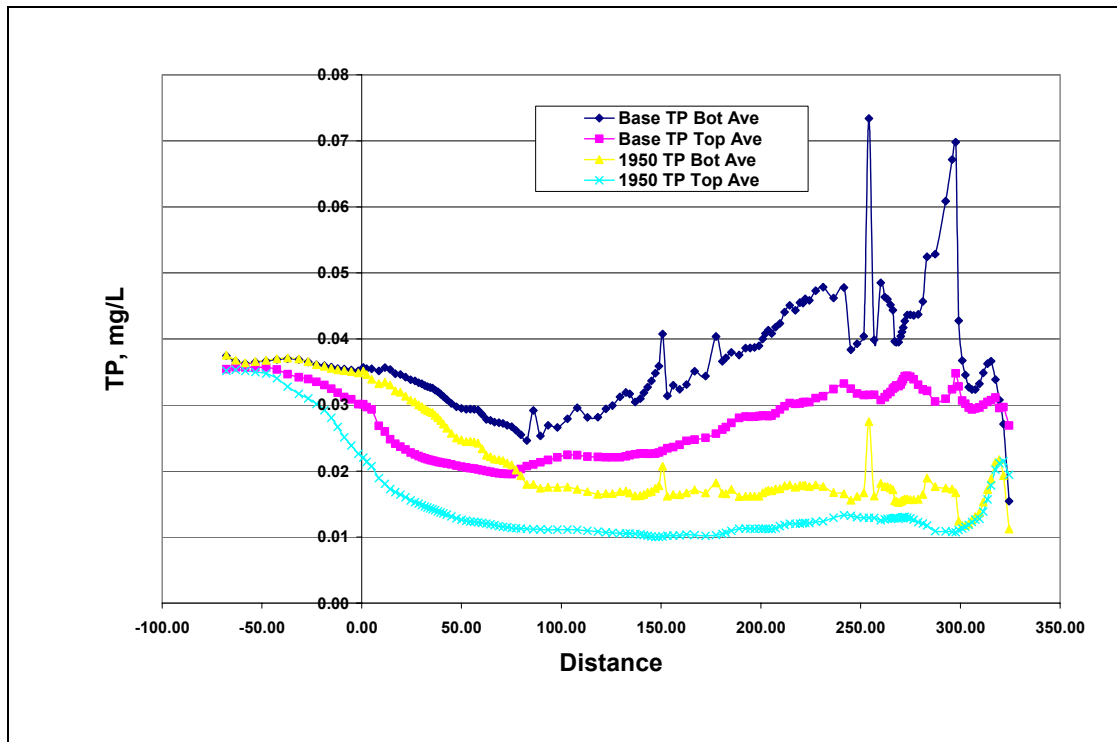


Figure 5.28. Comparison of summer averaged (1985-1987) TP results longitudinally from the Susquehanna River (≈ 325 km) to the open ocean (≈ -70 km).

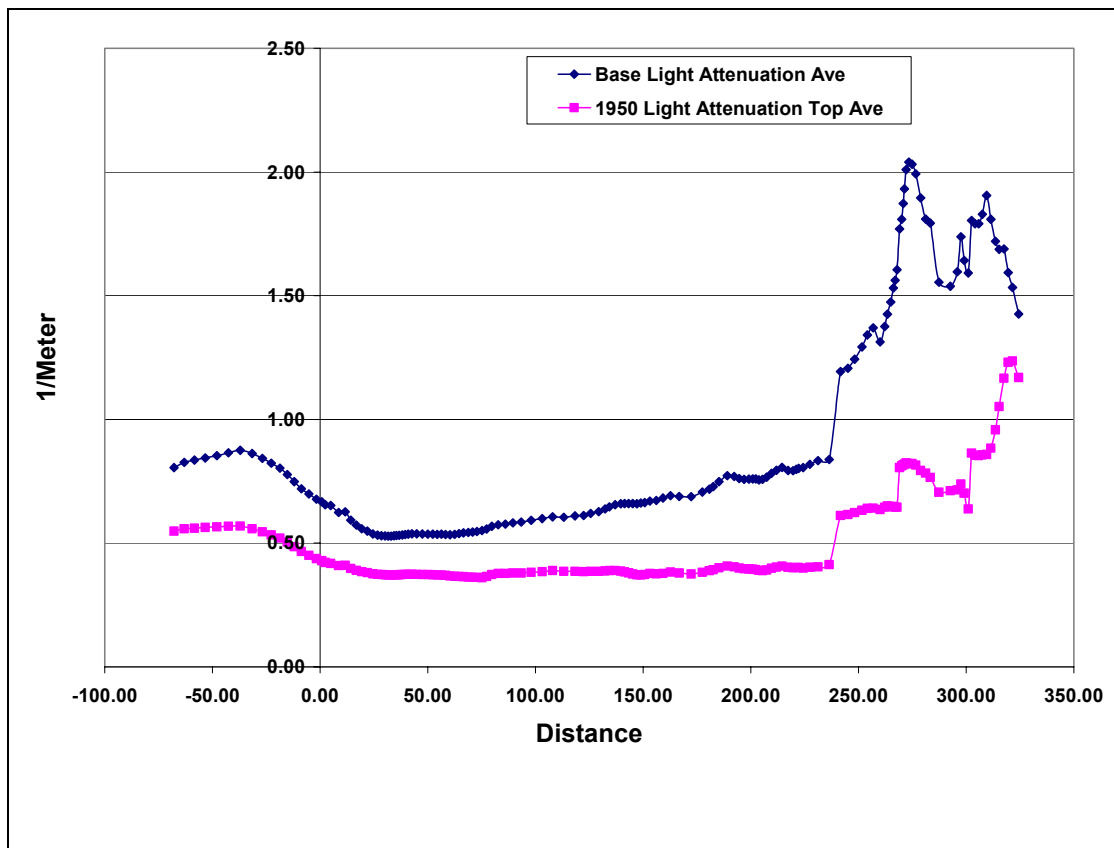


Figure 5.29. Comparison of summer averaged (1985-1987) light extinction results longitudinally from the Susquehanna River (≈ 325 km) to the open ocean (≈ -70 km).

5.4.3. DO Volume-Day Plots

Plots presenting anoxia and hypoxia in the three regions of the Chesapeake Bay (Figure 3.6) were plotted for the simulation period (1985 to 1987) and are shown in Figures 5.29 through Figure 5.31. Two lines on each plot symbolize predictions from the base and 1950's restored mid Bay runs. Each line contains symbols that denote the 30-day average of DO for a specific DO

interval. There were four DO intervals analyzed:

- DO values 0.1 mg/L or <
- DO values 1 mg/L or <
- DO values 2 mg/L or <
- DO values 5 mg/L or <

The statistic to calculate the DO Volume-day came from Cerco and Cole (1994) and is defined as:

$$DOV = \sum_{i=1, j=1}^{n, m} V_i \Delta t_j \quad \text{if } DO \leq \text{interval} \quad \text{Eq. 5.8}$$

where DOV is the Volume-day for interval ($\text{m}^3 \text{ day}$), V_i is the volume of model cell (m^3), Δt_j is the finite-difference integration time step (day), DO is the dissolved oxygen concentration (gm m^{-3}), n is the number of model cells in a region, and m is the number of time steps during the averaging period.

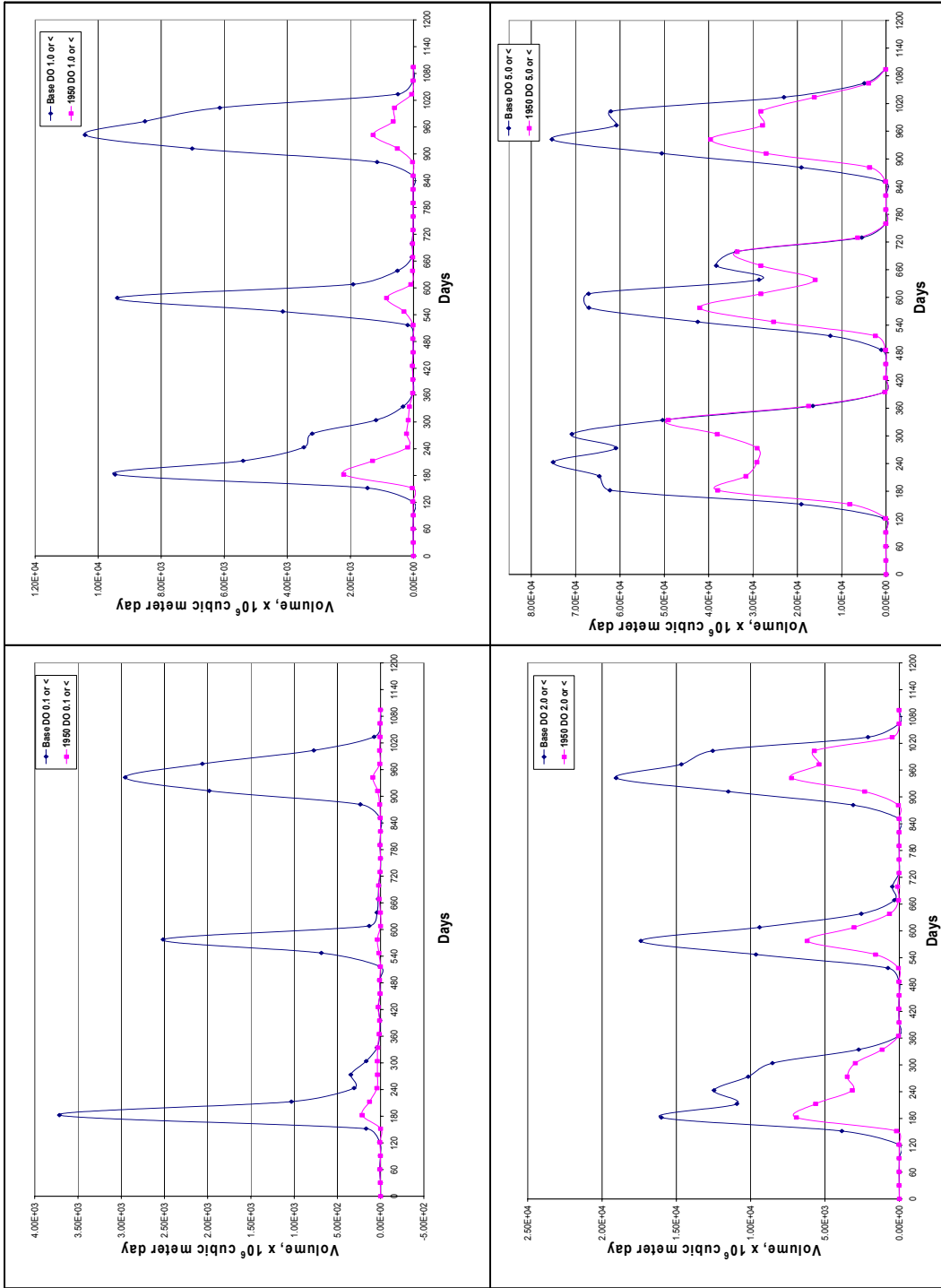


Figure 5.30. DO Volume-day for upper Chesapeake Bay region for DO <= 0.1, 1.0, 2.0 and 5.0.

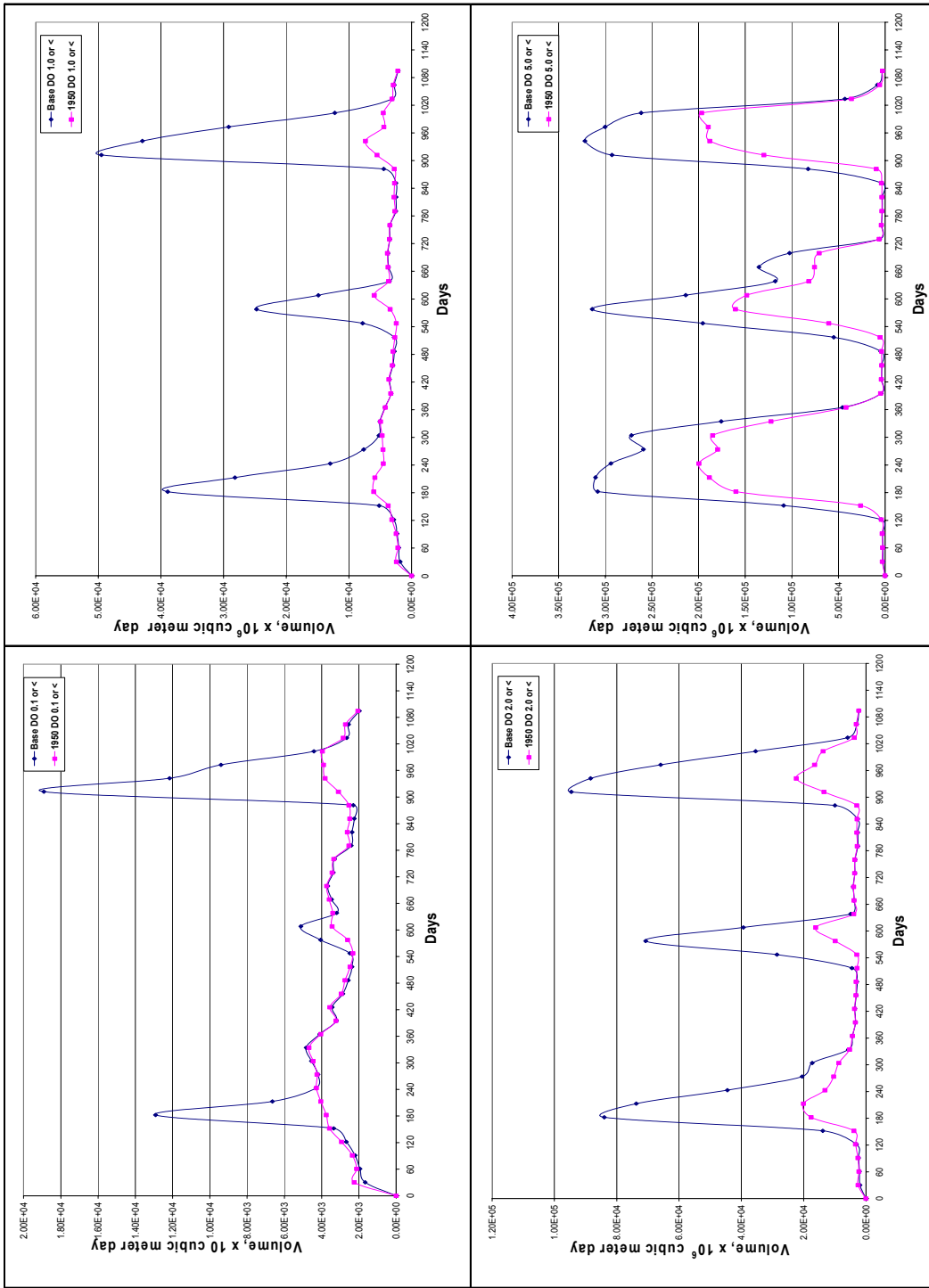


Figure 5.31. DO Volume-day for mld Chesapeake Bay region for DO <= 0.1, 1.0, 2.0 and 5.0.

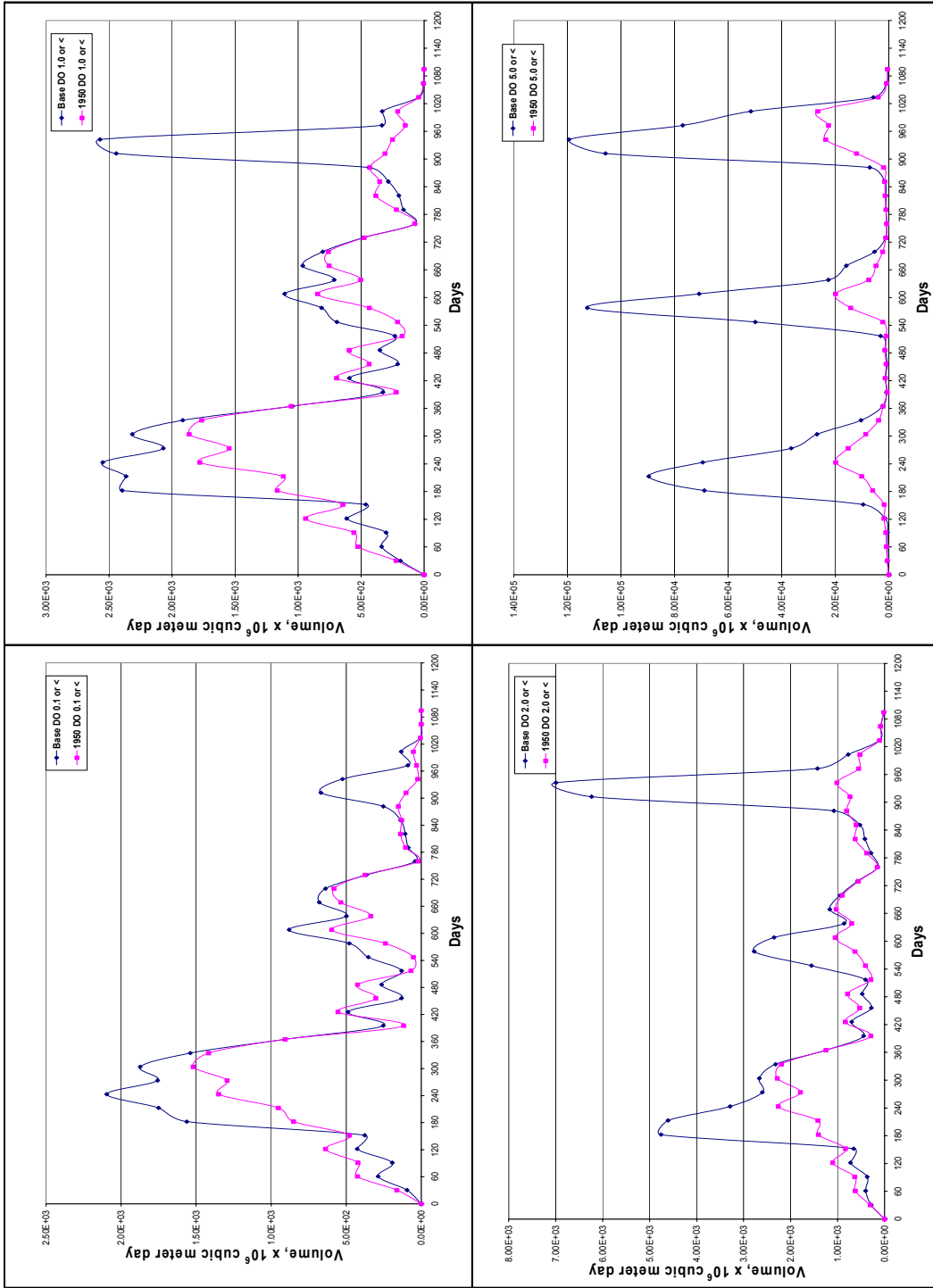


Figure 5.32. DO Volume-day for lower Chesapeake Bay region for DO \leq 0.1, 1.0, 2.0 and 5.0.

5.5. Results and Discussion

Results will be presented for the ICM base run representing the modern mid bay to the 1950's restored Bay run. This was an attempt to try and recreate more pristine conditions that existed in the Bay at one time. By changing nutrients, light attenuation and/or patchiness of the SAVs, will the Bay recover?

5.5.1. Base Verses Sensitivity Runs

The model output will be presented in several graphical formats for the base and sensitivity runs.

5.5.1.1. Histograms of CE-QUAL-ICM to Ecopath Parameters: Biomass, P/B Ratio, Q/B Ratio and UA/B Ratio

Unquestionably, the most responsive indicator of nutrient enrichment (N and P) in the Chesapeake Bay or anywhere is chlorophyll *a* expressed as phytoplankton biomass (Harding and Perry, 1997). From the 1950's to the 1990's, Harding and Perry (1997) show in the mid Bay an increase of about 2-fold for chlorophyll *a*. Boynton et al. (1995) estimated increases of TN and TP loadings to be 6-fold to 8-fold and 13-fold to 23-fold, respectively, since pre-colonial times. However, since the 1970's TP loadings have been greatly reduced. With this in mind, reducing the external nutrient (N and P) loads 50% coming from the watershed causes reduction in the phytoplankton biomass by approximately 24% when compared to base results (Figure 5.5). This does not produce a 2-fold decrease in phytoplankton biomass as might be expected. Moreover, this implies that there is not a one-to-one correspondence of reducing loads by 50% to get reduced biomass of 50%. As is the norm in any natural water body system, there are other factors influencing phytoplankton biomass besides the external loads entering the system from the watershed. Boynton et al. (1995) in their conceptual model of the Chesapeake Bay nutrient

budget included sediment nutrient fluxes and atmospheric loads (above and below hydrologic fall-lines) in addition to diffuse source and point source loads from the watershed. Another thing to consider here is the type of flow years used in the simulation. Harding and Perry (1997) suggest that the strong correlation between nutrient input and freshwater flow may cloud the issue of whether phytoplankton biomass increase or decrease is due to eutrophication or climate conditions. Chlorophyll *a* and primary production (PP) of the Chesapeake Bay have been shown to be strongly influenced by the flow from the Susquehanna River which delivers approximately 60% of the freshwater flow to the Bay (Malone et al. 1988; Harding 1994).

In the SR2 both nutrient loads and K_c are reduced 50%, but there is only a slight additional decrease (i.e., 3% more) in phytoplankton biomass from the SR1. Decreased light attenuation could be considered equivalent to improvement in water clarity. Thus, it would be expected for the phytoplankton biomass to increase somewhat since more light is reaching deeper in the water column. However, it appears the benthic algae are utilizing more of the nutrients before the phytoplankton in the water column have access to it. Figure 5.5 shows definite increases when comparing the benthic algal biomass in both sensitivity runs to base results.

From Figure 5.6, the P/B ratio for phytoplankton and benthic algae follows the same trend as biomass when compared to base results. As biomass is reduced for phytoplankton, the P/B ratio is reduced, and as biomass is increased for benthic algae, the P/B ratio also increased. According to Kemp et al. (2005) increases in phytoplankton production and biomass have been related to decreased water clarity and growth of benthic diatoms as a direct result of nutrient enrichment. Conversely, through nutrient reduction, is it not conceivable to possibly create a shift in community production back to benthic algae having a greater role in the primary

production of the Chesapeake Bay system? Increased benthic algal biomasses presented in Figure 5.5 appear to support this postulation.

Zooplanktons are represented by two groups in CE-QUAL-ICM (microzooplankton and mesozooplankton). Figures 5.5 and 5.6 show that biomass and P/B ratio results for both groups were reduced in the SR1 compared to base results. As discussed previously, CE-QUAL-ICM model formulation allows microzooplankton to graze on phytoplankton and DOC, while mesozooplankton are allowed equal weighting factors for grazing on phytoplankton and microzooplankton. Consequently, decreased phytoplankton and dissolved organic carbon (DOC) biomass affect zooplankton grazing since food source availability becomes an issue. With phytoplankton biomass being at least an order of magnitude greater than microzooplankton, microzooplanktons are essentially absent from mesozooplankton diet (Cercio and Tillman 2008). Mesozooplankton results from the SR2 follow the behavior seen in the SR1 (Figures 5.5 and 5.6) in that their biomass and P/B ratio are both reduced. This is not the case for the microzooplankton. Their biomass actually increases slightly in the SR2 probably as a result of less predation from mesozooplankton. On the other hand, their P/B ratio remains similar to the value from the SR1 and by formulation, this would still indicate increased production. Cercio and Noel (2004) have suggested that the temperature function governing zooplankton grazing be revisited to allow more grazing at temperatures above 25 °C. Heinle (1966) has noted from feeding and bioenergetics studies that zooplankton growth is not usually limited by food. Their abundance and production can be affected by overabundance of nutrients through changes in their habitat (i.e., increases in bottom water hypoxia).

Comparison of the Q/B ratio response of both zooplankton groups (Figure 5.7) of SR1 results to the base results follows the trend of their P/B ratio response. As food sources of microzooplankton and mesozooplankton are diminished, a 10% and 18% reduction of the Q/B

ratio (consumption rate) is observed, respectively. SR2 results compared to SR1 results did not show a noticeable decrease in the Q/B ratio for microzooplankton simply because there was very little change in the consumption rate and biomass, but the Q/B ratio of mesozooplankton was further decreased an additional 4% from the SR1 results. Again this was attributed to the decrease in biomass of food sources. The Q/B ratio could increase with decreased biomass only if consumption rate has increased. That is possible if grazing by a predator is as fast or faster than growth.

There is very little or no change for the UA/Q ratio (the unassimilated food to consumption) in comparison of base results to SR1 and SR2 results (Figure 5.8). Unassimilated food is usually considered the by-products of urea and feces. The only group where there is a noticeable change is the suspension feeders.

5.5.1.2. Time Series of Nutrient Limitation in the Mid Bay

There is a consensus among many scientists that the limiting factors affecting phytoplankton growth are strongly influenced by temporal and spatial variations in the Chesapeake Bay (Kemp et al. 2005). Fisher et al. (1994) substantiate this observation by showing both N and P limit phytoplankton growth during different seasons and at different locations within the Chesapeake Bay. The upper/oligohaline (0.5-5‰ salinity) regions of the Chesapeake Bay exhibit P and Si limitation at times through the year while the mid/mesohaline (5-18‰ salinity) and the lower/polyhaline (18-27‰ salinity) regions are most susceptible to N limitation for phytoplankton growth (Harding and Perry 1997). The Chesapeake Bay exhibits a 2 phase annual cycle of phytoplankton production (Adolf et al. 2006; Conley and Malone 1992) with increased production in the spring (April-May time frame) resulting from freshwater riverine nutrient loads and a summer maximum supported by regeneration of nutrients from the

sediments. With this in mind, analyses of nutrient limitation for all primary producer groups, not just phytoplankton in the mid Bay were considered for both sensitivity runs.

Figure 5.3 corroborates for the base results at least for summer periods (June 1 through August 31) in the mid Bay what has been noted previously for phytoplankton growth limitation - phytoplankton growth is limited by N or co-limited by N and P in the summer and is limited by P the rest of the year Figure (16 from Kemp et al. 2005). In early March of all years simulated, there are small dips in silica (Si) limitation with results from the third year (1987) showing Si and P co-limiting for a short period of time. This probably corresponds to diatom spring bloom dynamics and Si uptake. Sellner and Brownlee (1988) estimate the composition of algal abundance in the spring as being composed of 80 to 90% diatoms. Moreover, spring limitation of diatoms by Si has been noted by Conley and Malone (1992). They agree that Si limitation may be an important factor in reducing the spring algal biomass maximum and go on to infer that this could have important implications for nutrient management strategies.

When nutrient loads (N and P) are reduced 50% in SR1, summer periods of N and P co-limitation become more pronounced (Figure 5.2) with the Chesapeake Bay system becoming more N limited at times. Another difference noted from base results is the extended duration of limiting conditions for both N and P. As discussed previously phytoplankton biomass was reduced but not by the same percentage as nutrients. Consequently, the phytoplankton groups are demanding more nutrients increasing the N and P limitations during prime growth periods. Nutrient reduction has affected Si limitation opposite of N and P. The dips in Si limitation noticeable in the base results during early spring are barely visible. This indicates that the phytoplankton group feeding on Si has been reduced to the point that it is no longer in as much demand.

From Figure 5.2, results from the SR2 show it is clearly evident that the mid Chesapeake Bay is more P limited than either of the previous runs. Before, P and N shared the role as limiting nutrient at certain times of the year with P being the limiting nutrient the rest, but this is not the case for this run. The major difference between this run and the other two is that the SAV group and not just the benthic algae group has increased in biomass (Figure 5.5). This implies that through nutrient reduction and reduced turbidity, SAV and benthic algae have increased growth thus adding to the production of the system. This is consistent (at least for SAVs) with other field and modeling studies that identified improved water clarity and reduced nutrients as means to recover SAV beds (Kemp et al. 2005). N and Si limitation followed similar trends as observed in the SR1. N limitation followed the same pattern but the range of limitation is not as pronounced (i.e., most limiting value 0.46 compared to 0.28). Si limitation values looked almost identical to these results leading to the same conclusion presented previously about the phytoplankton group.

Limitations for benthic algae from the comparison of the base with SR1 results denoted slight decreases to N and P limitation values, although the trends through the years were similar (Figure 5.3). This was attributed to the increase in benthic algal biomass and production resulting from nutrient load reduction. Either from less phytoplankton demand (i.e., decreased biomass) or benthic algae having up taken nutrients first, N and P became more limiting than they normally would be. Nevertheless, light limitation still remained the limiting factor for both of these runs. With the addition of reduced light attenuation, results from SR2 when compared to the two previous runs show a remarkable change to P limitation. As illustrated in Figure 5.3 for the early to late winter periods in all years modeled, P and light became co-limiting nutrients. This probably corresponds to winter diatom algal blooms.

Patterns of limiting variables of SAV for the two sensitivity runs showed the smallest change from base results than exhibited for the other two primary producers. There is consensus (Cooper and Brush 1993; Davis 1985, Orth and Moore 1983) that light is the main limiting variable for SAV, and this is demonstrated for all runs conducted. Results show a cyclic pattern of light being less limiting in the winter to more limiting in the summer. SR1 with nutrient load reduction produced minimal change to the light limitation with slightly more change to P limitation; N limitation actually became less limiting. In terms of production, SAV biomasses were reduced but P/B ratio actually showed an increase implying an increased production rate. Since production of SAV in CE-QUAL-ICM is dependent on light, it is possible to see increased production rate with decreased biomass. Results from SR2 show SAV biomass and P/B ratio have increased causing slightly more P limitation resulting in the winter period. As with benthic algae, P and light co-limit growth during this period with light limitation being the limiting factor the rest of the time. N limitation does not appear to play any role in SAV growth.

5.5.2. Base Verses 1950's Restored Mid Bay Run

5.5.2.1. Histograms of CE-QUAL-ICM to Ecopath Parameters: Biomass, P/B Ratio, Q/B Ratio and UA/B Ratio

In Figure 5.2, biomass of the primary producers for the 1950's RMB1 compare similarly to results from the SR2 run next to base results. For the 1950's RMB1 and SR2 results, phytoplankton biomass decreases while biomasses of the other two groups increase similar amounts. Accordingly, their differences from base results are about the same. There is a plausible explanation for this. Specifically, the nutrient loads for both runs were reduced by similar amounts (e.g., 0.57 and 0.70, respectively, for 1950's RMB1 and 0.5 for both N and P for the SR2). At the time SR2 was conducted, the loads for the 1950's RMB1 had not been

estimated so it was not known they would be so comparable. Based on this and the fact that the SAV biomass needed to be more in line with Hagy (2002), it was decided to adjust the patchiness coefficient to try to increase SAV biomass. This run was designated as the 1950's RMB2. By adjusting patchiness from 0.1 to 0.5, SAV was allowed to grow in 50% of the cells modeled as SAV beds instead of 10%. By doing this, SAV biomass certainly increased although perhaps a bit too much (Figure 5.2). The P/B ratios of most groups modeled for the 1950's RMB2 were reduced from base except for benthic algae and SAV. Similar to the SR1 and SR2 results, the P/B ratio for all groups follows the same trend as biomass results next to base results; as biomass is reduced for phytoplankton, zooplankton, deposit feeders, and suspension feeders, the P/B ratio is reduced, and as biomass is increased for benthic algae and SAV, the P/B ratio also increased. Again this represents a reduction in production rate for all groups except benthic algae and SAV.

Comparison of the Q/B ratio response of the zooplankton and benthos groups (Figure 5.7) from the 1950's RMB1 and the 1950's RMB2 to the base results follows similar trends of their P/B ratio response. As food sources of microzooplankton and mesozooplankton are diminished, a 10% and 28% reduction of the Q/B ratio is observed, respectively. Results from the 1950's RMB1 and 1950's RMB2 compared to each other did not show a noticeable decrease in the Q/B ratio for microzooplankton possibly because: their food source biomass did not change a great deal, their consumption rate probably remained the same, and their biomass was not changed. Mesozooplankton Q/B ratio did show a little more variation from one scenario to the next with the 1950's RMB2 showing a greater decrease from base than the 1950's RMB1. This could have resulted from decreased phytoplankton biomass although the consumption rate between the two was not so different. The Q/B ratios for the deposit and suspension feeders show opposite behavior when compared to base results. In particular, deposit feeders have

increased in biomass for both 1950's RMB1 and SR2 when compared to base results, although the P/B ratio is less than base for both. Without a doubt, increased biomass is a direct result of increased benthic algae as well as sediment particulate organic carbon (POC). Both of these are allowed as food sources for the benthos in CE-QUAL-ICM. Suspension feeder Q/B ratios show only slight changes from base to 1950's RMB1 and SR2 results even though their biomasses show significant differences from base. Consumption rates seem to vary only slightly among runs (i.e., 0.14 day⁻¹ for base, 0.135 day⁻¹ for 1950's RMB1, and 0.156 day⁻¹ for 1950's RMB2)

There is very little or no change for the UA/Q ratio in comparing base results to 1950's RMB1 and 1950's RMB2 results. Like the sensitivity scenario runs, the only group showing a noticeable change is the suspension feeders.

5.5.2.2. Time Series and Longitudinal Plots

Concentrations of chlorophyll *a* in the surface waters of each region (i.e., upper, mid, and lower denoted in Figure 5.9) demonstrate what has been observed by many scientists (Harding, 1994; Harding and Perry 1997; Fisher et al. 1988): strong seasonal variation of chlorophyll *a* with increased production in the spring and a second high productivity period in the summer driven by remnants of the spring bloom. This is observed in the pycnocline and deep layers of the Bay as well (Figures 5.9, 5.14 and 5.18). Comparing chlorophyll *a* base results to the 1950's RMB2 results reveals a number of observations. First, during high spring and summer production periods in the surface layer, base results are 30% to 50% higher than 1950's RMB2 results in the mid and lower Bay but although higher do not show great differences in the upper Bay. This coincides with the 2-fold increase reported by Harding and Perry (1997) for the increase in chlorophyll concentration from the 1950s to present day. Additionally, winter concentrations between the two runs are quite similar. In a previous discussion, lower chlorophyll concentrations for the 1950's RMB2 are attributed to the reduction in nutrient loads;

however, this does not eliminate the summer maxima from occurring in any of the regions indicating the regeneration of N and P from the spring blooms continue to support summer growth. Secondly, in the pycnocline and deep layers of the mid and lower Bay during spring and summer periods of high production, we again see higher concentrations of chlorophyll *a* in the base results which can be up to approximately 40% greater than 1950's RMB2 results. Upper Bay results for these layers show differences between the runs but are again less than what was observed for the other two regions. The chlorophyll *a* concentrations in the pycnocline layer of the upper Bay only show small differences during the spring bloom, and in the deep layer show greater differences than in the pycnocline but not near the range as seen in the mid and lower Bay for these layers.

A longitudinal plot (Figure 5.25) of chlorophyll *a* from the Susquehanna River confluence (distance \approx 325 km on figure) to the ocean boundary (distance \approx -50 km on figure) indicates the highest chlorophyll *a* concentrations occur in the mid Bay region followed by the lower region. Kemp et al. (2005) have indicated this same chlorophyll trend throughout the Bay. Of the three regions, the mid Bay shows the most change in chlorophyll *a* from base results when comparing the 1950's RMB2 results. This is probably related to freshwater in flows from the Susquehanna River and possibly regenerated nitrogen from spring blooms being depleted through the Bay as it flows to the mouth. Longitudinal N depletion can be seen in Figure 5.27 for the base and 1950's RMB runs. This is in agreement with Harding and Perry (1997) who have related the lower mesohaline and polyhaline chlorophyll *a* concentrations to N supply and state that concentrations are mostly lower than those found in the more northern areas.

Regional plots of chlorophyll *a* on an areal basis (mg/m^2) show chlorophyll concentrations follow similar trends and patterns to chlorophyll *a* observed in the surface layer (Figures 5.22 – 5.24). This may be because the surface layer encompasses more of the regional

area weighting the estimated concentrations so that they look like what occurs in the surface layer more than the other.

Just as chlorophyll *a* concentrations vary seasonally in the Chesapeake Bay, DO concentrations do the same. Plots of DO concentrations for all layers and regions (Figures 5.10, 5.15 and 5.19) show increased DO concentrations during the spring season corresponding to the spring diatom bloom. This is demonstrated in the base and 1950's RMB2 runs. DO concentrations decrease until the lowest values occur in the early summer of all regions. This is initiated by organic matter decay from the spring algal bloom that lasts through the summer and begins recovery in the fall (Hagy et al. 2004). Equally important, the results of the 1950's RMB2 run show shortly after the minima, DO concentrations in the upper Bay show a climb in concentration to a second maximum in concert with the summer algal bloom. This is most noticeable in the surface and pycnocline layers. Of the modifications made to conduct the 1950's RMB2 run, decreased light attenuation in all likelihood is what produced this behavior. DO concentrations approach anoxic conditions in the pycnocline of the upper Bay and the deep layer of the upper and mid Bay. Anoxic conditions do not form in the lower Bay because most of the organic matter has been depleted in the upper and mid Bay. Illustrating this fact, the longitudinal plot (Figure 5.26) of surface and bottom DO show that most of the anoxic/hypoxic water occurs between 140 km to 255 km from the ocean boundary of the Bay. These observations have been documented by Cerco and Cole (1994).

Nutrient behavior through the Bay follows the same trend as chlorophyll *a* and DO. This is seen in Figures 5.11, 5.12, 5.16, 5.17, 5.20, and 5.21 as N and P concentrations are highest in the upper Bay in the spring, show a period of decline in summer, rise again in the later summer, and decline to a minimum in the late autumn. This cycle is repeated in all years modeled. The high nutrient concentrations in the spring coincide with the spring freshet bringing nutrients from

the watershed and in summer are from dead algal matter and sediment resuspension. Model predictions have produced similar findings by Adolf et al. (2006) and Harding et al. (2002) in that flora and algal community composition and primary productivity are highly influenced by the magnitude of the flows coming from the Susquehanna River which control the timing, spatial extent, and extent of the spring algal bloom through regulation of the light and nutrients.

Spatially, Figures 5.26 and 5.27 illustrate this point as N and P concentrations are reduced as one moves down the Chesapeake Bay main longitudinal axis beginning at the confluence of the Susquehanna River to the Bay (distance ≈ 325 km) and ending at the ocean boundary (distance ≈ 0.0 km). Both runs show decreased nutrient concentrations with top and bottom concentration similar in value. Differences between run results are simply from loads reduction for the 1950's RMB2 run.

As seen for other constituents, light attenuation longitudinally decreases through the Bay (Figure 5.29) for Base and the 1950's. It is highest in the shallow upper Bay and remains fairly constant until it reaches the ocean. Because of the inflow from the Susquehanna River, the upper Bay receives higher total suspended solids than the mid and lower Bay probably increasing the light attenuation in this area. Also this area is susceptible to spring algal blooms creating large amounts of suspended solids. Light attenuation values reported by Kemp et al. (2005) in the most saline area of the Patuxent River were in the range of 0.97 m^{-1} for the 1930's and 1.38 m^{-1} for the 1990's. Although, we do not see these values around 165 km on Figure 29, we do see the same trend of light extinction increasing from the 1950's to the 1980's.

5.6. DO Volume-Day

Figures 5.30 through 5.32 show that of all the regions, the mid Bay was the most susceptible to anoxia during the summer months. It has almost twice as much water approaching

anoxia (DO concentration < 1) as the other two regions. All regions show the cyclic pattern of low DO in the summer with increasing DO concentrations in the fall.

Data from Hagy et al. (2004) for the July monthly average for years from 1985-1987 were compared to ICM output averaged over the same period. There were differences in the data that had to be overcome before comparisons were made. First, the anoxic data presented by Hagy was for the whole main stem of the Bay while the ICM data represented values for each of the three regions. To compensate for this, relative values were found by normalizing to the average of the combination of the 1950's and 1980's July monthly data for ICM output and Hagy's observed values. Before data could be normalized, ICM values were converted to the same units as Hagy's values (m^3). ICM values carried the units of m^3/day so they were divided by 30 days to get m^3 . Comparisons were made between ICM 1980's and 1950's data then to Hagy's to see if the same behavior patterns of anoxia followed the observed. Results are shown in Figures 5.33 and 5.34. Each figure contains three plots for the intervals of $DO \leq 0.1$, $DO \leq 1.0$, and $DI \leq 2.0$ and on each plot are the 1950's and 1980's data from ICM and Hagy, respectively. It should be pointed out that Hagy's et al. (2004) lower interval was less than 0.2 as opposed to 0.1. From the figures, the amount of anoxic volume water for both Hagy and ICM for all intervals increased from the 1950's to the 1980's. Eutrophication has been blamed for increased anoxia in the Chesapeake Bay (Cooper and Brush 1993; Kemp et al. 2005; Burnett 1997) so by reducing the loads and light attenuation the amount of anoxia was reduced. Comparing the time series results (Figures 5.29 – 5.31) for base to the 1950's RMB2 showed the volume of anoxic water has increased from the 1950's RMB2 conditions during the summer periods for all years as much as 4 times for the interval of 1.0 or less.

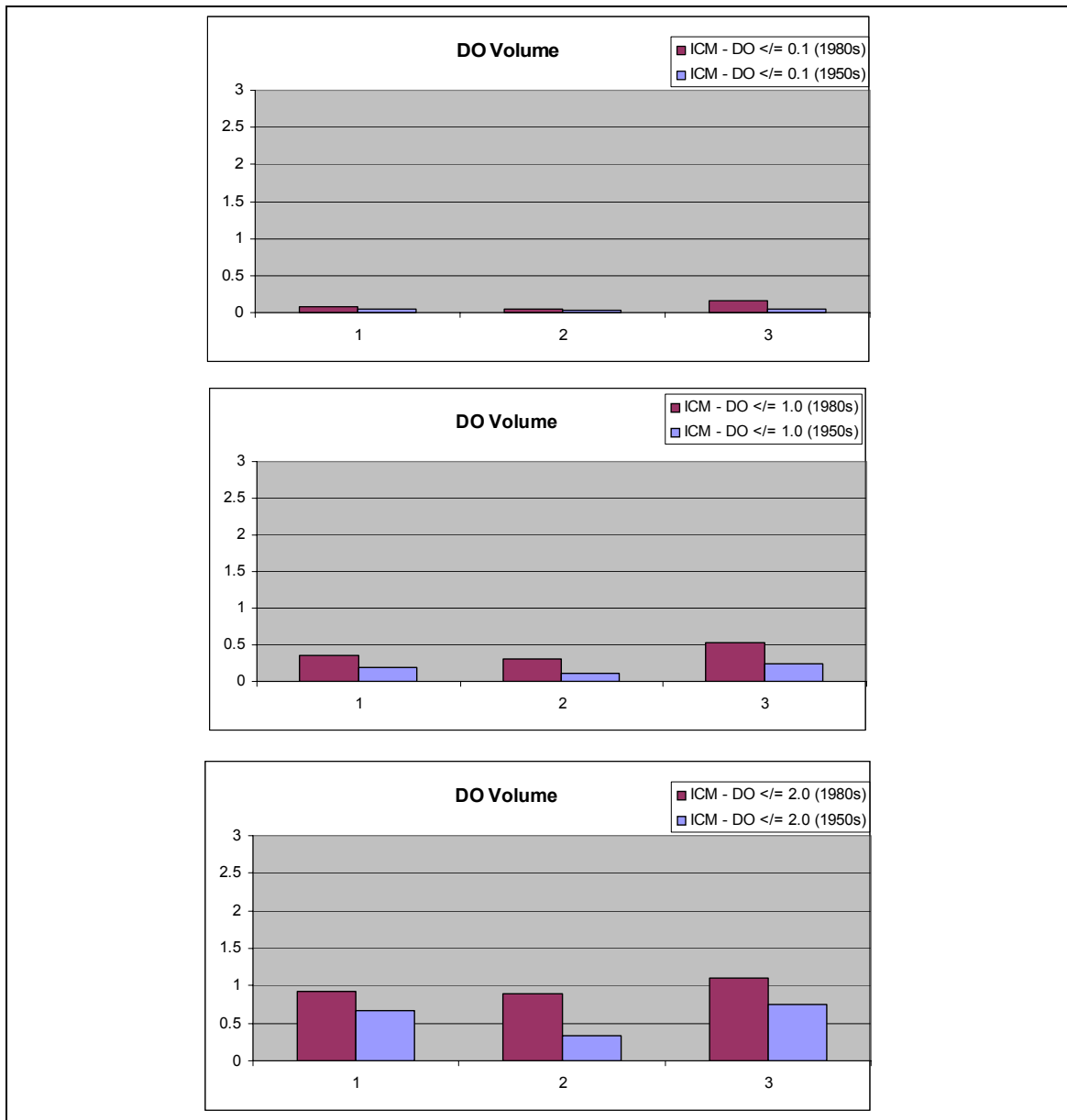


Figure 5.33. ICM normalized DO Volume water at three intervals: upper – DO ≤ 0.1 , middle – DO ≤ 1.0 , and lower – DO ≤ 2.0 .

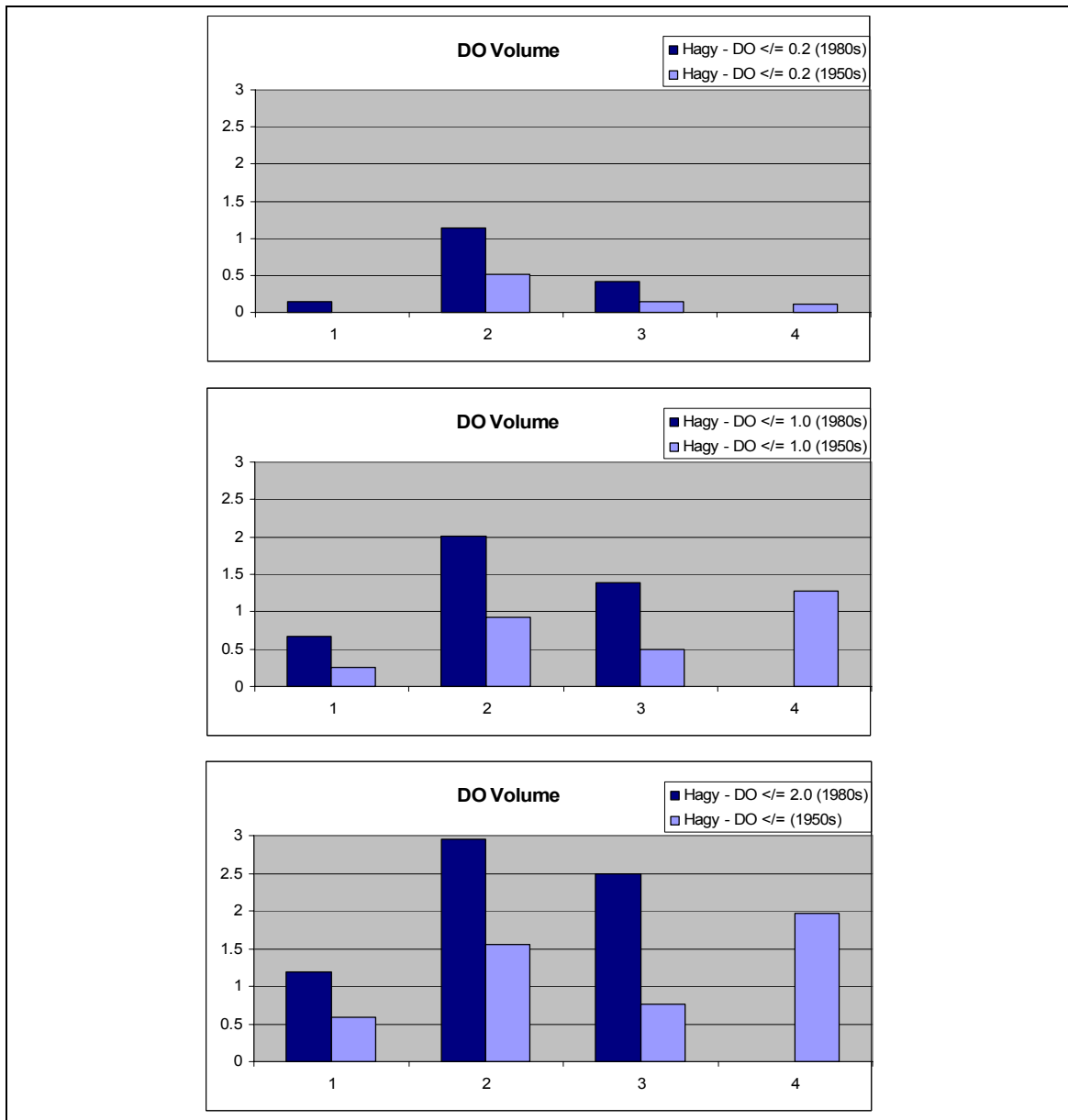


Figure 5.34. Hagy et al. (2004) normalized DO Volume water at three intervals: upper – DO \leq 0.1, middle – DO \leq 1.0, and lower – DO \leq 2.0.

5.7. Summary and Conclusions

Five simulations using the 2002 CBEM were conducted with analyses only discussed for the mid Bay. All model runs were simulated for the same time period, 1985 through 1994, but only analyzed for the 1985 through 1987 period. These runs included:

- 2002 calibration run: base
- Sensitivity run 1: SR-1
- Sensitivity run 2: SR-2
- 1950's restored mid Bay run 1: 1950's RMB1
- 1950's restored mid Bay run 2: 1950's RMB2

Reproducing the biomass of phytoplankton for the 1950's RMB2 was achieved by reducing the nutrient loads by 0.57 TN and 0.703 TP and light attenuation was reduced by half. Initially, halving the loads by themselves did not produce the desired effect on chlorophyll a ; thus, light attenuation had to be reduced as well. These values coincide with values reported by Harding and Perry (1997) for the chlorophyll a concentrations of the 1950s and 1960s.

Patchiness was adjusted to allow SAV to grow in more of the cell where SAV beds exist. From this, the SAV biomass was slightly higher than the values estimated by Hagy (2004) and increased from the ICM base run. Biomasses of the benthic organisms could not be reproduced to the values used by Hagy but were increased for deposit feeders and decreased for suspension feeders. This was attributed to prey of deposit feeders increasing and prey of suspension feeders decreasing. All in all, biomass of the primary producers was very similar to the values Hagy set for the 1950s. Production rates (P/B) for most groups were increased or remained similar for the 1950's RMB2 run compared to the base run. The only groups that were adversely affected were the zooplankton groups. With the combination of them being predators

of phytoplankton and prey for the benthos their reduction in biomass and production is believed to stem from this. Consumption rates (Q/B) do not change much from the base except for the deposit feeders. They do vary greatly from values Hagy used for his 1950's restored mid Bay Ecopath model. However, it can be noted that he did not change the Q/B from values he used in his base run.

Time series of limitations plots on phytoplankton growth show that the SR-1 produces a co-limiting of N and P in the summer months and becomes P limiting the rest of the year. Adding reduced light attenuation causes the mid Bay to be dominated by P limiting conditions all year. For benthic algae and SAV light is always the limiting factor for growth. This was shown for all scenarios run. SR-2 results show that with both loads and light attenuation reduced, P becomes more limiting through out the year than before for benthic algae. There were no early observed data from the 1950's or 1960's to verify this though. SAV limitation results for light show a cyclic pattern with less light limitation in the winter months which probably coincide with the non-growing season. Again there was no data to verify this.

DO concentrations follow similar behavior of chlorophyll *a* in that there is variation seasonally. There are increased concentrations in the spring with summer depletion in the upper and mid Bay. In the upper and mid Bay, longer periods of anoxic are observed more than anywhere else. The upper Bay has an anoxic period corresponding to the spring algae bloom that gets transported to the mid Bay. In the bottom waters for the 1950's RMB2 run, periods of anoxia are of shorter duration which has historically been observed (Hagy et al. 2004; Kemp et al. 2005). Anoxic volume day plots also illustrate that the conditions of anoxic water from the 1950's RMB2 run have been reduced. For the interval of 1 or less, the 1950's conditions of anoxia have been reduced about 4 times less than what occurs in modern times. Comparing to

DO anoxic volume from Hagy et al. (2004) shows that ICM does produce the behavior of DO anoxia increasing from the 1950's to the 1980's.

Overall, ICM produced reasonable results for conditions that could have occurred in the 1950's. Although observed data were scarce from the 1950's or 1960's to make comparisons, the results follow behavior described in literature by other researchers. These runs demonstrate the ability of ICM to reasonably predict past or future conditions/ behavior of a system if the appropriate boundary conditions are known. As demonstrated in the previous chapter, primary producer information from ICM combined with an already available Ecopath model can be a useful tool used to answer critical questions about management strategies. As changes occur in the environment (manmade or naturally), a coupled ICM /Ecopath tool can be useful in considering consequences to the upper and lower trophic levels in the ecosystem.

CHAPTER VI

SUMMARY AND CONCLUSIONS

The possibility of coupling a eutrophication model to a fisheries network model was explored. Coupling of these two models will provide managers a new perspective on how to improve management strategies and help answer questions such as: 1) how will management of watershed impact fisheries, or 2) can management of fisheries replace/supplement nutrient control? The models being considered were CE-QUAL-ICM (ICM) and Ecopath with Ecosim, (Ecopath), respectively. CE-QUAL-ICM is a time and spatially varying multi-dimensional water quality model, and Ecopath is a fisheries network model with no temporal or spatial resolution. Both models have previously been applied to the Chesapeake Bay.

Chapter II gave an overview of the ICM and Ecopath models chosen for this study. The fundamental equations of each model were presented briefly. Differences in model framework were stressed to show that coupling a three-dimensional model to a zero-dimensional model takes some consideration of how to deal with the time and the spatial aspect of the two. Both models solve for mass balance and use similar rates and processes to attain it.

Coupling the ICM and Ecopath models was presented in Chapter III. Common links between the two models were identified. Because ICM's and Ecopath's model frameworks were so vastly different, results from ICM were aggregated temporally and spatially so that its values could be compared to values used in Ecopath. Results from comparisons indicate that generally ICM and Ecopath values were similar to each other (e.g., within an order of magnitude or less). It is unreasonable to expect values from both models to be exactly the same, especially since model formulations are different. Many of the constituents and rates in ICM are calculated based on environmental conditions while Ecopath values are estimated from literature. Also, in this

chapter, two Ecopath models were created using common links from an ICM base run and the Ecopath-CB Ecopath input data for the upper Chesapeake Bay region. This exercise was performed to see Ecopath's interpretation of the same system using two different data sources for the same region. From this, the consequences of ICM under-predicting benthos and zooplankton biomasses became evident. Improvements to ICM formulations for some of the groups identified (i.e., benthos) will help to enhance the ICM predictive capabilities and bring ICM's view of the ecosystem more in line with Ecopath so that through coupling their information, answers can be found for nutrient and fishery management questions.

In Chapter IV, ICM was used to predict carbon production for the mid CB for three separate runs to replace common variables of primary producer biomasses and P/B ratios in the original Ecopath base model developed by Hagy (2002). This was an exercise to see if ICM predictions could maintain the higher trophic level organisms in Ecopath for the mid CB. In addition to the three Ecopath models developed from using ICM variables, another Ecopath model was developed by increasing the original menhaden biomass by 20%. In general, the results from the three modified EWE-ICM runs indicate that some higher trophic level groups (i.e., blue crab, white perch, spot, croaker, hogchoker, and catfish) cannot be supported without adjustments to their prey biomasses and diet compositions. The imbalance of the system for the three modified EWE runs was attributed to lower ICM primary producer biomass values (especially for net phytoplankton and microphytobenthos) and lower values of ICM net primary production rates for all primary producers except for the EWE-ICM 20%P run. These runs demonstrate the usefulness of coupling information from ICM to an existing Ecopath model to test management strategies that would take years of data collection to verify.

One of the questions this research explored is that knowing what we know about the driving forces of over abundance of nutrients and decreased water clarity, can we go back to

conditions that were found in the 1950's mid Bay by applying some type of management strategy for nutrients? This question was explored in Chapter V using ICM to simulate conditions where adjustments were made to loads and coefficients controlling eutrophication. These adjustments were made based on observations from the 1950s and 1960s. This was an attempt to try to predict primary producer biomasses similar to values Hagy (2002) used in his 1950's restored Chesapeake Bay Ecopath model. Reproducing the biomass of phytoplankton for the 1950's RMB2 was achieved by reducing the nutrient loads by 0.57 TN and 0.703 TP and light attenuation by half. Before an ICM run was made with these conditions, two sensitivity runs were made by simply halving the loads and the light attenuation coefficient. Halving the loads by themselves did not produce the desired effect on chlorophyll *a* so light attenuation had to be reduced as well. These ICM chlorophyll *a* results coincide with values reported by Harding and Perry (1997) for the chlorophyll *a* concentrations of the 1950's and 1960's.

In Chapter V, ICM produced reasonable results for conditions that could have occurred in the 1950s. Although observed data were scarce from that period to make comparisons, the results follow behavior described in literature by other researchers. If more data could be found, they would be beneficial for comparison purposes to support these observations and give more confidence to model predictions. These runs demonstrate the usefulness of using ICM to predict conditions or behavior of past or future events by setting the appropriate boundary conditions to see the effect. Taking this information and coupling it with Ecopath gives the added benefit and confidence predicting outcomes of management strategies implemented. As changes occur in the environment through anthropogenic actions or nature, a coupled ICM /Ecopath tool can be useful in considering consequences to any trophic level in an ecosystem.

During this research it was determined that a true coupling of ICM with Ecopath (i.e., exchanging of information from one model to the other and back) could not be accomplished

because the model frameworks are too different. In spite of this, the exchange of information from ICM to Ecopath is very worthwhile. A gui is being developed to automate this exchange to combine ICM information with an existing Ecopath model or as a stand alone. A exported *.eii file from Ecopath is read into the gui along with the Ecopath specific output file from the ICM post-processor. Once in the gui, any of the ten groups from ICM and their associated parameters can replace the variables in the Ecopath model. The user can exchange all or be more specific and exchange particular groups (i.e., only primary producers). Coupling the models in this way will allow modeling of upper trophic levels such as fish without adding to the computational burden of developing new state variables for ICM.

Presently, addressing interactions between water quality, habitat condition, food availability, and fisheries population dynamics from coupling ICM with Ecopath will be limited by results being a static mass-balance snapshot over an arbitrary period such as a year or seasonal period. To realize the full benefits of coupling the Ecopath with ICM, future developments should explore the possibility of coupling ICM with Ecosim and Ecospace (the dynamic, spatial version of Ecopath). Ecosim provides temporal capabilities at the ecosystem level. It uses a system of differential equations that express biomass flux rates. By doing iterative simulations, Ecosim can fit predicted biomasses to time series data. Like Ecosim, Ecospace consists of a series of coupled differential equations derived from the Ecopath master equation and is solved for each cell in the region being modeled. This would allow managers to explore temporally as well as spatially effects of fishing or to fishing from changes to different groups or rates within the ecosystem.

REFERENCES

- Adolf, J.E., Yeager, C. L., Miller, W. D., Malone, M. E., and Harding Jr., L. C. (2005).
“Environmental forcing of phytoplankton floral composition, biomass, and primary productivity
in Chesapeake Bay, USA.” *Estuarine, Coastal and Shelf Science*, 67 (2006), 108-122.
- Angelini, R. and Agostinho, A. A. (2005). “Food web model of the Upper Parana River floodplain:
Description and aggregation effects.” *Ecological Modeling*, 181(2-3), 109-121.
- Baird, D., and Ulanowicz, R.E., (1989.) “The seasonal dynamics of the Chesapeake Bay
ecosystem.” *Ecol. Monogr.* 59, 329–364.
- Bayley, S., Stotts, V. D., Springer, P. R., and Stennis, J. (1978). “Changes in submerged aquatic
macrophyte populations at the head of Chesapeake Bay, 1958-1975.” *Estuaries*, 1, 73-84.
- Bicknell, B., Imhoff, J., Kittle, J., Donigian, A., Johanson, R., and Barnwell, T. (1996). “Hydrologic
simulation program - FORTRAN user’s manual for release 11,” United States Environmental
Protection Agency Environmental Research Laboratory, Athens, GA.
- Boesch, D. F. (2000). “Measuring the health of the Chesapeake Bay: Toward integration and
prediction.” *Environ Res*, 82, 134-42.
- Boesch, D. F., Brinsfield, R. B., and Magnien, R. E. (2001). “Chesapeake Bay eutrophication:
Scientific understanding, ecosystem restoration, and challenges for agriculture.” *Journal of
Environmental Quality*, 30, 303-320.
- Boynton, W. R., Garber, J. H., Summers, R., and Kemp, W. M. (1995). “Inputs, transformations
and transport of nitrogen and phosphorus in Chesapeake Bay and selected tributaries.” *Estuaries*,
18, 285– 314.
- Bradford, J. M., Probert, P. K., Nodder, S. D., Thompson, D., Hall, J., Hanchet, S., Boyd, P.,
Zeldis, J., Baker, A., Best, H. A., Broekhuizen, N., Childerhouse, S., Clark, M., Hadfield, M.,

- Safi, K., and Wilkinson, I. (2003). "Pilot trophic model for subantarctic water over the Southern Plateau, New Zealand: A low biomass, high transfer efficiency system." *Journal of Experimental Marine Biology and Ecology*, 289(2), 223-262.
- Breitburg, D. L. (1990). "Nearshore hypoxia in Chesapeake Bay: Patterns and relationships among physical factors." *Estuarine Coastal Shelf Sci.*, 30, 593– 609.
- Breitburg, D. L. (1992). "Episodic hypoxia in Chesapeake Bay: Interacting effects of recruitment, behavior, and physical disturbance." *Ecological Monographs*, 64(2), 525-546.
- Breitburg, D. L., Loher, T., Pacey, C. A., and Gerstein, A. (1997). Varying effects of low dissolved oxygen on trophic interactions in an estuarine food web. *Ecological Monographs*, 67, 489–507.
- Bunch, B., Cerco, C., Dortch, M., Johnson, B., and Kim, K. (2000). "Hydrodynamic and water quality model study of San Juan Bay and Estuary," ERDC TR-00-1, U.S. Army Engineer Research and Development Center, Vicksburg MS.
- Bunch, B. W., Channell, M., Corson, W. D., Ebersole, B. A., Lin, L., Mark, D. J., McKinney, J. P., Pranger, S. A., Schroeder, P. R., Smith, S. J., Tillman, D. H., Tracy, B. A., Tubman, M. W., Welp, T. L. (2003). "Evaluation of island and nearshore confined disposal facility alternatives, Pascagoula River Harbor dredged material management plan" ERDC TR-03-3, U.S. Army Engineer.
- Bundy, A. (2005). "Structure and functioning of the eastern Scotian Shelf ecosystem before and after the collapse of groundfish stocks in the early 1990s." *Can J. Fish. Aquat. Sci.*, 62, 1453-1473.
- Burnett, L. E. (1997). "The challenges of living in hypoxic and hypercapnic aquatic environments." *Amer. Zool.*, 37, 633-640.
- Campbell, N. A. (1987). *Biology*. The Benjamin/Cummings Publishing Company, Inc. Redwood City, CA.

- Cerco, C. F. (1995). "Response of Chesapeake Bay to nutrient load reduction." *Journal of Environmental Engineering*, 121(8), 549-557.
- Cerco, C. and Bunch, B. (1997). "Passaic River tunnel diversion model study, Report 5, water quality modeling," Technical Report HL-96-2, U.S. Army Engineer Waterways Experiment Station, Vicksburg, MS.
- Cerco, C., and Cole, T. (1994). "Three-dimensional eutrophication model of Chesapeake Bay," Technical Report EL-94-4, US Army Engineer Waterways Experiment Station, Vicksburg, MS.
- Cerco, C., and Noel, M. (2004). "The 2002 Chesapeake Bay eutrophication model," EPA 903-R-04-004, Chesapeake Bay Program Office, US Environmental Protection Agency, Annapolis, MD.
- Cerco, C., and Tillman, D. H. (2008). "Use of coupled eutrophication and network models for examination of fisheries and eutrophication processes," ERDC/EL TR-08-10, US Army Engineer Research and Development Center, Vicksburg, MS.
- Cerco, C., Bunch, B., Cialone, M., and Wang, H. (1994). "Hydrodynamic and eutrophication model study of Indian River and Rehoboth Bay, Delaware," Technical Report EL-94-5, US Army Engineer Waterways Experiment Station, Vicksburg, MS.
- Cerco, C. F., Bunch, B. W., Teeter, A. M., and Dortch, M. S. (2000). "Water Quality Model of Florida Bay," ERDC/EL TR-00-10, U.S. Army Engineer Research and Development Center, Vicksburg, MS.
- Chambers, P. A., Meissner, R., Wrona, F. J., Rupp, H., Guhr, H., Seeger, J., Culp, J. M., and Brua, R. B. (2006). "Changes in nutrient loading in an agricultural watershed and its effects on water quality and stream biota." *Hydrobiologia*. 556, 399-415.
- Christensen, V. (1995a). Ecosystem maturity - towards quantification. *Ecological Modelling*, 77(1), 3-32.

- Christensen, V. (1995b). "A model of trophic interactions in the North Sea in 1981, the year of the Stomach." *Dana*, 11(1), 1-28.
- Christensen, V., and Walters, C. J. (2004). "Ecopath with ecosim: methods, capabilities and limitations." *Ecological Modelling*, 172(2-4), 109-139.
- Christensen, V., Walters, C., and Pauly, D. (2000). *Ecopath with ecosim: A user's guide*. Fisheries Centre, Vancouver, BC: University of British Columbia.
- Christensen, V., Walters, C., and Pauly, D. (2004). "Ecopath with Ecosim: A user's guide," Fisheries Centre, University of British Columbia.
- Christensen, V., Walters, C., and Pauly, D. (2005). *Ecopath with Ecosim: A user's guide*. Fisheries Centre, Vancouver, BC: University of British Columbia.
- Conley, D. J., and Malone, T. C., (1992). "The annual cycle of dissolved silicate in Chesapeake Bay: Implications for the production and fate of phytoplankton biomass." *Marine Ecology Progress Series*, v. 81, p. 121–128.
- Cooper, S. R. and Brush, G. S. (1991). "Long-term history of Chesapeake Bay anoxia." *Science*, 254, 992-996.
- Cooper, S. R., and Brush, G. S., (1993). "A 2500-year history of anoxia and eutrophication in Chesapeake Bay." *Estuaries*, 16, 617–626.
- Criales-Hernandez, M. I., Duarte, L. O., Garcia, C. B., and Manjarres, L. (2005). "Ecosystems impacts of the introduction of bycatch reduction devices in a tropical shrimp trawl fishery: Insights through simulation." *Fisheries Research*, 77(3), 333-342.
- Crump, B. C., Peranteau, C., Beckingham, B., and Cornwell, J. C., (2007). "Respiratory succession and community succession of bacterioplankton in seasonally anoxic waters." *Applied and Environmental Microbiology*, Nov. 2007, 6802-6810.

- Dauer, D. M., Weisberg, S. B., Ranasinghe, J. A., (2000). "Relationships between benthic community condition, water quality, sediment quality, nutrient loads, and land use patterns in Chesapeake Bay." *Estuaries* 23, 80–96.
- Davis, F. D. (1985). "Historical changes in submerged macrophyte communities of upper Chesapeake Bay." *Ecology*, 66(3), 981–993.
- Diaz, R. J. and Rosenberg, R. (1995). "Marine benthic hypoxia: A review of its ecological effects and the behavioral responses of benthic macrofauna." *Oceanography and Marine Biology Annual Review*, 33, 245–303.
- DiToro, D., and Fitzpatrick, J. (1993). *Chesapeake Bay sediment flux model*. Contract Report EL-93-2. Vicksburg, MS: U.S. Army Engineer Waterways Experiment Station, Environmental Laboratory.
- Dortch, M., Chapman, R. and Abt., S. (1992). "Application of three dimensional Lagrangian residual transport." *Journal of Hydraulic Engineering*, 118, 831-848.
- Editorial. (2004). "Placing fisheries in their ecosystem context, an introduction." *Ecological Modeling*. 172, 103-107.
- Environmental Protection Agency (EPA). (1983). "1983 Chesapeake Bay agreement." U.S. EPA, Chesapeake Bay Program Office, Annapolis, MD.
- Fetahi, T. and Mengistou, S. (2007). "Trophic analysis of Lake Awassa (Ethiopia) using mass-balance Ecopath model." *Ecological Modelling*, 201(3-4), 398-408.
- Fisher, T. R., Harding, L. W., Stanley, D. W., and Ward, L. G. (1988). "Phytoplankton, nutrients, and turbidity in the Chesapeake, Delaware, and Hudson estuaries." *Estuar. Coast. Shelf Sci*, 27, 61-93.
- Hagy III, James Dixon. (2002). "Eutrophication, hypoxia and trophic transfer efficiency in Chesapeake Bay." Diss., University of Maryland, College Park.

- Hagy, J. D., Boyton, W. R., Keefe, C. W., and Wood, K. V. (2004). "Hypoxia in Chesapeake Bay, 1950–2001: Long-term change in relation to nutrient loading and river flow." *Estuaries*, 27, 634–658.
- Harding, L.W., (1994). "Long-term trends in the distribution of phytoplankton in Chesapeake Bay: Roles of light, nutrients, and stream flow." *Marine Ecology Progress Series*, 104, 267-291.
- Harding, L. W., Jr. and Perry, E. (1997). "Long-term increase of phytoplankton biomass in Chesapeake Bay," *Mar. Ecol. Prog. Ser.*, 157, 39–52.
- Harding, L. W., Jr., Mallonee, M. E., and Perry, E. (2002). "Toward a predictive understanding of primary productivity in a temperate, partially stratified estuary." *Estuarine Coastal Shelf Sci.*, 55, 437-463.
- Heinle, D. R. (1966). "Production of a calanoid copepod, *Acartia tonsa*, in the Patuxent River estuary." *Chesapeake Sci.*, 7, 59-74.
- Heymans, J. J., and Baird, D. (2000). "A carbon flow model and network analysis of the northern Benguela upwelling system, Namibia." *Ecol. Model.* 126 (1), 9–32.
- Heymans, J. J., and McLachlan, A. (1996). "Carbon budget and network analysis of a high-energy beach: Surf-zone ecosystem." *Est. Coast. Shelf Sci.*, 43, 485–505.
- Holland, A. F., Shaughnessy, A. T., and Hiegel, M. H. (1987). "Long-term variation in mesohaline Chesapeake Bay macrobenthos: Spatial and temporal patterns." *Estuaries*, 10, 227–245.
- HydroQual. (2000). *Development of a suspension feeding and deposit feeding benthos model for Chesapeake Bay*. Project No. USCE0410. Mahwah, NJ, HydroQual Inc.
www.chesapeakebay.net/modsc.htm.
- Jaworski, N. A., Groppman, P. M., Keller, A. A., and Prager, J. C. (1992). "A watershed nitrogen and phosphorus balance: The Upper Potomac River Basin." *Estuaries*, 15, 83-95.

- Johnson, B., Heath, R., Hsieh, B., Kim, K., and Butler, L. (1991). "Development and verification of a three-dimensional numerical hydrodynamic, salinity, and temperature model of Chesapeake Bay," HL-91-7, US Army Engineer Waterways Experiment Station, Vicksburg, MS.
- Johnson, B., Kim, K., Heath, R., Hsieh, B., and Butler, L. (1993). "Validation of a three dimensional hydrodynamic model of Chesapeake Bay," *Journal of Hydraulic Engineering*, 199(1), 2-20.
- Kavanagh, P., Newlands, n., Christensen, v., and Pauly, D. (2004). "Automated parameter optimization for Ecopath ecosystem models." *Ecological Modelling*, 172, 141–149.
- Kemp, W., Smith, E., DiPasquale, M., and Boynton, W. (1997). "Organic carbon balance and net ecosystem metabolism in Chesapeake Bay." *Marine Ecology Progress Series*, 150, 229–248.
- Kemp, W. M., Sampou, P. A., Garber, J., Tuttle, J., and Boynton, W. R. (1992). "Seasonal depletion of oxygen from bottom waters of Chesapeake Bay: Roles of benthic and planktonic respiration and physical exchange processes." *Marine Ecology Progress Series* 85: 137-152.
- Kemp, W. M., Twilley, R. R., Stevenson, J. C., Boynton, W. R., and Means, J. C. (1983). "The decline of submerged vascular plants in upper Chesapeake Bay: Summary of results concerning possible causes." *Mar Technol Soc J*, 17, 78–89.
- Kemp, W. M., Boynton, W. R., Adolf, J. E., Boesch, D. F., Boicourt, W. C., Brush, G., Cornwell, J. C., Fisher, T. R., Glibert, P. M., Hagy, J. D., Harding, L. C., Houde, E. D., Kimmel, D. G., Miller, W. C., Newell, R. I. E., Roman, M. R., Smith, E. M., and Stevenson, J. C. (2005). "Eutrophication of Chesapeake Bay: Historical trends and ecological interactions." *Marine Ecology Progress Series*, 303, 1-29.
- Kiely, Gerard. (1997). *Environmental Engineering*. The McGraw-Hill Companies, London, England.

- Korpinen, Samula, Joromalainin, Verijo, and Honkanen, Turja. (2007). "Bottom-up and cascading top-down control of macroalgae along a depth gradient." *J. of Experimental Marine Biology and Ecology*. 343, 52-63.
- Leonard, B. (1979). "A stable and accurate convection modelling procedure based on quadratic upstream interpolation," *Computer Methods in Applied Mechanics and Engineering*, 19, 59-98.
- Lindeman, R. L., (1942.) "The trophic-dynamic aspect of ecology." *Ecology*, 23, 399-418.
- Linker, L., Shenk, G., Dennis, R., and Sweeney, J. (2000). "Cross-media models of the Chesapeake Bay watershed and airshed," *Water Quality and Ecosystem Modeling*, 1(1-4), 91-122.
- Loeuille, N. and Loreau, M., (2004). "Nutrient enrichment and food chains: Can evolution buffer top-down control." *Theoretical Population Biology*, 65, 285-298.
- Malone, T. C., Crocker, L. H., Pike, S. E., Wendler, B. (1988). "Influences of river flow on the dynamics of phytoplankton production in a partially stratified estuary." *Mar. Ecol. Prog.Ser.*, 48, 235-249.
- Marshall, H. G., (1994). "Chesapeake Bay phytoplankton: I. Composition." *Proceedings of the Biological Society of Washington*, 107, 573-585.
- Mason, C. F. (1991). *Biology of Freshwater Pollution*, 2nd edn, Longman Scientific & Technical, Harlow, Essex, England.
- Meyer, E. I., and Poepperl, R. (2004). "Assessing food-web structure, matter fluxes, and system attributes of a Central European mountain stream by performing mass-balanced network analysis." *Can J. Fish. Aquat. Sci.*, 61, 1565-1581.
- Morales-Zarate, M. V., Arreguin-Sanchez, F., Lopez-Martinez, J., and Lluch-Cota, S. E. (2003). "Ecosystem trophic structure and energy flux in the Northern Gulf of California, Mexico." *Ecological Modelling*, 174(4), 331-345.

- Neira, S., and Arancibia, H. (2004). "Trophic interactions and community structure in the upwelling system off Central Chile (33-39°S)." *Journal of Experimental Marine Biology and Ecology*, 312(2), 349-366.
- Nestler, John M., Goodwin, R. A., and Loucks, D. P. (2005). "Coupling engineering and biological models for ecosystem analysis." *J. Water Resource Plann. Management*. 131(2), 101-109.
- Newcombe, C. L., and Horner, W. A. (1938). "Oxygen-poor waters of the Chesapeake Bay." *Science*, 88, 80-81.
- Nielsen, S. L., Sand-Jensen, K. Borum, J. and Geertz-Hansen, O. (2002). "Phytoplankton, nutrients, and transparency in Danish coastal waters." *Estuaries* 25: 930-937.
- Odum, H.T. (1971.) *Fundamentals of Ecology*. W. B. Saunders Company. Philadelphia, Pa.
- Officer, C. B., Biggs, R. B., Taft, J. L., Cronin, L. E., Tyler, M. A. And Boynton, W. R. (1984). "Chesapeake Bay anoxia: Origin, development, and significance." *Science*, 223, 22-27.
- Orth, R. J., and Moore, K. A.. (1983). "Chesapeake Bay: An unprecedented decline in submersed aquatic vegetation." *Science*, 222(5), 1-53.
- Ortiz, M., and Wolff, M. (2002.) "Trophic models of four benthic communities in Tongoy Bay (Chile): Comparative analysis and preliminary assessment of management strategies." *Journal of Experimental Marine Biology and Ecology*, 268, 205–235.
- Paerl, H. W., Valdes, L. M., and Peierls, B. L. (2006). "Anthropogenic and climatic influences on the eutrophication of large estuarine ecosystems." *Limnol. Oceanogr.*, 51(1, part 2), 2006, 448–462.
- Patricio, J., and Marques, J. C., (2006). "Mass balanced models of food web in three areas along a gradient of eutrophication symptoms in the south arm of the Mondego estuary (Portugal)." *Ecological Modeling*, 197, 21-34.

- Paul, R. W. (2001). "Geographical signature of middle Atlantic estuaries: Historical layers." *Estuaries*, 24, 151-166.
- Pikitch, E. K., Santora, E. A., Babcock, E. A., Bakun, A., Bonfil, R., Conover, D. O., Dayton, P., Doukakis, P., Fluharty, D., Heneman, B., Houde, E. D., Link, J., Livingston, P. A., Mangel, M., McAllister, M. K., Pope, J., Sainsbury, K. J. (2004). "Ecosystem-based fishery management." *Science*, 305, 346-347.
- Poepperl, R. (2003). "A quantitative food web model for the macro-invertebrate community of a northern German lowland stream." *Int. Rev. Hydrobiol.*, 88, 433-452.
- Polovina, J. J. (1984). "An overview of the ECOPATH model." *Fishbyte*, 2(2), 5-7.
- Rybarczyk, H. Elkaim, B., Ochs, L., and Loquet, N. (2003). "Analysis of the trophic network of a macrotidal ecosystem: The Bay of Somme (Eastern Channel)." *Estuarine and Coastal Shelf Science*, 58(3), 405-421.
- Scavia, D., Kelly, E. M. A., and Hagy, J. D. (2006). "A simple model for forecasting the effects of nitrogen loads on Chesapeake Bay Hypoxia." *Estuaries and Coasts*. 29(4), 674-684.
- Smith, V. H. (2003). "Eutrophication of freshwater and coastal marine ecosystems: A global problem." *Environ Sci Pollut Res* 10, 1-14.
- Scientific and Technical Advisory Committee (STAC). (2005). "Coupling water quality and upper trophic level models for Chesapeake Bay: A planning workshop." STAC Publication 05-002. <http://www.chesapeake.org/stac/stacpubs.html>.
- Taft, J. L., Taylor, W. R., Hartwig, E. O., and Loftus, R. (1980). "Seasonal oxygen depletion in Chesapeake Bay." *Estuaries*, 3, 242-247.
- Tchobanoglous, G. and Schroeder, E. D. (1987). *Water quality: Characteristics, modeling, modification*. Addison-Wesley Publishing Company, Inc. Reading, MA.

- Tillman, D., Cerco, C., and Noel, M. (2006). "Conceptual processes for linking eutrophication and network models." TN-SWWRP-0905. Environmental Laboratory, Vicksburg, MS: U.S. Army Engineer Research and Development Center.
- Tillman, Dottie H., Cerco, Carl F., Noel, Mark R., Martin, James L., and Hamrick, John (2004). "Three-dimensional eutrophication model of the Lower St. Johns River, Florida." ERDC/EL TR-04-13, US Army Engineer Research and Development Center, Vicksburg, MS.
- Twilley, R. R., and Barko, J. W. (1990). "The growth of submerged macrophytes under experimental salinity and light conditions." *Estuaries*, 13(3), 311-321.
- Ulanowicz, R.E., (1986). *Growth and development: Ecosystem phenomenology*. Springer-Verlag, New York, 203 pp.
- United States Geological Service (USGS). (2000). "Effects of climate variability and human activities on Chesapeake Bay and the implications for ecosystem restoration." USGS Fact Sheet FS-116-00, September 2000.
- Villanueva, M. C., Laleye, P., Albaret, J. J., Lae, R., Tito de Morais, L., and Moreau, J. (2006). "Comparative analysis of trophic structure and interactions of two tropical lagoons." *Ecological Modelling*, 197(3-4), 461-477.
- Westrich, J., and Berner, R. (1984). "The role of sedimentary organic matter in bacterial sulfate reduction: The G model tested," *Limnology and Oceanography*, 29(2), 236-249.
- Wolfe, D. A., Champ, M. A., Flemer, D. A., and Mearns, A. J. (1987). "Long-term biological data sets: Their role in research, monitoring, and management of estuarine and coastal marine systems." *Estuaries*, 10(3), 181-193.
- Worm, B., Lotze, H. K., and Sommer, U. (2000). "Coastal food web structure, carbon storage, and nitrogen retention regulated by consumer pressure and nutrient loading." *Limnol. Oceanogr.*, 45(2), 339-349.

Zimmerman, A. R., and Canuel, E. A. (2002). "Sediment geochemical records of eutrophication in the mesohaline Chesapeake Bay." *Limnology and Oceanography*, 47, 1084–1093.

APPENDIX A

This appendix contains the program listing for the post-processor /subroutine created to manipulated data to be compatible with Ecopath. The program can also solve for the ecotrophic efficiencies of the groups being modeled. This variable determines whether a group is being over-utilized causing mass balance problems. This program is written in FORTRAN.

c A rudimentary KFL processor for checking purposes.
 c Revised Feb 14, 2006 to go with new ecopath postprocessor
 c Revised Jul 19, 2007 to go calculate Diet Compositions and Detritus
 Fate

***** Parameter declarations

```

      INTEGER NCP, NBP, NQFP, NHQP, NSBP, NLP, NS1P, NS2P, NS3P,
      .         NBCP, NMP, NDP, NSAVP, NFLP, NOIP, NSSFP, NPES

```

```

      PARAMETER (NCP=24)

```

c Chesapeake Bay (for 1 PE run) 12000 cells

```

      PARAMETER (NBP=12920, NQFP=30835, NHQP=20876, NSBP=2961, NLP=19,
!CHESAPEAKE
      .         NS1P=4000, NS2P=4000,
!CHESAPEAKE
      .         NS3P=4000, NBCP=496, NMP=30, NDP=500, NSAVP=5,
!CHESAPEAKE
      .         NFLP=100, NOIP=10, NSSFP=3, NPES=1)
!CHESAPEAKE

```

```

      REAL E_BALG(NSBP), E_BNPP(NSBP), E_DFEED(NSBP), E_SAV(NSBP),
      .     E_CFLUX(NSBP), E_SAVNP(NSBP), E_BALGR(NSBP),
      .     E_BALGPR(NSBP), E_BALGC(NSBP), E_SFEED(NSBP), E_BURIAL(NSBP),
      .     E_SAV2SED(NSBP), E_SAV2POC(NSBP), E_SAV2DOC(NSBP),
      .     E_DFNP(NSBP), E_DFCON(NSBP), E_DFUAC(NSBP), E_SFNP(NSBP),
      .     E_SFTCON(NSBP), E_SFACON(NSBP), E_SFPCCON(NSBP), E_SFUAC(NSBP),
      .     E_ALG2SED(NSBP), E_SEDPOC(NSBP), E_SEDR(NSBP), E_DFR(NSBP),
      .     E_SFR(NSBP), E_SAVR(NSBP)

```

```

      REAL E_ALGC(NBP), E_ANPP(NBP), E_AGPP(NBP), E_MICRZ(NBP),
      .     E_MESoz(NBP), E_DOC(NBP), E_POC(NBP), E_DETC(NBP),
      .     E_APRED(NBP), E_ADOC(NBP), E_APOC(NBP), E_CRESP(NBP),
      .     E_MICRZR(NBP), E_MESozR(NBP), E_MIC2MES(NBP), E_MICRZNP(NBP),
      .     E_MESozNP(NBP), E_MICRZDOC(NBP),
      .     E_MICRZPOC(NBP), E_MESozPOC(NBP), E_MICRZPR(NBP),
      .     E_MESozPR(NBP), E_MICRZALG(NBP), E_MESozALG(NBP)

```

```

      REAL E_UADOCsz(NBP), E_UAPOCSz(NBP), E_UAPOCLz(NBP),
      .     E_UADOCCLz(NBP), E_POC2DOC(NBP), E_TCONLz(NBP),
      .     E_TCONsz(NBP)

```

```

      REAL COL_JDAY,          COL_ALGC,          COL_ANPP,
      .     COL_AGPP,          COL_APRED,          COL_ADOC,
      .     COL_APOC,
      .     COL_DOC,          COL_POC,          COL_DETC,
      .     COL_CRESP,          COL_POC2DOC,          COL_MICRZ,
      .     COL_MICRZR,          COL_MICRZNP,          COL_MICRZDOC,
      .     COL_MICRZPOC,          COL_MICRZPR,          COL_MICRZALG,
      .     COL_TCONsz,          COL_UADOCsz,          COL_UAPOCSz,
      .     COL_MESoz,          COL_MESozR,          COL_MESozNP,
      .     COL_MESozPOC,          COL_MESozPR,          COL_MESozALG,
      .     COL_MIC2MES,          COL_TCONLz,          COL_UADOCCLz,
      .     COL_UAPOCLz

```

```

REAL COL_BURIAL,          COL_CFLUX,          COL_ALG2SED,
. COL_BALG,              COL_BALGR,
. COL_BALGPR,           COL_BALGC,          COL_BNPP,

. COL_SAV,              COL_SAVNP,          COL_SAV2SED,
. COL_SAV2POC,          COL_SAV2DOC,        COL_SFEED,
. COL_SFPN,             COL_SFTCON,         COL_SFACON,
. COL_SFPCCON,          COL_SFUAC,          COL_DFEED,
. COL_DFNP,             COL_DFTCON,         COL_DFUAC,
. COL_SEDPOC,           COL_SEDR,           COL_SFR,
. COL_DFR,              COL_SAVR

REAL REG_JDAY(10000),    REG_ALGC(10000),    REG_ANPP(10000),
. REG_AGPP(10000),      REG_APRED(10000),   REG_ADOC(10000),
. REG_APOC(10000),
. REG_DOC(10000),       REG_POC(10000),     REG_DETC(10000),
. REG_CRESP(10000),    REG_POC2DOC(10000), REG_MICRZ(10000),
. REG_MICRZR(10000),   REG_MICRZNP(10000), REG_MICRZDOC(10000),
. REG_MICRZPOC(10000), REG_MICRZPR(10000), REG_MICRZALG(10000),
. REG_TCONSZ(10000),   REG_UADOC SZ(10000), REG_UAPOC SZ(10000),
. REG_MESoz(10000),    REG_MESozR(10000), REG_MESozNP(10000),
. REG_MESozPOC(10000), REG_MESozPR(10000), REG_MESozALG(10000),
. REG_MIC2MES(10000), REG_TCONLZ(10000), REG_UADOC LZ(10000),
. REG_UAPOC LZ(10000)

REAL REG_BURIAL(10000), REG_CFLUX(10000), REG_ALG2SED(10000),
. REG_BALG(10000),     REG_BALGR(10000),
. REG_BALGPR(10000),  REG_BALGC(10000),  REG_BNPP(10000),

. REG_SAV(10000),     REG_SAVNP(10000),  REG_SAV2SED(10000),
. REG_SAV2POC(10000), REG_SAV2DOC(10000), REG_SFEED(10000),
. REG_SFPN(10000),    REG_SFTCON(10000), REG_SFACON(10000),
. REG_SFPCCON(10000), REG_SFUAC(10000),  REG_DFEED(10000),
. REG_DFNP(10000),    REG_DFTCON(10000), REG_DFUAC(10000),
. REG_SEDPOC(10000), REG_SEDR(10000),   REG_SFR(10000),
. REG_DFR(10000),     REG_SAVR(10000)

REAL MICRBENALG_DOC, MICRBENALG_POC, MICRBENALG_SedPOC

REAL EE(100), BIOM(100), PB(100), Consumpt(100),
. QB(100), UA(100), DC(20,20), BIOA(50),
. GSUMM2(100), PHI(100), Y(100),
. BA(100), E(100), Biomass(100), M2,
. EE_BIO(50), CANN(100), SAMEG(100)

```

```

REAL V1(0:NBP), SFA(NSBP), JDAY

INTEGER NB, NSB, SBN(NSBP), BBN(NSBP), CELL, B
INTEGER NBOXCOL(NSBP), BOX(NSBP,NLP), REG_CELL(1000)
INTEGER NGROUP, NPREDATOR,S_EE(50), S_Biom(50)

CHARACTER*72 TITLE(6)

LOGICAL SAV_CALC, BALGAE_CALC, SolEE(50), SolBiom(50)

DATA KFL /21/

OPEN(21,FILE='wqm_kfl.10YR_SENS153_new_grid_ISS_061408',
.   STATUS='UNKNOWN',FORM='UNFORMATTED')
OPEN(22,FILE='CBPSbylevel_MD2_2961_DHT.dat',STATUS='UNKNOWN')
OPEN(23,FILE='KFL_postpro_area_12000_ISS_061408.opt',
.   STATUS='UNKNOWN')
OPEN(24,FILE='col_ches_7_24_00.inp',STATUS='OLD')
C
C Set number of groups
C
  NGROUP = 10
  NPREDATOR = 10
  Do I = 1, NGROUP
    SolEE(I) = .false.
    SolBiom(I) = .false.
    BIOA(I) = 0.0
  END DO

C READ FILE THAT MAPS SURFACE BOXES TO REST OF COLUMN
C   DO I=1,729
C   DO I=1,3162
C     READ(24,*,END=50) idum,jdum,NBOXCOL(I), (BOX(I,J),
C       J=1,NBOXCOL(I))
C   END DO
50 Continue
C ZERO OUT AVERAGE REGIONAL SUMS

  DO I=1,10000
    AREG_JDAY=0.0
    AREG_ALGC=0.0
    AREG_ANPP=0.0
    AREG_AGPP=0.0
    AREG_APRED=0.0
    AREG_ADOC=0.0
    AREG_APOC=0.0

    AREG_DOC=0.0
    AREG_POC=0.0
    AREG_DETC=0.0
    AREG_CRESP =0.0
    AREG_POC2DOC =0.0

    AREG_MICRZ =0.0

```

```

AREG_MICRZR =0.0
AREG_MICRZNP =0.0
AREG_MICRZDOC =0.0
AREG_MICRZPOC =0.0
AREG_MICRZPR =0.0
AREG_MICRZALG =0.0
AREG_TCONSZ =0.0
AREG_UADOC SZ =0.0
AREG_UAPOC SZ =0.0

```

```

AREG_MES0Z =0.0
AREG_MES0ZR =0.0
AREG_MES0ZNP =0.0
AREG_MES0ZPOC =0.0
AREG_MES0ZPR =0.0
AREG_MES0ZALG =0.0
AREG_MIC2MES =0.0
AREG_TCONLZ =0.0
AREG_UAD0CLZ =0.0
AREG_UAPOCLZ =0.0

```

```

AREG_BURIAL = 0.0
AREG_CFLUX = 0.0
AREG_SEDR = 0.0
AREG_ALG2SED = 0.0
AREG_BALG = 0.0
AREG_BALGR = 0.0
AREG_BALGPR = 0.0
AREG_BALGC = 0.0
AREG_BNPP = 0.0

```

```

AREG_SAV = 0.0
AREG_SAVNP = 0.0
AREG_SAVR = 0.0
AREG_SAV2SED = 0.0
AREG_SAV2POC = 0.0
AREG_SAV2DOC = 0.0

```

```

AREG_SFEE D = 0.0
AREG_SFNP = 0.0
AREG_SFR = 0.0
AREG_SFTCON = 0.0
AREG_SFACON = 0.0
AREG_SFPCCON = 0.0
AREG_SFUAC = 0.0
AREG_DFEE D = 0.0
AREG_DFNP = 0.0
AREG_DFR = 0.0
AREG_DFTCON = 0.0
AREG_DFUAC = 0.0
AREG_SEDPOC = 0.0

```

```
END DO
```

```
ACOUNT = 0.
```

```
1 READ (KFL) (TITLE(I), I=1,6), NB, NSB, (SBN(B), B=1, NSB),
```

```

. (BBN(B),B=1,NSB),
. (V1(B),B=0,NB), (SFA(B),B=1,NSB), SAV_CALC, BALGAE_CALC
  Write(*,*) (TITLE(I),I=1,6)

```

```

READ(22,*,END=3) NCELL
READ(22,*) (REG_CELL(I),I=1,NCELL)

```

C GET REGIONAL AREA

```

REG_AREA = 0.0
DO I=1,NCELL
  CELL = REG_CELL(I)
  REG_AREA = REG_AREA + SFA(CELL)
END DO

```

C ZERO OUT REGIONAL SUMS

```

DO I=1,10000
  REG_JDAY(I) =0.0
  REG_ALGC(I) =0.0
  REG_ANPP(I) =0.0
  REG_AGPP(I) =0.0
  REG_APRED(I)=0.0
  REG_ADOC(I) =0.0
  REG_APOC(I) =0.0

  REG_DOC(I) =0.0
  REG_POC(I) =0.0
  REG_DETC(I) =0.0
  REG_CRESP(I) =0.0
  REG_POC2DOC(I) =0.0

  REG_MICRZ(I) =0.0
  REG_MICRZR(I) =0.0
  REG_MICRZNP(I) =0.0
  REG_MICRZDOC(I) =0.0
  REG_MICRZPOC(I) =0.0
  REG_MICRZPR(I) =0.0
  REG_MICRZALG(I) =0.0
  REG_TCONSZ(I) =0.0
  REG_UADOC SZ(I) =0.0
  REG_UAPOC SZ(I) =0.0

  REG_MESoz(I) =0.0
  REG_MESozR(I) =0.0
  REG_MESozNP(I) =0.0
  REG_MESozPOC(I) =0.0
  REG_MESozPR(I) =0.0
  REG_MESozALG(I) =0.0
  REG_MIC2MES(I) =0.0
  REG_TCONLZ(I) =0.0
  REG_UADOC LZ(I) =0.0
  REG_UAPOC LZ(I) =0.0

```

```

REG_BURIAL(I) = 0.0
REG_CFLUX(I) = 0.0
REG_SEDR(I) = 0.0
REG_ALG2SED(I) = 0.0
REG_BALG(I) = 0.0
REG_BALGR(I) = 0.0
REG_BALGPR(I) = 0.0
REG_BALGC(I) = 0.0
REG_BNPP(I) = 0.0

```

```

REG_SAV(I) = 0.0
REG_SAVNP(I) = 0.0
REG_SAVR(I) = 0.0
REG_SAV2SED(I) = 0.0
REG_SAV2POC(I) = 0.0
REG_SAV2DOC(I) = 0.0

```

```

REG_SFEED(I) = 0.0
REG_SFNP(I) = 0.0
REG_SFR(I) = 0.0
REG_SFTCON(I) = 0.0
REG_SFACON(I) = 0.0
REG_SFPCCON(I) = 0.0
REG_SFUAC(I) = 0.0
REG_DFEED(I) = 0.0
REG_DFNP(I) = 0.0
REG_DFR(I) = 0.0
REG_DFTCON(I) = 0.0
REG_DFUAC(I) = 0.0
REG_SEDPOC(I) = 0.0

```

```
END DO
```

```
NREAD=0
```

```
DO I=1,10000
```

```
  READ(KFL,END=2) JDAY
```

```
  NREAD = NREAD+1
```

```
  REG_JDAY(I) = JDAY
```

```
  READ(KFL) (E_ALGC(B),B=1,NB), (E_ANPP(B),B=1,NB),
```

```
  . (E_AGPP(B),B=1,NB), (E_APRED(B),B=1,NB),
```

```
  . (E_ADOC(B),B=1,NB), (E_APOC(B),B=1,NB)
```

```
  READ(KFL) (E_DOC(B),B=1,NB), (E_POC(B),B=1,NB),
```

```
  . (E_DETC(B),B=1,NB), (E_CRESP(B),B=1,NB),
```

```
  . (E_POC2DOC(B),B=1,NB)
```

```
  READ(KFL) (E_MICRZ(B),B=1,NB), (E_MICRZR(B),B=1,NB),
```

```
  . (E_MICRZNP(B),B=1,NB),
```

```
  . (E_MICRZDOC(B),B=1,NB), (E_MICRZPOC(B),B=1,NB),
```

```
  . (E_MICRZPR(B),B=1,NB), (E_MICRZALG(B),B=1,NB),
```

```
  . (E_TCONSZ(B),B=1,NB), (E_UADOC SZ(B),B=1,NB),
```

```
  . (E_UAPOC SZ(B),B=1,NB)
```

```
  READ(KFL) (E_MESoz(B),B=1,NB), (E_MESozR(B),B=1,NB),
```

```
  . (E_MESozNP(B),B=1,NB), (E_MESozPOC(B),B=1,NB),
```

```
  . (E_MESozALG(B),B=1,NB), (E_MIC2MES(B),B=1,NB),
```

```
  . (E_MESozPR(B),B=1,NB), (E_TCONLZ(B),B=1,NB),
```



```

.          (E_UADOCLZ(B),B=1,NB), (E_UAPOCLZ(B),B=1,NB)
.
.          READ(KFL) (E_SEDPOC(B),B=1,NSB), (E_BURIAL(B),B=1,NSB),
.                   (E_CFLUX(B),B=1,NSB), (E_ALG2SED(B),B=1,NSB),
.                   (E_SEDR(B),B=1,NSB)
.          READ(KFL) (E_BALG(B),B=1,NSB), (E_BNPP(B),B=1,NSB),
.                   (E_BALGR(B),B=1,NSB),
.                   (E_BALGPR(B),B=1,NSB), (E_BALGC(B),B=1,NSB)
.          READ(KFL) (E_SAV(B),B=1,NSB), (E_SAVNP(B),B=1,NSB),
.                   (E_SAV2SED(B),B=1,NSB), (E_SAV2POC(B),B=1,NSB),
.                   (E_SAV2DOC(B),B=1,NSB), (E_SAVR(B),B=1,NSB)
.          READ(KFL) (E_SFEED(B),B=1,NSB), (E_SFNP(B),B=1,NSB),
.                   (E_SFTCON(B),B=1,NSB), (E_SFACON(B),B=1,NSB),
.                   (E_SFPCON(B),B=1,NSB), (E_SFUAC(B),B=1,NSB),
.                   (E_SFR(B),B=1,NSB)
.          READ(KFL) (E_DFEED(B),B=1,NSB), (E_DFNP(B),B=1,NSB),
.                   (E_DFTCON(B),B=1,NSB), (E_DFUAC(B),B=1,NSB),
.                   (E_DFR(B),B=1,NSB)

```

C SUM THESE OVER ALL COLUMNS IN THE REGION

```
DO JJ=1,NCELL
```

C ZERO OUT COLUMN SUMS

```

COL_ALGC =0.0
COL_ANPP =0.0
COL_AGPP =0.0
COL_APRED=0.0
COL_ADOC =0.0
COL_APOC =0.0

COL_DOC =0.0
COL_POC =0.0
COL_DETC =0.0
COL_CRESP =0.0
COL_POC2DOC =0.0

COL_MICRZ =0.0
COL_MICRZR =0.0
COL_MICRZNP =0.0
COL_MICRZDOC =0.0
COL_MICRZPOC =0.0
COL_MICRZPR =0.0
COL_MICRZALG =0.0
COL_TCONSZ =0.0
COL_UADOC SZ =0.0
COL_UAPOC SZ =0.0

COL_MESoz =0.0
COL_MESozR =0.0
COL_MESozNP =0.0
COL_MESozPOC =0.0
COL_MESozPR =0.0
COL_MESozALG =0.0

```

```

COL_MIC2MES =0.0
COL_TCONLZ =0.0
COL_UADOCLZ =0.0
COL_UAPOCLZ =0.0

CELL = REG_CELL(JJ)

DO J=1,NBOXCOL(CELL)
  K=BOX(CELL,J)
  COL_ALGC=COL_ALGC+E_ALGC(K)
  COL_ANPP=COL_ANPP+E_ANPP(K)
  COL_AGPP=COL_AGPP+E_AGPP(K)
  COL_APRED=COL_APRED+E_APRED(K)
  COL_ADOC=COL_ADOC+E_ADOC(K)
  COL_APOC=COL_APOC+E_APOC(K)

  COL_DOC=COL_DOC+E_DOC(K)
  COL_POC=COL_POC+E_POC(K)
  COL_DETC=COL_DETC+E_DETC(K)
  COL_CRESP=COL_CRESP+E_CRESP(K)
  COL_POC2DOC=COL_POC2DOC+E_POC2DOC(K)

  COL_MICRZ=COL_MICRZ+E_MICRZ(K)
  COL_MICRZR=COL_MICRZR+E_MICRZR(K)
  COL_MICRZNP=COL_MICRZNP+E_MICRZNP(K)
  COL_MICRZDOC=COL_MICRZDOC+E_MICRZDOC(K)
  COL_MICRZPOC=COL_MICRZPOC+E_MICRZPOC(K)
  COL_MICRZPR=COL_MICRZPR+E_MICRZPR(K)
  COL_MICRZALG=COL_MICRZALG+E_MICRZALG(K)
  COL_TCONSZ=COL_TCONSZ+E_TCONSZ(K)
  COL_UADOC SZ=COL_UADOC SZ+E_UADOC SZ(K)
  COL_UAPOC SZ=COL_UAPOC SZ+E_UAPOC SZ(K)

  COL_MESoz=COL_MESoz+E_MESoz(K)
  COL_MESozR=COL_MESozR+E_MESozR(K)
  COL_MESozNP=COL_MESozNP+E_MESozNP(K)
  COL_MESozPOC=COL_MESozPOC+E_MESozPOC(K)
  COL_MESozPR=COL_MESozPR+E_MESozPR(K)
  COL_MESozALG=COL_MESozALG+E_MESozALG(K)
  COL_MIC2MES=COL_MIC2MES+E_MIC2MES(K)
  COL_TCONLZ=COL_TCONLZ+E_TCONLZ(K)
  COL_UADOCLZ=COL_UADOCLZ+E_UADOCLZ(K)
  COL_UAPOCLZ=COL_UAPOCLZ+E_UAPOCLZ(K)
END DO

C SAVE THE VARIABLES THAT ONLY EXIST AT THE BOTTOM

COL_SEDPOC = E_SEDPOC(CELL)
COL_BURIAL = E_BURIAL(CELL)
COL_CFLUX = E_CFLUX(CELL)
COL_ALG2SED = E_ALG2SED(CELL)
COL_SEDR = E_SEDR(CELL)

COL_BALG = E_BALG(CELL)

```

```

COL_BALGR = E_BALGR (CELL)
COL_BALGPR = E_BALGPR (CELL)
COL_BALGC = E_BALGC (CELL)
COL_BNPP = E_BNPP (CELL)

COL_SAV = E_SAV (CELL)
COL_SAVNP = E_SAVNP (CELL)
COL_SAVR = E_SAVR (CELL)
COL_SAV2SED = E_SAV2SED (CELL)
COL_SAV2POC = E_SAV2POC (CELL)
COL_SAV2DOC = E_SAV2DOC (CELL)

COL_SFEEED = E_SFEEED (CELL)
COL_SFNP = E_SFNP (CELL)
COL_SFR = E_SFR (CELL)
COL_SFTCON = E_SFTCON (CELL)
COL_SFACON = E_SFACON (CELL)
COL_SFPCCON = E_SFPCCON (CELL)
COL_SFUAC = E_SFUAC (CELL)

COL_DFEED = E_DFEED (CELL)
COL_DFNP = E_DFNP (CELL)
COL_DFR = E_DFR (CELL)
COL_DFTCON = E_DFTCON (CELL)
COL_DFUAC = E_DFUAC (CELL)

```

C SUM CELLS OVER REGION

```

REG_ALGC (I) = REG_ALGC (I) + COL_ALGC * SFA (CELL)
REG_ANPP (I) = REG_ANPP (I) + COL_ANPP * SFA (CELL)
REG_AGPP (I) = REG_AGPP (I) + COL_AGPP * SFA (CELL)
REG_APRED (I) = REG_APRED (I) + COL_APRED * SFA (CELL)
REG_ADOC (I) = REG_ADOC (I) + COL_ADOC * SFA (CELL)
REG_APOC (I) = REG_APOC (I) + COL_APOC * SFA (CELL)

REG_DOC (I) = REG_DOC (I) + COL_DOC * SFA (CELL)
REG_POC (I) = REG_POC (I) + COL_POC * SFA (CELL)
REG_DETC (I) = REG_DETC (I) + COL_DETC * SFA (CELL)
REG_CRESP (I) = REG_CRESP (I) + COL_CRESP * SFA (CELL)
REG_POC2DOC (I) = REG_POC2DOC (I) + COL_POC2DOC * SFA (CELL)

REG_MICRZ (I) = REG_MICRZ (I) + COL_MICRZ * SFA (CELL)
REG_MICRZR (I) = REG_MICRZR (I) + COL_MICRZR * SFA (CELL)
REG_MICRZNP (I) = REG_MICRZNP (I) + COL_MICRZNP * SFA (CELL)
REG_MICRZDOC (I) = REG_MICRZDOC (I) + COL_MICRZDOC * SFA (CELL)
REG_MICRZPOC (I) = REG_MICRZPOC (I) + COL_MICRZPOC * SFA (CELL)
REG_MICRZPR (I) = REG_MICRZPR (I) + COL_MICRZPR * SFA (CELL)
REG_MICRZALG (I) = REG_MICRZALG (I) + COL_MICRZALG * SFA (CELL)
REG_TCONSZ (I) = REG_TCONSZ (I) + COL_TCONSZ * SFA (CELL)
REG_UADOC SZ (I) = REG_UADOC SZ (I) + COL_UADOC SZ * SFA (CELL)
REG_UAPOC SZ (I) = REG_UAPOC SZ (I) + COL_UAPOC SZ * SFA (CELL)

REG_MESoz (I) = REG_MESoz (I) + COL_MESoz * SFA (CELL)
REG_MESozR (I) = REG_MESozR (I) + COL_MESozR * SFA (CELL)

```

```

REG_MESOZNP(I)=REG_MESOZNP(I)+COL_MESOZNP*SFA(CELL)
REG_MESOZPOC(I)=REG_MESOZPOC(I)+COL_MESOZPOC*SFA(CELL)
REG_MESOZPR(I)=REG_MESOZPR(I)+COL_MESOZPR*SFA(CELL)
REG_MESOZALG(I)=REG_MESOZALG(I)+COL_MESOZALG*SFA(CELL)
REG_MIC2MES(I)=REG_MIC2MES(I)+COL_MIC2MES*SFA(CELL)
REG_TCONLZ(I)=REG_TCONLZ(I)+COL_TCONLZ*SFA(CELL)
REG_UADOCLZ(I)=REG_UADOCLZ(I)+COL_UADOCLZ*SFA(CELL)
REG_UAPOCLZ(I)=REG_UAPOCLZ(I)+COL_UAPOCLZ*SFA(CELL)

```

```

REG_SEDPOC(I) = REG_SEDPOC(I)+COL_SEDPOC*SFA(CELL)
REG_SEDR(I) = REG_SEDR(I)+COL_SEDR*SFA(CELL)
REG_BURIAL(I) = REG_BURIAL(I)+COL_BURIAL*SFA(CELL)
REG_CFLUX(I) = REG_CFLUX(I)+COL_CFLUX*SFA(CELL)
REG_ALG2SED(I) = REG_ALG2SED(I)+COL_ALG2SED*SFA(CELL)

```

```

REG_BALG(I) = REG_BALG(I)+COL_BALG*SFA(CELL)
REG_BALGR(I) = REG_BALGR(I)+COL_BALGR*SFA(CELL)
REG_BALGPR(I) = REG_BALGPR(I)+COL_BALGPR*SFA(CELL)
REG_BALGC(I) = REG_BALGC(I)+COL_BALGC*SFA(CELL)
REG_BNPP(I) = REG_BNPP(I)+COL_BNPP*SFA(CELL)

```

```

REG_SAV(I) = REG_SAV(I)+COL_SAV*SFA(CELL)
REG_SAVNP(I) = REG_SAVNP(I)+COL_SAVNP*SFA(CELL)
REG_SAVR(I) = REG_SAVR(I)+COL_SAVR*SFA(CELL)
REG_SAV2SED(I) = REG_SAV2SED(I)+COL_SAV2SED*SFA(CELL)
REG_SAV2POC(I) = REG_SAV2POC(I)+COL_SAV2POC*SFA(CELL)
REG_SAV2DOC(I) = REG_SAV2DOC(I)+COL_SAV2DOC*SFA(CELL)

```

```

REG_SFEED(I) = REG_SFEED(I)+COL_SFEED*SFA(CELL)
REG_SFNP(I) = REG_SFNP(I)+COL_SFNP*SFA(CELL)
REG_SFR(I) = REG_SFR(I)+COL_SFR*SFA(CELL)
REG_SFTCON(I) = REG_SFTCON(I)+COL_SFTCON*SFA(CELL)
REG_SFACON(I) = REG_SFACON(I)+COL_SFACON*SFA(CELL)
REG_SFPCCON(I) = REG_SFPCCON(I)+COL_SFPCCON*SFA(CELL)
REG_SFUAC(I) = REG_SFUAC(I)+COL_SFUAC*SFA(CELL)

```

```

REG_DFEED(I) = REG_DFEED(I)+COL_DFEED*SFA(CELL)
REG_DFNP(I) = REG_DFNP(I)+COL_DFNP*SFA(CELL)
REG_DFR(I) = REG_DFR(I)+COL_DFR*SFA(CELL)
REG_DFTCON(I) = REG_DFTCON(I)+COL_DFTCON*SFA(CELL)
REG_DFUAC(I) = REG_DFUAC(I)+COL_DFUAC*SFA(CELL)

```

END DO

C DIVIDE REGIONAL SUMS BY SURFACE AREA

```

REG_ALGC(I)=REG_ALGC(I)/REG_AREA
REG_ANPP(I)=REG_ANPP(I)/REG_AREA
REG_AGPP(I)=REG_AGPP(I)/REG_AREA
REG_APRED(I)=REG_APRED(I)/REG_AREA
REG_ADOC(I)=REG_ADOC(I)/REG_AREA
REG_APOC(I)=REG_APOC(I)/REG_AREA

```

```

REG_DOC(I)=REG_DOC(I)/REG_AREA

```

REG_POC(I)=REG_POC(I)/REG_AREA
 REG_DETC(I)=REG_DETC(I)/REG_AREA
 REG_CRESP(I)=REG_CRESP(I)/REG_AREA
 REG_POC2DOC(I)=REG_POC2DOC(I)/REG_AREA

REG_MICRZ(I)=REG_MICRZ(I)/REG_AREA
 REG_MICRZR(I)=REG_MICRZR(I)/REG_AREA
 REG_MICRZNP(I)=REG_MICRZNP(I)/REG_AREA
 REG_MICRZDOC(I)=REG_MICRZDOC(I)/REG_AREA
 REG_MICRZPOC(I)=REG_MICRZPOC(I)/REG_AREA
 REG_MICRZPR(I)=REG_MICRZPR(I)/REG_AREA
 REG_MICRZALG(I)=REG_MICRZALG(I)/REG_AREA
 REG_TCONSZ(I)=REG_TCONSZ(I)/REG_AREA
 REG_UADOCSZ(I)=REG_UADOCSZ(I)/REG_AREA
 REG_UAPOCSZ(I)=REG_UAPOCSZ(I)/REG_AREA

REG_MESoz(I)=REG_MESoz(I)/REG_AREA
 REG_MESozR(I)=REG_MESozR(I)/REG_AREA
 REG_MESozNP(I)=REG_MESozNP(I)/REG_AREA
 REG_MESozPOC(I)=REG_MESozPOC(I)/REG_AREA
 REG_MESozPR(I)=REG_MESozPR(I)/REG_AREA
 REG_MESozALG(I)=REG_MESozALG(I)/REG_AREA
 REG_MIC2MES(I)=REG_MIC2MES(I)/REG_AREA
 REG_TCONLZ(I)=REG_TCONLZ(I)/REG_AREA
 REG_UADOCLZ(I)=REG_UADOCLZ(I)/REG_AREA
 REG_UAPOCLZ(I)=REG_UAPOCLZ(I)/REG_AREA

REG_SEDPOC(I) = REG_SEDPOC(I)/REG_AREA
 REG_BURIAL(I) = REG_BURIAL(I)/REG_AREA
 REG_CFLUX(I) = REG_CFLUX(I)/REG_AREA
 REG_SEDR(I) = REG_SEDR(I)/REG_AREA
 REG_ALG2SED(I) = REG_ALG2SED(I)/REG_AREA

REG_BALG(I) = REG_BALG(I)/REG_AREA
 REG_BALGR(I) = REG_BALGR(I)/REG_AREA
 REG_BALGPR(I) = REG_BALGPR(I)/REG_AREA
 REG_BALGC(I) = REG_BALGC(I)/REG_AREA
 REG_BNPP(I) = REG_BNPP(I)/REG_AREA

REG_SAV(I) = REG_SAV(I)/REG_AREA
 REG_SAVNP(I) = REG_SAVNP(I)/REG_AREA
 REG_SAVR(I) = REG_SAVR(I)/REG_AREA
 REG_SAV2SED(I) = REG_SAV2SED(I)/REG_AREA
 REG_SAV2POC(I) = REG_SAV2POC(I)/REG_AREA
 REG_SAV2DOC(I) = REG_SAV2DOC(I)/REG_AREA

REG_SFEEED(I) = REG_SFEEED(I)/REG_AREA
 REG_SFNP(I) = REG_SFNP(I)/REG_AREA
 REG_SFR(I) = REG_SFR(I)/REG_AREA
 REG_SFTCON(I) = REG_SFTCON(I)/REG_AREA
 REG_SFACON(I) = REG_SFACON(I)/REG_AREA
 REG_SFPCCON(I) = REG_SFPCCON(I)/REG_AREA
 REG_SFUAC(I) = REG_SFUAC(I)/REG_AREA

```

REG_DFEED(I) = REG_DFEED(I)/REG_AREA
REG_DFNP(I) = REG_DFNP(I)/REG_AREA
REG_DFR(I) = REG_DFR(I)/REG_AREA
REG_DFTCON(I) = REG_DFTCON(I)/REG_AREA
REG_DFUAC(I) = REG_DFUAC(I)/REG_AREA
C
C Find Average Regional values over seasons
C
  JREG_DAY=REG_JDAY(I)
  WRITE(*,*)'JDAY = ',JREG_DAY
  IF(JREG_DAY .eq. 243. .or. JREG_DAY .eq. 608.
*   .or. JREG_DAY .eq. 973.)then
    ACOUNT =ACOUNT + 1.
C
    WRITE(*,*)'JDAY = ',REG_JDAY(I)
    AREG_ALGC=REG_ALGC(I)+AREG_ALGC
    AREG_ANPP=REG_ANPP(I)+AREG_ANPP
    AREG_AGPP=REG_AGPP(I)+AREG_AGPP
    AREG_APRED=REG_APRED(I)+AREG_APRED
    AREG_ADOC=REG_ADOC(I)+AREG_ADOC
    AREG_APOC=REG_APOC(I)+AREG_APOC

    AREG_DOC=REG_DOC(I)+AREG_DOC
    AREG_POC=REG_POC(I)+AREG_POC
    AREG_DETC=REG_DETC(I)+AREG_DETC
    AREG_CRESP=REG_CRESP(I)+AREG_CRESP
    AREG_POC2DOC=REG_POC2DOC(I)+AREG_POC2DOC

    AREG_MICRZ=REG_MICRZ(I)+AREG_MICRZ
    AREG_MICRZR=REG_MICRZR(I)+AREG_MICRZR
    AREG_MICRZNP=REG_MICRZNP(I)+AREG_MICRZNP
    AREG_MICRZDOC=REG_MICRZDOC(I)+AREG_MICRZDOC
    AREG_MICRZPOC=REG_MICRZPOC(I)+AREG_MICRZPOC
    AREG_MICRZPR=REG_MICRZPR(I)+AREG_MICRZPR
    AREG_MICRZALG=REG_MICRZALG(I)+AREG_MICRZALG
    AREG_TCONSZ=REG_TCONSZ(I)+AREG_TCONSZ
    AREG_UADOC SZ=REG_UADOC SZ(I)+AREG_UADOC SZ
    AREG_UAPOC SZ=REG_UAPOC SZ(I)+AREG_UAPOC SZ

    AREG_MESoz=REG_MESoz(I)+AREG_MESoz
    AREG_MESozR=REG_MESozR(I)+AREG_MESozR
    AREG_MESozNP=REG_MESozNP(I)+AREG_MESozNP
    AREG_MESozPOC=REG_MESozPOC(I)+AREG_MESozPOC
    AREG_MESozPR=REG_MESozPR(I)+AREG_MESozPR
    AREG_MESozALG=REG_MESozALG(I)+AREG_MESozALG
    AREG_MIC2MES=REG_MIC2MES(I)+AREG_MIC2MES
    AREG_TCONLZ=REG_TCONLZ(I)+AREG_TCONLZ
    AREG_UADOC LZ=REG_UADOC LZ(I)+AREG_UADOC LZ
    AREG_UAPOC LZ=REG_UAPOC LZ(I)+AREG_UAPOC LZ

    AREG_SEDPOC = REG_SEDPOC(I)+AREG_SEDPOC
    AREG_BURIAL = REG_BURIAL(I)+AREG_BURIAL
    AREG_CFLUX = REG_CFLUX(I)+AREG_CFLUX
    AREG_SEDR = REG_SEDR(I)+AREG_SEDR
    AREG_ALG2SED = REG_ALG2SED(I)+AREG_ALG2SED

```

```

AREG_BALG = REG_BALG(I)+AREG_BALG
AREG_BALGR = REG_BALGR(I)+AREG_BALGR
AREG_BALGPR = REG_BALGPR(I)+AREG_BALGPR
AREG_BALGC = REG_BALGC(I)+AREG_BALGC
AREG_BNPP = REG_BNPP(I)+AREG_BNPP

AREG_SAV = REG_SAV(I)+AREG_SAV
AREG_SAVNP = REG_SAVNP(I)+AREG_SAVNP
AREG_SAVR = REG_SAVR(I)+AREG_SAVR
AREG_SAV2SED = REG_SAV2SED(I)+AREG_SAV2SED
AREG_SAV2POC = REG_SAV2POC(I)+AREG_SAV2POC
AREG_SAV2DOC = REG_SAV2DOC(I)+AREG_SAV2DOC

AREG_SFEED = REG_SFEED(I)+AREG_SFEED
AREG_SFNP = REG_SFNP(I)+AREG_SFNP
AREG_SFR = REG_SFR(I)+AREG_SFR
AREG_SFTCON = REG_SFTCON(I)+AREG_SFTCON
AREG_SFACON = REG_SFACON(I)+AREG_SFACON
AREG_SFPCCON = REG_SFPCCON(I)+AREG_SFPCCON
AREG_SFUAC = REG_SFUAC(I)+AREG_SFUAC

AREG_DFEED = REG_DFEED(I)+AREG_DFEED
AREG_DFNP = REG_DFNP(I)+AREG_DFNP
AREG_DFR = REG_DFR(I)+AREG_DFR
AREG_DFTCON = REG_DFTCON(I)+AREG_DFTCON
AREG_DFUAC = REG_DFUAC(I)+AREG_DFUAC
ENDIF
END DO

C WRITE THESE OUT
2   CONTINUE

C NOW TRY TO WRITE OUT THINGS THAT ECOPATH NEEDS
666 CONTINUE
DO I=1,NREAD
WRITE(23,40) REG_JDAY(I), REG_AREA
40  FORMAT(//'   DAY ',F10.1,' AREA ',E14.6,' SQ M')

C SEDIMENTS
WRITE(23,20)
20  FORMAT('/' SEDIMENTS',' B ',' FR ALGAE',' FR DETR',
$   ' FR SAV ',' DEP FEED ',' SUS FEED ',' BENTH ALG ',
$   ' BURIAL RESP')
WRITE(23,21) REG_SEDPOC(I),REG_ALG2SED(I),REG_CFLUX(I),
$   REG_SAV2SED(I),
$   REG_DFUAC(I),REG_SFUAC(I),REG_BALGC(I),REG_BURIAL(I),
$   REG_SEDR(I)
21  FORMAT(10X,9F10.3)

C WATER COLUMN POC
WRITE(23,22)
22  FORMAT('/' POC ',' B ',' FROM ALG ',' FR MIZOO ',

```

```

$ ' FR MEZOO ',' FROM SAV ',' TO MIZOO ',' TO MEZOO ',
$ ' TO SEDS ',' TO DOC ')
WRITE(23,23) REG_POC(I),REG_APOC(I),REG_UAPOCSZ(I),
$
REG_UAPOCLZ(I),REG_SAV2POC(I),REG_MICRZPOC(I),REG_MESozPOC(I),
$ REG_CFLUX(I),REG_POC2DOC(I)
23 FORMAT(10X,9F10.3)

C WATER COLUMN DOC
WRITE(23,24)
24 FORMAT(/' DOC ',' B ',' FR ALGAE',' FR MIZOO ',
$ ' FR MEZOO ',' FR SAV ',' TO MIZOO CRESP')
WRITE(23,25) REG_DOC(I),REG_ADOC(I),REG_UADOCsz(I),
$ REG_UADOCCLZ(I),REG_SAV2DOC(I),REG_MICRZDOC(I),REG_CRESP(I)
25 FORMAT(10X,7F10.3)

C PHYTOPLANKTON
WRITE(23,26)
26 FORMAT(/' ALGAE ',' B ',' NPP ',' TO DOC ',
$ ' TO POC ',' TO MIZOO ',' TO MEZOO ',' TO SEDS RESP')
WRITE(23,27) REG_ALGC(I),REG_ANPP(I),REG_ADOC(I),REG_APOC(I),
$ REG_MICRZALG(I),REG_MESozALG(I),REG_ALG2SED(I),
$ REG_AGPP(I)-REG_ANPP(I)
27 FORMAT(10X,8F10.3)

C MICROZOOPLANKTON
WRITE(23,28)
28 FORMAT(/' MICRO Z ',' B ',' PROD ',' TCON ',
$ ' UCON ',' DOC IN ',' POC IN ',' ALGAE IN ',
$ ' DOC OUT ',' POC OUT ',' TO MEZOO RESP')
WRITE(23,29) REG_MICRZ(I),REG_MICRZNP(I),REG_TCONsz(I),
$ REG_UADOCsz(I)+REG_UAPOCSZ(I),REG_MICRZDOC(I),
$ REG_MICRZPOC(I),REG_MICRZALG(I),REG_UADOCsz(I),
$ REG_UAPOCSZ(I),REG_MIC2MES(I),REG_MICRZR(I)
29 FORMAT(10X,11F10.3)

C MESOZOOPLANKTON
WRITE(23,30)
30 FORMAT(/' MESO Z ',' B ',' PROD ',' TCON ',
$ ' UCON ',' POC IN ',' ALGAE IN ',' MICRO IN ',
$ ' DOC OUT ',' POC OUT RESP')
WRITE(23,31) REG_MESoz(I),REG_MESozNP(I),REG_TCONCLZ(I),
$ REG_UADOCCLZ(I)+REG_UAPOCLZ(I),
$ REG_MESozPOC(I),REG_MESozALG(I),REG_MIC2MES(I),
$ REG_UADOCCLZ(I),REG_UAPOCLZ(I),REG_MESozR(I)
31 FORMAT(10X,10F10.3)

C SAV
WRITE(23,32)
32 FORMAT(/' SAV ',' B ',' NPP ',' TO DOC ',
$ ' TO POC ',' TO SEDS RESP')
WRITE(23,33) REG_SAV(I),REG_SAVNP(I),REG_SAV2DOC(I),
$ REG_SAV2POC(I),REG_SAV2SED(I),REG_SAVR(I)
33 FORMAT(10X,6F10.3)

```



```

C BENTHIC ALGAE
      WRITE(23,34)
34     FORMAT(/'BENTHIC ALG','      B      ','      NPP ',' TO SEDS ',
$      '      RESP')
      WRITE(23,35) REG_BALG(I),REG_BNPP(I),REG_BALGC(I),REG_BALGR(I)
35     FORMAT(10X,4F10.3)

C DEPOSIT FEEDERS
      WRITE(23,36)
36     FORMAT(/'  DEP FEED ','      B      ','      PROD ','      TCON      ',
$      '  UCON ',' FROM SED ','      TO SED ','      RESP')
      WRITE(23,37) REG_DFEEED(I),REG_DFNP(I),REG_DFTCON(I),
$      REG_DFUAC(I),REG_DFTCON(I),REG_DFUAC(I),REG_DFR(I)
37     FORMAT(10X,7F10.4)

C FILTER FEEDERS
      WRITE(23,38)
38     FORMAT(/'  SUS FEED ','      B      ','      PROD ','      TCON      ',
$      '  UCON ',' FROM ALG ',' FROM POC ','      TO SED      ',
$      '      RESP')
      WRITE(23,39) REG_SFEEED(I),REG_SFNP(I),REG_SFTCON(I),
$      REG_SFUAC(I),REG_SFACON(I),REG_SFPCCON(I),REG_SFUAC(I),
$      REG_SFR(I)
39     FORMAT(10X,8F10.3)

C
C Production/Biomass ratio
C

      OPEN(20,FILE='EE_BIO.txt',STATUS='OLD')

      IF(REG_BNPP(I).le.0.0)then
        REG_BNPP(I) = 0.001
      END IF
      IF(REG_ANPP(I).le.0.0)then
        REG_ANPP(I) = 0.001
      END IF
      IF(REG_MICRZNP(I).le.0.0)then
        REG_MICRZNP(I) = 0.001
      END IF
      IF(REG_MESozNP(I).le.0.0)then
        REG_MESozNP(I) = 0.001
      END IF
      IF(REG_SAVNP(I).le.0.0)then
        REG_SAVNP(I) = 0.001
      END IF
      IF(REG_DFNP(I).le.0.0)then
        REG_SFNP(I) = 0.001
      END IF

      PB_BALGRatio = REG_BNPP(I)/REG_BALG(I)
      PB_ALGRatio = REG_ANPP(I)/REG_ALGC(I)
      PB_Z1Ratio = REG_MICRZNP(I)/REG_MICRZ(I)

```

```

PB_Z2Ratio = REG_MESOZNP(I)/REG_MESoz(I)
PB_SAVRatio = REG_SAVNP(I)/REG_SAV(I)
PB_DFRatio = REG_DFNP(I)/REG_DFEED(I)
PB_SFRatio = REG_SFNP(I)/REG_SFEED(I)

WRITE(23,67)
67  FORMAT(/' P/B BALG  ',' P/B ALG  ',' P/B Z1  ',' P/B Z2
',
*      'P/B SAV  ',' P/B DF  ','P/B SF  ')
WRITE(23,68) PB_BALGRatio,PB_ALGRatio,PB_Z1Ratio,PB_Z2Ratio,
*           PB_SAVRatio,
*           PB_DFRatio,PB_SFRatio
68  FORMAT(7F10.3)

C
C Consumption/Biomass
C
QB_Z1Ratio = REG_TCONSZ(I)/REG_MICRZ(I)
QB_Z2Ratio = REG_TCONLZ(I)/REG_MESoz(I)
QB_DFRatio = REG_DFTCON(I)/REG_DFEED(I)
QB_SFRatio = REG_SFTCON(I)/REG_SFEED(I)

WRITE(23,71)
71  FORMAT(/' Q/B Z1  ',' Q/B Z2  ',
*          'Q/B DF  ',' Q/B SF  ')
WRITE(23,72) QB_Z1Ratio,QB_Z2Ratio,
*           QB_DFRatio,QB_SFRatio
72  FORMAT(7F10.3)

C
C Uassimilated/Consumption
C
UATC_Z1Ratio = (REG_UADOCsz(I)+REG_UAPOCSz(I))/REG_TCONSZ(I)
UATC_Z2Ratio = (REG_UADOCCLZ(I)+REG_UAPOCLZ(I))/REG_TCONLZ(I)
UATC_DFRatio = REG_DFUAC(I)/REG_DFTCON(I)
UATC_SFRatio = REG_SFUAC(I)/REG_SFTCON(I)

WRITE(23,73)
73  FORMAT(/' UA/Q Z1  ',' UA/Q Z2  ',
*          ' UA/Q DF  ','UA/Q SF  ')
WRITE(23,74) UATC_Z1Ratio,UATC_Z2Ratio,
*           UATC_DFRatio,UATC_SFRatio
74  FORMAT(7F10.3)

C
C Diet Compostion
C
C Z1 Diet Compostion
Z1DCDOC = REG_MICRZDOC(I)/(REG_MICRZDOC(I)+REG_MICRZPOC(I)+
* REG_MICRZALG(I))
Z1DCPOC = REG_MICRZPOC(I)/(REG_MICRZDOC(I)+REG_MICRZPOC(I)+
* REG_MICRZALG(I))
Z1DCALG = REG_MICRZALG(I)/(REG_MICRZDOC(I)+REG_MICRZPOC(I)+
* REG_MICRZALG(I))

```

```

        WRITE(23,69)
69      FORMAT(/' Z1 DC From DOC ','Z1 DC From POC ',
*          'Z1 DC From ALG ')
        WRITE(23,70) Z1DCDOC,Z1DCPOC,Z1DCALG
70      FORMAT(3(5X,F10.3))

C Z2 Diet Compostion
      Z2DCPOC = REG_MESOZPOC(I)/(REG_MIC2MES(I)+REG_MESOZPOC(I)+
*      REG_MESOZALG(I))
      Z2DCZ1 = REG_MIC2MES(I)/(REG_MIC2MES(I)+REG_MESOZPOC(I)+
*      REG_MESOZALG(I))
      Z2DCALG = REG_MESOZALG(I)/(REG_MIC2MES(I)+REG_MESOZPOC(I)+
*      REG_MESOZALG(I))
        WRITE(23,42)
42      FORMAT(/' Z2 DC From POC ',' Z2 DC From Z1 ',
*          ' Z2 DC From ALG ')
        WRITE(23,70) Z2DCPOC,Z2DCZ1,Z2DCALG
41      FORMAT(10X,3F10.3)

C Deposit Feeders (DF) Diet Compostion
      DFDCSedPOC = REG_DFUAC(I)/REG_DFUAC(I)
        WRITE(23,43)
43      FORMAT(/' DF DC From SedPOC ')
        WRITE(23,70) DFDCSedPOC
44      FORMAT(10X,3F10.3)

C Filter Feeders (SF) Diet Compostion
      SFDCPOC = REG_SFPCCON(I)/(REG_SFPCCON(I)+REG_SFACON(I))
      SFDCALG = REG_SFACON(I)/(REG_SFPCCON(I)+REG_SFACON(I))
        WRITE(23,45)
45      FORMAT(/' SF DC From POC ',' SF DC From ALG ')
        WRITE(23,70) SFDCPOC,SFDCALG
46      FORMAT(10X,3F10.3)

C
C Detrital Fate
C

C Microphytobenthos Detrital Fate
      MICRBENALG_SedPOC = REG_BALGC(I)/REG_BALGC(I)
      MICRBENALG_POC = 0.
      MICRBENALG_DOC = 0.
      BAExport = 0.
      BATotal =
MICRBENALG_SedPOC+MICRBENALG_POC+MICRBENALG_DOC+Export
        WRITE(23,47)
47      FORMAT(/' BALG DF to DOC ',' BALG DF to SedPOC ',
*          ' BALG DF to POC ',' BA Export',' Total Sum')
        WRITE(23,48) MICRBENALG_DOC,MICRBENALG_SedPOC,MICRBENALG_POC,
*          BAExport,BATotal
48      FORMAT(f10.3,9x,f10.3,10x,f10.3,3x,f10.3,4x,f10.3)

C Phytoplankton Detrital Fate
      ALG_SedPOC = REG_ALG2SED(I)/(REG_ADOC(I)+REG_APOC(I)+

```

```

*           REG_ALG2SED(I))
ALG_POC = REG_APOC(I) / (REG_ADOC(I)+REG_APOC(I)+REG_ALG2SED(I))
ALG_DOC = REG_ADOC(I) / (REG_ADOC(I)+REG_APOC(I)+REG_ALG2SED(I))
AlgExport = 0.
AlgTotal = ALG_SedPOC+ALG_POC+ALG_DOC+AlgExport
WRITE(23,49)
49  FORMAT(/' ALG DF to DOC ',' ALG DF to SedPOC ',
*       ' ALG DF to POC ',' ALG Export ',' Total Sum')
WRITE(23,48) ALG_DOC,ALG_SedPOC,ALG_POC,
*           AlgExport,AlgTotal

C Microzooplankton Detrital Fate
Z1_SedPOC = 0.
Z1_POC = REG_MICRZPOC(I) / (REG_MICRZDOC(I)+REG_MICRZPOC(I))
Z1_DOC = REG_MICRZDOC(I) / (REG_MICRZDOC(I)+REG_MICRZPOC(I))
Z1_POC = REG_UAPOCSZ(I) / (REG_UAPOCSZ(I)+REG_UADOCSZ(I))
Z1_DOC = REG_UADOCSZ(I) / (REG_UAPOCSZ(I)+REG_UADOCSZ(I))
Z1Export = 0.
Z1Total = Z1_SedPOC +Z1_POC +Z1_DOC +Z1Export
WRITE(23,51)
51  FORMAT(/' Z1 DF to DOC ',' Z1 DF to SedPOC ',
*       ' Z1 DF to POC ',' Z1 Export ',' Total Sum')
WRITE(23,48) Z1_DOC,Z1_SedPOC,Z1_POC,
*           Z1Export,Z1Total

C Mesozooplankton Detrital Fate
Z2_SedPOC = 0.
Z2_POC = REG_UAPOCLZ(I) / (REG_UAPOCLZ(I)+REG_UADOCLZ(I))
Z2_DOC = REG_UADOCLZ(I) / (REG_UAPOCLZ(I)+REG_UADOCLZ(I))
Z2Export = 0.
Z2Total = Z2_SedPOC +Z2_POC +Z2_DOC +Z2Export
WRITE(23,53)
53  FORMAT(/' Z2 DF to DOC ',' Z2 DF to SedPOC ',
*       ' Z2 DF to POC ',' Z2 Export ',' Total Sum')
WRITE(23,48) Z2_DOC,Z2_SedPOC,Z2_POC,
*           Z2Export,Z2Total

C SAV Detrital Fate
SAV_SedPOC = REG_SAV2SED(I) / (REG_SAV2DOC(I)+REG_SAV2POC(I)+
*           REG_SAV2SED(I))
SAV_POC = REG_SAV2POC(I) / (REG_SAV2DOC(I)+REG_SAV2POC(I)+
*           REG_SAV2SED(I))
SAV_DOC = REG_SAV2DOC(I) / (REG_SAV2DOC(I)+REG_SAV2POC(I)+
*           REG_SAV2SED(I))
SAVExport = 0.
SAVTotal = SAV_SedPOC +SAV_POC +SAV_DOC +SAVExport
WRITE(23,55)
55  FORMAT(/' SAV DF to DOC ',' SAV DF to SedPOC ',
*       ' SAV DF to POC ',' SAV Export ',' Total Sum')
WRITE(23,48) Z2_DOC,Z2_SedPOC,Z2_POC,
*           Z2Export,Z2Total

C Deposit Feeders Detrital Fate
DF_SedPOC = REG_DFUAC(I) / REG_DFUAC(I)

```

```

    DF_POC = 0.
    DF_DOC = 0.
    DFExport = 0.
    DFTotal = DF_SedPOC+DF_POC+DF_DOC+DFExport
    WRITE(23,57)
57  FORMAT(/' DF DF to DOC ',' DF DF to SedPOC ',
*      ' DF DF to POC ',' DF Export ',' Total Sum')
    WRITE(23,48) DF_DOC,DF_SedPOC,DF_POC,
*      DFExport,DFTotal

C Suspension Feeders Detrital Fate
    SF_SedPOC = REG_SFUAC(I)/REG_SFUAC(I)
    SF_POC = 0.
    SF_DOC = 0.
    SFExport = 0.
    SFTotal = SF_SedPOC+SF_POC+SF_DOC+SFExport
    WRITE(23,59)
59  FORMAT(/' SF DF to DOC ',' SF DF to SedPOC ',
*      ' SF DF to POC ',' SF Export ',' Total Sum')
    WRITE(23,48) SF_DOC,SF_SedPOC,SF_POC,
*      SFExport,SFTotal

C DOC Detrital Fate
    DOC_SedPOC = 0.
    DOC_POC = 0.
    DOC_DOC = 0.
    DOCExport = 1.
    DOCTotal = DOC_SedPOC +DOC_POC +DOC_DOC +DOCExport
    WRITE(23,61)
61  FORMAT(/' DOC DF to DOC ',' DOC DF to SedPOC ',
*      ' DOC DF to POC ',' DOC Export ',' Total Sum')
    WRITE(23,48) DOC_DOC,DOC_SedPOC,DOC_POC,
*      DOCExport,DOCTotal

C Sed POC Detrital Fate
    SedPOC_SedPOC = 0.
    SedPOC_POC = 0.
    SedPOC_DOC = 0.
    SedPOCExport = 1.
    SedPOCTotal = SedPOC_SedPOC+SedPOC_POC+SedPOC_DOC+SedPOCExport
    WRITE(23,63)
63  FORMAT(/' SedPOC to DOC ',' SedPOC to SedPOC ',
*      ' SedPOC to POC ',' SedPOC Export',' Total Sum')
    WRITE(23,48) SedPOC_DOC,SedPOC_SedPOC,SedPOC_POC,
*      SedPOCExport,SedPOCTotal

C POC Detrital Fate
    POC_SedPOC = REG_CFLUX(I)/(REG_CFLUX(I)+REG_POC2DOC(I))
    POC_POC = 0.
    POC_DOC = REG_POC2DOC(I)/(REG_CFLUX(I)+REG_POC2DOC(I))
    POCExport = 0.
    POCTotal = SF_SedPOC+SF_POC+SF_DOC+SFExport
    WRITE(23,65)
65  FORMAT(/' POC DF to DOC ',' POC DF to SedPOC ',

```

```

*          ' POC DF to POC ',' POC Export ',' Total Sum')
WRITE(23,48) POC_DOC,POC_SedPOC,POC_POC,
*          POCEXport,POCTotal
C
C Detritus flow to calculate EE of Detritus Compartments
C
  DETDOCIN=REG_SAV2DOC(I)+REG_MICRZDOC(I)+REG_ADOC(I)+
*          REG_POC2DOC(I)
  DETDOCOUT= REG_UADOCLZ(I)+REG_UADOCSZ(I)
  DETPOCIN=REG_SAV2POC(I)+REG_MICRZPOC(I)+REG_APOC(I)+
*          REG_MESozPOC(I)
  DETPOCOUT= REG_UAPOCLZ(I)+REG_UAPOCSZ(I)
  DETSEDIN=REG_DFUAC(I)+REG_SFUAC(I)+REG_BALGC(I)
*          +REG_SAV2SED(I)
*          +REG_ALG2SED(I)+REG_CFLUX(I)
  DETSEDOUT=REG_DFTCON(I)
C
C          Calculate Bioaccumulation
C
  DO IBA = 1, NGROUP
    IF(I .gt. 1)then
      IF(IBA .eq. 1)THEN
        BIOA(1) = REG_BALG(I-1)-REG_BALG(I)
        write(27,*)'Bioa = ',BIOA(1)
      ELSE IF(IBA .eq. 2)THEN
        BIOA(2) = REG_ALGC(I-1)-REG_ALGC(I)
      ELSE IF(IBA .eq. 3)THEN
        BIOA(3) = REG_MICRZ(I-1)-REG_MICRZ(I)
      ELSE IF(IBA .eq. 4)THEN
        BIOA(4) = REG_MESoz(I-1)-REG_MESoz(I)
      ELSE IF(IBA .eq. 5)THEN
        BIOA(5) = REG_SAV(I-1)-REG_SAV(I)
      ELSE IF(IBA .eq. 6)THEN
        BIOA(6) = REG_DFEED(I-1)-REG_DFEED(I)
      ELSE IF(IBA .eq. 7)THEN
        BIOA(7) = REG_SFEED(I-1)-REG_SFEED(I)
      ELSE IF(IBA .eq. 8)THEN
        BIOA(8) = REG_DOC(I-1)-REG_DOC(I)
      ELSE IF(IBA .eq. 9)THEN
        BIOA(9) = REG_SEDPOC(I-1)-REG_SEDPOC(I)
      ELSE IF(IBA .eq. 10)THEN
        BIOA(10) = REG_POC(I-1)-REG_POC(I)
      END IF
    END IF
  END DO
C
C Calculate EE(I) of any Group or Biomass(I) of Predators Only
C
C If calculating Biomass
C
  DO IB = 1,NGROUP
    READ(20,15,END=16)S_EE(IB),S_Biom(IB),EE_BIO(IB)

```

```

15      write(*,15)S_EE(IB),S_Biom(IB),EE_BIO(IB)
      format(2I5,f8.0)
      IF(S_EE(IB) .eq. 1)THEN
        SolEE(IB) = .true.
      ENDIF
      IF(S_Biom(IB) .eq. 1)THEN
        SolBiom(IB) = .true.
      ENDIF
C      Write(27,*)SolEE(I),SolBiom(I)
      End do
16 Continue
      Close (20)
C If calculating EE
C
C Set Biomass, P/B & Q/B arrays
C
      IG_COUNT = 0
      DO IBIO = 1, NGROUP
        IG_COUNT = IG_COUNT + 1
        IF (IG_COUNT .EQ. 1)THEN
          BIOM(1) = REG_BALG(I)
          PB(1) = PB_BALGRatio
          QB(1) = 0.0
          UA(1) = 0.0
        ELSE IF(IG_COUNT .EQ. 2)THEN
          BIOM(2) = REG_ALGC(I)
          PB(2) = PB_ALGRatio
          QB(2) = 0.0
          UA(2) = 0.0
        ELSE IF(IG_COUNT .EQ. 3)THEN
          BIOM(3) = REG_MICRZ(I)
          PB(3) = PB_Z1Ratio
          QB(3) = QB_Z1Ratio
          UA(3) = UATC_Z1Ratio
          Consumpt(3) = REG_TCONSZ(I)
          write(27,*)'Consumpt 3 = ',Consumpt(3)
        ELSE IF(IG_COUNT .EQ. 4)THEN
          BIOM(4) = REG_MESoz(I)
          PB(4) = PB_Z2Ratio
          QB(4) = QB_Z2Ratio
          UA(4) = UATC_Z2Ratio
          Consumpt(4) = REG_TCONLZ(I)
          write(27,*)'Consumpt 4 = ',Consumpt(4)
        ELSE IF(IG_COUNT .EQ. 5)THEN
          BIOM(5) = REG_SAV(I)
          PB(5) = PB_SAVRatio
          QB(5) = 0.0
          UA(5) = 0.0
        ELSE IF(IG_COUNT .EQ. 6)THEN
          BIOM(6) = REG_DFEED(I)
          PB(6) = PB_DFRatio
          QB(6) = QB_DFRatio
          UA(6) = UATC_DFRatio
          Consumpt(6) = REG_DFTCON(I)

```

```

        write(27,*)'Consumpt 6 = ',Consumpt(6)
ELSE IF(IG_COUNT .EQ. 7)THEN
    BIOM(7) = REG_SFEED(I)
    PB(7) = PB_SFRATIO
    QB(7) = 0.0
    UA(7) = 0.0
    Consumpt(7) = REG_SFTCON(I)
    write(27,*)'Consumpt = 7 ',Consumpt(7)
ELSE IF(IG_COUNT .EQ. 8)THEN
    BIOM(8) = REG_DOC(I)
    PB(8) = 0.0
    QB(8) = 0.0
    UA(8) = 0.0
ELSE IF(IG_COUNT .EQ. 9)THEN
    BIOM(9) = REG_SEDPOC(I)
    PB(9) = 0.0
    QB(9) = 0.0
    UA(9) = 0.0
ELSE IF(IG_COUNT .EQ. 10)THEN
    BIOM(10) = REG_POC(I)
    PB(10) = 0.0
    QB(10) = 0.0
    UA(10) = 0.0
ENDIF
END DO

C
C Set Diet Comp array
C
DO IDC = 1, NGROUP
    DO IPRED = 3, NPREDATOR
        DC(IPRED, IDC) = 0.0
        IF(IPRED .eq. 3 .and. IDC .eq. 8)THEN
            DC(IPRED, IDC) = Z1DCDOC
        ELSE IF (IPRED .eq. 3 .and. IDC .eq. 10)THEN
            DC(IPRED, IDC) = Z1DCPOC
        ELSE IF (IPRED .eq. 4 .and. IDC .eq. 2)THEN
            DC(IPRED, IDC) = Z2DCALG
        ELSE IF (IPRED .eq. 4 .and. IDC .eq. 3)THEN
            DC(IPRED, IDC) = Z2DCZ1
        ELSE IF (IPRED .eq. 4 .and. IDC .eq. 10)THEN
            DC(IPRED, IDC) = Z2DCPOC
        ELSE IF (IPRED .eq. 6 .and. IDC .eq. 9)THEN
            DC(IPRED, IDC) = DFDCSedPOC
        ELSE IF (IPRED .eq. 7 .and. IDC .eq. 2)THEN
            DC(IPRED, IDC) = SFDCALG
        ELSE IF (IPRED .eq. 7 .and. IDC .eq. 10)THEN
            DC(IPRED, IDC) = SFDCPOC
        END IF
    END DO
END DO

C
C Set Catch, Biomass Accumulation, & Emigration
C Will read in when get actual data.

```



```

C
DO IYBAE = 1, NGROUP-3
  Y(IYBAE) = 0.0
  IF(IYBAE .eq. 1)then
    BA(IYBAE) = 0.0
  ELSE
    BA(IYBAE) = BIOA(I)
  END IF
  E(IYBAE) = 0.0
END DO

C
C Calculate EE
C
SUMM2 = 0.0
DO IG = 1, NGROUP
  IF (IG .lt. 8)THEN
    IF (Solee(IG) .ne. .false.)THEN
      Do J = 3, NGROUP
        M2 = BIOM(J)*QB(J)*DC(J,IG)
        SUMM2 = SUMM2 + M2
      END DO
      GSUMM2(IG) = SUMM2
      write(*,*)BIOM(IG),PB(IG)
      PHI(IG) = BIOM(IG)*PB(IG)
      EE(IG) = (GSUMM2(IG) + Y(IG) + BA(IG) + E(IG))/PHI(IG)
      IF (EE(IG) .GT. 1.0)THEN
        WRITE(23,75)EE(IG)
        WRITE(*,*)'EE = ',EE(IG)
75      FORMAT(8x,'EE .GT. 1; Unbalanced Model',
              EE = ',f8.3)
        ELSE
76      WRITE(23,76)IG,EE(IG)
        FORMAT('Group = ',I5,'EE = ',f8.3)
      END IF
    END IF
  ELSE IF (IG .gt. 7)THEN
    IF(IG .eq. 8)THEN
      EE(IG) = DETDOCOUT/DETDOCIN
      WRITE(23,76)IG,EE(IG)
    ELSE IF (IG .eq. 9)THEN
      EE(IG) = DETPOCOUT/DETPOCIN
      WRITE(23,76)IG,EE(IG)
    ELSE IF (IG .eq. 10)THEN
      EE(IG) = DETSEDOUT/DETSSEDIN
      WRITE(23,76)IG,EE(IG)
    END IF
  END IF
  SUMM2 = 0.0
END DO

C
C Calculate Biomass for Predators Only
C
DO IBG = 1, NGROUP
  Do J = 3, NGROUP-3

```

```

      If (J .ne. 5) then
        M2 = (Consumpt(J)*DC(J,IBG)) - (Consumpt(IBG)*
*         DC(IBG,IBG))
        SUMM2 = SUMM2 + M2
      END IF
    END DO
    GSUMM2(IBG) = SUMM2
    CANN(IBG) = (QB(IBG)*DC(IBG,IBG))
    SAMEG(IBG) = (PB(IBG)*EE_BIO(IBG))
    IF (CANN(IBG) .gt. SAMEG(IBG)) Then
      CANN(IBG) = SAMEG(IBG) - 0.01
    ENDIF
    IF (SAMEG(IBG) .ne. 0.0) then
      Biomass(IBG) = (GSUMM2(IBG) + Y(IBG) + BA(IBG) +
*         E(IBG)) / (SAMEG(IBG) - CANN(IBG))
      IF (IBG .eq. 3 .or. IBG .eq. 4 .or. IBG .eq. 6
*         .or. IBG .eq. 7) then
        WRITE(23,77) IBG, Biomass(IBG)
77      FORMAT('Group = ',I5,'Biomass = ',e12.8)
      END IF
    END IF
    SUMM2 = 0.0
  END DO
END DO

```

```

C
C Caculate Average Seasonal Values
C

```

```

AREG_ALGC=AREG_ALGC/ACOUNT
AREG_ANPP=AREG_ANPP/ACOUNT
AREG_AGPP=AREG_AGPP/ACOUNT
AREG_APRED=AREG_APRED/ACOUNT
AREG_ADOC=AREG_ADOC/ACOUNT
AREG_APOC=AREG_APOC/ACOUNT

AREG_DOC=AREG_DOC/ACOUNT
AREG_POC=AREG_POC/ACOUNT
AREG_DETC=AREG_DETC/ACOUNT
AREG_CRESP=AREG_CRESP/ACOUNT
AREG_POC2DOC=AREG_POC2DOC/ACOUNT

AREG_MICRZ=AREG_MICRZ/ACOUNT
AREG_MICRZR=AREG_MICRZR/ACOUNT
AREG_MICRZNP=AREG_MICRZNP/ACOUNT
AREG_MICRZDOC=AREG_MICRZDOC/ACOUNT
AREG_MICRZPOC=AREG_MICRZPOC/ACOUNT
AREG_MICRZPR=AREG_MICRZPR/ACOUNT
AREG_MICRZALG=AREG_MICRZALG/ACOUNT
AREG_TCONSZ=AREG_TCONSZ/ACOUNT
AREG_UADOC SZ=AREG_UADOC SZ/ACOUNT
AREG_UAPOC SZ=AREG_UAPOC SZ/ACOUNT

AREG_MESoz=AREG_MESoz/ACOUNT
AREG_MESozR=AREG_MESozR/ACOUNT

```

```

AREG_MESOZNP=AREG_MESOZNP/ACOUNT
AREG_MESOZPOC=AREG_MESOZPOC/ACOUNT
AREG_MESOZPR=AREG_MESOZPR/ACOUNT
AREG_MESOZALG=AREG_MESOZALG/ACOUNT
AREG_MIC2MES=AREG_MIC2MES/ACOUNT
AREG_TCONLZ=AREG_TCONLZ/ACOUNT
AREG_UADOCLZ=AREG_UADOCLZ/ACOUNT
AREG_UAPOCLZ=AREG_UAPOCLZ/ACOUNT

AREG_SEDPOC = AREG_SEDPOC/ACOUNT
AREG_BURIAL = AREG_BURIAL/ACOUNT
AREG_CFLUX = AREG_CFLUX/ACOUNT
AREG_SEDR = AREG_SEDR/ACOUNT
AREG_ALG2SED = AREG_ALG2SED/ACOUNT

AREG_BALG =AREG_BALG/ACOUNT
AREG_BALGR =AREG_BALGR/ACOUNT
AREG_BALGPR = AREG_BALGPR/ACOUNT
AREG_BALGC =AREG_BALGC/ACOUNT
AREG_BNPP = AREG_BNPP/ACOUNT

AREG_SAV = AREG_SAV/ACOUNT
AREG_SAVNP = AREG_SAVNP/ACOUNT
AREG_SAVR = AREG_SAVR/ACOUNT
AREG_SAV2SED = AREG_SAV2SED/ACOUNT
AREG_SAV2POC = AREG_SAV2POC/ACOUNT
AREG_SAV2DOC = AREG_SAV2DOC/ACOUNT

AREG_SFEEED = AREG_SFEEED/ACOUNT
AREG_SFNP = AREG_SFNP/ACOUNT
AREG_SFR = AREG_SFR/ACOUNT
AREG_SFTCON = AREG_SFTCON/ACOUNT
AREG_SFACON = AREG_SFACON/ACOUNT
AREG_SFPCCON = AREG_SFPCCON/ACOUNT
AREG_SFUAC =AREG_SFUAC/ACOUNT

AREG_DFEED =AREG_DFEED/ACOUNT
AREG_DFNP = AREG_DFNP/ACOUNT
AREG_DFR = AREG_DFR/ACOUNT
AREG_DFTCON =AREG_DFTCON/ACOUNT
AREG_DFUAC = AREG_DFUAC /ACOUNT
WRITE(23,80)
80  FORMAT(// ' Average Seasonal Values ')

C SEDIMENTS
  WRITE(23,20)
  WRITE(23,21) AREG_SEDPOC,AREG_ALG2SED,AREG_CFLUX,
$  AREG_SAV2SED,
$  AREG_DFUAC,AREG_SFUAC,AREG_BALGC,AREG_BURIAL,
$  AREG_SEDR

C WATER COLUMN POC
  WRITE(23,22)
  WRITE(23,23) AREG_POC,AREG_APOC,AREG_UAPOCSZ,

```

```

$  AREG_UAPOCLZ,AREG_SAV2POC,AREG_MICRZPOC,AREG_MESozPOC,
$  AREG_CFLUX,AREG_POC2DOC

C WATER COLUMN DOC
  WRITE (23,24)
  WRITE (23,25) AREG_DOC,AREG_ADOC,AREG_UADOCsz,
$  AREG_UADOCCLZ,AREG_SAV2DOC,AREG_MICRZDOC,AREG_CRESP

C PHYTOPLANKTON
  WRITE (23,26)
  WRITE (23,27) AREG_ALGC,AREG_ANPP,AREG_ADOC,AREG_APOC,
$  AREG_MICRZALG,AREG_MESozALG,AREG_ALG2SED,
$  AREG_AGPP-AREG_ANPP

C MICROZOOPLANKTON
  WRITE (23,28)
  WRITE (23,29) AREG_MICRZ,AREG_MICRZNP,AREG_TCONsz,
$  AREG_UADOCsz+AREG_UAPOCSZ,AREG_MICRZDOC,
$  AREG_MICRZPOC,AREG_MICRZALG,AREG_UADOCsz,
$  AREG_UAPOCSZ,AREG_MIC2MES,AREG_MICRZR

C MESOZOOPLANKTON
  WRITE (23,30)
  WRITE (23,31) AREG_MESoz,AREG_MESozNP,AREG_TCONLZ,
$  AREG_UADOCCLZ+AREG_UAPOCLZ,
$  AREG_MESozPOC,AREG_MESozALG,AREG_MIC2MES,
$  AREG_UADOCCLZ,AREG_UAPOCLZ,AREG_MESozR

C SAV
  WRITE (23,32)
  WRITE (23,33) AREG_SAV,AREG_SAVNP,AREG_SAV2DOC,
$  AREG_SAV2POC,AREG_SAV2SED,AREG_SAVR

C BENTHIC ALGAE
  WRITE (23,34)
  WRITE (23,35) AREG_BALG,AREG_BNPP,AREG_BALGC,AREG_BALGR

C DEPOSIT FEEDERS
  WRITE (23,36)
  WRITE (23,37) AREG_DFEED,AREG_DFNP,AREG_DFTCON,
$  AREG_DFUAC,AREG_DFTCON,AREG_DFUAC,AREG_DFR

C FILTER FEEDERS
  WRITE (23,38)
  WRITE (23,39) AREG_SFEED,AREG_SFNP,AREG_SFTCON,
$  AREG_SFUAC,AREG_SFACON,AREG_SFPCCON,AREG_SFUAC,
$  AREG_SFR

C
C Production/Biomass ratio
C
  APB_BALGRatio = AREG_BNPP/AREG_BALG
  APB_ALGRatio = AREG_ANPP/AREG_ALGC

```

```

APB_Z1Ratio = AREG_MICRZNP/AREG_MICRZ
APB_Z2Ratio = AREG_MESozNP/AREG_MESoz
APB_SAVRatio = AREG_SAVNP/AREG_SAV
APB_DFRatio = AREG_DFNP/AREG_DFEED
APB_SFRatio = AREG_SFNP/AREG_SFEED

WRITE (23, 67)
WRITE (23, 68) APB_BALGRatio, APB_ALGRatio, APB_Z1Ratio, APB_Z2Ratio,
*             APB_SAVRatio,
*             APB_DFRatio, APB_SFRatio

C
C Consumption/Biomass
C
    AQB_Z1Ratio = AREG_TCONSZ/AREG_MICRZ
    AQB_Z2Ratio = AREG_TCONLZ/AREG_MESoz
    AQB_DFRatio = AREG_DFTCON/AREG_DFEED
    AQB_SFRatio = AREG_SFTCON/AREG_SFEED

    WRITE (23, 71)
    WRITE (23, 72) AQB_Z1Ratio, AQB_Z2Ratio,
*                 AQB_DFRatio, AQB_SFRatio

C
C Uassimilated/Consumption
C
    AUATC_Z1Ratio = (AREG_UADOCsz+AREG_UAPOCSz)/AREG_TCONSZ
    AUATC_Z2Ratio = (AREG_UADOCCLz+AREG_UAPOCLz)/AREG_TCONLz
    AUATC_DFRatio = AREG_DFUAC/AREG_DFTCON
    AUATC_SFRatio = AREG_SFUAC/AREG_SFTCON

    WRITE (23, 73)
    WRITE (23, 74) AUATC_Z1Ratio, AUATC_Z2Ratio,
*                 AUATC_DFRatio, AUATC_SFRatio

C
C Diet Compostion
C
C Z1 Diet Compostion
    AZ1DCDOC = AREG_MICRZDOC/ (AREG_MICRZDOC+AREG_MICRZPOC+
*                             AREG_MICRZALG)
    AZ1DCPOC = AREG_MICRZPOC/ (AREG_MICRZDOC+AREG_MICRZPOC+
*                             AREG_MICRZALG)
    AZ1DCALG = AREG_MICRZALG/ (AREG_MICRZDOC+AREG_MICRZPOC+
*                             AREG_MICRZALG)
    WRITE (23, 69)
    WRITE (23, 70) AZ1DCDOC, AZ1DCPOC, AZ1DCALG

C Z2 Diet Compostion
    AZ2DCPOC = AREG_MESozPOC/ (AREG_MIC2MES+AREG_MESozPOC+
*                             AREG_MESozALG)
    AZ2DCZ1 = AREG_MIC2MES/ (AREG_MIC2MES+AREG_MESozPOC+
*                             AREG_MESozALG)
    AZ2DCALG = AREG_MESozALG/ (AREG_MIC2MES+AREG_MESozPOC+

```

```

*           AREG_MESOZALG)
WRITE(23,42)
WRITE(23,70) AZ2DCPOC,AZ2DCPOC,AZ2DCALG

C Deposit Feeders (DF) Diet Compostion
ADFDCSedPOC = AREG_DFUAC/AREG_DFUAC
WRITE(23,43)
WRITE(23,70) ADFDCSedPOC

C Filter Feeders (SF) Diet Compostion
ASFDCPOC = AREG_SFPCCON/(AREG_SFPCCON+AREG_SFACON)
ASFDCALG = AREG_SFACON/(AREG_SFPCCON+AREG_SFACON)
WRITE(23,45)
WRITE(23,70) ASFDCPOC,ASFDCALG

C
C Detrital Fate
C
C Microphytobenthos Detrital Fate
AMICRBENALG_SedPOC = AREG_BALGC/AREG_BALGC
AMICRBENALG_POC = 0.
AMICRBENALG_DOC = 0.
ABAExport = 0.
ABATotal =
AMICRBENALG_SedPOC+AMICRBENALG_POC+AMICRBENALG_DOC+AExport
WRITE(23,47)
WRITE(23,48) AMICRBENALG_DOC,AMICRBENALG_SedPOC,AMICRBENALG_POC,
*           ABAExport,ABATotal

C Phytoplankton Detrital Fate
AALG_SedPOC = AREG_ALG2SED/(AREG_ADOC+AREG_APOC+
*           AREG_ALG2SED)
AALG_POC = AREG_APOC/(AREG_ADOC+AREG_APOC+AREG_ALG2SED)
AALG_DOC = AREG_ADOC/(AREG_ADOC+AREG_APOC+AREG_ALG2SED)
AAlgExport = 0.
AAlgTotal = AALG_SedPOC+AALG_POC+AALG_DOC+AAlgExport
WRITE(23,49)
WRITE(23,48) AALG_DOC,AALG_SedPOC,AALG_POC,
*           AAlgExport,AAlgTotal

C Microzooplankton Detrital Fate
AZ1_SedPOC = 0.
AZ1_POC = AREG_UAPOCSZ/(AREG_UAPOCSZ+AREG_UADOC SZ)
AZ1_DOC = AREG_UADOC SZ/(AREG_UAPOCSZ+AREG_UADOC SZ)
AZ1Export = 0.
AZ1Total = AZ1_SedPOC +AZ1_POC +AZ1_DOC +AZ1Export
WRITE(23,51)
WRITE(23,48) AZ1_DOC,AZ1_SedPOC,AZ1_POC,
*           AZ1Export,AZ1Total

C Mesozooplankton Detrital Fate
AZ2_SedPOC = 0.
AZ2_POC = AREG_UAPOCLZ/(AREG_UAPOCLZ+AREG_UADOC LZ)

```

```

AZ2_DOC = AREG_UADOCLZ/ (AREG_UAPOCLZ+AREG_UADOCLZ)
AZ2Export = 0.
AZ2Total = AZ2_SedPOC +AZ2_POC +AZ2_DOC +AZ2Export
WRITE(23,53)
WRITE(23,48) AZ2_DOC,AZ2_SedPOC,AZ2_POC,
*           AZ2Export,AZ2Total

C SAV Detrital Fate
ASAV_SedPOC = AREG_SAV2SED/ (AREG_SAV2DOC+AREG_SAV2POC+
*           AREG_SAV2SED)
ASAV_POC = AREG_SAV2POC/ (AREG_SAV2DOC+AREG_SAV2POC+
*           AREG_SAV2SED)
ASAV_DOC = AREG_SAV2DOC/ (AREG_SAV2DOC+AREG_SAV2POC+
*           AREG_SAV2SED)
ASAVExport = 0.
ASAVTotal = ASAV_SedPOC +ASAV_POC +ASAV_DOC +ASAVExport
WRITE(23,55)
WRITE(23,48) AZ2_DOC,AZ2_SedPOC,AZ2_POC,
*           AZ2Export,AZ2Total

C Deposit Feeders Detrital Fate
ADF_SedPOC = AREG_DFUAC/AREG_DFUAC
ADF_POC = 0.
ADF_DOC = 0.
ADFExport = 0.
ADFTotal = ADF_SedPOC+ADF_POC+ADF_DOC+ADFExport
WRITE(23,57)
WRITE(23,48) ADF_DOC,ADF_SedPOC,ADF_POC,
*           ADFExport,ADFTotal

C Suspension Feeders Detrital Fate
ASF_SedPOC = AREG_SFUAC/AREG_SFUAC
ASF_POC = 0.
ASF_DOC = 0.
ASFExport = 0.
ASFTotal = ASF_SedPOC+ASF_POC+ASF_DOC+ASFExport
WRITE(23,59)
WRITE(23,48) ASF_DOC,ASF_SedPOC,ASF_POC,
*           ASFExport,ASFTotal

C DOC Detrital Fate
ADOC_SedPOC = 0.
ADOC_POC = 0.
ADOC_DOC = 0.
ADOCExport = 1.
ADOCTotal = ADOC_SedPOC +ADOC_POC +ADOC_DOC +ADOCExport
WRITE(23,61)
WRITE(23,48) ADOC_DOC,ADOC_SedPOC,ADOC_POC,
*           ADOCExport,ADOCTotal

C Sed POC Detrital Fate
ASedPOC_SedPOC = 0.
ASedPOC_POC = 0.
ASedPOC_DOC = 0.

```

```
ASedPOCExport = 1.
ASedPOCTotal =
ASedPOC_SedPOC+ASedPOC_POC+ASedPOC_DOC+ASedPOCExport
WRITE(23,63)
WRITE(23,48) ASedPOC_DOC,ASedPOC_SedPOC,ASedPOC_POC,
*           ASedPOCExport,ASedPOCTotal

C POC Detrital Fate
APOC_SedPOC = AREG_CFLUX/(AREG_CFLUX+AREG_POC2DOC)
APOC_POC = 0.
APOC_DOC = AREG_POC2DOC/(AREG_CFLUX+AREG_POC2DOC)
APOCExport = 0.
APOCTotal = ASF_SedPOC+ASF_POC+ASF_DOC+ASFExport
WRITE(23,65)
WRITE(23,48) APOC_DOC,APOC_SedPOC,APOC_POC,
*           APOCExport,APOCTotal

C
C
REWIND (KFL)
GO TO 1
3 STOP
END
```


APPENDIX B

This appendix contains a table listing code names and definitions for the common links between ICM and Ecopath.

Table B.1 Glossary terms for common variables (Cerco and Tillman 2008)

Symbol	Units	Definition
BBM	g C m^{-2}	Benthic algae
BMalg	d^{-1}	Algal basal metabolism
BMba	d^{-1}	Benthic algae basal metabolism
BMIz	d^{-1}	Mesozooplankton basal metabolism
BMRT	d^{-1}	SAV root metabolism
BMsav	d^{-1}	SAV basal metabolism
BMSH	d^{-1}	SAV shoot metabolism
BMsZ	d^{-1}	Microzooplankton basal metabolism
B2	g C m^{-3}	Spring diatoms
B3	g C m^{-3}	Green algae
CFECES	$\text{mg C m}^{-2} \text{d}^{-1}$	Labile carbon feces produced by filter feeders
CP	$\text{g C m}^{-3} \text{d}^{-1}$	Detritus production by phytoplankton metabolism
CPSFEC	$\text{mg C m}^{-2} \text{d}^{-1}$	Labile carbon pseudo-feces produced by filter feeders
DF	mg C m^{-2}	Deposit feeders
DOC	g C m^{-3}	Dissolved organic carbon
DOCalg	$\text{g C m}^{-3} \text{d}^{-1}$	Phytoplankton dissolved organic carbon production rate
Elz	$0 < \text{Elz} < 1$	Mesozooplankton efficiency
Esz	$0 < \text{Esz} < 1$	Microzooplankton efficiency
FCD	$0 < \text{FCD} < 1$	Fraction of phytoplankton metabolism excreted as dissolved organic carbon
FCDP	$0 < \text{FCDP} < 1$	Fraction of non-specific predation on phytoplankton released as dissolved organic carbon
FCDSH	$0 < \text{FCDSH} < 1$	Fraction of SAV metabolism excreted as DOC
FCDSL	$0 < \text{FCDSL} < 1$	Fraction of SAV leaf sloughing released as DOC

Table B.1 Continued.

Symbol	Units	Definition
FILTCT	$\text{m}^3 \text{g}^{-1} \text{filter feeder carbon d}^{-1}$	Filtration rate as determined by temperature, dissolved oxygen, and other factors
Gdf	d^{-1}	Deposit feeder specific growth rate as determined by local temperature, dissolved oxygen concentration, and food availability
G1	mg C m^{-3}	Labile sediment particulate organic carbon
G2	mg C m^{-3}	Refractory sediment particulate organic carbon
G3	mg C m^{-3}	Inert sediment particulate organic carbon
H	m	Depth of water column
KLPOC	d^{-1}	Labile particulate organic carbon dissolution rate
KRPOC	d^{-1}	Refractory particulate organic carbon dissolution rate
LPOC	g C m^{-3}	Labile particulate organic carbon
LZ	g C m^{-3}	Mesozooplankton
M2	mg m^{-3}	Bed sediment solids concentration
Palg	d^{-1}	Algal specific production rate as determined by local irradiance, temperature, and nutrient availability
Pba	d^{-1}	Benthic algae specific production rate as determined by local irradiance, temperature, and nutrient availability
POC _{alg}	$\text{g C m}^{-3} \text{d}^{-1}$	Phytoplankton particulate organic carbon production rate
Psav	d^{-1}	SAV specific production rate as determined by local irradiance, temperature, and nutrient availability
PATCH	$0 < \text{PATCH} < 1$	Product of coverage and patchiness
POC1	mg C m^{-3}	G1 carbon concentration in bed sediments
POC2	mg C m^{-3}	G2 carbon concentration in bed sediments
POC2DOC	$\text{g C m}^{-2} \text{d}^{-1}$	Particulate organic carbon dissolution to dissolved organic carbon
POC2SED	$\text{g C m}^{-2} \text{d}^{-1}$	Particulate organic carbon deposition to sediments
POC3	mg C m^{-3}	G3 carbon concentration in bed sediments
PRAsz	g C m^{-3}	Prey available to microzooplankton
PRalg	$\text{g C m}^{-3} \text{d}^{-1}$	Non-specific predation on phytoplankton
PRA _{lz}	g C m^{-3}	Prey available to mesozooplankton
PRSPalg	$0 < \text{PRSPalg} < 1$	Algal photorespiratory fraction

Table B.1 Continued.

Symbol	Units	Definition
RCFECES	$\text{mg C m}^{-2} \text{ d}^{-1}$	Refractory carbon feces produced by filter feeders
RCPSFEC	$\text{mg C m}^{-2} \text{ d}^{-1}$	Refractory carbon pseudo-feces produced by filter feeders
Rdf	d^{-1}	Deposit feeder specific respiration rate
RESPff	$\text{mg C m}^{-2} \text{ d}^{-1}$	Filter feeder respiration
RFlz	$0 < \text{RFlz} < 1$	Mesozooplankton active respiration
RFsz	$0 < \text{RFsz} < 1$	Microzooplankton active respiration
RPOC	g C m^{-3}	Refractory particulate organic carbon
Rlz	d^{-1}	Mesozooplankton specific ration as determined by local temperature and prey availability
Rsz	d^{-1}	Microzooplankton specific ration as determined by local temperature and prey availability
RT	g C m^{-2}	SAV roots
SEDalg	$\text{g C m}^{-2} \text{ d}^{-1}$	Phytoplankton sedimentation rate
SF(I)	mg C m^{-2}	Filter feeder group I
SH	g C m^{-2}	SAV shoots
SL	d^{-1}	SAV leaf sloughing rate
SZ	g C m^{-3}	Microzooplankton
TCONff	$\text{mg C m}^{-2} \text{ d}^{-1}$	Filter feeder total consumption
UB2lz	$0 < \text{UB2lz} < 1$	Utilization of spring diatoms by mesozooplankton
UB2sz	$0 < \text{UB2sz} < 1$	Utilization of spring diatoms by microzooplankton
UB3lz	$0 < \text{UB3lz} < 1$	Utilization of green algae by mesozooplankton
UB3sz	$0 < \text{UB3sz} < 1$	Utilization of green algae by microzooplankton
UCONff	$\text{mg C m}^{-2} \text{ d}^{-1}$	Filter feeder unassimilated consumption
UDOCsz	$0 < \text{UDOCsz} < 1$	Utilization of dissolved organic carbon by microzooplankton
ULlz	$0 < \text{ULlz} < 1$	Utilization of labile particulate organic carbon by mesozooplankton
ULsz	$0 < \text{ULsz} < 1$	Utilization of labile particulate organic carbon by microzooplankton
URLz	$0 < \text{URLz} < 1$	Utilization of refractory particulate organic carbon by mesozooplankton

Table B.1 Concluded.

Symbol	Units	Definition
URsz	$0 < URsz < 1$	Utilization of refractory particulate organic carbon by microzooplankton
USZlz	$0 < USZlz < 1$	Utilization of microzooplankton by mesozooplankton
WSalgNET	$m\ d^{-1}$	Net phytoplankton settling rate into bottom sediments
WSLNET	$m\ d^{-1}$	Net labile particulate organic carbon settling rate into bottom sediments
WSRNET	$m\ d^{-1}$	Net refractory particulate organic carbon settling rate into bottom sediments
xki0	$mg\ sediment\ mg^{-1}\ deposit\ feeder\ carbon\ d^{-1}$	Ingestion rate, as influenced by temperature
xpoc1lim	Function that saturates deposit feeder G1 carbon uptake at high concentrations	$0 < xpoc1lim < 1$
xpoc2lim	Function that saturates deposit feeder G2 carbon uptake at high concentrations	$0 < xpoc2lim < 1$
$\alpha 1$	G1 carbon assimilation efficiency	$0 < \alpha 1 < 1$
$\alpha 2$	G2 carbon assimilation efficiency	$0 < \alpha 2 < 1$

VITA

Name: Dorothy Hamlin Tillman

Office Address: 3909 Halls Ferry Rd.
Vicksburg, MS., 39180

Email Address: Dorothy.H.Tillman@erdc.usace.army.mil

Work Experience: Research Civil Engineer in the Water Quality and Contaminant Modeling
Branch, EL ERDC (1981-present)

Education: Mississippi State University (1973-1977)
B.S.: Major - Zoology
Mississippi State University (1980-1984)
B.Eng.: Major - Biological Eng.
Mississippi State University (1986-1991)
M. Eng.: Major - Civil Engineering
Texas A&M University (1997-2008)
Ph. D.: Major - Civil Engineering